



1990

## Electrophysiological and Ultrastructural Analysis of Subsidiary Pacemakers in the Cat Right Atrium

Donald S. Rubenstein  
*Loyola University Chicago*

Follow this and additional works at: [https://ecommons.luc.edu/luc\\_diss](https://ecommons.luc.edu/luc_diss)



Part of the [Microbiology Commons](#)

---

### Recommended Citation

Rubenstein, Donald S., "Electrophysiological and Ultrastructural Analysis of Subsidiary Pacemakers in the Cat Right Atrium" (1990). *Dissertations*. 2690.  
[https://ecommons.luc.edu/luc\\_diss/2690](https://ecommons.luc.edu/luc_diss/2690)

This Dissertation is brought to you for free and open access by the Theses and Dissertations at Loyola eCommons. It has been accepted for inclusion in Dissertations by an authorized administrator of Loyola eCommons. For more information, please contact [ecommons@luc.edu](mailto:ecommons@luc.edu).



This work is licensed under a [Creative Commons Attribution-NonCommercial-No Derivative Works 3.0 License](#).  
Copyright © 1990 Donald S. Rubenstein

ELECTROPHYSIOLOGICAL AND ULTRASTRUCTURAL ANALYSIS  
OF SUBSIDIARY PACEMAKERS IN THE CAT RIGHT ATRIUM

By

Donald S. Rubenstein, M.D.

A Dissertation Submitted to  
the Faculty of the Graduate School  
of Loyola University of Chicago in Partial Fulfillment  
of the Requirements for the Degree of  
Doctor of Philosophy

April

1990

((c), Donald S. Rubenstein)

## ACKNOWLEDGEMENTS

I would like to express my most sincere thanks to Dr. Stephen Lipsius for his invaluable advice, inspiration, and expertise. Without his knowledgeable insight and guidance this dissertation would not have been possible. His selfless time and effort has taught me the patience and skill needed for scientific research. I am most grateful for his devotion to science and the scientific method which have been instilled in my own ability to become a medical scientist.

Enormous thanks are extended to Linda Fox, for her superior technical supervision, and photographic skill that enabled us all to see the intricate beauty of the heart. Her friendship and humor over the years have been truly appreciated.

I also wish to thank the entire Faculty of the Physiology Department for their unsurpassed excellence in teaching and research. Their enthusiasm and open-door policy generated the ideal environment for the creation and development of new ideas.

Most especially, I want to thank my parents, Beverly and Van, and sister, Randi. It is with their continued support, guidance, and trust, that has provided me the opportunity to reach for my dreams. This dissertation is dedicated to them. For my past achievements, as well as all my future ones, they have my immeasurable gratitude.

## VITA

The author, Donald S. Rubenstein, was born on June 8, 1958, in Encino, California.

He graduated from Adlai E. Stevenson High School in Prairie View, Illinois in 1976. In August of that year, he enrolled at the University of Illinois, Champaign-Urbana, Illinois. During his undergraduate years, he entered into a combined degree program to receive degrees in Biology and Mechanical Engineering. In May of 1980, he received his Bachelor of Science degree in Biology. In August of 1981, he received his Masters of Science degree in Mechanical Engineering. At the end of August in 1981, he enrolled in Medical School at Loyola University of Chicago, and in June of 1983 entered into a combined M.D./Ph.D. degree program with the Physiology Department. In June of 1987, he received his Doctor of Medicine degree. Dr. Rubenstein is a member of the American Medical Association and the American Association for the Advancement of Science.

The author has worked under the direction of Dr. Stephen L. Lipsius. Dr. Rubenstein's publications include:

RUBENSTEIN, D.S., L.M. Fox, J.A. McNulty, and S.L. Lipsius. Electrophysiology and ultrastructure of Eustachian ridge from cat right atrium: a comparison with SA node. J. Mol. Cell. Cardiol. 19: 965-976, 1987.

Lipsius, S.L. and D.S. RUBENSTEIN. Cyclic bradycardias generated by atrial subsidiary pacemakers. J. Electrophys. 2: 90-103, 1988.

RUBENSTEIN, D.S., S.L. Lipsius. Mechanisms of automaticity in subsidiary pacemakers from cat right atrium. Circ. Res. 64: 648-657, 1989.

RUBENSTEIN, D.S., J.P. Zbilut, C.L. Weber, and S.L. Lipsius. Cardiac Sarcoplasmic Reticulum Mediates Periodic and Irregular Voltage Waveforms (submitted).

Wu, J., D.S. RUBENSTEIN, S.L. Lipsius. Inhibitory Effects of Extracellular Magnesium on Right Atrial Pacemakers (in preparation).

### Abstracts

Lipsius, S.L. and D.S. RUBENSTEIN. Ionic components of subsidiary automaticity in the canine right atrium. Fed.Proc. 42: 580, 1983.

RUBENSTEIN, D.S. and S.L. Lipsius. Electrophysiology of atrial pacemakers in the Eustachian ridge of the cat heart. The Physiologist 27: 215, 1984.

RUBENSTEIN, D.S. and S.L. Lipsius. Mechanisms of brady-tachy dysrhythmia. Circulation 70 II: 223, 1984.

RUBENSTEIN, D.S. and S.L. Lipsius. Autonomic initiation of subsidiary atrial pacemaker activity. Fed. Proc. 44: 1361, 1985.

Lipsius, S.L., L. Fox, J.A. McNulty, and D.S. RUBENSTEIN. Electrophysiology and ultrastructure of fibers in the Eustachian ridge of the cat heart. Fed. Proc. 44: 739, 1985.

Lipsius, S.L. and D.S. RUBENSTEIN. Slow inward current and intracellular calcium mediate subsidiary atrial pacemaker automaticity. J. Physiol. (Lond.) 371: 193P, 1986.

RUBENSTEIN, D.S. and S.L. Lipsius. Mechanisms of atrial pacemaker activation by norepinephrine. Fed. Proc. 46: 1260, 1987.

## TABLE OF CONTENTS

	<u>Page</u>
ACKNOWLEDGEMENTS .....	ii
VITA .....	iii
LIST OF TABLES .....	ix
LIST OF ILLUSTRATIONS .....	x
 CHAPTER	
I. INTRODUCTION .....	1
II. LITERATURE REVIEW .....	4
A. THE ORIGIN OF THE HEARTBEAT AND ITS HIERARCHY .....	4
1. Sinus Node .....	4
2. Subsidiary Pacemakers .....	5
a. <u>In vivo</u> -General History .....	5
b. Confirmation and Importance of Low Right Atrial Subsidiary Pacemakers .....	12
c. Coronary Sinus Rhythms .....	15
d. Subsidiary Pacemaker Instability .....	16
e. <u>In Vitro</u> .....	17
f. Other Atrial Subsidiary Pacemaker Sites .....	21
B. STRUCTURE-FUNCTION .....	22
1. Atrial Embryology .....	22
2. Cellular Structure and Function .....	25
a. Glycocalyx and Cell Membrane .....	27
b. Caveolae or T-tubules .....	27
c. Nucleus .....	28
d. Myofibrils .....	29
e. Mitochondria .....	29
f. Sarcoplasmic Reticulum .....	30
g. Intercellular Junctions .....	31
i) Intercalated Discs .....	31
ii) Desmosomes .....	31
iii) Intermediate Junctions .....	32
iv) Nexal connections .....	32

<u>CHAPTER</u>	<u>Page</u>
3. Internodal Tracts .....	33
<b>C. CELLULAR ELECTROPHYSIOLOGY OF PACEMAKER ACTIVITY</b>	<b>35</b>
1. The Heart as an Oscillator .....	35
2. Mechanisms of Diastolic Depolarization .....	39
a. $P_{Na}/P_K$ ratio .....	40
b. $I_K$ current .....	41
c. $I_f$ current .....	42
d. Calcium currents .....	45
e. Sodium Calcium Exchange and SR Components .....	48
f. $I_{Na}$ current .....	52
g. Summary .....	52
3. Autonomic Modulation of Pacemaker Activity .....	53
a. Adrenergic .....	54
i) $\beta$ -Adrenergic .....	54
ii) $\alpha$ -Adrenergic .....	57
iii) Summary .....	58
b. Cholinergic (Muscarinic) .....	59
<b>D. CLINICAL ATRIAL ECTOPIC DYSRHYTHMIAS</b> .....	<b>62</b>
1. Ectopic Supraventricular Tachycardias .....	62
2. Surgical Trauma .....	63
3. Sick Sinus Syndrome .....	65
4. Summary .....	67
<b>III. METHODS</b> .....	<b>69</b>
<b>A. PREPARATION AND EXPERIMENTAL SETUP</b> .....	<b>69</b>
<b>B. RECORDING OF TRANSMEMBRANE POTENTIALS</b> .....	<b>73</b>
<b>C. DATA MEASUREMENT</b> .....	<b>74</b>
<b>D. ULTRASTRUCTURE STUDIES</b> .....	<b>78</b>
<b>E. DRUG PROTOCOLS</b> .....	<b>80</b>
1. Preparation of Solutions .....	80
2. Autonomic Neuromediators .....	81
3. Pharmacological Agents .....	82
<b>F. DATA ANALYSIS</b> .....	<b>83</b>



IV. RESULTS .....	84
A. ELECTROPHYSIOLOGY AND ULTRASTRUCTURE OF EUSTACHIAN RIDGE FROM CAT RIGHT ATRIUM: A COMPARISON WITH SA NODE ( <u>J. Mol. Cell. Cardiol.</u> , 19: 965-976, 1987) .....	84
1. Electrophysiology .....	84
2. Morphology .....	87
3. Quantification .....	92
B. MECHANISMS OF AUTOMATICITY IN SUBSIDIARY PACEMAKERS FROM CAT RIGHT ATRIUM ( <u>Circ. Res.</u> , 64: 648-657, 1989) .....	97
1. Cesium .....	97
2. Norepinephrine and Bay K 8644 .....	100
3. Verapamil and Tetrodotoxin .....	100
4. Ryanodine .....	103
C. CYCLIC BRADYDYSRHYTHMIAS GENERATED BY ATRIAL SUBSIDIARY PACEMAKERS ( <u>J. Electrophys.</u> , 2: 90-103, 1988) .....	110
D. SUBSIDIARY PACEMAKER RESISTANCE TO $[K]_o$ .....	124
1. $P_{Na}/P_K$ Ratio .....	124
2. Effect of $[K]_o$ on Spontaneous Activity .....	127
E. MECHANISMS OF INITIATION OF ATRIAL SUBSIDIARY PACEMAKER ACTIVITY .....	129
1. Effect of Adrenergic Blockade .....	129
2. Effect of Dibutyryl Cyclic AMP .....	132
3. Effect of Bay K 8644 .....	132
4. Effect of Cesium .....	135
5. Effect of Tetrodotoxin .....	135
6. Effect of Verapamil .....	135
7. Effect of Low Sodium .....	136
8. Effect of Acetylstrophanthidin .....	138
9. Effect of Ryanodine .....	138
V. DISCUSSION .....	140
A. ELECTROPHYSIOLOGY AND ULTRASTRUCTURE OF EUSTACHIAN RIDGE FROM CAT RIGHT ATRIUM: A COMPARISON WITH SA NODE ( <u>J. Mol. Cell. Cardiol.</u> , 19: 965-976, 1987) .....	140
1. Electrophysiology .....	140

<u>CHAPTER</u>	<u>Page</u>
2. Morphology .....	141
B. MECHANISMS OF AUTOMATICITY IN SUBSIDIARY PACEMAKERS FROM CAT RIGHT ATRIUM ( <u>Circ. Res.</u> , 64: 648-657, 1989) .....	144
C. CYCLIC BRADYDYSRHYTHMIAS GENERATED BY ATRIAL SUBSIDIARY PACEMAKERS ( <u>J. Electrophys.</u> , 2: 90-103, 1988) .....	150
D. SUBSIDIARY PACEMAKER RESISTANCE TO $[K]_o$ .....	156
E. MECHANISMS OF PACEMAKER INITIATION .....	157
SUMMARY .....	162
BIBLIOGRAPHY .....	164

## LIST OF TABLES

TABLE	<u>Page</u>
1. Composition of Tyrode's Solution .....	70
2. Comparative Action Potential Measurements .....	86
3. Relative Volume Densities .....	96
4. Pacemaker Action Potential Measurements in Cat Right Atrium .....	99
5. Effect of $[K]_o$ on Atrial Subsidiary Pacemaker Action Potential Measurements .....	130

## LIST OF ILLUSTRATIONS

<u>Figure</u>	<u>Page</u>
1. Location of the Eustachian Ridge .....	71
2. Fast-Flow Chamber .....	72
3. Tension Transducer .....	75
4. Calibration of Tension Transducer .....	76
5. Action Potential Measurements .....	77
6. Spontaneous Action Potentials from SA Node and Eustachian Ridge .....	85
7. Low Power Electron Micrograph of Eustachian Ridge .....	88
8. Electron Micrograph of SA Nodal Cells at the Site of Earliest Activation .	89
9. Electron Micrograph of Eustachian Ridge P Cells at the Site of Earliest Activation .....	90
10. Electron Micrograph of P Cell and Transitional Cell in the Eustachian Ridge .....	91
11. Electron Micrograph of Nexal Connections in the Eustachian Ridge .....	93
12. Electron Micrograph of Directly Apposed Subsarcolemmal Cisternae ....	94
13. High Power Electron Micrograph of Directly Apposed Subsarcolemmal Cisternae .....	95
14. Effect of Cesium on Pacemaker Action Potentials . .....	98
15. Effect of Bay K 8644 on Pacemaker Action Potentials and Tension .....	101
16. Effect of Verapamil on Pacemaker Action Potentials .....	102
17. Effect of Ryanodine on Subsidiary Pacemaker Action Potentials and Tension .....	104
18. Superimposed Action Potentials During Ryanodine Administration .....	106

<u>Figure</u>	<u>Page</u>
19. Effect of Bay K 8644 in the Presence of Ryanodine .....	108
20. Effect of Cesium in the Presence of Ryanodine .....	109
21. Voltage and Tension Records of a Typical Cyclic Bradycardia .....	111
22. Beat to Beat Changes in Spontaneous Cycle Length and Maximum Diastolic Potentials .....	112
23. Cyclic Bradycardia Induced by High $[Ca]_o$ .....	115
24. Effect of Acetylcholine on Cyclic Bradycardias .....	117
25. Effect of Electrical Pacing of a Dysrhythmic Eustachian Ridge .....	119
26. Effect of 5.4 mM $[Ca]_o$ on a Dysrhythmic Eustachian Ridge .....	120
27. Effect of Norepinephrine on Cyclic Bradycardias .....	122
28. Ryanodine Induced Bradycardia .....	123
29. $P_{Na}/P_K$ Ratio With and Without Acetylcholine .....	125
30. Subsidiary Pacemaker Automaticity is Resistant to High $[K]_o$ .....	128
31. Initiation of Activity with Norepinephrine and Acetylcholine: Different Effects of Ryanodine .....	131
32. Initiation of Activity with Dibutyryl cAMP .....	133
33. Initiation of Activity with Bay K 8644 .....	134
34. Initiation of Activity with Low Sodium .....	137

## CHAPTER I

### INTRODUCTION

Previous viewpoints on the hierarchy of pacemaker activity, claimed that sites within the atrioventricular (AV) node acquired the primary role after the sinoatrial (SA) node was suppressed (257,536,537). This perspective continued until the late 1970's, when investigations by two separate laboratories found contradicting evidence. Sealy and associates (464,466,467) and Randall and associates (149,178,267,268,420-422,444) demonstrated that after SA node excision in the canine model, the permanent subsidiary pacemaker that emerged was located still within the right atrium. Jones and coworkers (267,268) systematically mapped the site of these pacemakers and found them to lie at the junction of the inferior vena cava (IVC) and the posterior wall of the right atrium. It was observed that atrial subsidiary pacemakers (ASPs) exhibited significantly slower rates and a greater overdrive suppression than the SA node (420), and were under autonomic regulation (149,332,420). An in vitro model of the canine ASPs was developed, and reinforced the above results using extracellular and intracellular techniques (443,444). Furthermore, Rozanski and Lipsius (442) demonstrated that fibers within this preparation can generate triggered activity. The results of these studies suggested a revision in the hierarchy of supraventricular pacemakers, as well as demonstrated the possibility that ASPs may be a focus for atrial dysrhythmias.

Intracellular recordings of ASP action potentials displayed prominent diastolic depolarization, a significantly lower maximum diastolic potential and peak upstroke velocity when compared to surrounding atrial muscle (442). However, an analysis of the

cellular electrophysiological mechanisms responsible for this subsidiary pacemaker automaticity have yet to be performed. Preliminary experiments revealed that the same region of the cat right atrium beat spontaneously. In addition, this tissue was thinner, more prominent, and more stable for intracellular electrode experiments than that found in the dog. As a result, the cat right atrial model was chosen to study the ASP mechanisms. This dissertation proposes to develop an in vitro model of the cat ASPs. Modifications of ionic composition of Tyrode's solution and/or applications of specifically-acting pharmacological agents will allow the study of possible mechanisms of subsidiary pacemaker automaticity. The isolated in vitro preparation provides a method to selectively study these pacemakers in a controlled extracellular environment.

The Eustachian ridge (ER) of the dog, located at the junction of the IVC and right atrium, was ultrastructurally described by James and associates to be comprised of 6 cellular types, one of which was labelled as P-cells for their similarity to P-cells found in the SA node (473). Sherf and James (473) postulated that cells within the internodal pathways (including the ER) may exhibit automaticity, however no recordings were attempted. The ultrastructure of the cat ER has not been described. Therefore in a combined anatomical and physiological study, a structure-function relationship will be completed for the ER in comparison to cat SA node. Although there have been several morphological studies of SA node in different animals, at the onset of this study, there had yet to be published any ultrastructural description of the cat SA node. By the conclusion of this investigation however, to the best of our knowledge, one anatomical study of the cat SA node was published (397). Therefore, this work will also provide some of the first structure-function information on cat SA node.

In several experiments the ER was quiescent after isolation yet could initiate activity by slight alterations in ionic concentrations or by specific pharmacologic agents. The mechanisms of this pacemaker initiation also will be investigated.

Therefore the purpose of this investigation is to: 1) develop an in vitro model to study right atrial subsidiary pacemaker function, 2) analyze the electrophysiological mechanisms responsible for atrial subsidiary pacemaker automaticity, 3) describe the ultrastructural characteristics of atrial subsidiary pacemaker fibers, and 4) determine fundamental mechanisms of subsidiary pacemaker initiation.



## CHAPTER II

### LITERATURE REVIEW

#### A. THE ORIGIN OF THE HEARTBEAT AND ITS HIERARCHY

##### 1. Sinus Node.

In an electrophysiologic investigation of impulse generation of the heart, one must begin by locating the site of the impulse generator. Methods of applying direct stimuli to specific locales were first achieved by Erlanger and Blackman (147) in 1907. By regional clamping, cutting, torsion or crushing, the only site found to consistently exhibit rate modification was the junctional region between the great veins and the right atrium. Only a few months prior, Keith and Flack (286) found morphologic evidence from several mammalian species including humans that a small region of cells at the junction of the superior vena cava (SVC) and the right atrium were similar in structure to fibers found by Tawara (504) and Aschoff (10) in the atrioventricular (AV) node. Specifically, Keith and Flack (286) found cells resembling embryonic fibers, which had less fibrillar content giving them a pale appearance in contrast to atrial muscle cells. In addition, the fibers were not aligned in a parallel manner as typical atrial or ventricular muscle.

It wasn't until 1910 that the first electrical manipulations were used to firmly reinforce this site of primary pacemaker activity. Lewis et al. (320) placed a small trout hook on the tip of several electrodes that were attached to specific areas of either the left or right atrium. Small induction shocks were delivered to the heart via these electrodes while the resulting electrical complex was continuously monitored. Lewis

believed an artificial electrical impulse activating only at the precise spot of the pacemaker could generate an electrical waveform that was similar to that produced spontaneously. His findings consistently demonstrated that only shocks delivered to the right atrial inlet of the SVC could generate closely similar, if not identical, waveforms. Importantly, this was also the first direct evidence of the intimate association between electrical and mechanical events. Although Lewis associated his evidence with the work of Keith and Flack, he had not yet obtained any direct histologic evidence that these sites were within the SA node.

Later in the same year, Lewis (319), and Wybauw (586) separately developed a second galvanometric method of localizing the pacemaker. Each mapped the surface of the right atrium for the site of primary (or earliest) electrical negativity. Both obtained the same result; that the site of the primary pacemaker was at the junction of right atrium and the SVC. Lewis (319), had one important addition in their paper. Lewis's coworkers were from Keith's laboratory and had histologically examined the tissues that demonstrated the primary negativity. Invariably, the site lay directly over the sinoatrial (SA) node with a propensity of being toward the cephalic end.

In the next several years, experiments were focused on pacemakers outside the SA node (subsidiary pacemakers). Jaeger (250) selectively cauterized the entire region of the SA node and found that the heart continued beating with only a slight change in rate. Erlanger and Blackman (147) had similar results 3 years earlier, but their ablation techniques were attempts to find the primary not the subsidiary pacemakers.

## 2. Subsidiary Pacemakers.

### a. In Vivo - General History

Similar to Jaeger, Brandenburg and Hoffman (56) and Zahn (595), either physically clamped or burned the SA node. Again, the heart continued to beat, although

this new site of activity originated within the atria (by ECG recordings), it was not pinpointed by the method of primary negativity. In 1914, Meek and Eyster (357) identified the SA node by initial electric negativity and then observed the effects of directly and reversibly inhibiting the pacemakers at this site. They stitched several recording electrodes on the surface of the heart to obtain a general region of where the pacemaker would shift. Vagal stimulation by tetanizing currents, ice pencils, ethyl chloride spray, or selective KCl injection changed the site of dominant pacemaker activity to a lower region within the specialized tissue. Weak vagal stimulation or application of local cold was found to shift the pacemaker to a more caudal region within the SA node. However, either stronger vagal stimuli or more diffuse cooling of the SA node by ethyl chloride spray caused the pacemaker to relocate, usually in the AV node. Interestingly, the method used for locating the site of subsidiary pacemaker activity was by a comparison of electrical records from 4 stationary electrodes; three vertically arranged within the SA node and the fourth electrode placed by the AV node.

Two important considerations must be introduced at this point, both of which were seemingly ignored and subsequently caused over a half century to pass before the correct hierarchy of pacemakers was established. First, the site of the subsidiary pacemaker found by Meek and Eyster was never systematically mapped (357). The pacemaker was considered to be residing in the AV node when the fixed electrode in AV region registered its electrical activity prior to the electrodes within the SA node. The area of tissue that could cause this electrical event certainly may have been within the AV node, yet it would also include a relatively large area of adjacent tissue. Second, in an experiment after KCl injection the pacemaker although close to the electrodes, did not seem to reside either in the SA node or the AV node (357). The nearest identifiable structure in the heart near the entrance of the IVC was the coronary sinus, thus the name, coronary sinus rhythm. Therefore, by not systematically

mapping the new site of initial negativity after SA node suppression, the AV node became the second most important pacemaker in the heart. The region near the coronary sinus had a rhythm named after it for subsidiary pacemaker sites not found within the AV node, but near the junction of the IVC.

Eyster and Meek (150) continued their investigations of subsidiary pacemakers in the dog heart by either clamping or crushing the SA node. The pacemaker exhibiting dominance in these acute experiments was found to be either within the AV node or lie in a region surrounding the coronary sinus. The pacemakers were again grossly located using immobile surface electrodes. Although this coronary sinus rhythm occurred in 10 of 55 experiments, its average rate was faster than the rates observed of pacemakers within the AV node. Three years earlier, Eyster and Meek (356) demonstrated that isolating the SA node with surgical cuts produced AV nodal rhythm in five of eight experiments. However, if the SA node was inhibited by crushing instead of cuts, coronary sinus rhythm appeared in five of five experiments. Although it remained unclear which pacemakers were to predominate in the chronic condition, conclusions drawn from the above experiments added momentum to the belief that the AV node contained the second most dominant pacemakers.

In 1922, Eyster and Meek (151) performed the first experiments to study the effects of SA node excision on the development of a chronic subsidiary pacemaker. Following SA node excision, the site of primary negativity was systematically mapped by moving a pair of surface electrodes across the atria. These sites were determined at a time ranging from 48 hours to 97 days. Seven of ten dogs demonstrated initial AV nodal rhythms (by ECG), while three others had a shortened P-R interval and were therefore considered to have a rhythm "with its origin in the region of the coronary sinus." Five of the dogs with initial AV nodal rhythm displayed a transition to a coronary sinus rhythm. This transition occurred at varying times from 30 minutes up

to 9 days. Both dogs that did not experience a transition died spontaneously on the 5th day. The authors observed a considerable difference in the animals' health before and after the transitions. During AV nodal rhythm the animals were lethargic, easily becoming cyanotic and dyspneic with the slightest exertion. With the onset of "coronary sinus rhythm," significant improvements were readily seen. In the last seven experiments, the excised SA node was fixed and verified histologically as was the surrounding tissue at the time of death. Five of these were determined to have had complete excision, while two had residual, less than one tenth of the original nodal tissue (151).

An interesting relation became apparent on the automaticity of the three different pacemaker regions. The control SA rate averaged 115/min, the "coronary sinus rhythm" averaged 86/min, while the average AV nodal rhythm was 60/min. Meek and Eyster (151,357) concluded that the automaticity of the specialized tissues along the great veins gradually diminished in the caudal direction. In three dogs the influence of exercise on heart rate was also compared. The heart rate increased from a control (prior to SA node excision) of 140 to an average 220 in the SA node, the coronary sinus rates increased from 100 to 142, and the rate increase of rhythms originating in the AV node was essentially insignificant. Therefore, the amount of sympathetic regulation also seemed to diminish from above downward. Furthermore, they found that the coronary sinus was under more vagal control compared to the AV node. Atropine caused greater acceleration in coronary sinus rhythms than AV nodal rhythms. These experiments were reviewed in more detail since many similar experiments were included in later studies of atrial subsidiary function (267,268,420,421,444,464,466).

In 1927, Borman and McMillan (47) criticized Eyster and Meek's method of SA node destruction. They believed that the surgical excision was too rapid or traumatic an event to observe where the resulting subsidiary pacemaker originates. They repeated

the experiments using a more gradual destruction of the SA node, specifically by the implantation of radon seeds. The progressive destruction of the SA node over 30 days, was considered to parallel a more realistic progression of a disease state. Borman and Meek (48) found no permanent AV nodal rhythms with this new technique. In three of seven dogs automaticity was still generated from the SA node. In the other four animals, the initial negativity was found to be near the region of the coronary sinus (again the site was not systematically mapped). Therefore, it was concluded that no matter how acute or chronic the disease state, the pacemaker that permanently gained control was near the coronary sinus. Although the authors histologically examined the SA node region, there was no examination of the resultant subsidiary pacemaker regions.

Noteworthy is the fact that the coronary sinus region is near the AV node, and investigators have further confused the issue by considering the entire coronary sinus region to be an upper portion of the AV node. In actuality, Tawara (504), Aschoff (11), Koch (295) and Kung (305) found that in the region of the coronary sinus, nodal looking cells were in continuity with the posterior region of the AV node. Koch (295) and Kung (305) also added that this zone was infiltrated with a multitude of nerve fibers and ganglion cells. Later (252), this span of tissue was clarified as a portion of the posterior internodal pathway before it adjoins to the posterior aspect of the AV node.

In 1946, the confusion concerning this zone broadened with the statement by Sherf and Harris' (459) that "coronary sinus rhythm" was a rhythm which had its origin in the upper part of the AV node. Specifying electrocardiographic criteria for coronary sinus rhythm, they found an incidence of this rhythm to be about 13 per 10,000 in the general human population, eighty percent of which had evidence of heart disease. Experimentally they showed that a warming electrode which was directly applied to these pacemakers in the dog could reproduce the same electrocardiographic waveform

(inverted P waves in leads II and III).

Analysis of their method (459) included the placement of a thermal electrode on the "wall of the inferior vena cava" at the junction of the right atrium and pressing it to the area around the orifice of the coronary sinus. They did not appear to be aware that warming through the IVC was likely to stimulate the posterior internodal pathway preferentially. No direct histologic verification of a systematically mapped region generating subsidiary automaticity was made until 1985 (442).

A series of papers produced from James' lab used selective perfusion of parasympathomimetic agents through the sinus node artery to suppress SA node automaticity (257,259,536,537). Their conclusions from these experiments repeatedly emphasized that the AV node was the dominant subsidiary pacemaker site (257,259,536,537). "There appear to be only two major centres of automaticity in the normal canine heart, in and near the sinus node and in and near the AV junction (537)." James and coworkers (257), had never observed any stable rhythm other than AV junctional rhythm in any of their acute experiments. The obvious question arises as to why were the stable rhythms they recorded (257,259,536,537) different in location from previous investigators. It would seem that their method of SA node suppression may have unmasked a different subsidiary pacemaker.

Although the results of these investigations were certainly reliable for the subsidiary pacemakers they studied (257,259,536,537), the conclusions they reached do not appear to be justified. Their method of suppressing the SA node was not as selective as they believed. The evidence is based on four separate results that differed from previous works. First, the ECG recordings from the previous investigators (47,48,150,151,357,457-459) all recorded shifts in pacemaker dominance to a more caudal site. This was identified by either mapping the primary negativity or the finding of a normal to decreased P-R interval. Urthaler et al. (536) never demonstrated P waves;

They stated "all atrial complexes are within the ventricular complex." By ECG, they had unmasked a different subsidiary pacemaker.

Second, postmortem angiograms illustrating their perfusion technique (258,259), showed contrast material not only reaching the SA node, but also along the entire cristae terminalis extending down to the IVC by several branches. Apparently, they were suppressing a far larger area of specialized tissue throughout the region between the great veins than just the SA node at the SVC junction. More evidence of the distribution of the SA node artery will be presented later.

Third, Urthaler et al. (536), found that after SA node suppression, the subsidiary pacemaker that emerged had a rate 66% of the control SA node rate. This percent decline in rate is notably larger than all previous rates measured from coronary sinus rhythms (47,48,150,151). If one aberrant result is excluded (n=7), the acute coronary sinus rhythms had a mean rate of 79.5 % of the SA node rate (150). Furthermore coronary sinus rhythms in the chronic experiments had rates >75% of the control SA node rates (47,48,151). Eyster and Meek's observation of the gradual decline in automaticity from the anatomical position, above downward (151) suggested that James' lab had indeed suppressed the pacemakers in the entire region between the vena cava and were studying an anatomically different pacemaker based solely on its inherent rate.

Fourth, all experiments performed by James and coworkers were acute experiments (257,259,536,537). No chronic investigations were performed to see if this AV junctional pacemaker was permanent, let alone stable over a long period of time. Therefore by ECG, angiograms, rate, and all being acute experiments, they were likely studying a subsidiary pacemaker region, but not necessarily the second most important or dominant one.



b. Confirmation and Importance of  
Low Right Atrial Subsidiary Pacemakers

Sealy et al. (465), correlated the development of atrial dysrhythmias in patients after repairs of atrial secundum defects. They suggested that formation of the dysrhythmias may have been secondary to disruption of the internodal tracts. Although the presence of preferential conducting pathways (internodal tracts) to the AV node remains controversial, experimental support for this suggestion was obtained in the canine model (230). In control experiments, paced stimulations at the SA node showed almost a three-fold increase in conduction velocity in the internodal tracts compared to right atrial muscle (230). Furthermore, sequential division of the tracts resulted in a 30-50% prolongation in the P-R interval. Seventy percent of the animals exhibited an AV nodal rhythm when the stimulator was off. The remaining 30% were described to generate rhythms emanating from the region near the coronary sinus (230). This led to the suggestion that during atrial surgery, one should attempt to avoid low transection of the posterior internodal pathway and thereby preserve this region of pacemaker tissue (465). The more superior approach might therefore prevent the seriously symptomatic AV nodal rhythm.

Sealy continued investigation of atrial subsidiary pacemakers by the method of surgical exclusion of the SA node (464). This was an incision made completely transmural and circumferentially around the SA node. As the incision was made, the two cut ends were resutured in place, thus electrically isolating an island of SA node cardiac tissue. Immediately after SA node exclusion in 17 dogs, 4 maintained an atrial rhythm and 13 developed an AV nodal rhythm. The animals with AV nodal rhythm developed arrhythmias which appeared to be a competition between ectopic atrial and AV nodal foci. Twelve of the thirteen dogs stabilized into regular atrial rhythms within 3 to 15 days. Post-operative atrial rhythms beat an average of 17 beats/min

slower than the pre-operative SA node rhythm (83% of the original rate). ECG recordings demonstrated slight changes in P wave amplitude and configuration, but frequently normal P-R intervals. Systematic mapping of primary negativity was performed in five dogs 8 to 10 months post-operatively. The electrically isolated SA node region was discharging approximately 10 beats faster than the atrial rhythm. The atrial subsidiary site of earliest activation was adjacent to the coronary sinus.

Interestingly the ECGs did not correlate with some previously established criteria for coronary sinus rhythm. Hurst and Logue (233) had claimed that the P-R interval must be greater than 0.12s and there must be retrograde activation of the atria. Scherf et al. (458) stated there should be normal P-R intervals, however the P waves must be inverted in leads II, aVR, and aVF. Sealy's results (464) corresponded more closely to results of Moore et al. (364), in which there were normal P-R intervals and P wave polarity. Although mapping the site of earliest activation revealed low atrial subsidiary pacemakers, establishing this rhythm by ECG recordings does not appear to be meaningful.

Sealy and Seaber (467) performed another series of experiments on the size of exclusion of the SA node and the effects on the cardiac rhythm. In the first group of dogs, they made an incision that excluded specifically the SA node region of the heart. In a second group of dogs, the incision excluded almost the entire right atrium, leaving in continuity the atrial septum, coronary sinus, left atrium, and the inferior vena caval ostium. The first group showed stable low atrial pacemakers which emerged within two weeks of SA node exclusion. The second group however developed chronically unstable junctional rhythms. Although Sealy and Seaber left the low atrial region intact with the AV node, the low atrial region did not develop a dominant rhythm. They suggested that the atrial subsidiary pacemakers were suppressed by a factor of "summation," meaning the region lacked atrial tissue that could generate summing wavefronts.

However a more likely cause of the unstable junctional rhythms, was that the arterial blood supply to the low atrial site was interrupted. Examination of the diagrams of their incision techniques, illustrated that the entire cristae terminalis down to the inlet of the IVC was separated. Such an incision would transect branches of the SA node artery that are distributed to the inferior right atrium, and compromise the low right atrial subsidiary pacemakers. Their methods included no evidence of sparing the SA node artery.

Separate investigations of SA node excision showed similar results. In 1973, Goldberg et al. (192) studied pacemaker shifts from the dog SA node elicited by selective stellate stimulation before and after SA node excision. They found that after SA node excision, but prior to stellate stimulation, 54% of the control pacemakers were located within the posterior internodal tract region. Histologic studies of the internodal pathways already had demonstrated cells having nodal characteristics to be along the posterior internodal pathway especially within the ER and near the coronary sinus (260,262,473).

In 1978, Jones et al. (267) found that after excision of the canine SA node along with 3-4 cm of the sulcus terminalis, most developed a stable low right atrial rhythm within a few weeks. After meticulous mapping, eighty percent of the animals demonstrated pacemaker location at the junction of the IVC and posterior right atrium. Further functional investigations were performed on these ASPs to study the response to autonomic blockade and exercise (422). In twelve dogs, after SA node excision, several bipolar electrodes were sutured on the epicardial surface of the atrium. Pacemaker activity was initially unstable but within several days, a low right ASP became dominant. In addition, they found a consistent waxing and waning in frequency similar to "sinus arrhythmia" which was abolished by atropine. The increased heart rate observed during exercise was markedly reduced after administering

propranolol. They concluded from these experiments that ASPs are regulated by both sympathetic and parasympathetic divisions of the autonomic nervous system.

The results from this series of experiments are in agreement with those performed by Eyster and Meek (151), but differ from those obtained by Urthaler et al. (536,537). It was suggested that the discrepancy may have been due a nonselective suppression method used by Urthaler et al. (536,537).

Suppression of the SA node was achieved by cannulating the SA node artery and injection of eserine (536,537). However, the angiograms (258,259), as well as injections of vinylite (254), radioactive microspheres (572), and indocyanine green dye (209), consistently showed a nonselective nutrient distribution of the SA node artery. In fact, the arterial distribution included the entire region of the sulcus terminalis and the junctional region between the IVC and the right atrium (209). The subsidiary pacemaker region identified by Jones et al. (267,268) was well within the distribution of the SA node artery. Therefore, the eserine injections by Urthaler et al. (536,537) were also likely suppressing this specialized area.

### c. Coronary Sinus Rhythms

A clarification must be made about "coronary sinus rhythms." In 1922, following SA node excision in the dog, Eyster and Meek (151) also observed up to 2 weeks of unstable junctional rhythms. Eventually a stable dominant atrial pacemaker emerged that was mapped epicardially "in the region of the coronary sinus." This region has been described in relatively vague terms over several decades. Any activity originating in this general area was given the name coronary sinus rhythm (48,150,151,356,457-459). Yet, after two similarly described methods of SA node excision, both with histological verification (151,267,268,422), the more advanced mapping technique (267,268) determined the site of earliest activation to be at the IVC-inferior right atrial junction

(a region adjacent to, but not within, the coronary sinus). Furthermore, Sealy and Seaber stated that the subsidiary pacemakers emerged from a region "low in the right atrium not far from the coronary sinus (466)." In addition, during exercise and cholinergic blockade, both Eyster and Meek (151) and Randall et al. (422) showed similar effects on the subsidiary pacemakers (151,422).

In fact, thermal probe stimulation on the endocardial surface of the coronary sinus in situ generated AV nodal rhythms, but failed to elicit coronary sinus rhythms (457). Coronary sinus rhythms (P waves occurring prior to the QRS) were observed only when the coronary sinus was stimulated epicardially and through the IVC (457). Thus any pacemakers warmed in this region, which now includes the region found by Jones et al.(267,268), were likely responsible for generating coronary sinus rhythms.

Isolated preparations that included the coronary sinus and several millimeters of the posterior right atrial wall generated automatic and triggered activity in the presence of norepinephrine (578). Although, automaticity was not seen in the coronary sinus after it was separated from the atrial muscle, the coronary sinus did exhibit triggered activity (578). It is not known if the coronary sinus rhythms seen in vivo were triggered rhythms, or what type of ECG waveform would have been generated by this form of activity.

However, in the chronic SA node excision or exclusion experiments, the accumulated evidence obtained from mapping, stimulation, progressive stability, spontaneous rate, and response to exercise and cholinergic blockade, all strongly suggest that the subsidiary pacemaker regions of Eyster and Meek (151), Randall and coworkers (267,268,421,422) and Sealy et al. (464,466) were emanating from a similar site.

#### d. Subsidiary Pacemaker Instability

In all studies of acute selective suppression of SA node pacemakers by either

excision or exclusion techniques, a 2-3 week instability period of junctional pacemakers was present (151,267,268,467). Thereafter, the low right atrial pacemakers emerged as the dominant stable pacemakers. Experiments by Euler et al. (149) suggested the instability may be autonomically mediated. In a typical experiment, they demonstrated a conversion from the unstable junctional rhythm to a stable atrial rhythm after injection of atropine. Since it had been previously shown that vagal effects may be more pronounced on low atrial rhythms than AV nodal rhythms (151,421), it would appear that specifically inhibiting these effects, allowed the stable dominant pacemaker to emerge. In addition, the ASP pacemakers may also be more sensitive to direct vagal influence than SA node pacemakers. Direct stimulation of the vagus during ASP automaticity caused complete asystole and prolonged recovery (332,421), compared to an earlier recovery from postvagal tachycardia seen with intact SA nodes. Furthermore, in vitro experiments on canine subsidiaries showed a significantly greater negative chronotropic effect of acetylcholine on the ASPs than the SA node pacemakers (443).

Another possible mechanism may exist for causing the instability period. Overdrive suppression initially following SA node excision caused significantly prolonged corrected recovery times. Over the next several weeks, a progressive decrease occurred until the corrected recovery times approached control values (420,444). Thus suggesting adaptations at the intracellular level may gradually occur after the pacemaker shifts. A slow rate of adjustment may explain why it was found that no instability period occurred when gradually destroying the SA node (47,48). The specific cause of such an adjustment remains unknown.

#### e. In Vitro

The information gained about mechanisms of automaticity in the atrial subsidiary pacemakers was reaching its limits with in vivo experiments. The need to isolate this

site was essential in order to study these mechanisms. Methods of isolating and maintaining selected regions of cardiac tissue stem from experiments performed by Draper and Weidmann (132). They isolated canine Purkinje fibers and placed them in a tissue chamber with continuous perfusion of oxygenated Tyrode's solution. Using Ling and Gerard (324) type microelectrodes, they recorded the first mammalian automatic action potentials. Hoffman and Cranefield (226), clarified that automatic cells were those "which show spontaneous depolarization during phase 4." This phase of the action potential is synonymous with the diastolic depolarization. They also distinguished the difference between true pacemakers and latent (subsidiary) pacemakers. A latent pacemaker is one "which shows spontaneous depolarization but which is excited by the arrival of a propagated action potential before it excites itself." In 1952, Trautwein and Zink (524) recorded the first true pacemaker action potentials from frog SA node. Three years later, the first true pacemaker action potentials from a mammalian species was recorded from the rabbit SA node by West (570). Transmembrane potentials demonstrating diastolic depolarization smoothly merging into the upstroke of the action potential serve as a reference for distinguishing characteristics of a true pacemaker. Other potentials recorded from adjacent tissue, demonstrating diastolic depolarization with a more abrupt transition into the upstroke, were indicative for subsidiary pacemakers.

Many pacemaking cells, either true or subsidiary, in the mammalian right atrium were found to be embryologically derived from within or immediately adjacent to the sinus venosus (286,542,589). This includes the entire area surrounding the SVC, venous valves, cristae terminalis, and the region of the coronary sinus (286,542,589). Paes de Carvalho (402) described these areas in the adult mammalian heart as the SA ring bundle. It was found that transmembrane potentials recorded from cells down the cristae terminalis away from the SA node had progressively less diastolic slope (401,402).

This corroborates the results of Eyster and Meek's finding of decreasing spontaneous rates (151,357). Also, the cristae terminalis had much faster conduction times, thus providing a specialized pathway towards the AV node (230,402). Because the cristae terminalis contained cells exhibiting "pacemaker potentiality" (subsidiary pacemakers), Paes de Carvalho (402) further speculated that under certain conditions pacemaker function may shift to other regions of the SA ring bundle.

Davis et al. (106) performed experiments on isolated canine atria, and found that within the cristae terminalis, cells demonstrated transmembrane action potentials similar to Purkinje fibers, exhibiting a significant plateau. Hogan and Davis (228) demonstrated that these plateau fibers exhibited diastolic depolarization with abrupt transitions into the upstroke. The rate and magnitude of diastolic depolarization could be enhanced by isoproterenol or norepinephrine (105). Furthermore, the activity of these cells was relatively resistant to elevated extracellular potassium, similar to findings reported of the SA node and AV node (110,335,550). These similar characteristics, but from different species, added support to the existence of a functionally specialized SA ring bundle. Hogan and Davis (229) later showed that plateau fibers along this tract had a 2-3 times faster conduction velocity than surrounding atrial muscle. Therefore, the posterior internodal pathway along the cristae terminalis is a faster conducting path between SA and AV nodes than via typical atrial muscle.

An in vitro right atrial preparation (90,584,585) was modified by Rozanski et al. (443,444) for studying the canine atrial subsidiary pacemakers at the IVC-right atrial junction. The isolated preparation, excluding the coronary sinus and AV node, was placed in a tissue chamber superfused with warmed oxygenated Tyrode's solution and perfused by a cannula placed within the SA node artery. A ligature was placed distally on the SA node artery midway up the sulcus terminalis, cutting off flow to the SA node



and maintaining flow to the ASP region. In the presence of  $10^{-8}$  M norepinephrine, the new site of earliest activation was mapped to a low atrial region at the junction of the IVC in 73% of preparations. The isolated preparation exhibited similar subsidiary pacemaker characteristics as those found in vivo. The atrial subsidiary pacemakers had an average spontaneous rate of 86 beats per minute, significantly slower than the average SA rate of 101 beats per minute. Increasing concentrations of norepinephrine caused significant increases in spontaneous rate of both SA node pacemakers (SNPs) and ASPs, with the ASP maximum rate significantly slower than SNPs. The ASP region was significantly more sensitive to acetylcholine than SNPs, causing a greater negative chronotropic response. Rozanski et al. (443,444) also demonstrated significant increases in corrected recovery time of ASPs versus SNPs following rapid pacing.

This in vitro right atrial preparation was also used to study the differences between the acute and chronic ASP after SA node excision (444). They found no difference in ASP sites between the acute and chronic states. Also similar to acute ASPs, the chronic ASPs were less sensitive to adrenergic stimulation and more sensitive to cholinergic stimulation than SNPs. However, the chronic ASPs were found to be less dependent than acute ASPs upon background concentrations of norepinephrine to maintain spontaneous activity. Furthermore, the chronic ASPs became less sensitive to acetylcholine and overdrive pacing with time. These results suggests that the ASPs electrophysiologically change with time.

In a later study, Rozanski and Lipsius (442) used standard intracellular microelectrode techniques to electrophysiologically characterize the pacemakers at the IVC-right atrial junction. A small section of atrial tissue was isolated from perfused right atrial preparations. This tissue had been electrophysiologically mapped and contained ASP activity after SA node artery ligation. The endocardial surface of this tissue included the ER, a vestigial IVC valve leaflet. In comparison with stimulated

atrial muscle action potentials, the ASP spontaneous action potentials exhibited a prominent diastolic depolarization, a significantly lower maximum diastolic potential, takeoff potential, overshoot, amplitude, and rate of rise. Relatively low concentrations of acetylcholine (ACh;  $<10^{-7}$  M), were found to inhibit conduction as well as decrease the diastolic depolarization, thereby decreasing spontaneous rate. It was also found that in quiescent preparations in the presence of norepinephrine, this tissue site could generate triggered activity.

#### f. Other Atrial Subsidiary Pacemaker Sites

Although selective suppression of the SA node allows the emergence of low right atrial pacemakers, other ectopic atrial pacemakers exist and may contribute to pacemaker activity as well as significant dysrhythmias. Boineau et al. (42-44) showed a multicentric pacemaker complex along the SVC-right atrial junction. Thus the functional location of primary pacemaker activity was found to exceed the histologic dimensions of the canine SA node.

After Paes de Carvalho found that cells within the cristae terminalis had diastolic depolarization (402), related findings of possible pacemaker activity were obtained by other investigators in the cristae terminalis of the rabbit heart (110,223,449) and dog heart (223,228,268). In one study, sequentially inferior excisions of the cristae terminalis produced more inferior pacemaker sites with progressively less intrinsic rates (268).

De Mello and Hoffman (110) also found that these subsidiary pacemakers were similar to the SA node when exposed to elevated levels of extracellular potassium ( $[K]_o$ ). The higher  $[K]_o$  depressed the excitability of working atrial muscle cells. Comparing resting potentials with equilibrium potentials in different  $[K]_o$ , the SA node cells were found to be significantly more depolarized compared to the calculated potential. They

suggested the difference might be that SA node cells were less permeable to  $[K]_o$  than atrial muscle. The cells within the SA node, cristae terminalis, and AV node all demonstrated the resistance to elevated  $[K]_o$  (110,228). This further suggested that the cells within the specialized tracts or SA ring bundle may all have a relatively decreased permeability to  $[K]_o$ .

Isolated tissues from the coronary sinus region in the dog have shown both automatic and triggered activity dependent on the presence of norepinephrine (578,579). Furthermore, Wit and coworkers have demonstrated sustained rhythmic activity in the mitral valve leaflet in dog (158,580), monkey (577), and human (581). Similar findings of automatic and triggered activity have been found in the tricuspid valve of dogs (16,440,441). Even areas within the left atrium at the entrance of the pulmonary veins has been shown to elicit pacemaker activity (359). All these areas have potential to generate dysrhythmias, yet it appears that the most consistent and stable pacemakers to emerge after SA node suppression are those found at the junction of the low right atrium and the IVC.

## B. STRUCTURE-FUNCTION

### I. Atrial Embryology

Many potential pacemaker sites exist within the atria. It will be shown, that many locations containing either primary or subsidiary pacemakers, can be localized to special regions within the atria. These sites, in the fully developed mammalian heart, form a SA ring bundle (45,86,261,402,517). The ring bundle includes fibers within the SA node, cristae terminalis, and internodal tracts. Recently, monoclonal antibodies were used to bind a neurofilament-like protein in myocytes along the cardiac conduction system (197). Even in the very early embryological stages of development, a ring-shaped distribution of these cells was found between the SA and AV nodes, along the cristae

terminalis and interatrial septum, and around the inflow tract of the superior and IVC (197). Recently, it has been suggested that the sites of atrial pacemaker activity and internodal conduction may have been derived from neural crest cells (196), instead of subendocardial mesoderm (554).

Within the first three weeks of mammalian development, angiogenic cell clusters coalesce and form a lumen. This plexus of newly formed small blood vessels is horseshoe-shaped (542). The most anterior central region of the horseshoe is the cardiogenic area. From either side of the horseshoe, two symmetric heart tubes approach each other and fuse. At day 23, the heart is basically a straight tube. The most caudal portion (venous pole) of the valveless heart tube is the sinus venosus and the primitive atria, also called the sinoatrial ostium. The sinus venosus is composed of right and left sinus horns (developed from the two limbs of the horseshoe) and an intermediate transverse region. Three pairs of primitive veins develop and enter laterally into the sinus venosus. This includes the omphalomesenteric, common cardinal, and umbilical veins which merge on either side to form the right and left sinus horns of the sinus venosus. About day 22, the heart tube begins to pulsate (113). It had been previously thought that the first site of electrical activity was located in pre-SA nodal tissue (540). However, pre-destined mid-ventricular tissue has recently been determined to be the actual initial automatic site (224,492). Similar to intestinal motility, blood is moved through the tube by peristaltoid motion (406,407,541). In the next few days, the pacemaking site gradually shifts caudally. Meda and Ferroni (540) and Van Mierop (540) have determined that by the 8-13th somite stage in the chick embryo (about day 24 in human development), the pacemaker site is within the sinoatrial region.

At approximately day 26, the sinus venosus and atria have passively formed two septa (right and left sinus valves) by an infolding at the sinoatrial venous inlet junction (157). Further in development, the left sinus valve is reduced in size and has blended

within the atrial septum (542). In addition, the superior portion of the right sinus valve later diminishes in size and becomes incorporated within the future region of the crista terminalis. The inferior segment of the right sinus valve persists and fuses with another passively formed septa (between the orifice of the omphalomesenteric vein and the orifice of the coronary ostium). This terminal portion of the right omphalomesenteric vein will later form the IVC-right atrial junction. Thus the inferior right sinus valve remains in the adult as the larger Eustachian valve (ER) at the opening of the IVC and the Thebesian valve at the orifice of the coronary sinus (542).

In the next several days, functionally important sites within the atria begin to emerge. The SA node becomes morphologically distinct by day 30 and is derived from the ventrolateral wall of the right sinus horn (589). Near day 35, the proximal left sinus horn and the transverse portion between the two horns form a distinct coronary sinus. The distal left sinus horn and left common cardinal vein attenuate in size and function to the point of becoming a functionless ligament (ligament of Marshall). However, the proximal left sinus horn is later found to develop into the proximal innervated portion of the AV node (6). The umbilical veins of both horns degenerate and disappear. The right sinus horn enlarges with the proximal right cardinal and omphalomesenteric veins. The anterior and posterior cardinal veins will become the SVC and the azygos vein respectively.

Areas within the adult left atrium, that were embryologically adjacent to the sinus venosus, have been shown to be capable of pacemaker function. The pulmonary veins arise from an outpocketing of tissue by the fourth week which is immediately adjacent to the transverse tissue between the two sinus horns (542). Mirowski (359) has shown that some dysrhythmias in dogs were generated from subsidiary pacemakers located adjacent to the pulmonary venous inlet of the left atrium. The regions of the adult heart that were derived embryologically from cells within or immediately

adjacent to the sinus venosus are: the SA node, crista terminalis, coronary sinus, ER, proximal portion of the AV node and the pulmonary venous-left atrial junction. Therefore, the embryologic pacemakers within the sinus venosus are associated with the adult primary and subsidiary pacemakers within these regions (105,106,229,267,268,321,358,401,402,578). The Eustachian valve or ridge, embryologically within the sinus venosus, has been shown to be within a region of the low right atrium that is associated with important subsidiary pacemaker activity (150,151,267,268,442-444,464,467).

## 2. Cellular Structure and Function

The mammalian SA node is located at the junction of the SVC and the free wall of the right atrium (286). This first morphologic investigation of the SA node described cells that were fusiform in shape with elongated nuclei. Although having the typical striated appearance, the cells were more pale than the surrounding atrial muscle tissue (286). The size of the SA node ranges with the type and size of mammal. For example, the SA node area in the cat is about 10 mm<sup>2</sup> (397), but in the pig it is about 60 mm<sup>2</sup> (394,395). Collagen fibers have been found to be densely packed throughout the SA node (286,394-397). Fetal or newborn SA node tissue have minimal collagen content, whereas adult SN tissue is predominantly composed of collagen (255,394). Opthof (394) found that within the cat and pig SN region, fibroblasts and collagen fibers make up approximately 75% - 95% of the entire volume density. Five to twenty percent of the SN volume was myocytes, with the rest being blood vessels and nerve tissue.

Recent investigations using electron microscopic techniques (87,262,342,344,394-397,513,523,553) have further described the SN to be composed primarily of three cardiac cells types. The three forms of cardiac cells include: 1) pale cells (P cells), 2) working atrial muscle cells, and 3) transitional cells (an intermediate

classification between P cells and atrial muscle cells). Abrupt transitions among cell types are typical in the dog, pig and human SA node (255,262,395). The rabbit (37,344,394,396), guinea pig (396), bat (312) or monkey (95), however, were found to be more homogeneous, having a gradual transition from P cells to the working atrial myocytes. P cells were found to be adjacent to one another or a transitional cell, but never a working atrial myocyte. Transitional cells could be found adjacent to either a P cell, transitional cell, or working atrial muscle cell (262).

For many years it had remained elusive as to which of the cardiac cell types was responsible for pacemaker activity. In an ultrastructural analysis, Trautwein and Uchinozo (523) dissected small tissue sections containing the electrophysiologically identifying pacemaker cells from the rabbit SN. They found that the majority of cardiac cells were small and spindle shaped, with sparse myofibrillar content. Direct confirmation that these were in fact the pacemakers was achieved by Taylor et al. (505). After recording transmembrane action potentials from spontaneously beating SA node preparations, intracellular ionophoretic injection of lanthanum was used to mark the true pacemaker cells (505). Electrophysiological criteria used for identification of the true pacemakers were: low maximum diastolic potential, smooth transition of the phase 4 diastolic depolarization into the the phase 0 upstroke, slow upstroke velocity, and minimal overshoot. Structural examination of these tissues demonstrated lanthanum to be almost exclusively within P cell types. The ultrastructural characteristics of the P cell (described below) is considered unique and therefore predictive of having pacemaker potential (344).

It has been estimated that the rabbit SA node has approximately 5000 typical P cells (37), while in the cat at most 2000, and the guinea pig with only 1000. Furthermore, some SA node preparations contained about 300 cells and still demonstrated ordinary pacemaking function (397). This suggests that normal

pacemaker function of the SA can be maintained with relatively few numbers of automatic cells.

#### a. Glycocalyx and Cell Membrane

Mammalian P cells are relatively small in diameter (5-7  $\mu$ ; (262,394,395,397)) in comparison with atrial muscle cells (10-20  $\mu$ ), and are spindle shaped (longitudinal axis of 20-40  $\mu$ ; (87,342,397)). P cells are grouped in grapelike clusters that are surrounded by a basement membrane or glycocalyx (262), ranging in thickness from 40 - 500 Å (171,262,353). The glycocalyx is an electron dense matrix rich in polysaccharides and acidic residues (21,231). There is evidence that this matrix may be an important modulator of cellular calcium permeability (309). Calcium-free perfusion (100), hypoxic (213) or ischemic conditions (266) cause disruption of the glycocalyx, all of which have been shown to increase intracellular calcium concentration (291,316). Therefore the glycocalyx may serve as an extracellular calcium buffer (310).

#### b. Caveolae or T-tubules

Along the cell membrane numerous caveolae or invaginations (previously called pinocytotic vesicles) are evident. The caveolae are more numerous at regions where cells are not closely apposed to one another. Numerous caveolae are present in the mammalian SA node (343,395-397). Caveolae are far more abundant in the SA node P-cells than in atrial muscle (262). The presence of caveolae greatly increases the sarcolemmal surface area (317,343). In rat atria, the amount of caveolae has been found to be inversely proportional to the complexity of the T-tubules. Atrial muscle cells lacking a T-system contained abundant caveolae, conversely other atrial cells with a highly developed T-system had almost no caveolae (169). In cat SA node P-cells (397) or in amphibian hearts (189), no T-tubules are evident, yet the sarcolemma is abundant in caveolae. These findings suggest caveolae are either a rudimentary form of T-tubules



or that T-tubules are formed by caveolar fusion (165,166,168,249,365).

Along the sarcolemma of atrial muscle cells small T-tubular invaginations begin near the Z-band level (169,365). The T-tubules range from 350-1000 Å in diameter and the basement membrane remains continuous within the tubule. T-tubules quickly branch, becoming smaller in diameter (483), tortuous and longitudinally oriented (169). There is a large diversity in the extent of T-tubules within atrial muscle cells among the different species. Mouse atrial cells have an elaborate T-tubular system, while evidence of T-tubules in cat atria was relatively scarce (353). Rat atria demonstrated a combination, cells were either found with an extensive T-tubular system, or devoid of any system (169). Furthermore, atrial cells without T-tubules were generally located toward the endocardial surface (482).

In comparison to ventricular cells, atrial cells were found to have a less complex system (13,159,353). Of note is the fact that twice as many right atrial cells generally are found without a T-system than left atrial cells (49). These findings suggest that cells without T-tubules (less cellular membrane capacitance) were part of the atrial conducting system (49,483,487). This is further supported by the finding that the distribution of cells lacking T-tubules tends to occur along the internodal tracts (45,86,261,402,517,553).

### c. Nucleus

The nucleus, is generally located near the center of the cell, is ovoid or fusiform in shape (368). The nuclear chromatin is enclosed within a nuclear membrane which is interrupted periodically by nuclear pores. It is hypothesized that the pores serve to allow selective exchange between the nucleus and cytoplasm (155).

#### d. Myofibrils

Myofibrils of P cells, composed of actin and myosin filaments, combine in a specialized orientation called sarcomeres. In mammalian SA node studies, 15% to 36% of cell volume (nuclear volume excluded) was filled with myofibrillar material in SA node studies of various mammals (342,394,396,397). This was significantly less than the corresponding atrial muscle (48% - 53%) and therefore accounts for the more pale appearance of the SA node (286,342,344,394,396,397).

An interesting correlation was found between myofibrillar density and primary pacemaker activity. By extracellular ionophoretic marking, the dominant pacemaker activity in rabbit SA node was localized to the region of cells with the least myofibrillar density (344). These results were confirmed in other mammalian species (396,397). Furthermore, it has been demonstrated that regions of cells with the least cellular density of myofilaments was associated with the lowest rate of rise in the action potential upstroke (344). Within individual SA node P cells, the myofibrils were randomly oriented. Transitional cells also exhibit this apparent random orientation (396,397), however the myofibrillar density is intermediate of P cells and atrial muscle cells.

The density of myofilaments seen in atrial muscle cells are less than ventricular cells (365). The fibers are arranged in sarcomeres and are aligned parallel to the longitudinal axis of the cell (353). Typically, there is a perinuclear region absent of myofilaments (365).

#### e. Mitochondria

Mitochondria are small membrane bound organelles that are closely apposed to the myofilaments. Mitochondria have important function in energy maintenance through oxidative phosphorylation, and act as an important intracellular calcium buffer

(311). The inner mitochondrial membrane has convoluted folds that make-up the mitochondrial cristae (353). P cells contain relatively few mitochondria in comparison to working atrial myocytes, possibly related to the lack of contractile material and function. They are randomly dispersed throughout the cytosol. However, in atrial muscle the mitochondria are found between the densely packed myofibrils and just beneath the plasma membrane. Although their sizes in P-cells and atrial myocytes are similar (ranging from 0.5 to 1.0  $\mu$ ), P-cell mitochondria have less intricate internal cristae structure than atrial muscle (262).

#### f. Sarcoplasmic Reticulum

The endoplasmic reticulum within cardiac cells form a fine network of tubules 200-600 Å in diameter which are in direct continuity with the nuclear membrane (483). Their membrane surface is generally devoid of ribosomes (typical of smooth endoplasmic reticulum) and has been labeled the sarcoplasmic reticulum (155). The tubules of the sarcoplasmic reticulum (SR) are in close proximity of the sarcolemma and myofibrils. Portions of the SR network that are in close apposition with the cell membrane (within 150 -200 Å) or T-tubules are termed subsarcolemmal cisternae or junctional SR (155,415). Because P-cells of the SA node lack a T-tubular system (262,553), their junctional SR refer only to SR apposed to the sarcolemma. Junctional SR appear as flattened saccules (516,553), and are rarely found more than 1 micron from the myofilaments of the I band (413). Free SR tubules, 200-600 Å in diameter, are found deeper within the cell. They form a fine network among myofilament bundles and mitochondria (155). Spheroidal vesicles (700-1100 Å in diameter) called corbular SR are coupled to free SR tubules via peduncles (484). Corbular vesicles tend to be located mostly near Z-bands. Both junctional and corbular SR contain an electron opaque substance, whereas the free SR appears lucent (155,167,484,512). Immunocytochemical studies have demonstrated a preferential localization of

$\text{Ca}^{++}\text{Mg}^{++}\text{ATPase}$  in free SR (271,275) and calsequestrin in the junctional and corbular SR (271-274). This suggests different forms of SR have different functions: junctional and corbular SR serve in calcium storage and release (514,571), whereas the free SR is responsible for calcium uptake (271-274).

### g. Intercellular Connections

#### i) Intercalated Discs

Intercalated discs are localized regions of intercellular connections that include desmosomes (macula adherens), intermediate junctions (fascia adherens), and nexuses. In general, most intercalated discs are associated with end-to-end connections (154,351,480). However, intercalated discs have also been found to make side-to-side contacts between cells (207,220,352). At the intercalated disc, the ends of cells interdigitate with one another resulting in a zig-zag appearance. Thus the intercalated discs are divided into transverse and longitudinal segments (261). Most intercalated discs are associated with a terminal Z-line of the myofilaments (365). Although they are abundant in atrial muscle and transitional cells, discs are seldomly observed between SA node P cells (95,255,262).

#### ii) Desmosomes (Macula Adherens)

Desmosomes are an apposing pair of thickened, electron dense round spots of plasma membrane between two cells. The thickening is due to the desmosome being a site for the attachment of cytoplasmic tonofilaments. These slender filaments have been found to connect with other desmosomes and may function as a cytoskeleton (353). Dimensions in the dog and man are 1000 Å along the plane of the plasma membrane and 700-900 Å in thickness (perpendicular to the plane of the plasma membrane). Intercellular distances at these sites are approximately 200 Å (261) filled with a

granular amorphous material. In the SN, connections between cells predominantly consist of scattered desmosomes (262). In the transition to atrial muscle cells, desmosomes become numerous, and more frequent nexal connections appear.

### iii) Intermediate Junctions (Fascia Adherens)

Similar to desmosomes, the intercellular gap distance of intermediate junctions is approximately 200 Å and filled with a dense amorphous material. The actin filaments of the terminal I bands are found to insert into the filamentous mat. These myofibrillar insertion plaques are the point at which tension is generated during cell shortening (261,368). However, in the SA node the myofibrils are scarce and the number of intermediate junctions is proportional to the number of myofibrils (261). When intercalated discs are present, intermediate junctions constitute a major part of the transverse sections of the zig-zag (483). Therefore, intermediate junctions have been ascribed the function of intercellular adhesion (351,483).

### iv) Nexal Connections

Nexal connections are the sites of closest apposition of two cell membranes. The junctions are regions of secure cohesion (133,284,369). Although sparse in P-cells, they are abundant between atrial muscle cells. These sites have been suggested to be regions of low electrical resistance between cells (107,108,114,119,120,333,334). It was also thought that the nexus was a site of membrane fusion between cells (15,284). Later, it was found that there was actually a small 20 Å gap between cells by utilizing a different staining technique (433).

McNutt (351) found hexagonal arrays of small pits on the inner face of the nexal membranes. These pits were found to be intercellular channels (493). Recently, single channel electrical events have been recorded across gap junctions (75). The nexus and

therefore electrical coupling has been found to be sensitive to intracellular divalent cation levels (101,107,109,115,411). Therefore, besides intercellular cohesion, the nexus is likely a site of low electrical resistance. Although nexal connections have been observed in the mammalian SA node, they have not been quantitated due their sparseness (394,396). Importantly, it has been calculated that just one nexal connection between P cells would be enough to maintain synchronous pacemaker activity (112).

Description of smaller organelles such as centrioles, lysosomes, cytoplasmic granules, and Golgi complexes are not relevant to the present discussion.

### 3. Internodal Tracts

In the first morphologic description of the SA node by Keith and Flack, a possible specialized pathway to the AV node was also suggested (286). Three years later, Keith retracted this proposal (287). To this day, the controversy of the existence of internodal pathways has continued. In a histological study of the AV node, Baird and Robb (14) suggested that no specialized tracts led into the AV node. However, James (253) described three bundles of parallel aligned myocytes that adjoined the AV node. Similar observations were reported by Truex and Smythe (525) and Anderson et al. (4). It has since been suggested that the anterior, middle and posterior internodal tracts are preferential electrical conducting pathways between the SA and AV node (405,453,473,503,543,553,558,587). Recently, another extensive histologic study also confirmed the existence of three distinct bundles converging on the AV node (418).

The anterior internodal tract arises from the superior end of the SA node and loops around the SVC. After sending a bundle branch into the left atrium (Bachmann's bundle), the tract extends down the anterior portion of the interatrial septum, and enters the anterior region of the AV node (252).

The middle internodal tract arises from the inferior portion of the SA node and immediately curves behind the SVC. The pathway then courses down the dorsal portion of the interatrial septum and converges onto the middle superior region of the AV node (553).

The posterior internodal tract originates from the posterior edge of the SA node and enters directly into the crista terminalis. Small fan-like branches project laterally over the dorsal right atrium. The bundle that continues down the crista terminalis into the ER or valve, finally reaches the posterior margin of the AV node by traversing the coronary sinus (252,253,553).

Ultrastructurally in dog and man, all three internodal pathways show similar heterogeneity, being composed of at least five cell types (473). P cells were frequently seen dispersed throughout the tracts. P cells, most similar to SA node P cells, were found in the ER of the posterior internodal tract (473). The anterior internodal pathway demonstrated clusters of P cells similar to SA node P cells. However only individual P cells were observed within the ER (473). Similar to the SA node, P cells were found to be adjacent to either another P cell or a transitional cells. Gradual transitions to atrial muscle cells were typically seen (473,553).

Transitional cells as described above, have been further subdivided anatomically (473) into slender and broad types. The distinction is that slender transitional cells have both a shorter length and diameter relative to the broad types. Cell types larger than transitional cells are subdivided into myofibrillar rich and poor cells. The myofibrillar rich cells are the atrial working myocytes, as have been described above. The myofibrillar poor cells have taken on two names, Purkinje-like (252), or intercalated clear cells (553). They are large in diameter, similar to working atrial myocytes, but are sparse in myofibrillar content. Although smaller than ventricular Purkinje fibers, these cells share other similarities, including a very pale appearance and an absence of T-

tubules (473,553).

A sixth cell type, the ameoboid cell was identified in the ER (473). This cell type had several unique characteristics. The shape as the name implies, was ameoboid with several pseudopodic projections. The pseudopods were filled with electron-opaque granules. These cells had abundant myofibrillar material, numerous mitochondria, and a multilobular nucleus. Although the accumulated anatomic evidence suggest 3 pathways, electrophysiological verification has been more controversial. The anatomical pathways have demonstrated high conduction rates (42,195,222,230), and plateau action potentials with rapid rates of depolarization (228,229). Furthermore, Holsinger et al. (230) showed that transection of the anatomical paths caused an internodal conduction delay. However, others have reported no such functional evidence and that wavefronts over broad areas propagated to the AV node (263,486).

### C. CELLULAR ELECTROPHYSIOLOGY OF PACEMAKER ACTIVITY

#### 1. The Heart as an Oscillator

An oscillator is a system that exhibits a cyclic or rhythmic change in a measurable quantity, which has a relatively constant waveform (172). There are numerous examples of biological oscillators, but the one most investigated is probably the heart. The heart, as an entire organ, oscillates or contracts rhythmically. Over three and a half centuries have passed since William Harvey found that the heart was made up of even smaller oscillators (210). While observing the rhythmic nature of fish and animal hearts, he noted that even small isolated sections of heart tissue could contract rhythmically (210). It has since been well established that the oscillatory nature of this multicellular organ is due to the synchronicity of its cellular oscillators. In general, cellular oscillators are of two distinct types, cytoplasmic or membrane oscillators (28). The membrane oscillators are further subdivided into metabolic and ionic flux oscillators (28). Thus,



the electrical activity of cardiac cells are considered to be an oscillation of ionic flux across the membrane.

In any biological system, there are at least three essential elements required to generate oscillations. The components are 1) an excitatory drive, 2) a restorative process, and 3) an inertial element (delay of action) which allows for an overshoot of a steady state value (172). Cardiac cells are electrically excitable. Action potentials are elicited by either an internal or external stimulus that causes the membrane potential to reach threshold. Surpassing the threshold potential results in a large inward flux of cations that rapidly depolarizes the cell. Following the depolarization, the cell repolarizes (the restorative process) after some delay from the excitatory event. However, only pacemaker cells have the first essential element: an internal excitatory drive to reach the threshold potential. The pacemaker cells are unique, they achieve the threshold potential by mechanisms which cause a diastolic depolarization of the membrane potential.

Engelmann (146) hypothesized that the heart's rhythmic activity was due to an increased sensitivity to a constant weak internal stimulus throughout diastole. Indirect confirmation of this process was obtained by extracellular potential measurements that showed slow voltage changes during diastole in the snail heart (9) and frog sinus venosus (54). The first direct confirmation was made by Draper and Weidman (132). Using intracellular microelectrodes to record transmembrane potentials, they observed a slow diastolic depolarization in Purkinje pacemaker cells. Similar diastolic depolarizations were soon found in the primary pacemakers of amphibian hearts (55,524) and in the SA node of mammalian hearts (570). Diastolic depolarizations have since been recorded in many types of cardiac pacemakers (40,62,98,214,222,336,401,440,442,580).

Diastolic depolarization is common to triggered and automatic activity which may

be experimentally difficult to differentiate. Triggered activity and automatic (spontaneous) activity can generate sustained rhythmic activity (577). Triggered activity is rhythmic activity initiated by one or more driven action potentials, such that a quiescent fiber remains quiescent unless driven by an action potential (577). Automaticity, on the other hand, is activity which occurs without the necessity of a prior action potential.

The delayed afterdepolarization observed in triggered activity is caused by events (described below) during the previous action potential (8,527,577). According to Glass and Mackey (190), fibers exhibiting triggered activity have bistability. A stable steady-state resting membrane potential or a stable oscillatory activity can be observed, depending on the immediate history of its activity. Thus, if left undisturbed from external influences, a quiescent fiber will remain quiescent or a rhythmically active fiber will remain rhythmically active. One method to distinguish triggered from automatic activity involves characteristic differences arising from single pulse voltage stimulations at different points in the cycle (phases) of the oscillation (190). Single pulse stimulations of an oscillator causes phase shifts (permanent advances or delays) of the oscillatory cycle (575).

Theoretically, it has been determined that a stimulus delivered within a narrow range of phases and of a specific strength can completely stop (annihilate) the oscillator (200,575). However, only the triggered oscillatory activity has this stable second state (resting membrane potential), also termed a black hole (190,576). Theoretically, true automatic oscillators have only an unstable singular point, a singularity, that would cause annihilation (190,576). Experimentally, it is impossible to annihilate this automatic biological oscillator, due to the instability of the singularity (190). The smallest noise will start the voltage back into oscillations again. Therefore if one is to distinguish between triggered activity and spontaneous activity, one should be able to

experimentally annihilate a triggered rhythm but not an automatic one. In fact, Wit and Cranefield (577) showed annihilation of a triggered activity with a single pulse in a simian mitral valve preparation.

Jalife and Antzelevitch (251) were able to annihilate pacemaker activity in the SA node, which has been considered to be a site of automatic pacemakers (99). However, Glass and Mackey (190) suggested that the annihilation of these pacemakers were performed in abnormal conditions which may have converted the automatic activity into a triggered activity. Furthermore, it was speculated that this conversion could only occur under pathological conditions (190).

Atrial subsidiary pacemakers have exhibited both automatic and triggered activity either under control solutions or an added beta adrenergic agonist (228,229,327,441-443,449,577). After SA node excision (149,267,305,420-422,444) or selective suppression (332,449), the junctional region of the inferior right atrium and IVC assumed pacemaker control in the canine model. Initial functional characteristics of these subsidiary pacemakers showed important differences from SA node pacemakers. Specifically, the atrial subsidiary pacemakers displayed a dependency of  $\beta$ -adrenergic stimulation (442,449), and an increased sensitivity to both parasympathetic stimulation (149,332,444,449) and overdrive pacing (420,449). Electrophysiological characteristics of pacemakers within this region exhibited prominent diastolic depolarization, relatively low maximum diastolic potential, and slow upstroke velocity (442). Although the differences in characteristics may have lessened after chronic control (444), disparities still existed. The mechanisms of pacemaker activity (diastolic depolarization) in these atrial subsidiary pacemakers have not been investigated.

Analysis of cellular membrane ionic flux oscillators among different cell types are generally shown to be dependent upon at least two separate channels (28). An inward current channel (usually carrying sodium and calcium) permits the excitatory

or depolarizing phase, and the delayed outward current (usually carrying potassium) restores or repolarizes the membrane potential. Active ion pumps that maintain the ionic gradient driving force would be required if an oscillator were to remain functional over an extended time (28). True or subsidiary cardiac pacemakers, whether automatic or triggered, have special currents or combination of currents that result in diastolic depolarization (99). Thus, the currents responsible for generating the diastolic depolarization are considered as pacemaker currents.

Therefore, the focus of this portion of the review will be on the cause of diastolic depolarization in cardiac pacemakers such as in the SA node. Since the pacemakers of the ER have embryologic origins similar to the SA node, it is hypothesized that these two sites share similar pacemaker mechanisms.

## 2. Mechanisms of Diastolic Depolarization

Application of the voltage clamp technique to the SA node was initially technically difficult due to its structure, but its development (240,382) has led to a long and changing course of the ionic current mechanisms involved in pacemaker activity. There are now at least 5 currents identified as contributors to the development of diastolic depolarization of the mammalian SA node. Ionic currents in general, as well as those specifically involved in diastolic depolarization, may take two forms: time dependent or time independent. Both types may contribute to the depolarization. The magnitude and the kinetics of the time dependent currents are important factors that would control pacemaker rate. However, only the magnitude is important in rate control for time independent currents (65). Examples of time independent currents are the background leak currents responsible for the level of the resting membrane potential.

a.  $P_{Na}/P_K$  ratio

The resting membrane potential (RMP) of the SA node (-40 to -60 mV) is relatively low compared to Purkinje fibers. It was hypothesized that the low RMP was a result of a higher ratio of the resting sodium and potassium permeabilities, a high  $P_{Na}/P_K$  ratio (241,490). In support of this, the SA node resting membrane potential is fairly constant with relatively large changes in extracellular potassium ( $[K]_o$ ; (380,543)). Similar findings were observed in isolated tissues of the coronary sinus (53). One possible mechanism of changing the  $P_{Na}/P_K$  ratio may be related to the level of an outward background potassium current,  $i_{K1}$  (383). In ventricular cells this current is responsible for the large inward rectification seen in the I/V relationship (386,451). However, in the SA node and crista terminalis, the  $i_{K1}$  current was found to be much less pronounced (183,386,450). Furthermore, if less  $i_{K1}$  is responsible for the decreased potassium permeability in nodal cells, then it would be expected that nodal cells would have a greater specific membrane resistance. In fact, Noma et al. (386) found over a tenfold higher resistance in SA node cells compared to ventricular cells.

Another contribution to the RMP may emanate from an inward sodium leak. If the inward  $i_f$  current (described below) contributes to the passive membrane properties, then, without a strong outward current, less negative membrane potentials would be expected (243). In fact, sudden sodium chloride removal in SA node (380,471), embryonic cell aggregates (354), or coronary sinus tissue (53) caused a large hyperpolarization of the resting membrane potential. Although sudden sodium chloride removal may cause artifactual liquid junction potentials (491), control studies showed insignificant alteration of the experimental results (354). In the embryonic cell aggregates, it was found that the hyperpolarization could be blocked by cesium, a blocker of  $i_f$  current (354). Thus two currents,  $i_f$  and  $i_{K1}$  may contribute to the low resting membrane potential. A relative decrease in  $i_{K1}$  density, would cause a relative

decrease in  $P_K$  compared to Purkinje fibers. The resultant increase in the  $P_{Na}/P_K$  ratio would, thereby, generate a more positive resting membrane potential.

Cells of similar embryonic origin, within the SA ring bundle, appear to have a relative insensitivity to moderately elevated  $[K]_o$  (53,110,335,336,440,543,549). The cells within the ER, also of similar origin, exhibit relatively low RMPs or maximum diastolic potentials (442). It therefore is hypothesized that the atrial subsidiary pacemakers have a relatively high  $P_{Na}/P_K$  ratio.

#### b. $I_K$ current

$I_K$  is a time dependent outward potassium current, with a reversal potential at approximately -90 mV (127,381). Activation of the current occurs at potentials positive to -50 mV, and further depolarizations exhibits a slight inward rectification (65,127,381,592). Therefore, this outward current is activated during the upstroke of the action potential and is major component of repolarization of the action potential to the maximum diastolic potential (68,244,476). After full repolarization, the conductance decreases, resulting in a decaying outward  $i_K$  current, which may contribute to diastolic depolarization (65,68,244,476,592). However, if there is no preceding depolarizing voltage clamp or action potential, then this current would contribute little if any to pacemaker mechanisms (65).

After measuring paracellular  $K^+$  activity ( $[K]_o$  very close to the cell), the contribution of  $i_K$  to diastolic depolarization of the SA node was challenged (348,349). If the  $i_K$  current was turned off during diastolic depolarization, it was hypothesized that the rate of change of  $[K]_o$  should also change during this time (349). However, the rate of  $[K]_o$  change remained nearly constant, and it was therefore concluded that  $i_K$  decay was not an important factor of pacemaker activity (348,349). This conclusion came under scrutiny, since the method of measuring paracellular  $[K]_o$  caused an

enlarged paracellular space (349). Mathematical computation of such a systematic error was found to skew the results toward a constant rate of change (68,377).

### c. $I_f$ current

First discovered in the SA node, the  $i_f$  current is activated by hyperpolarization and is a time dependent inward current (64,381,382,469,592). Several names have been associated with this current,  $i_h$ ,  $i_f$ , and  $i_p$  (63,349,381), for clarity, only  $i_f$  will be used. By analyzing tail currents, the reversal potential was about -25 mV, halfway between  $E_K$  and  $E_{Na}$ , and could carry both sodium and potassium ions (63,126,129,348). Activation of the  $i_f$  current begins at potentials negative to -50 mV (126,129,592). However, the maximum diastolic potential of cells within the SA node is in the range of -50 to -60 mV. Therefore, this suggests that  $i_f$  is not fully activated in the spontaneous SA node preparation (68,377). Although the current can be elicited in the SA node, its participation in pacemaker activity was questioned.

Low concentrations of cesium (1 mM) have a fairly specific blocking effect on  $i_f$  (125,129). Yet, the exposure of a spontaneously beating SA node preparation to 1 mM cesium only slightly increased the cycle length (348,385). Furthermore, a separate study evaluating relative contributions of pacemaker currents, determined that the proportion of contribution to diastolic depolarization,  $i_f:i_K$ , was approximately 1:4 (65). Thus, the voltage dependency, as well as minimal effects of cesium, suggests a minor importance for  $i_f$  in pacemaker depolarization of the SA node. Although it seems  $i_f$  may not be a major contributor to diastolic depolarization, it has been considered to be an important factor in the background inward current (243,354).

The discovery of the  $i_f$  current in the SA node led to the alteration of pacemaker mechanisms in the Purkinje fiber. This change was provoked by noticing similar characteristics between SA node pacemaker currents and barium treated Purkinje fiber

currents (122,123,129). In addition,  $i_f$  was found to be sensitive to  $[Na]_o$  in the SA node (129,388,470), similar to the previous  $i_{K2}$  current of Purkinje fibers (122,129,350). Initial studies of pacemaker activity generated in Purkinje fibers showed an increase in total membrane resistance during diastolic depolarization (568), and was suggested to be due to a decrease in potassium conductance (135,522). This was later supported by voltage clamp studies at potential levels equal to the maximum diastolic potential (544). During the clamp, brief square wave current pulses were imposed to measure total membrane conductance changes during the clamp (544). Since conductance decreased with the duration of the clamp, it was suggested that the results were due to a decreasing outward current,  $i_{K2}$ . Furthermore, the  $i_{K2}$  current exhibited a reversal potential that approximated  $E_K$ , and a sensitivity to  $[K]_o$  that resulted in a slope of 60 mV/decade change in  $[K]_o$ . Thus, leading to the conclusion that the pacemaker current in Purkinje fibers was a deactivating outward pure potassium current,  $i_{K2}$  (377,379,410,544).

Two major problems existed with this conclusion for Purkinje fiber pacemaker mechanisms. First, the apparent reversal potential of  $i_{K2}$ , although approximating  $E_K$ , was consistently more negative than the predicted Nernst potential (93,124,379,410,544). Second, the  $i_{K2}$  current might not have been a pure potassium current since it significantly depended upon the  $[Na]_o$  (122,129,350).

A reversal potential more negative than  $E_K$  led to the assumption of a local K depletion compared to the bulk concentration. For example, voltage clamp to potentials more negative to  $E_K$  would cause an inward  $i_{K1}$  potassium current. The inward flux of potassium would then deplete the intercellular cleft concentration of potassium, causing a decay in current as well as shift  $E_K$  to more negative levels. Conversely, voltage clamp to potentials positive to  $E_K$  would cause potassium accumulation in the clefts. Potassium accumulation would decrease its gradient and cause a decay of outward current. Potassium accumulation/depletion at the intercellular clefts was found to



cause significant changes in current measurements (18,128,294,347,376). Subtracting the decaying  $i_{K1}$  current enabled the inward  $i_f$  current to be unmasked (122,123). After elevating  $[K]_o$  to reduce depletion effects, or applying 5 mM barium to block  $i_{K1}$  (203,592), the total membrane conductance was remeasured (123,129). As  $i_f$  activated during the clamp, an increase in conductance was observed (123,124,129) contrary to Vassalle's (544) result. Thus, the same current,  $i_{K1}$ , determined to cause the RMP of Purkinje fibers to be more negative than SA node, was also likely masking the  $i_f$  current.

Accumulation/depletion effects from  $i_{K1}$  cannot entirely explain the overlapping current decay. In single cell patch clamps, where depletion/accumulation effects should be absent, decaying kinetics of  $i_{K1}$  were still present (78,452). However, if no depletion occurred in the multicellular preparations, then one would not expect any apparent shift in  $E_K$ . Therefore, it seems likely that a combination of channel kinetics and depletion may be responsible for the  $i_{K1}$  decay.

After blocking  $i_{K1}$  in Purkinje fibers with barium, reducing the extracellular Na shifted the  $i_f$  reversal potential to more negative levels (122,124). Shifting the reversal potential away from  $E_{Na}$  is in good agreement with sodium crossing this channel (122,124). Furthermore, the I/V relationships at differing sodium concentrations were remarkably parallel, suggesting that changing the  $[Na]_o$  did not affect the channel conductance, but only altered the driving force. This is in contrast to the effects of  $[K]_o$  on the  $i_f$  current (469). Increasing  $[K]_o$  from 3 to 36 mM shifted the reversal potential by 25 mV in the positive direction. However, the slopes of the I/V relationships were not parallel. Increasing  $[K]_o$  was found to cause greater currents, thus increasing the slope conductance (125). Therefore,  $[K]_o$  affects channel conductance as well as the driving force. It was concluded that at least both Na and K ions contribute to the  $i_f$  current (63,348).

Recently, the  $i_f$  current has also been found to be sensitively modulated by the

$[Ca]_i$  (201). Increased  $[Ca]_i$  in the physiologic range was found to depolarize the threshold of activation of  $i_f$  by more than 10 mV, therefore, further into the diastolic depolarization range (201). This would suggest that the calcium released from the SR might have a significant effect on increasing the contribution of  $i_f$  on pacemaker activity. Although cesium does not have much of a negative chronotropic effect on normal tissue (348,385), it may have more negative influence in a calcium overloaded tissue.

The cesium sensitive,  $i_f$  pacemaker current has been identified in the S-A node (63,126,129,348,385,590), Purkinje fibers (78,122,123,126,246), and atrial muscle (83,138). It has recently been suggested that  $i_f$  may also contribute to ectopic atrial pacemakers in the tricuspid valve (440). Specifically, 1 mM cesium decreased the slope of  $D_1$ , the early portion of diastolic slope (440). However, SCL was not significantly increased in that tissue.

In atrial subsidiary pacemakers of the ER, the dependency of an  $i_f$  current has not been investigated. The maximum diastolic potential of these fibers was approximately -70 mV (442), which is 10 - 20 mV more negative than typical SA node pacemakers (63,335,349,570). Because of the SA node pacemaker having a more positive diastolic membrane potential, the amount of  $i_f$  contribution was shown to be minimal. Therefore it might be expected that cesium may have more of an inhibitory effect on automaticity of the ASPs.

#### d. Calcium Currents

The slow inward current,  $i_{si}$ , is an inward current that persists in the absence of sodium ions (388,427). The current carries mainly sodium and calcium ions (428,431,518), and was shown to be responsible for the upstroke of the action potential in the SA node (62,299). Verapamil (62,297,298), D-600 a methoxy derivative of

verapamil (243,297), and Mn (97,204,205) block  $i_{\text{si}}$ .  $I_{\text{si}}$  currents recorded in the multicellular tissues show large variations in activation and inactivation kinetics (438). However, in the single cellular studies, multiple components of the  $i_{\text{si}}$  were observed, some of which exhibited kinetics 10 times faster than the multicellular results (361). One explanation of the different results obtained from the two different methods, may have been due to masking by the calcium activated transient outward current in the multicellular tissue. In support of this hypothesis, buffering intracellular calcium with EGTA, thus removing the induced outward current, caused a much faster and larger inward current (477). Another source for result differences between methods may have been related to an added series resistance that would be expected between multiple cell membranes with voltage clamp circuit (247,378). An increase in series resistance would cause artifactual slower kinetics.

Two components of the old  $i_{\text{si}}$  current have now been identified as 2 separate types of calcium channels found in atrial myocytes (19), ventricular myocytes (19,374), Purkinje cells (221), and in SA node pacemaker cells (202). The faster activating current has been labelled  $i_{\text{T}}$  or T-type, and the slower, but longer lasting current,  $i_{\text{L}}$  or L-type (374). The two calcium currents are differentiated by different holding potentials (19,202,374) and show large differences in kinetics and magnitudes.

The  $i_{\text{T}}$  current has a threshold of activation between -60 to -50 mV (202), coincident with diastolic depolarization (19,202). The activation threshold for  $i_{\text{L}}$  current is about 10 mV more positive than T-type channels (19,374). Current densities among different regions of the heart show that T-type current in the SA node is almost 10 times greater than that seen in atrial or ventricular cells (19,202,374). Therefore, it has been suggested that T-type channels contribute more to the action potential configuration in SA node pacemaker cells than to other cardiac cell types (202). Although the T-type current is much lower in magnitude than L-type current, T-type

current is active in the voltage range that contributes more to diastolic depolarization (19,202).

Both  $i_L$  and  $i_T$  currents are similar in that both can be blocked by 2 mM cobalt (19,202), and neither can be blocked by TTX (19,202,374). Although there are several similarities of the two currents, important differences do exist. Only the L-type channels are blocked by the dihydropyridines calcium channel antagonists (19,202,374) or D600 (202). Furthermore, only L-type channels are activated by the dihydropyridine calcium channel agonist, Bay K 8644 (19,202,221,374), and modulated by beta adrenergic stimulation (19). Therefore, the increased calcium current seen with increasing ATP or cAMP (242) has been shown to be a specific L-type current enhancement (529).

Attempts to find specific blocking agents of T-type channels have thus far yielded agents which only show a concentration dependent difference. For example, relatively low concentrations of either the TTX derivative, tetramethrin (0.1  $\mu\text{M}$ ), or nickel (40  $\mu\text{M}$ ) has been found to be a specific T-type channel blocker. However, larger concentrations of each have been shown to block both L and T-type channels (202). When 40  $\mu\text{M}$  Ni or 0.1  $\mu\text{M}$  tetramethrin was applied to a spontaneously beating SA node cell, the diastolic slope decreased, especially during the later half (202). Although the  $i_T$  current has significance for pacemaker activity in the SA node, the same cannot be assumed for Purkinje pacemakers since the T-type channel activation potential is too positive compared to its pacemaker voltage range (221).

In the ASPs, triggered activity was elicited in the presence of exogenous norepinephrine (442). In the presence of verapamil, stimulated action potentials were still generated, but no triggered beats could be elicited (442). It was apparent that verapamil decreased the stimulated action potential amplitude but did not prevent an all-or-none response. If we assume that verapamil had achieved block of the L-type channels during repetitive stimulation, then the upstroke of the stimulated action

potentials may suggest participation of fast sodium channels. The contribution of L-type calcium channels or fast sodium channels to the development of automatic activity in the atrial subsidiary pacemakers has not been investigated.

#### e. Sodium Calcium Exchange and SR Components

In voltage clamp studies of rabbit S-A node, Brown et al. (69), presented evidence for another component of the old  $i_{\text{si}}$  current, possibly mediated by intracellular calcium release from the sarcoplasmic reticulum. In addition, Escande et al. (148), have shown that an SR calcium-mediated component may participate in pacemaker activity recorded from abnormal, partially depolarized human atrial tissues. However, participation of such a current in atrial pacemaker automaticity may not necessarily result from an abnormal condition (69).

The calcium mediated component may be similar if not identical to mechanisms that generate the transient inward current,  $i_{\text{ti}}$ , seen in calcium overloaded states (139,279,280,282,314). Delayed afterdepolarizations, shown to be responsible for the development of triggered activity (98,577,578) are considered to be generated by  $i_{\text{ti}}$ . In fact, a recent report by Tseng and Wit (527) showed that transient inward currents were responsible for delayed afterdepolarizations recorded from atrial tissue isolated from the canine coronary sinus.

In calcium overloaded multicellular tissues, a transient or oscillatory inward current was identified (279,282,552). Similarly, in the single cell studies, when  $[\text{Ca}]_i$  is increased either by solution manipulations or SR release, an inward current is generated which is dependent on the transmembranous gradients of sodium and calcium (7,66,292,293,326,355). Furthermore, by the calcium dye, fura-2, cells demonstrating spontaneous oscillatory SR calcium release were found to have an elevated baseline of  $[\text{Ca}]_i$  (573). The synchronized oscillatory release of calcium from the sarcoplasmic

reticulum has been determined to generate the  $i_{ti}$  current as well as the concurrent after-contraction (3,191,280,301,328,574).

In calcium overloaded states, junctional sarcoplasmic reticulum of papillary muscles have been demonstrated to accumulate calcium (273). During this condition, the SR spontaneously releases calcium in multiple cardiac cell types (153,281,301,308,346,398,574). Furthermore, in single cells, it has been shown that the more synchronized as opposed to unifocal release of SR calcium, the greater the depolarizing effect (81). Membrane voltage changes such as repolarization from an action potential have been shown to aid in synchronizing the following spontaneous SR release (281,538). Thus, stimulated action potential as in triggered activity appear to be necessary in calcium overload to generate currents in the diastolic voltage range large enough to reach threshold.

The role of the SR in the generation of this current has been well established, since the transient inward current is abolished by agents (caffeine and ryanodine) that deplete SR stores of calcium (8,121,208,276,279,339,439,497,547,566). Caffeine depletes SR calcium by enhanced release (39,89) and inhibition of sequestration (29,218). Ryanodine has been shown to specifically interact with calcium release channels of the SR and thereby functionally eliminate SR calcium release (439). According to Rousseau (439), ryanodine causes a sudden increase in the open probability time of SR release channels, leading to gradual depletion of SR calcium stores. By inhibiting calcium release from the SR, ryanodine has also been shown to reduce calcium-activated outward currents in Purkinje fibers (497) and to delay inactivation of slow inward current in ventricular myocytes (362). Both ryanodine and caffeine were found to prevent triggered activity in atrial fibers from the coronary sinus (8).

The mechanism of SR calcium release generating  $i_{ti}$  has been associated with enhancement of a Na/Ca exchange current ( $i_{Na/Ca}$ ), and/or activation of a nonspecific

cation current. Sodium calcium exchange was first proposed by Reuter and Seitz (432) when they found that the flux of the two ions were interdependent. After multiple separate investigations, the ratio of exchange (stoichiometry) of ions across the sarcolemma has been approximated at 3:1,  $\text{Na}^+:\text{Ca}^{2+}$  (for reviews see (140,426,474). Thus three monovalent cations in exchange for 1 divalent cation causes the exchanger to be electrogenic. The reversal potential (370) of the exchanger ranges from -10 to about -25 mV, dependent upon concentrations of control solutions and tissues used (292,325). At the diastolic potential range, an inward current is generated by the exchanger since intracellular calcium is being exchanged for extracellular sodium.

The  $i_{\text{Ca}}$  current generated from SR release of calcium has failed to show a reversal potential with normal  $[\text{Na}]_o$  (92,279,326), and therefore is in accordance with Na/Ca exchange ( $i_{\text{Na/Ca}}$ ). The current generated in response to sudden increase in  $[\text{Ca}]_i$  would show a negative (inward) deflection, no matter which side of the reversal potential ( $E_{\text{Na/Ca}}$ ) of Na/Ca exchange that the membrane potential was voltage clamped (140,325). For example, if the membrane potential is clamped negative to  $E_{\text{Na/Ca}}$ , then the  $[\text{Ca}]_i$  surge causes the  $E_{\text{Na/Ca}}$  to shift in the positive direction away from the clamped membrane potential. The calcium induced shift of  $E_{\text{Na/Ca}}$  results in an increased driving force, causing an increased inward current (downward deflection) (140,326). However, if the membrane potential is clamped more positive to the  $E_{\text{Na/Ca}}$ , the Na/Ca exchange current reverses, outward current (3 sodium out for 1 calcium in). Importantly, a  $[\text{Ca}]_i$  surge still shifts  $E_{\text{Na/Ca}}$  to more positive levels, closer to the clamped membrane potential. Thus, the calcium induced shift of the  $E_{\text{Na/Ca}}$  now decreases the driving force, causing a decreased outward current (again a downward deflection) (140,326). By the exchanger mechanism, an  $[\text{Ca}]_i$  surge would drive this current and would be expected to cause downward deflections and not reverse direction. This is in contrast to typical channel kinetics where equilibrium potentials remain fairly constant,

and it is the voltage changes, not surges in concentration, that elicits current formation. Therefore,  $i_{\text{Na/Ca}}$  does have a predicted reversal potential given specific intracellular and extracellular sodium and calcium concentrations. But  $i_{\text{ti}}$ , which in actuality is likely the  $i_{\text{Na/Ca}}$  current during an intracellular calcium surge, causes a surge in the reversal potential ( $E_{\text{Na/Ca}}$ ) to more positive levels. Therefore voltage clamping at any potential during SR release would always show downward current deflections, due to the consistent directional change of concentration gradients. Under special conditions, however, even in normal  $[\text{Na}]_o$ , it has been hypothesized that  $i_{\text{ti}}$  may demonstrate an apparent reversal potential (140).

Another possible mechanism of the transient inward current is a calcium activated nonspecific cation channel (80,96). This current is not dependent on  $[\text{Na}]_o$  (80,96,354). The nonspecific channel can carry sodium and potassium ions preferentially, but calcium ions were also found to contribute to the current (80). However, the findings of a strong dependence of the  $i_{\text{ti}}$  current to  $[\text{Na}]_o$  and  $[\text{Ca}]_o$  in more physiologic conditions (355), and a voltage dependence of calcium extrusion (evidenced by incomplete relaxation), strongly suggested a more important role of Na/Ca exchange (355). Furthermore, coexistence of both Na/Ca exchange has been suggested (92,354). Na/Ca exchange would predominate in the more physiological presence of  $[\text{Na}]_o$ , yet the calcium activated nonspecific current would prevail in a sodium free environment (354).

ASPs from the junctional region of the IVC and inferior right atrium have demonstrated triggered activity (440,442). Development of these rhythms from quiescent preparations required norepinephrine to increase  $[\text{Ca}]_i$  (440,442). Atrial tissue from a variety of species was found to need less calcium to mediate SR release than in either ventricular or Purkinje fibers (153). It has not been investigated if an SR mediated component contributes to normal automaticity in this region.



### f. $I_{Na}$ Current

Although the fast sodium current,  $i_{Na}$ , can be elicited in mammalian SA node preparations (304,330,382,388) and in isolated nodal cells (390), it has been shown to have minor importance for diastolic depolarization (304,330,348,388,588).  $I_{Na}$  exhibits more importance in the upstroke of the action potential of atrial cells (62,438), Purkinje fibers (134), and ventricular cells (392). The minor  $i_{Na}$  component of the SA node action potential upstroke was enhanced when the maximum diastolic potential was shifted to more negative levels by acetylcholine (330). Therefore, it appears that the amount of contribution of  $i_{Na}$  to the upstroke in the SA node is voltage dependent. The atrial subsidiary pacemakers exhibited a mean maximum diastolic potential near -70 mV (442). Therefore, it is hypothesized that the atrial subsidiary pacemakers will demonstrate a relatively greater response to  $i_{Na}$  blockade by TTX.

### g. Summary

At this point in time, five currents:  $i_K$ ,  $i_f$ ,  $i_L$ ,  $i_T$ , and  $i_{Na/Ca}$  are considered to contribute to diastolic depolarization. Importantly, the relative contribution of each of the individual currents varies from preparation to preparation. In view of the definitions of triggered activity and automatic activity, one might be able to categorize the currents as either triggered currents or automatic currents. A triggered current would be a current that is activated by the upstroke or repolarization of the action potential, and generates its effect during diastolic depolarization. The  $i_{Na/Ca}$  ( $i_{ti}$  component) current would be considered as a triggered current. Automatic currents would be the  $i_f$ ,  $i_L$ , and  $i_T$  currents, since these currents exist without a prior action potential. It is hypothesized that triggered activity does not have a large enough density of automatic currents to spontaneously reach threshold. Thus a slight enhancement of an automatic current could transform a triggered focus into an automatic one.

Conversely, a slight degradation of an automatic current could transform an automatic focus into a triggered focus. Such a mechanism may have occurred in the experiments to cause annihilation in the SA node (251). Furthermore, if the  $i_{ti}$  current is enhanced by increasing  $[Ca]_i$  into an oscillatory current (i.e.  $i_{Na/Ca}$  during calcium overload), then the  $i_{ti}$  current would be apparent without a prior action potential. Thus, in this condition,  $i_{ti}$  would be a component of automatic but not triggered activity. It is speculated that through these mechanisms, slight alterations in a current intensity could significantly alter its pacemaker characteristics. For example, raising or lowering  $[Ca]_i$  would cause activation or inhibition of spontaneous SR calcium release, and therefore result in either automatic or triggered activity respectively. Similar conclusions were reached in a recent investigation of ventricular cell preparations from 24 hour infarcts (102). They demonstrated automatic and triggered activity from ventricular cells which normally do not demonstrate either of these forms of activity. Similar preparations 3-4 days post-infarct also did not exhibit this activity (102). Investigations into which currents may have been altered have yet to be performed.

In view of the increasing number of pacemaker currents over the last few years, Brown said it best: " One thing that is perhaps already clear is that there is no single pacemaker current in the SA node but that nodal pacemaking depends upon a balance of membrane currents (65)."

### 3. Autonomic Modulation of Pacemaker Activity.

Although the heart can function autonomously of neural input, it is richly innervated and sensitively modulated by both branches of the autonomic nervous system. Even in the unstressed mammal, autonomic outflow generates moderate fluctuations in the beat to beat rate (370). Virtually all rate fluctuations of normal SA node automaticity above 0.03 Hz (a change in rate over 1.8 beats/min) have been

determined to be caused by a change in autonomic input. Specifically, rate changes of more than 9 beats/min were found to be mediated solely by changes in parasympathetic influence, whereas changes less than 9 beats/minute heart were secondary to changes in both sympathetic and parasympathetic inputs (2,23,403,414). With the identification of specific transmembranous currents, the last decade has brought an enormous wealth of information on mechanisms of autonomic modulation of these currents.

### a. Adrenergic

#### i) $\beta$ -Adrenergic

Adrenergic stimulation of the heart is mediated by norepinephrine, released from sympathetic efferents, binding to either  $\alpha$  or  $\beta$  receptors. There are two forms of  $\beta$  receptors,  $\beta_1$  and  $\beta_2$ . In the ventricle, the majority of  $\beta$ -receptors on the myocytes (85%) are of the  $\beta_1$  subtype (371). However, arterioles exhibit almost exclusively  $\beta_2$  receptors (371).  $\beta_1$  receptor activation on the myocytes has been related to increased heart rate and contractility (495,564).  $\beta_2$  receptor activation on myocytes also have positive chronotropic and inotropic responses similar to  $\beta_1$  activation, although  $\beta_2$  stimulation is much weaker (12,59,60,136,238,283). The primary role of  $\beta_2$  receptors apparently is focused more on their presence in arterioles, and mediate a dilatory function in the coronary vasculature (156,404,437,593).

$\beta_1$  receptor stimulation activates adenylate cyclase and increases the formation of cAMP (73,211,373,399,530). A stimulatory G-protein has been suggested to couple the  $\beta$  receptor to adenylate cyclase (216). Increased cAMP results in activation of cAMP-dependent protein kinases, and thereby allows phosphorylation of specific intracellular proteins (198,278). One such phosphorylation activates the L-type calcium channel (278,488,520,529). It is proposed that the activation of the calcium channel by phosphorylation is a mechanism independent of the voltage gated mechanism

(429,430,489). Phosphorylated channels have an increased functional availability during a membrane depolarization (430), as well as an increased open state probability (74,77). This is in contrast to the mechanism of increased current by Bay K 8644. Bay K 8644 does not increase cAMP, and appears to increase current by prolonging the open state of the channel (217,300,529).

Another current possibly regulated by a cAMP mediated phosphorylation is the delayed rectifier  $i_K$  current. Stimulation of ventricular cells with a  $\beta_1$  agonist, forskolin, or cAMP, elicited significant increases in  $i_K$  (22,561). Furthermore, the increase was determined to be separate from a possible secondary influence of  $[Ca]_i$  (22,561). However, increased  $i_K$  also may be mediated through protein kinase C from  $\alpha_1$  receptor stimulation (511), and/or be a secondary effect of the increased  $[Ca]_i$  directly enhancing  $i_K$  (511).

Increased contractility through  $\beta$ -stimulation has been primarily related to the increased intracellular calcium from increased calcium influx through the L-type channels. Recently, additional contribution to the increased inotropy has been associated with cAMP dependent phosphorylation of phospholamban (46). Phospholamban is a SR protein that regulates the SR calcium pump (499,501). Phosphorylation of phospholamban causes significant increases in calcium transport into the SR (500,501). In addition to cAMP mediated phosphorylation of phospholamban (313,323,499,556), a calcium calmodulin-dependent phosphorylation (35,313), or a calcium activated phospholipid-dependent protein kinase phosphorylation (366), have also been shown. However, the calmodulin dependent mechanism may occur only as a supplemental pathway during high elevations of cAMP (556). The increase calcium pump activity is presumed to be the mechanism by which isoproterenol stimulation increases myocardial relaxation (323,499,555). Furthermore, the resultant increased calcium sequestration within the SR would enable an enhanced release of

calcium, causing an increased contractility (499). In addition to increased contractility, it is known that  $\beta$ -stimulation increases  $i_{Li}$  (46,527). Therefore, indirect enhancement of  $i_{Na/Ca}$  can be elicited through  $\beta$ -stimulation which had increased SR release of calcium.

Epinephrine was found to increase  $i_f$  in the SA node (63,64,67,126), atrial muscle cells (138), and Purkinje fibers (78). Similar results were obtained in experiments using isoproterenol, an almost pure  $\beta_1$  agonist, in the SA node (126,201). These results were, in part, due to a mechanism involving activation of adenylate cyclase and increased levels of cyclic AMP (201). The increased current was determined to be due to a shift of  $i_f$  activation threshold to more positive levels, similar to an increased  $[Ca]_i$  effect (126,201). However, a change in rate constants, not observed with increased  $[Ca]_i$ , was noted during  $\beta$ -stimulation of  $i_f$ , and may suggest a phosphorylation mechanism (201). Calcium was determined to have a direct effect on the channel without mediation through protein kinase C or calmodulin (201). Therefore  $i_f$  current may be enhanced by  $\beta_1$ -receptor stimulation through a secondary effect of increased calcium current, as well as a possible phosphorylation of a regulatory channel protein.

$\beta_1$  stimulation also may increase K accumulation within cardiac myocytes (143,546,557), possibly by activating the Na/K pump (118,315,408,563). However, it has also been observed that NE induced a hyperpolarization in Purkinje fibers (173) and the coronary sinus (52). It has been suggested that the effect on the resting membrane potential was due to an increased  $P_K$  (52,173). This was supported by an initial increase of K efflux in the first minute following in vivo isoproterenol infusion in pig hearts (143), but soon after, a large sustained K influx was noted. The K influx is likely mediated by increasing cAMP activating the Na/K pump, since forskolin, an adenylate cyclase activator (143) or exposure to dibutyryl cyclic AMP (408) also caused a significant K accumulation (143).

## ii) $\alpha$ -Adrenergic

Norepinephrine may also bind to myocardial  $\alpha_1$  receptors (20,72) to regulate myocardial contractility (363,460). The effects of  $\alpha$ -stimulation are due to mechanisms other than activation of adenylate cyclase (76), or elevation of cAMP levels (61). Although the mechanisms are not entirely clear, it has recently been shown that  $\alpha$  receptor stimulation increases contractility, in part, by increasing the myofibrillar protein sensitivity to calcium (144).

In addition,  $\alpha_1$  receptors are coupled to the turnover of phosphatidylinositol (71,296,461). The binding to an  $\alpha_1$  receptor activates phospholipase C, which recently has been determined to be mediated by a pertussis toxin insensitive G-protein (GTP-binding transducer protein) (494). Phospholipase C selectively hydrolyzes phosphatidylinositol (26,71,296). Two of several products of phosphatidylinositol turnover are (1,4,5)-inositol triphosphate (IP3) and diacylglycerol (DG) (26). IP3 and DG act as second messengers in the heart (26,494). Although it remains controversial if IP3 enhances SR calcium release (289,367,389), IP3 continues to be the primary hypothesized pathway for  $\alpha_1$  receptor mediated increased inotropy. DG, on the other hand, has been implicated both to enhance and inhibit SR release (for review see (27)). DG function has been shown to be mediated by activation of protein kinase C (26). Protein kinase C is capable of phosphorylating phospholamban, however this action is relatively weak compared to cAMP (322).

$\alpha_1$  receptor stimulation is also associated with activating another pathway involving G-proteins, which may be more important in chronotropic changes. Alpha adrenergic stimulation has been observed to increase automaticity in rat atria (162,163), as well as elicit both a positive chronotropic effect in about 1/3 and a negative chronotropic effect in 2/3 of canine Purkinje fibers (416,436). The different directions of rate change in Purkinje fibers has been related to the concentration of a different

specific G protein, that is pertussis toxin-sensitive (436). Higher levels of this substrate are associated with a decrease in Purkinje fiber automaticity following stimulation by phenylephrine (436). However, after inactivation of this G-protein with pertussis toxin, phenylephrine caused an increased automaticity (436). The decreased automaticity in Purkinje fibers by  $\alpha_1$ -adrenergic stimulation is likely mediated by stimulation of the Na/K pump ( $i_{\text{pump}}$ ), distinct from a cAMP activation (472). Supportive evidence for pump activation was obtained by a resultant decrease in intracellular sodium activity after  $\alpha_1$  receptor stimulation (562,596). It has been suggested that the pertussis toxin sensitive G-protein couples  $\alpha_1$  receptor stimulation to Na/K pump stimulation (472). Possibly the same pertussis toxin sensitive G-protein is now implicated in a muscarinic activation pathway that also slows automatic rate (345,412).

Rate changes secondary to phenylephrine also have been associated with a decrease in potassium conductance (363,472). Although the mechanism is not clearly established, it has been suggested that  $\alpha$ -receptor stimulation may inhibit  $i_{\text{K1}}$  (363) through a GTP regulatory protein that is insensitive to pertussis toxin (436,472). Suppression of  $i_{\text{K1}}$  by  $\alpha_1$ -stimulation in atrial and Purkinje fibers resulted in a depolarization of the membrane potential and increased net inward current during diastolic depolarization (363). Although significant  $\alpha_1$ -mediated chronotropic effects are elicited in Purkinje fibers, no chronotropic changes have been observed in the SA node (219).

### iii) Summary

In summary,  $\beta$  receptor stimulation can increase the rate of diastolic depolarization through multiple direct and indirect mechanisms. Specifically, norepinephrine will increase  $i_f$  and  $i_L$  by cAMP mediated events. Secondary to the

increased  $[Ca]_i$  from enhancing  $i_L$ , subsequent augmentation of  $i_f$  and  $i_{Na/Ca}$  would also likely occur. On the other hand,  $\alpha$  receptor stimulation activates at least 2 forms of G-proteins. The pertussis toxin sensitive G-protein may be coupled to Na/K pump to mediate the decrease in automaticity seen in Purkinje fibers. The pertussis toxin insensitive G-protein may be coupled to hydrolysis of phosphatidylinositol to mediate increased contractility and automaticity, possibly by enhancement of  $i_K$ , but inhibition of  $i_{K1}$ . It is not known if this is mediated by all the same form of pertussis toxin insensitive G-protein. Thus sympathetic discharge may affect automaticity by modulation of at least four currents in the SA node ( $i_K$ ,  $i_f$ ,  $i_L$ , and  $i_{Na/Ca}$ ) and four currents in Purkinje fibers ( $i_f$ ,  $i_{Na/Ca}$ ,  $i_{K1}$ , and  $i_{pump}$ ).

$\beta$ -adrenergic stimulation of atrial subsidiary pacemakers has been shown to have a positive chronotropic and dromotropic effect on in vivo (192,269,444) and in vitro (248,440,442) experiments. Similar propagation dependency on adrenergic stimulation has been demonstrated in other atrial sites (16,441). Furthermore, pacemakers that emerge, after SA node excision, show a dependence on  $\beta$ -adrenergic stimulation (442-444). The dependence wanes in the chronic animal experiments (444). In several in vitro experiments, true automatic pacemakers were evident without any background NE (442). NE exposure ( $2 \times 10^{-8}$  M) almost doubled the spontaneous rate, hyperpolarized the MDP, and doubled the upstroke velocity (442). From the increased diastolic depolarization, it is obvious that NE enhanced one or more of the pacemaker currents in this preparation. It is not known which currents may be responsible for this increase, if any  $\alpha$  receptor mediated effects are seen, or if any concomitant increase in contractility occurred.

#### b. Cholinergic (Muscarinic)

Acetylcholine (ACh) stimulation of muscarinic receptors exerts most of its electrophysiological effects by increasing potassium conductance (84,180,235,329,521)



by possibly opening ACh activated potassium channels (84,237,387,400,450,481). Stimulation of the muscarinic receptor activates a membrane bound G-protein (145,485) that may be directly coupled to the potassium channel,  $i_{K-ACh}$  (412,481).

The  $i_{K-ACh}$  current is time and voltage dependent (387,400). Membrane potential effects are seen within 30 msec after ACh application (387,400). The G-protein activator of  $i_{K-ACh}$  has been shown to be pertussis toxin sensitive (41,145,412,485). Administering pertussis toxin, blocks the negative chronotropic response of muscarinic stimulation, and may even result in a positive chronotropic response in atrial and SA node tissue (1,41,533).

Muscarinic stimulation is also known to inhibit adenylate cyclase (565), and therefore reduces cAMP (215,285). Suppression of adenylate cyclase is modelled as muscarinic activation of an inhibitory G-protein (131,164,215). This inhibition has been suggested to cause the decreased calcium current observed during muscarinic stimulation (161,506,519). Support of a G-protein pathway was added when it was found that pertussis toxin blocks muscarinic inhibition of adenylate cyclase (345,412). Subsequent muscarinic stimulation after toxin exposure was associated with an increase in contractility, demonstrating that a muscarinic path, possibly to phosphatidylinositol, was still functional (485).

Furthermore, muscarinic stimulation has been shown to increase  $[Na]_i$  in Purkinje fibers likely by inhibition of the Na/K pump (236,302) or an increase in sodium conductance (502). The muscarinic stimulation was also associated with increased contractility in ventricular cells (302) and Purkinje fibers, which may be related to the increased  $[Na]_i$  by altering Na/Ca exchange (303), or through hydrolysis of phosphatidylinositol (70,71). Similar to  $\alpha_1$  stimulation (322,494), muscarinic stimulation activates phospholipase C also by a pertussis toxin insensitive G-protein (345).

ACh has been found to cause an inhibition of the  $i_f$  current by shifting its

activation voltage range to more negative levels (130). The mechanism of inhibition is related to a decrease in cAMP levels (131). Recently, acetylcholine has been found to have no effect on  $i_f$  in Purkinje fibers in the absence of  $\beta$ -agonist stimulation (88). It is hypothesized that the difference seen between Purkinje fibers and SA node pacemakers, may be that Purkinje fibers have a much lower basal level of cAMP (88). Therefore, it appears that  $i_f$  is closely regulated by cAMP levels which sympathetic stimulation can increase but which is secondarily regulated by parasympathetic stimulation. In a similar vein, the cAMP enhanced  $i_K$  described above, can be antagonized by muscarinic stimulation (215).

In summary, acetylcholine can inhibit automaticity by direct activation of  $i_{K-ACh}$  and by indirect suppression of  $i_j$ ,  $i_K$ , and  $i_f$  through inhibition of adenylate cyclase. Accentuated antagonism of sympathetic activity by parasympathetic stimulation has been determined to be caused by both interneuronal and intracellular mechanism (for review see (419)). Since  $\beta_1$  stimulation activates adenylate cyclase, and muscarinic stimulation can inhibit this activation, one can now see the specific currents involved in the intracellular mechanisms of accentuated antagonism. ASPs were found to be significantly more sensitive to acetylcholine effects on automatic rate (443,444) than SA node, by producing a significant decrease in the rate of diastolic depolarization (442). In fact, the sensitivity may have been a result of accentuated antagonism, since it had been shown that the ASPs are dependent upon, as well as regulated by sympathetic stimulation (442-444). ACh was found to block propagation of activity to surrounding fibers as well as cause pacemaker shifts (442). At high concentrations of ACh ( $> 10^{-7}$  M), complete suppression of automaticity was observed, and likely were secondary to a profound hyperpolarization of the membrane potential (442).

Autonomic innervation and modulation of atrial subsidiary pacemakers has been well established (149,192,332,422,443). The effects not only alter rates of activity, but

have been associated with pacemaker shifts (51,402,421,443) as well as development of dysrhythmias (149,332,402,422). The electrophysiologic mechanisms of the autonomic modulation of atrial subsidiary pacemakers have not been investigated.

#### D. CLINICAL ATRIAL ECTOPIC DYSRHYTHMIAS

Atrial ectopic dysrhythmias are well recognized to generate clinically significant rhythm disturbances. The emergence of atrial subsidiary pacemaker activity may be related to a variety of abnormalities including congenital malformations of the heart, genetic tendencies (i.e. in collagen vascular diseases), post-surgical complications, myocardial infarcts, and aging. Seventy-five percent of the patients found with significant ECG changes significant for ectopic rhythms had heart disease of either atherosclerotic or rheumatic origin (360).

Ectopic atrial dysrhythmias, as well as all cardiac dysrhythmias, result from abnormal automaticity and/or abnormal conduction (227). Thus, the ASP emerges if there is a depression of automaticity of the SA node pacemaker as seen by cholinergic interactions (337,360), or by enhancement of automaticity of the subsidiary pacemaker through sympathetic influences (337,456,532). Another mechanism for the ASP emergence is through abnormal conduction. The most well recognized clinical example is from either atrial surgery for correction of an atrial septal defect or transposition of the great arteries (212,465).

##### 1. Ectopic Supraventricular Dysrhythmias

An infrequent form of dysrhythmia generated by an atrial subsidiary pacemaker is the ectopic supraventricular tachycardia. There are two forms of atrial tachycardias: reentrant rhythms, and ectopic pacemakers (186). The ectopic form of atrial tachycardias, although rare in adults, is found more commonly in children (184,194,455).

The incidence has been reported to occur in about 1 of every 25,000 children (184). Specific mapping to identify the site of origin has included areas near the junction of the IVC and the right atrium (106), a site well documented experimentally for subsidiary pacemaker activity (267,268,421,422,464,467).

Gillette and Garson (186) investigated treatments of reentrant atrial dysrhythmias versus ectopic atrial dysrhythmias. Although digoxin was found to be most effective for reentrant rhythms, it had little or no effect in controlling ectopic rhythms. The beta blocker propranolol was found to be effective in managing reentrant better than the ectopic types (186). Furthermore, digoxin, quinidine and procainamide also have shown minimal efficacy (212). Although verapamil may initially give good results, it is too dangerous to administer in infants due to their greater sensitivity of the drug to the SA and AV nodes (179). Recently, catheter ablation techniques (104,188,478) or encainide (212) have proved more successful in the treatment of the ectopic forms.

## 2. Surgical Trauma

Most of the atrial ectopic dysrhythmias are a result of surgical repairs in the atria near the SA node or internodal tracts. Transposition of the great arteries appears in about 9% of all congenital heart disease (288). One surgical repair, the Mustard procedure, developed in 1964 (372), involves creation of a baffle to separate the vessels. The original procedure was performed by excising the atrial septum and suturing a pericardial flap (baffle) to the atrial wall. The baffle is placed so that the pulmonary and systemic inflow are redirected to opposite ventricles (372). The suture line around the pericardial flap runs in close proximity to the the SA and atrioventricular node (597). Postoperative atrial dysrhythmias have been reported ranging from 20-90%, many of which were generated from ectopic sites (91,142,185,318,448). Many of these dysrhythmias were noted to be similar to those seen in sick sinus syndrome (141,199),

including ectopic atrial tachycardia (212).

Several studies have shown that the repair may cause damage to the SA node or its arterial supply (142,187), to any or all three internodal pathways (245,318,448,583), or direct damage to the AV node (32,57). One study stated that part of their procedure included specific resection of the ER with the tissue margins sewn over (583). In addition, partial damage has been related to suture placement that resulted in SA node artery hemorrhage, narrowing, or occlusion from intimal sclerosis (142), or fibrotic scarring within the internodal tracts (33,318). Furthermore, it was observed that just the placement and securing of the venous cannulae for the circulatory bypass, may create damage to the SA node or its artery (91,185).

After modification of the procedure, aimed at protecting the SA node and its arterial supply, a reduction of atrial dysrhythmias by up to 35% was observed (141,318,526,535). However, long term follow-up of this modified procedure noted a regression of stable SA rhythm (137). In fact, many required pacemaker implantation for symptomatic development of sick sinus syndrome (137).

Another surgical repair for transposition of the great arteries is the Senning procedure (468). Diversion of blood flow in this technique is made by reconstruction of the right atrial free wall and the interatrial septum. A conduit is made that diverts blood flow from the SVC and IVC to the mitral valve (468). Initial studies comparing the resultant postoperative dysrhythmias between the Senning and Mustard procedure showed no difference (111,341,534). Furthermore, the dysrhythmias after the Senning procedure also were shown to be similar to the sick sinus syndrome (594). The late follow-up of patients who had either the Mustard or Senning procedure showed significant degeneration of SA node stability, requiring implantation of a pacemaker in up to 10% of patients (111,534).

In an experimental study to investigate arrhythmogenesis, bipolar electrodes were

implanted in the internodal tracts of dogs (340). The Mustard and the Senning procedure produced varying degrees of damage to the anterior and posterior internodal tracts. However significant damage to the region of the posterior internodal tract was seen consistently by both techniques. In fact, it was suggested that sutures placed in the posterior internodal pathway was the likely cause of the atrioventricular block seen in some animals (340). Furthermore, a close association with the more lethal forms of AV block were also related to damage of the posterior internodal pathway (318).

Repair of atrial septal defects also have been found to develop similar postoperative dysrhythmias (36,199,391,465). As would be expected, the etiology of the dysrhythmias has been related to SA node injury during the repair (199).

Pharmacological regimens to treat atrial dysrhythmias in the postoperative infants has been restricted to digoxin. Beta blockers are contraindicated in these patients. It has been found that whatever rhythm the patients do generate, it is exquisitely sensitive to the depressant effects of the medication (212). If digoxin does not stabilize the rhythm, implantation of a pacemaker is indicated (212).

### 3. Sick Sinus Syndrome

Sick sinus syndrome is a grouping of clinical signs and symptoms secondary to a dysfunctional SA node (281). Disease involvement of the SA node directly and/or its preferential conducting pathways may result in clinically significant dysrhythmias. Disease or trauma to the arterial supply (SA node artery) of the SA node and its adjacent tissue may also result in SA node dysfunction. Furthermore, dysfunctional autonomic regulation of the SA node may affect automaticity or its conduction to generate acutely symptomatic dysrhythmias. Therefore, any dysfunction in the mechanisms that sustain or regulate the normal function or cellular integrity of the SA node may result in the sick sinus syndrome. If the dysfunction is confined to the SA

node, a pacemaker shift to an atrial subsidiary pacemaker may occur (290).

Any of the following six electrocardiographic criteria may determine the presence of sick sinus syndrome (281,290): 1) Persistent bradycardia; 2) Sinus pause or arrest with or without an emerging ectopic escape rhythm; 3) Sinoatrial exit block; 4) Chronic atrial fibrillation; 5) Insensitive atrial fibrillation to DC cardioversion; 6) Bradycardia-tachycardia syndrome. Symptomatic features of sick sinus syndrome include syncope (25-45%), dizziness, dyspnea, or chest pain (each 10-40%; (447,496)).

Two classifications of the disease have been assigned to sick sinus syndrome. Both classes have identical symptomatology, but the distinction is made by the effect of autonomic blockade (270,290). Signs and symptoms that persist after the administration of atropine and propranolol are classified as intrinsic. Conversely, if autonomic blockade abolishes the rhythm disturbance, then the classification is extrinsic. Both hypersensitive carotid sinus syndrome and orthostatic hypotension are examples of the extrinsic or autonomic mediated symptoms of sick sinus syndrome (103,510). Occasionally, both intrinsic and extrinsic forms of the syndrome may coexist in the same patient (290).

Direct involvement of SA node tissue may occur from the normal aging process. Sick sinus syndrome is a clinical entity that is normally associated with the elderly population (281,290). It has been found that with increasing age, there is an increased collagen density within the heart (117,255,424). The collagen vascular disease, amyloidosis has similar SA node infiltration as aging (255,393). Amyloid has been related to the development of significant atrial dysrhythmias including bradycardia and atrioventricular block (85).

Patients with HLA B27 associated rheumatic disorders (ankylosing spondylitis, sacroiliitis, uveitis), have shown a high incidence (2-10%; (24,375)) of atrial brady-tachy dysrhythmias, as well as all degrees of atrioventricular block (24,25,50). Development

of these forms of dysrhythmias have been linked to the diffuse increase in myocardial interstitial connective tissue (58).

Diseases that involve the arterial supply to the SA node may include polyarteritis nodosa or atherosclerosis. Polyarteritis nodosa commonly affects the medium and small sized arteries such as the coronary arteries, by causing a necrotizing inflammation (417). Furthermore, the SA node artery is frequently affected and results in atrial conduction abnormalities (256,508). Atherosclerosis involving the right coronary or left circumflex causing inferior wall infarctions commonly demonstrate SA node dysfunction (434,479).

The natural outcome of sick sinus syndrome has generally been indicated to have a good prognosis (425,454). Treatment of sick sinus syndrome has been directed at the symptomatic patient by implantation of an artificial pacemaker (290). Pharmacologic agents for use in therapy, as well as for testing, must be carefully monitored. The present function of the SA node in this disease may hazardously deteriorate in the presence of sympatholytic agents such as alpha-methyldopa and guanethidine (456). Furthermore, it should be remembered that in experimental animals, the atrial subsidiary pacemaker function showed a dependence on sympathetic stimulation (442-444). Recent clinical support of this caution has been documented for the use of propranolol in patients with sick sinus syndrome (532).

#### 4. Summary

The hierarchy of atrial pacemaker activity has been established (423). However, the ability of subsidiary pacemakers to maintain "normal cardiac rhythm" will depend on the extent of the disease, or trauma. Therefore disease entities causing a dysfunctional SA node may require atrial subsidiary pacemakers to maintain adequate cardiac function. In fact, patients with sick sinus syndrome generally remain asymptomatic until the subsidiary sites also fail (290). Furthermore, subsidiary



pacemaker failure is associated with a decline in the patient's prognosis (290). Therefore, diseases that may affect both the SA node and the atrial subsidiary pacemaker regions, such as those affecting their arterial supply (myocardial infarcts, polyarteritis nodosa, atrial surgical procedures), or diffuse tissue infiltration (amyloidosis, rheumatic disorders, aging), may cause more serious symptomatic dysrhythmias (i.e. complete AV block). One should recall the results of SAN excision experiments of Eyster and Meek (151): premature death occurred in those dogs that did not develop a transition from AV nodal rhythm to an atrial subsidiary rhythm. Thus, if the SA node is dysfunctional, it is seems clearly advantageous to maintain the integrity and function of the atrial subsidiary pacemakers.

### III. METHODS

#### A. Preparation and Experimental Set-Up

Cats (N = 154) of either sex weighing 2 to 4 kg were anesthetized with sodium pentobarbital (50 mg/kg, i.p.). A right thoracotomy was performed through the fifth intercostal space. The heart, including 2 to 3 cm of both vena cavae was quickly excised and placed into a dissecting dish containing a modified Tyrode's solution (composition is listed in Table 1) that was bubbled with 95% O<sub>2</sub>, 5% CO<sub>2</sub> and warmed to between 33-35° C. The ventricles were separated from the atria by cutting a few millimeters below the atrioventricular sulcus and across the interventricular septum. The atria were then placed into a second dissecting dish containing fresh, warmed oxygenated Tyrode's solution. The right atrium was separated from the left and opened to expose the atrial free wall. The Eustachian ridge is located on the endocardial surface, at the junction of the inferior vena cava and the posterior wall of the right atrium (Figure 1). The Eustachian ridge varied in form, appearing in some preparations as only a small raised ridge on the endocardial surface, while in others it took the form of a delicate, thin sheet of tissue resembling a valve leaflet. Approximately a 5 mm x 3 mm strip of the Eustachian ridge was carefully excised and placed into a small tissue bath (Figure 2), similar to the chamber used in studies by Gadsby et al. (175-177). This fast-flow chamber provides a method for rapidly altering the extracellular solution.

The tissue was gravity superfused with Tyrode's solution at a rate of 5 ml/min and warmed to 36 ± 0.5° C by a thermostatically controlled circulator (Haake, Model D8L). A two-path valve (Hamilton) for switching solutions was positioned very close

TABLE 1  
COMPOSITION OF TYRODE'S SOLUTION

---

NaCl	-	125.0
KCl	-	4.0
NaHCO <sub>3</sub>	-	24.0
NaH <sub>2</sub> PO <sub>4</sub>	-	1.2
CaCl <sub>2</sub>	-	1.8
MgCl <sub>2</sub>	-	1.0
Glucose	-	11.0

---

pH  $7.35 \pm 0.02^*$

Osmolarity  $293 \pm 0.9$  mOsm/L (n=5)\*\*

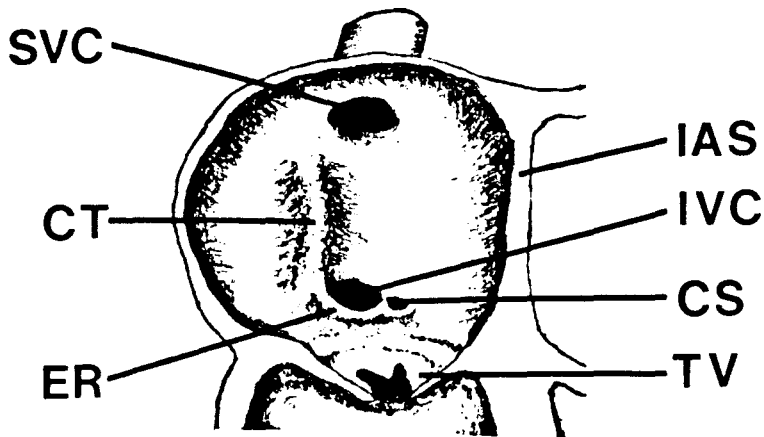
---

\*Measured by Beckman  $\Phi$  60 pH Meter

\*\*Measured by Advanced Instruments Osmometer

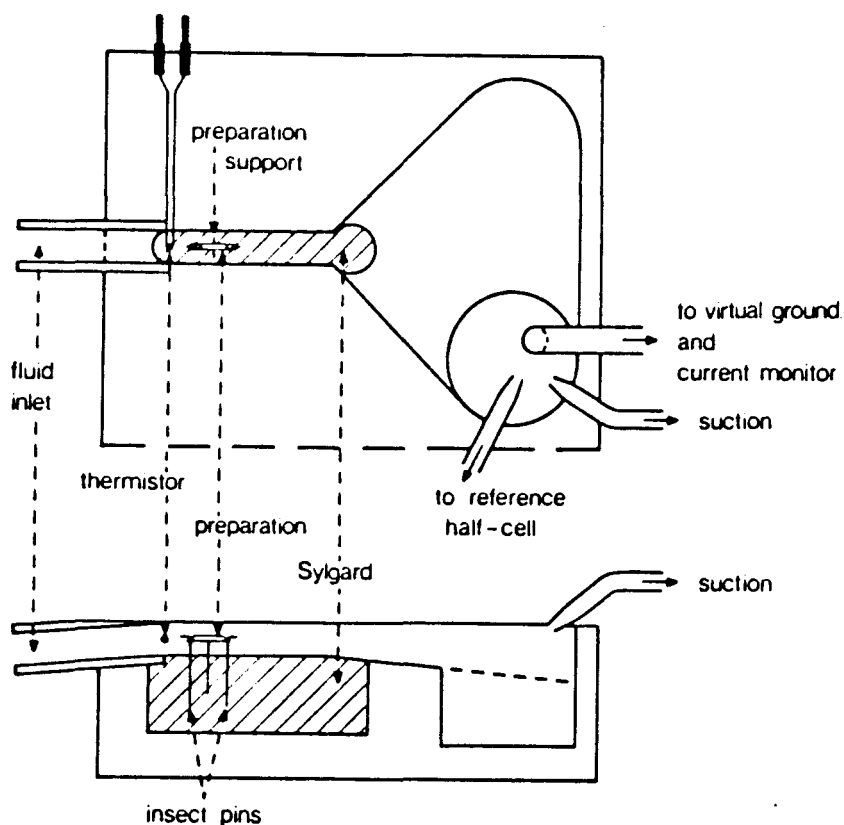
Tyrode's solution was prepared the morning of each experiment and only twice distilled, deionized water was used.

FIGURE 1  
LOCATION OF THE EUSTACHIAN RIDGE



Schematic endocardial view of the posterior wall of the right atrium. SVC = superior vena cava, CT = crista terminalis, ER = Eustachian ridge, IAS = interatrial septum, IVC = inferior vena cava, CS = ostium of coronary sinus, TV = tricuspid valve.

FIGURE 2  
FAST FLOW CHAMBER  
(TOP AND FRONT VIEW)



Schematic diagram of the fast-flow chamber taken from Gadsby and Cranefield's modification (175) of the Hodgkin-Horowitz tissue chamber.

to the inlet of the bath. A magnet placed within the valve handle completed a circuit, causing a 5 volt deflection whenever the valve position was switched. This voltage deflection was recorded and used to precisely indicate changes in bath solution. At a flow rate of 5 ml/min, the half-time for solutions to change in the middle of the bath channel was 0.5 seconds (175). The preparation was carefully pinned to the Sylgard (Dow Corning) floor of the tissue bath with stainless steel pins. After recording initial spontaneous rates, the tissue was often cut down into 2-3 preparations, each being 1-2 mm<sup>2</sup> in area.

### B. Recording of Transmembrane Potentials

Standard intracellular recording techniques were used to record transmembrane potentials. Ling and Gerard type glass microelectrodes (324), were made using a vertical pipette puller (David Kopf Instruments, Model 700c) and filled with a 3 M KCl solution. Each microelectrode was placed into a microelectrode holder (WPI, MEH-3R) filled with 3 M KCl and containing a Ag-Ag/Cl half cell. Each microelectrode holder was then attached to a probe mounted on a micromanipulator (Prior). Each probe was connected to a high impedance preamplifier (WPI, Model 750) with capacitance neutralization. The two unity gain outputs from the preamplifier were subtracted and then amplified 10x via a custom-made differential amplifier. The resulting signal was fed into a connecting circuit which allowed it to be simultaneously displayed on a dual beam storage oscilloscope (Tektronix 5113), a two channel chart recorder (Gould 220), and recorded on a 4 channel FM tape recorder (Racal 4DS). Action potential signals were also fed into a differentiator to determine the maximum rate of rise of the upstroke.

The tissue bath was grounded by a KCl agar bridge connecting to a pot containing 3 M KCl. The pot had a Ag-Ag/Cl wire immersed within it that was connected to virtual ground. The microelectrode resistances were measured by placing

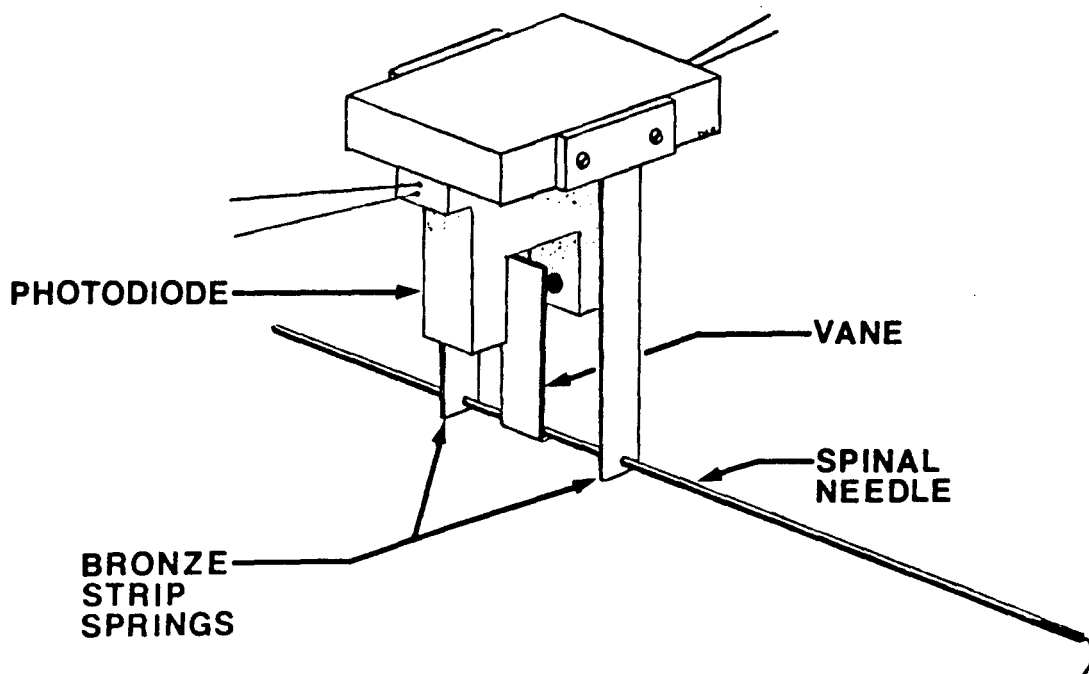
the tip of a microelectrode in the tissue bath containing Tyrode's solution and passing a 50 mV pulse across a 50 Mohm resistor in series with the microelectrode. The resultant voltage drop across the microelectrode was displayed on the storage oscilloscope and the microelectrode resistance was calculated. Only electrodes with tip resistances of 20-50 Mohms were used.

Tension was measured using a home-made (plans obtained from A. Wasserstrom, University of Chicago) tension transducer (Figure 3). A dissecting pin was glued to the end of a spinal needle and used to hook the edge of the tissue. The spinal needle was supported by two thin strips of bronze (.002" thick), acting as springs that were clamped to a micromanipulator. Attached to the needle between the bronze strips was a thin metallic vane. With each contraction, the vane passed in front of a photodiode (Texas Instruments, TIL-138) fixed to the micromanipulator. The output of the photodiode was fed into a variable gain amplifier with a variable noise filter. Calibration of the transducer demonstrated a linear relationship between force and voltage output over the range of 10 - 70 mg (Figure 4). Control tension was determined by pulling the needle and thus stretching the tissue to produce a tension that was 75% of the maximum.

### C. Data Measurement

To study subsidiary pacemaker characteristics, control action potentials were measured and compared to those obtained during a test response. Action potentials were replayed from the FM tape recordings at real time into a three channel chart recorder (Gould 2400S). The schematic diagram in Figure 5 (Panel A) demonstrates the values of the action potential measurements. The basic cycle length (BCL) was measured in milliseconds (msec) and is defined as the time between the peak upstrokes of two consecutive action potentials. The maximum diastolic potential (MDP) refers to the most negative voltage of the action potential, and the peak potential (PP) which

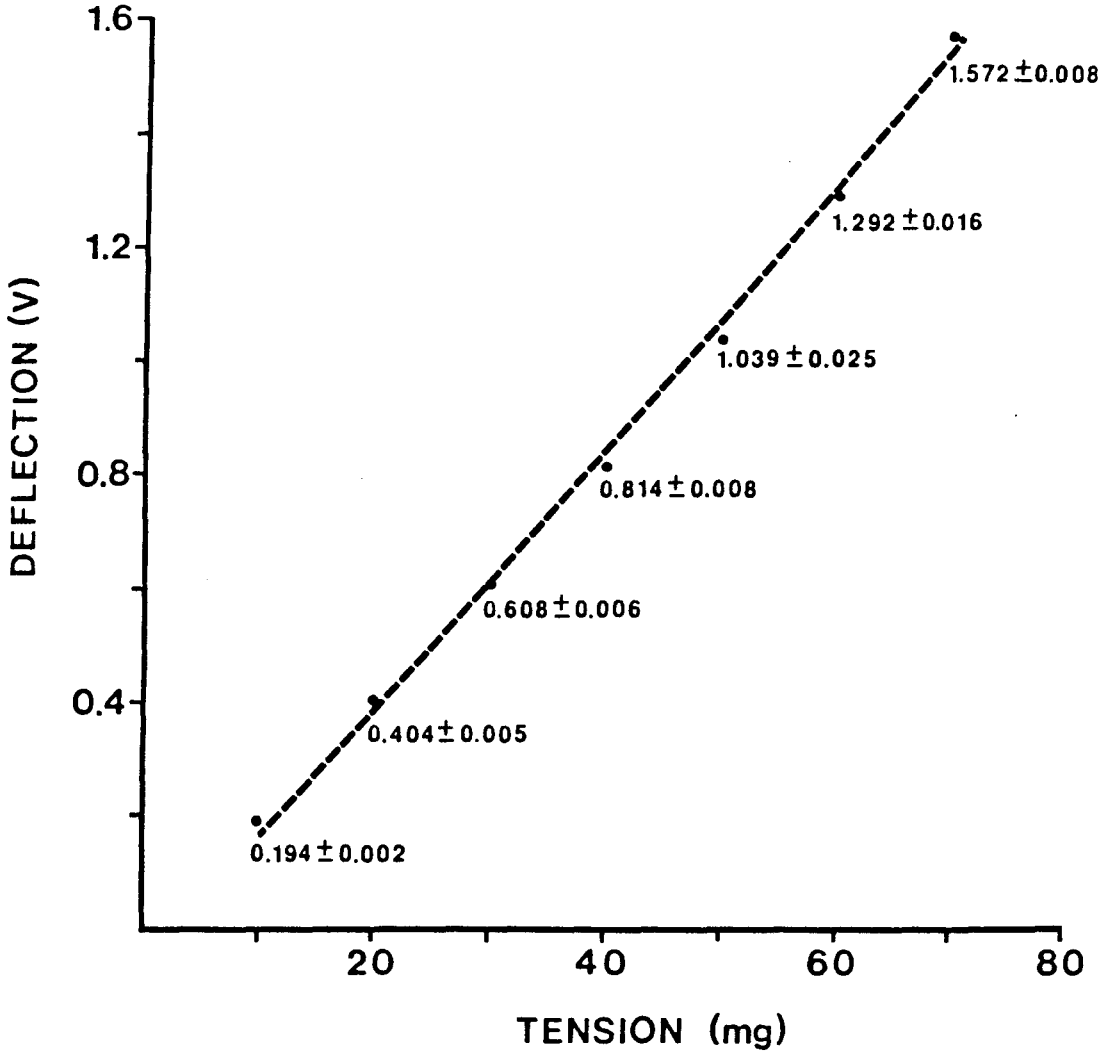
FIGURE 3  
TENSION TRANSDUCER



Pin at end of needle was used to carefully hook one edge of the tissue. Contractions generated slight back-and-forth motion in spinal needle by the bronze strip springs. The vane attached to the spinal needle passed in front of photodiode.

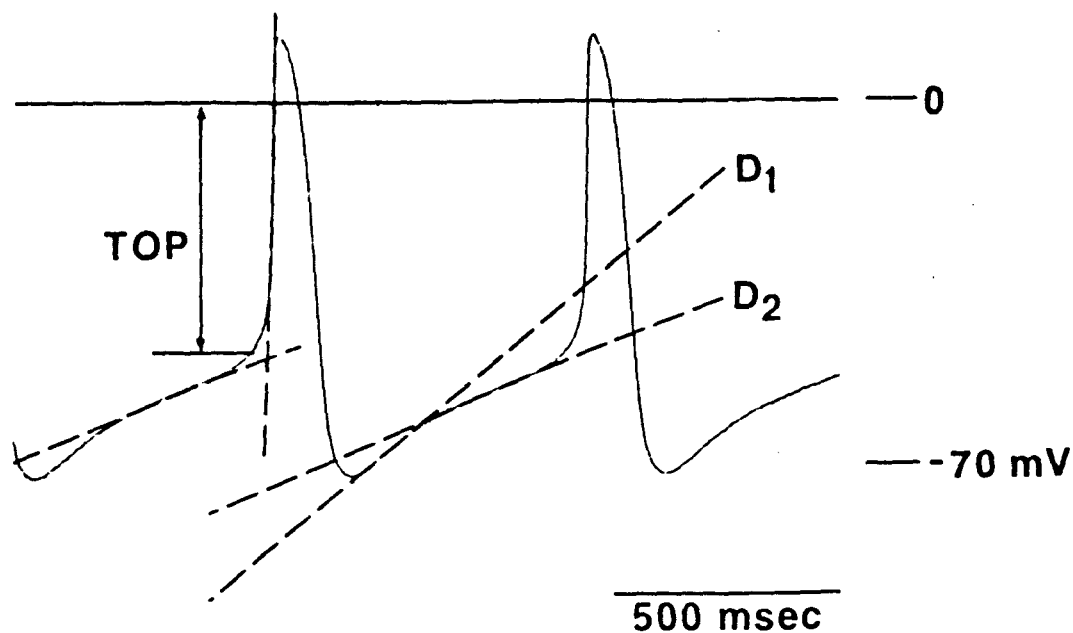


FIGURE 4  
CALIBRATION OF TENSION TRANSDUCER



The tension transducer was loaded from 10 mg to 70 mg in increments of 10 mg (N=3). At a gain of 500, the voltage was plotted above as the mean  $\pm$  SE.

FIGURE 5  
ACTION POTENTIAL MEASUREMENTS



Spontaneous subsidiary pacemaker action potentials exhibiting two phases of diastolic depolarization. Slope of early ( $D_1$ ) and late ( $D_2$ ) phase was measured as a line drawn tangent with linear portion of each phase. Takeoff potential (TOP) was measured at intersection of lines drawn tangent with late phase of diastolic depolarization and upstroke.

describes the peak positive voltage. Both are measured from the zero potential and are in units of millivolts (mV). The action potential amplitude is the absolute value of the voltage difference between the MDP and PP. Action potential duration (APD) was measured at 60% of repolarization from the PP. The diastolic slope, measured in millivolts/second (mV/s), was separated into two components,  $D_1$  and  $D_2$ .  $D_1$  and  $D_2$  were measured as the slope of a line drawn tangent to the first and second portions of diastolic depolarization, respectively (Figure 5). Although, this form of diastolic depolarization was frequently found, if the depolarization did not demonstrate both components, then  $D_1$  and  $D_2$  were assumed to have the same value. The take-off potential (TOP) was measured at the intersection of lines drawn tangent to  $D_2$  and the steepest portion of the action potential upstroke.

Tension was measured as an estimated index of the intracellular calcium concentration. Since the experiments were designed to observe relative changes, tension values were normalized. In addition, due to variability in the amount of working atrial muscle among preparations, measurements of absolute tension would have been inappropriate.

#### D. Ultrastructure Studies

A series of experiments were done to correlate the structural and functional characteristics of fibers within Eustachian ridge and to compare these characteristics with those of sinus node and working atrial muscle. In seven preparations the Eustachian ridge, sinus node, and a portion of the right atrial appendage were isolated. The sinus node region and a strip of right atrial appendage was superfused in a tissue bath simultaneously. All tissues were allowed to equilibrate for one hour before intracellular recordings were begun. The pacemaker site of earliest activation (SEA)

was electrophysiologically mapped in both SA node and Eustachian ridge by recording an extracellular bipolar electrogram from one end of the preparation, and making systematic, multiple intracellular impalements throughout the tissue. The site of earliest activation was defined as the location in which the action potential preceded the electrogram by the greatest time interval. Action potential configuration was also used as a criterion in estimating the site of earliest activation. None of the tissues isolated from the atrial appendage exhibited spontaneous activity, although they were electrically excitable with external stimulation (Pulsar 4i).

After intracellular recordings were completed in each tissue, the microelectrode was gently advanced, leaving the electrode tip at the site of earliest activation. Each tissue was then quickly placed in glutaraldehyde for fixation. To better visualize the recording site for later morphological analysis, the fixed tissue was placed under a dissecting microscope and a small dot of India ink (approx. 400  $\mu\text{m}$  diam.) was placed at the position of the electrode tip. In addition, a diagram was made, noting the position of the site of earliest activation, to aid in localizing the recording site. Tissues were exposed to Tyrode's solution for no more than 3 hours before being fixed.

Tissues were immersed in cold 4% glutaraldehyde in 0.15 N cacodylate buffer (pH 7.4), rinsed in cacodylate buffer. Following fixation, each tissue was cut in half directly through the center of the ink dot used to label the site of earliest activation. Each half of tissue was then postfixed in 1% osmium tetroxide in cacodylate buffer (pH = 7.4), dehydrated in graded series of acetone, and embedded in Epon. One micron sections were cut from each block face (through the site of earliest activation) using an LKB ultramicrotome with glass knives and stained with 1% toluidine blue for light microscopic evaluation using an Olympus AHBS compound microscope. Thin sections (70-80 nm) for electron microscopy were cut with a diamond knife, mounted on 200-mesh copper grids and stained with uranyl acetate and lead citrate to enhance contrast.

Sections were evaluated with an Hitachi H-600 electron microscope operated at 75 kV. Ten micrographs were taken of each tissue at random locations within the recording areas of both Eustachian ridge and SA node from each animal. The sampling method included systematically scanning one section per grid and recording the first ten grid spaces that contained P cells. In every case, the grid was positioned so as to selectively photograph only P cells in that grid space. Grid spaces which either contained artifact or did not contain P cells were excluded from the sample. The micrographs were photographically enlarged to a final magnification of 24,700 x and coded so that during analysis, the source of the tissue was not known. Volume densities of P cell nuclei, myofilaments, mitochondria and cytoplasm were estimated using a 99 point grid on a transparent overlay and applying standard point counting stereological methodologies (567). Apposed and unapposed subsarcolemmal cisternae in P cells was determined by directly counting each structure in both recording areas. Data for each variable measured was tested to determine if a significant difference existed between P cells in the Eustachian ridge and SA node by the Student's t test (two-tailed with a P value of less than 0.5 was considered statistically significant).

## E. Drug Protocols

### 1. Preparation of solutions

Tyrode's solution (concentrations listed above) was freshly made the morning of each experiment. All tissues were equilibrated in this solution for at least one hour before cellular recordings were attempted. In several experiments the ionic concentration of the Tyrode's solution was altered. To determine the  $P_{Na}/P_K$  ratio, the extracellular potassium concentration ( $[K]_o$ ) was randomly varied among 1, 2, 4, 8, 16, 32, 64, and 128 mM. The results from these experiments were plotted and fitted to curves calculated from the Goldman-Hodgkin-Katz equation (193,225). To maintain a

constant osmolarity, the extracellular sodium concentration ( $[Na]_o$ ) was adjusted proportionately in each of these solutions such that the sum of  $[K]_o + [Na]_o = 153$  mM. The preparations were exposed to each solution until a steady state potential was reached, usually about 3-5 minutes. The influence of acetylcholine (ACh) was tested after reaching a steady RMP by switching to the same  $[K]_o$  but with  $10^{-4}$  M ACh for 30 seconds. The ACh solution was washed out to the previous solution before the  $[K]_o$  was switched again. Chloride free solutions were not used since the permeability of chloride ions have been consistently shown to contribute little to the cardiac RMP (17,53,82,170,234).

In experiments that tested the effect of low  $[Na]_o$  (50%), sucrose was substituted for sodium (Na:sucrose = 1:1.8 in mM), to maintain constant osmolarity. Reducing the sodium, also causes a large reduction in the  $[Cl]_o$ , and to avoid changes in potentials due to the development of junction potentials, these experiments were performed by using a flowing 3 M KCl reference electrode (Fisher Scientific).

When the experimental protocol required altering calcium, no other adjustments were made. The concentrations of calcium examined ranged from 0.54 to 5.4 mM.

## 2. Autonomic Neurotransmitters

Norepinephrine (Levophed bitartrate, Winthrop-Breon) and isoproterenol (Isuprel, Winthrop-Breon) stock solutions were prepared in doubly distilled, deionized water. To prevent oxidation of norepinephrine in the Tyrode's solution, ascorbic acid (Sigma) was added at a concentration of  $6 \times 10^{-5}$  M (569). The stock solutions were all prepared the morning of each experiment. The effects of exogenous neuromediators were assessed by analyzing action potential characteristics in the absence (control) and presence (test) of the test solutions. Action potentials were measured every 15 seconds, but only values measured at 60 seconds were used for statistical analysis. Experiments

directed toward determining the mechanism of norepinephrine required several reapplications in the presence of different blocking agents. Therefore, control experiments were performed to demonstrate that this adrenergic agonist could repeatedly initiate activity without significant differences.

The autonomic receptor antagonists atenolol (Sigma), prazosin (Pfizer), and atropine (atropine sulfate, Sigma), were all prepared in stock solutions and kept refrigerated.

### 3. Pharmacological Agents

Channel blocking agents used to assess mechanisms of subsidiary pacemaker automaticity included: tetrodotoxin (Sigma), verapamil (+/- verapamil hydrochloride, Sigma), cesium (cesium chloride, Fisher Scientific). Stock solutions of each drug were made the morning of each experiment. The experimental drug Bay K 8644 (gift from Dr. Scriabine, Miles Laboratories, New Haven Connecticut), recently shown to enhance the slow inward current (462,463), was stored in a refrigerated stock solution of  $10^{-3}$  M in ethanol, contained within an amber glass jar. Bay K 8644 and norepinephrine have been shown to increase the classically described slow inward current by specifically enhancing the current through L-type calcium channels (19,202,374). Throughout the results and discussion sections, the terminology of slow inward current will be referring to this mechanism. Acetylstrophanthidin was prepared the morning of the experiment in a stock solution with 1% ethanol at a concentration of  $10^{-4}$  M.

Ryanodine (Penick Corp., Lyndhurst, NJ) a drug which has a direct influence on calcium movements from the sarcoplasmic reticulum (34,265,409,497,498), was prepared from a refrigerated stock solution, and used at  $10^{-6}$  M. The effects of ryanodine were irreversible. To assess the mechanism of norepinephrine action on SAP automaticity, dibutyryl cAMP ( $N^6$ -2'-O-dibutyryladenosine 3':5'-cyclic monophosphate, Sigma), was

tested.

#### F. Data Analysis

Action potential and membrane potential measurements and volume densities were all represented as the mean plus or minus the standard error of the mean ( $\bar{x} \pm \text{SEM}$ ). Analysis of electrophysiological data was performed by comparison of two paired or unpaired groups (control versus test) and by applying the appropriate student's t-test. The ultrastructural volume density data was analyzed by comparing the Eustachian ridge versus either the sinus node or atrial muscle. Differences were considered statistically significant at a  $p < 0.05$  (560).



## CHAPTER IV

### RESULTS

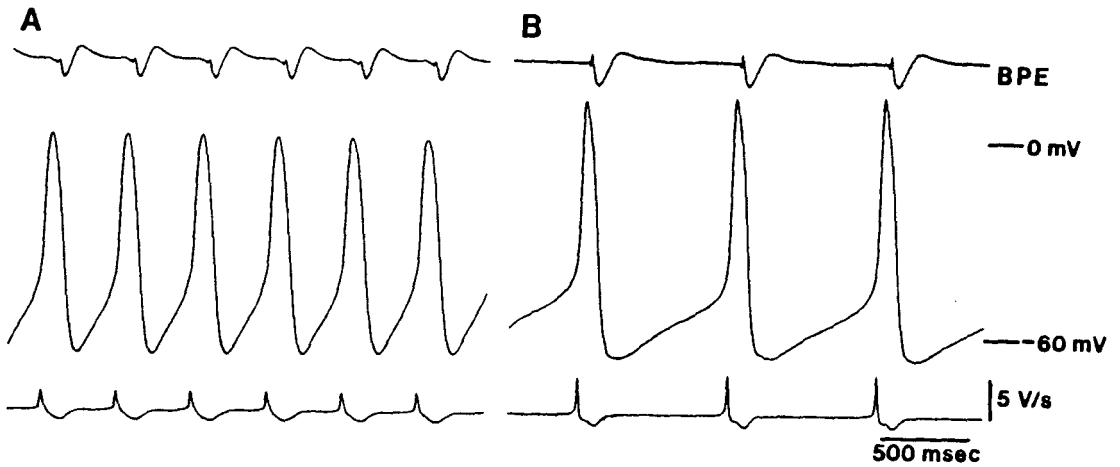
#### A. ELECTROPHYSIOLOGY AND ULTRASTRUCTURE OF EUSTACHIAN RIDGE FROM CAT RIGHT ATRIUM: A COMPARISON WITH SA NODE

(J.Mol.Cell.Cardiol. 19:965-967, 1987)

##### 1. Electrophysiology

Stable spontaneous activity was exhibited by six of seven SA node preparations and five of seven Eustachian ridge (ER) preparations. In the two quiescent ER preparations, norepinephrine (NE; approximately  $10^{-9}$ M) elicited sustained spontaneous activity. Action potentials from both SA node and ER preparations were recorded from the site of earliest activation and therefore represent the 'primary' pacemaker of each tissue. Figure 6 shows action potentials recorded from a spontaneously beating SA node [panel (a)] and ER preparation [panel (b)]. Table 2 summarizes the average value of each action potential parameter recorded from each tissue. The spontaneous cycle length of subsidiary pacemakers was more than twice that of SA node and was more variable among different preparations. Even though the maximum diastolic and take-off potentials of each pacemaker were similar, the amplitude of the overshoot and maximum rate of rise of subsidiary pacemakers were significantly greater than those in SA node. Although SA node exhibited a longer mean action potential duration, there was no statistical difference compared to subsidiary pacemakers.

**FIGURE 6**  
**SPONTANEOUS ACTION POTENTIALS FROM SA NODE**  
**AND EUSTACHIAN RIDGE**



Spontaneous action potentials recorded from the site of earliest activation in SA node (A) and Eustachian ridge (B). The top traces show bipolar electrograms (BPE) recorded from the periphery of each preparation. The bottom traces show the first derivative of maximum rate of rise of action potential upstroke (V/sec).

TABLE 2

	<u>Eustachian ridge</u>	<u>Sinus node</u>
SCL (ms)	948 ± 193 <sup>a</sup>	434 ± 8
MDP (mV)	-69.9 ± 1.7	-69.2 ± 1
OS (mV)	+7.7 ± 1.5 <sup>a</sup>	-6.4 ± 3.2
AMP (mV)	77.6 ± 1.7 <sup>a</sup>	63.2 ± 3.3
APD-60% (ms)	109 ± 2	132 ± 10
TOP (mV)	-52.5 ± 2.7	-53.3 ± 1.5
dV/dt (V/s)	5.5 ± 0.2 <sup>b</sup>	2.2 ± 0.4

SCL = spontaneous cycle length; MDP = maximum diastolic potential; OS = overshoot; AMP = amplitude; APD-60% = action potential duration at 60% repolarization; TOP = take-off potential; dV/dt = maximum rate of rise.

<sup>a</sup>p<0.05; <sup>b</sup>p<0.001--Significantly different from sinus node.

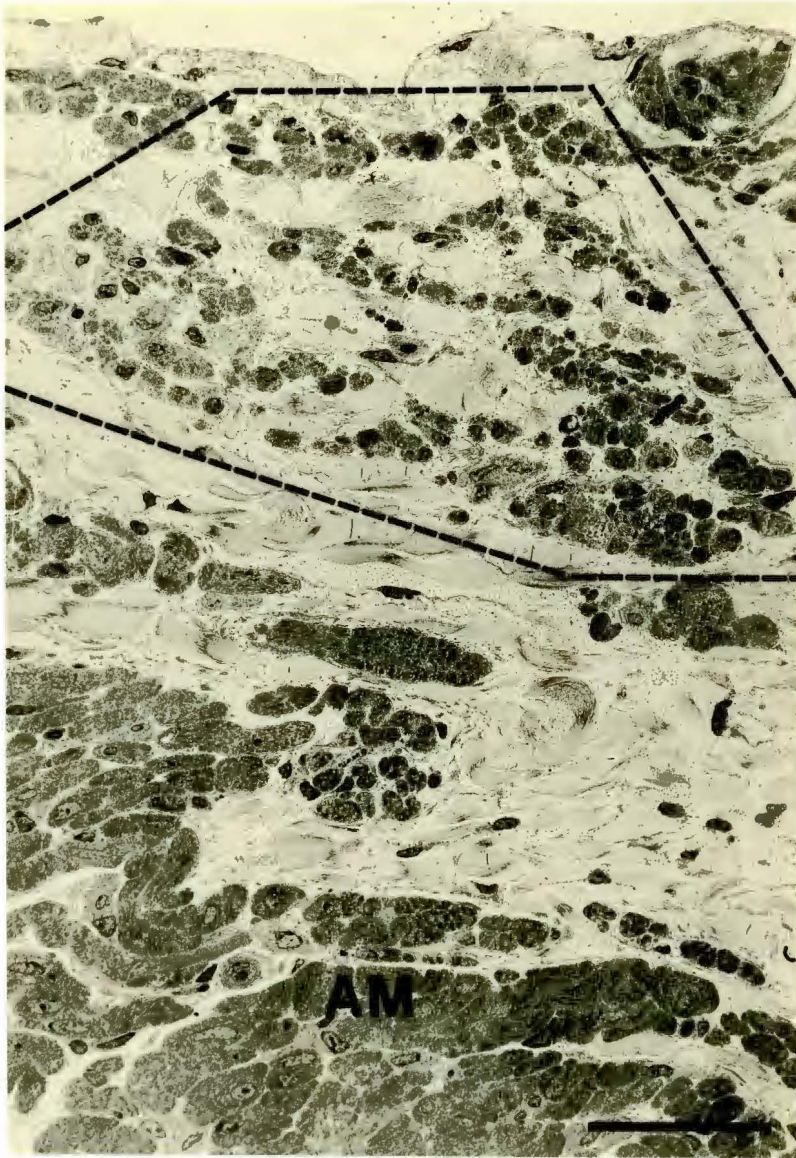
## 2. Morphology

Eustachian ridge tissues were more heterogenous than SA node, having at least four different types of myocardial cells. These could be broadly classified as P cells, transitional, typical working atrial muscle and ameoboid cells, as described by Sherf and James (473). The endocardial region from which the site of earliest activation was recorded consisted primarily of small cells (Fig. 7).

In both ER and SA node, electron microscopic examination of cells at the endocardial site of earliest activation revealed that P cells were the most predominant cell type. The P cells in the endocardial region of the Eustachian ridge had ultrastructural characteristics similar to those of P cells in SA node (compare Figs. 8 and 9). Typically, they were clustered in groups of three or more cell profiles surrounded by a single basal lamina. Cells were approximately 5 to 7  $\mu$  in diameter, were irregular in shape and showed a large variety of profile sizes in any one plane of section. The sparse content of internal organelles gave these cells the characteristic pale appearance. Myofibrillar content was sparse and randomly oriented. It was not unusual to see both longitudinal and cross sectional profiles of myofibrillar material within a single P cell (Fig. 10). Although an occasional Z line was observed, other components of a sarcomere were not clearly evident in P cells. Nuclei were relatively large in relation to cell size and centrally located. The nucleus was usually surrounded by endoplasmic reticulum, Golgi complexes, and small mitochondria. Mitochondria were also dispersed throughout the cytoplasm. Abundant small vesicles or calveoli were associated with the internal surface of the sarcolemmal membrane, at regions that did not directly appose another cell surface membrane. Vesicular mambranes were frequently continuous with the sarcolemma and therefore appeared pinocytotic.

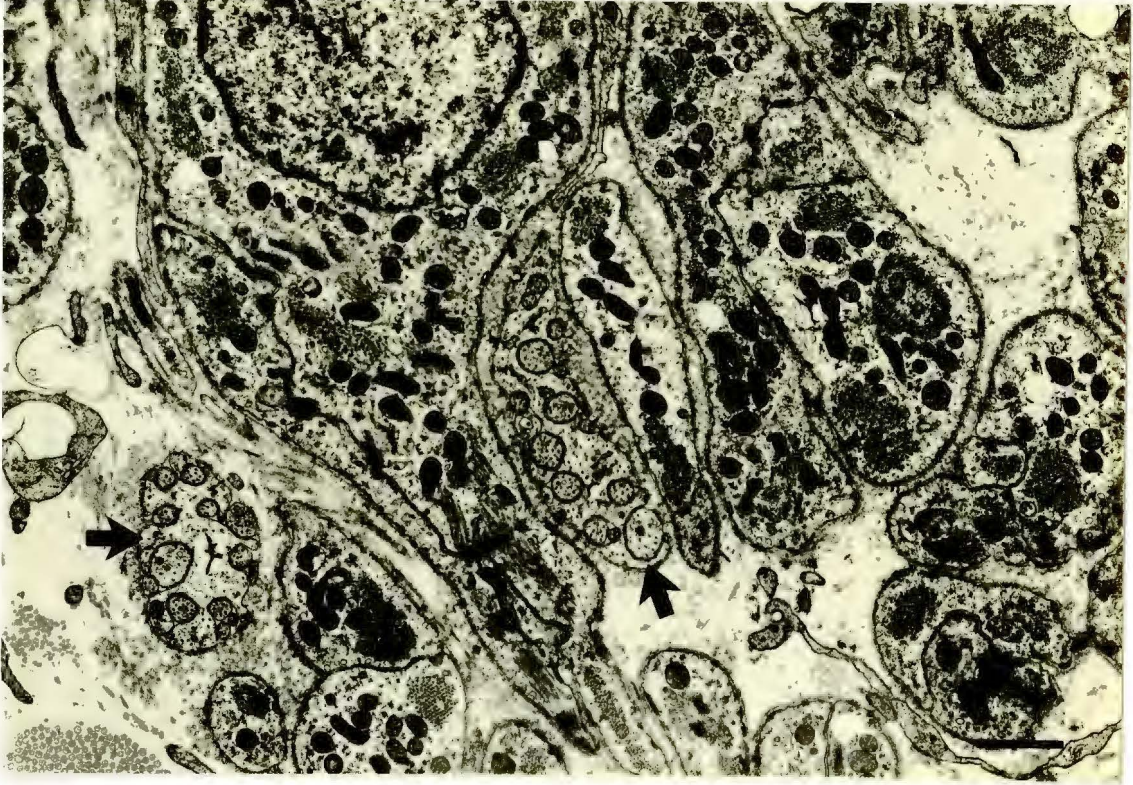
Both SA node and ER contained abundant nerve fibers in close proximity to P cells. Nerve fibers contained either clear or dense core vesicles and both types of fibers

## LOW POWER ELECTRON MICROGRAPH OF EUSTACHIAN RIDGE



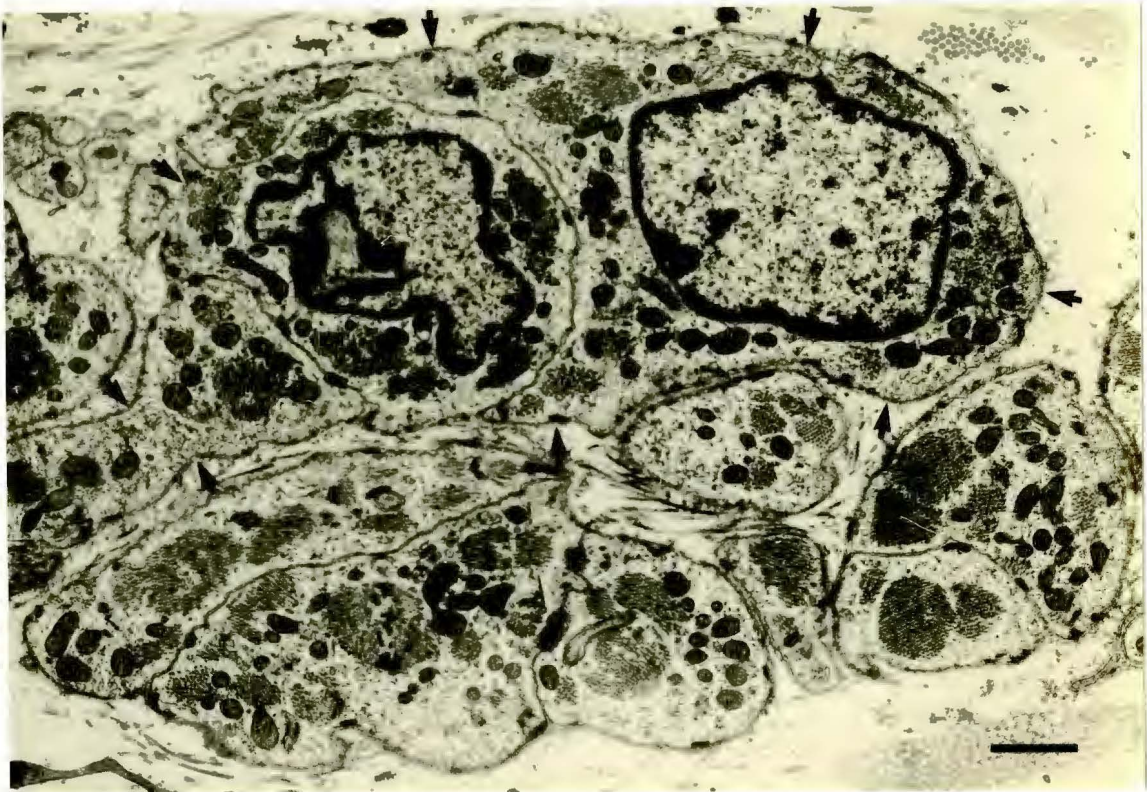
Low power electron micrograph of Eustachian ridge sectioned through the site of earliest activation. P cells clusters are scattered throughout the subendocardial region (dashed line). Connective tissue separates the subendocardial region from working atrial muscle cells (AM). Cell types were confirmed with high power electron microscopy. Bar indicates 40  $\mu\text{m}$ .

## FIGURE 8

ELECTRON MICROGRAPH OF SA NODAL CELLS  
AT THE SITE OF EARLIEST ACTIVATION

Electron micrograph showing SA nodal P cells taken at site of earliest activation. Note the sparse internal organelles and randomly oriented myofibrillar material. Bundles of axons (arrows) are observed in close proximity to P cells. Bar indicates 1.0  $\mu\text{m}$ .

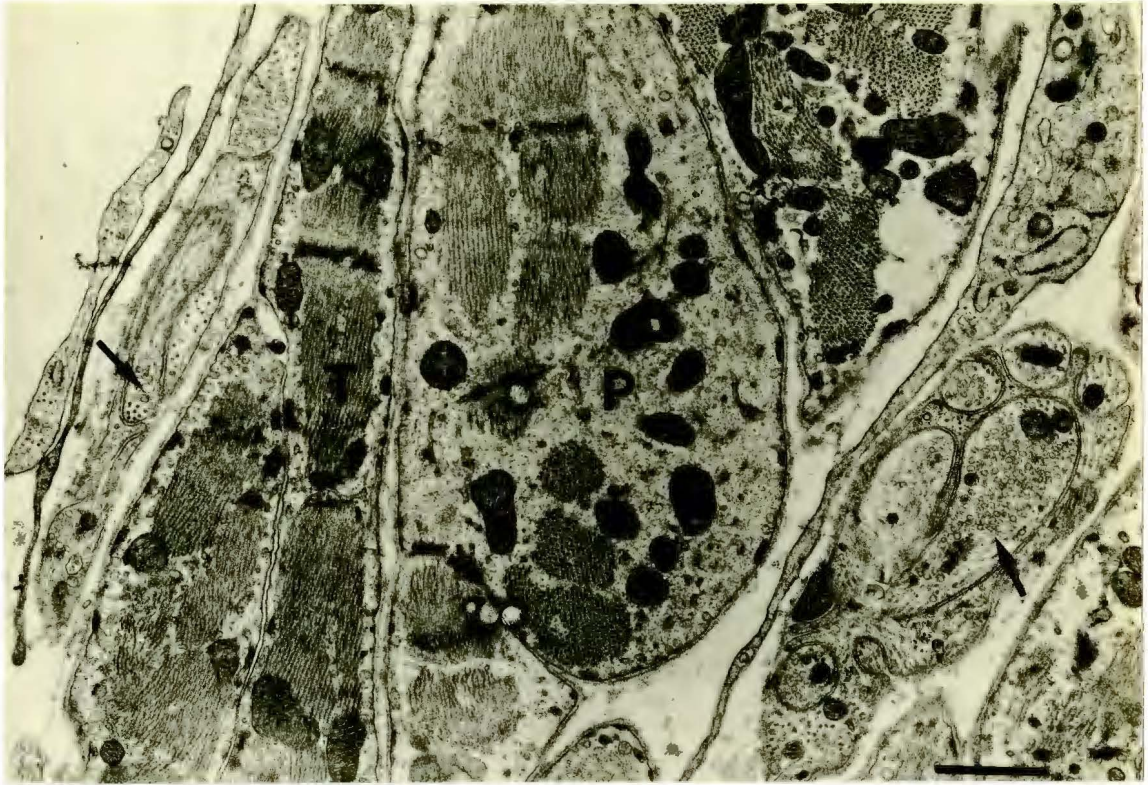
ELECTRON MICROGRAPH OF EUSTACHIAN RIDGE P CELLS  
AT THE SITE OF EARLIEST ACTIVATION



Electron micrograph of a typical cluster of Eustachian ridge P cells taken at the site of earliest activation. Each cluster is surrounded by a basal lamina (arrows). Some collagen fibers and occasional neural elements in the extracellular compartment are present. Bar indicates 1.0  $\mu\text{m}$ .

FIGURE 10

ELECTRON MICROGRAPH OF P CELL AND TRANSITIONAL CELL  
IN THE EUSTACHIAN RIDGE



P cell (P) adjacent to a transitional cell (T) in Eustachian ridge. In the vicinity are several nerve fibers (arrows) which contain numerous clear vesicles and occasional large dense-core vesicles. Bar indicates 1.0  $\mu\text{m}$ .



are seen within the same nerve bundle (Figs. 8, 9, 10).

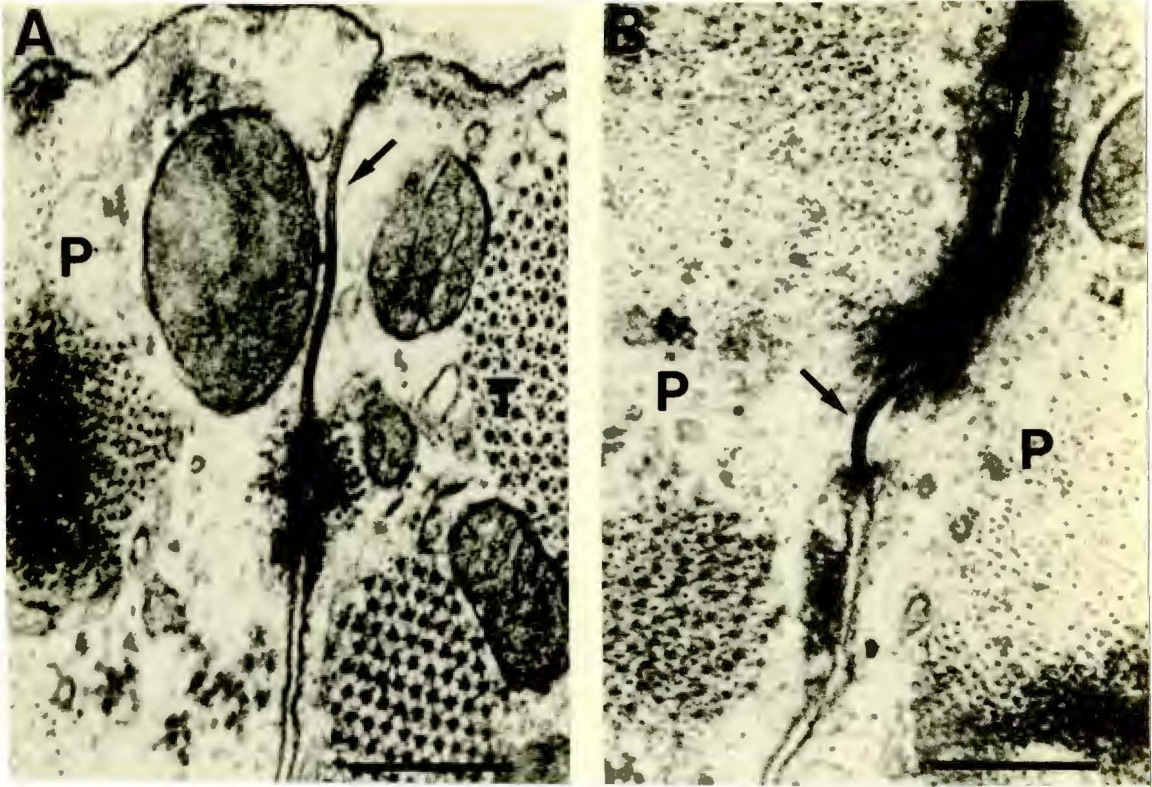
Intercellular junctions consisted primarily of undifferentiated regions, with some desmosomes and poorly developed fascia adherentes (Figs. 8, 9, 10, 12). In rare instances, nexal connections were observed between either a P cell and a transitional cell or between adjacent P cells in the ER (Fig. 11). There were no specialized junctional regions such as an intercalated disc. P cells appeared to make intercellular connections between other P cells or transitional cells. Transitional cells were considered those cells that were slightly larger in diameter than P cells and appeared to have a higher volume density of more organized myofibrillar material (Figs. 10 and 12).

The sarcoplasmic reticulum commonly formed subsarcolemmal cisternae along the cell margins with diffuse globular densities situated between each cisternae and the sarcolemma (Figs. 12 and 13). ER P cells had a unique organization of subsarcolemmal cisternae never seen in SA node P cells. The subsarcolemmal cisternae were often directly apposed to one another between connected P cells (Fig. 13) or between a connected P cell and a transitional cell (Fig. 12). In 79 random photomicrographs of ER tissue from a total of 227 subsarcolemmla cisterna, 18 subsarcolemmal cisternae were directly apposed to one another (9 pairs). These values do not include the subsarcolemmal cisternae shown in Figures 12 and 13, which were selected for illustration. An examination of 97 random photomicrographs of SA node revealed 298 subsarcolemmal cisternae and no directly apposed subsarcolemmal cisternae.

### 3. Quantification

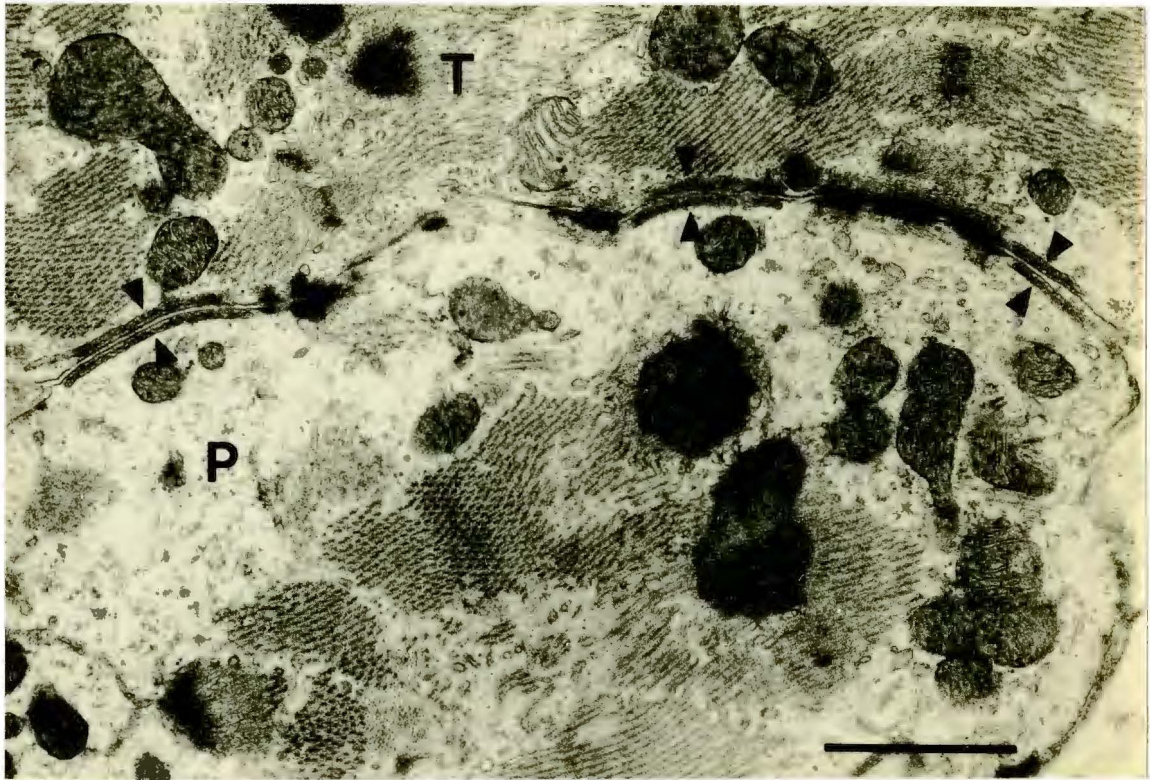
In four hearts, after electrophysiological recordings were made from both ER and SA node, each tissue was then morphologically analyzed to determine relative volume densities of nuclei, myofilaments, mitochondria, and cytoplasmic space. Table 3

FIGURE 11

ELECTRON MICROGRAPH OF NEXAL CONNECTIONS  
IN THE EUSTACHIAN RIDGE

Nexal connections (arrows) between a P cell (P) and transitional cell (T) (panel A) and between two adjacent P cells (panel B) in Eustachian ridge. Bar indicates 0.25  $\mu\text{m}$ .

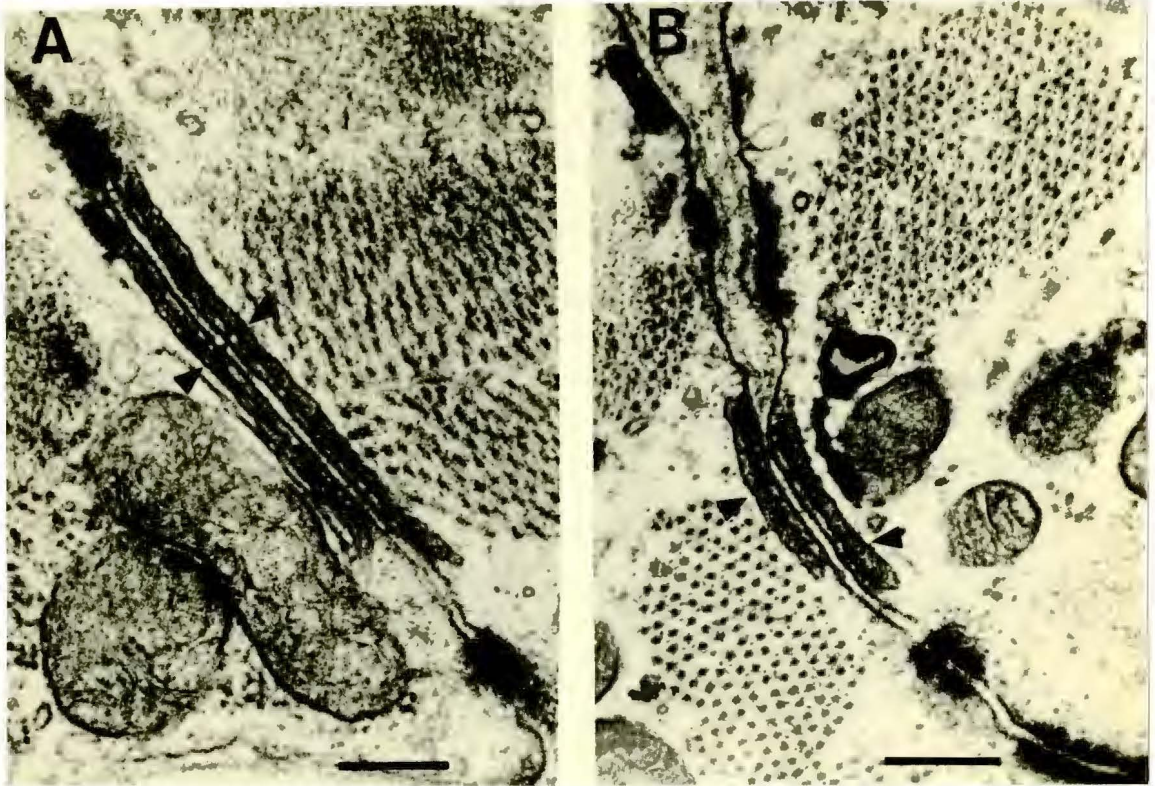
FIGURE 12  
ELECTRON MICROGRAPH OF DIRECTLY APPPOSED  
SUBSARCOLEMMA CISTERNAE



Direct apposition of subsarcolemmal cisternae (arrowheads) at three different sites in a P cell (P) and transitional cell (T) in Eustachian ridge. The cells are connected by several junctional complexes. Bar indicates 1.0  $\mu\text{m}$ .

FIGURE 13

HIGH POWER ELECTRON MICROGRAPH OF  
DIRECTLY APPOSED SUBSARCOLEMMA CISTERNAE



Two additional examples of paired subsarcolemmal cisternae (arrowheads) directly apposed to one another in Eustachian ridge P cells. Note that each apposed cisterna are approximately equal in length. Bar indicates  $0.25 \mu\text{m}$ .

TABLE 3RELATIVE VOLUME DENSITIES IN PERCENTS (N=4)

	<u>Eustachian Ridge</u>	<u>SA Node</u>
Myofilaments	26.5 ± 18.7	28.9 ± 6.8
Mitochondria	18.5 ± 5.6	15.9 ± 4.2
Nucleus	7.6 ± 9.8	6.9 ± 4.5
Cytoplasm	47.5 ± 10.8	48.4 ± 0.7

Values are expressed as the mean ± standard error of the mean and were obtained by Weibel's method of point counting. Statistical analysis was performed using Student's t test. P < 0.5 was considered statistically significant. No statistical differences were found between the values.

summarizes the results. There were no significant differences between P cells in ER and those in SA node.

## B. MECHANISMS OF AUTOMATICITY IN SUBSIDIARY PACEMAKERS FROM CAT RIGHT ATRIUM

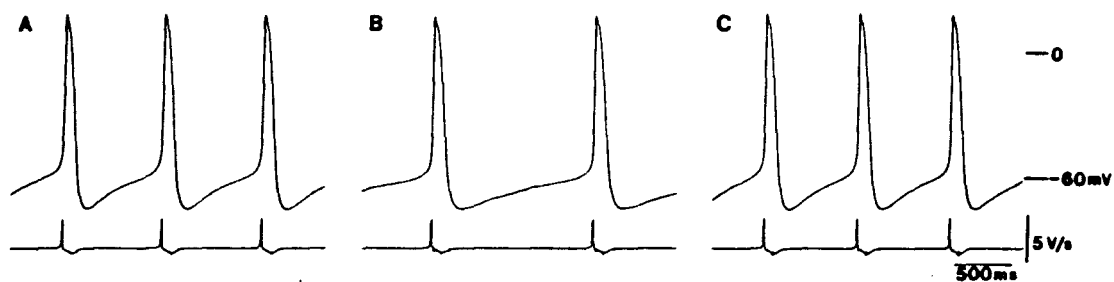
(Circ.Res. 64:648-657, 1989)

The following experiments were designed to determine mechanisms of automaticity of atrial subsidiary pacemakers. Only automatic isolated ER preparations (described in METHODS), which exhibited a discernible  $D_1$  and  $D_2$ , were used in this series of experiments. In eight control experiments, the slopes of  $D_1$  and  $D_2$  were  $55.3 \pm 8.1$  and  $39.6 \pm 4.5$  mV/sec, respectively ( $p < 0.05$ ). At a mean SCL of  $696.7 \pm 58.4$  msec the initial diastolic slope ( $D_1$ ) contributed 30.8% and the secondary slope ( $D_2$ ) contributed 69.2% of the the total time required for the diastolic membrane potential to depolarize from the maximum diastolic potential, that is, over the pacemaker voltage range (-75 to -55 mV). The transition from  $D_1$  to  $D_2$  was estimated at approximately 310 msec, measured from the action potential upstroke.

### 1. Cesium

The contribution of a cesium-sensitive pacemaker current to subsidiary pacemaker automaticity was assessed by exposure of spontaneously active preparations to 1 mM cesium. Figure 14A shows control pacemaker action potentials. In panel B, exposure to 1 mM cesium significantly decreased the slope of diastolic depolarization, resulting in a significant increase in spontaneous cycle length (SCL;  $+37.7 \pm 7.8\%$ ). As shown in Table 4, cesium significantly decreased the slope of  $D_1$  ( $-45 \pm 8.5\%$ ) and  $D_2$  ( $-33.6 \pm 7.6\%$ ), with the change in  $D_1$  being significantly greater than the change in  $D_2$  ( $p < 0.025$ ). The only other cesium-induced effect was a small but significant increase in

FIGURE 14  
EFFECT OF CESIUM ON PACEMAKER ACTION POTENTIALS



Panel A = control; panel B = effect of 1 mM cesium; panel C = recovery. The bottom trace shows the first derivative of action potential voltage changes. All action potentials were recorded from the same cell.

TABLE 4

	SCL (ms)	MDP (mV)	OSP (mV)	AMP (mV)	TOP (mV)	APD (ms)	D1 (mV/s)	D2 (mV/s)	dv/dt (V/s)	T (%)
CONTROL	727+47	-70.5+3.9	9.4+3.6	79.8+6.5	-52.3+3.4	116+6	51+7	33+4	5.4+1.0	
CESIUM (n=5)	987+23 <sup>#</sup>	-70.0+3.7	9.8+3.5	79.5+6.6	-55.2+3.4	119+9	25+1 <sup>*</sup>	21+1 <sup>a</sup>	6.0+1.3 <sup>a</sup>	
CONTROL	723+42	-73.8+3.0	12.7+2.2	86.6+3.0	-52.5+3.4	117+4	65+7	40+4	7.2+1.6	100
NE (n=7)	489+28 <sup>!</sup>	-75.3+3.2 <sup>a</sup>	14.6+2.2 <sup>#</sup>	89.9+2.9 <sup>#</sup>	-57.7+2.7 <sup>*</sup>	110+4 <sup>a</sup>	80+9 <sup>a</sup>	66+5 <sup>*</sup>	9.1+1.9 <sup>a</sup>	157+12 <sup>*</sup>
CONTROL	781+51	-75.8+4.4	12.1+1.8	88.2+4.5	-53.0+4.2	120+10	60+5	37+5	3.7+0.6	100
BAY K 8644 (n=6)	532+34 <sup>!</sup>	-76.9+4.3 <sup>#</sup>	14.6+1.7 <sup>+</sup>	91.8+3.9 <sup>*</sup>	-59.0+4.0 <sup>#</sup>	117+9	70+8 <sup>a</sup>	55+4 <sup>#</sup>	5.8+0.6 <sup>*</sup>	300+13 <sup>+</sup>
CONTROL	623+40	-77.4+1.8	13.0+0.9	90.4+2.0	-59.2+2.1	110+10	61+9	47+6	7.5+2.0	
TTX (n=5)	763+45 <sup>+</sup>	-77.0+2.1	11.4+1.0 <sup>a</sup>	88.4+2.5 <sup>+</sup>	-56.1+3.4 <sup>+</sup>	116+10	54+6	37+3 <sup>+</sup>	7.3+1.9	
CONTROL	757+79	-74.5+2.3	12.0+2.9	86.5+4.7	-53.1+1.7	104+12	51+8	39+4	5.4+1.2	100
RYANO-1	730+78 <sup>+</sup>	-74.2+2.2	13.0+2.4	87.2+3.9	-53.2+1.5	103+12	53+8	40+5	5.6+1.4	101+4
RYANO-15 (n=5)	2051+271 <sup>*</sup>	-70.9+1.9 <sup>*</sup>	22.9+1.1 <sup>*</sup>	93.7+2.0	-53.8+0.7	111+5	51+7	7+4 <sup>#</sup>	7.8+2.1	0

Values represent mean ± standard error of the mean. SCL = spontaneous cycle length; MDP = maximum diastolic potential; OSP = overshoot potential; AMP = total amplitude; TOP = take-off potential; APD = action potential duration (60%); D1 = slope of early diastolic depolarization; D2 = slope of late diastolic depolarization; T = percent change in tension development. RYANO-1 = ryanodine at 1 minute of exposure; RYANO-15 = ryanodine at 15 minutes of exposure. Concentrations of cesium = 1 mM; NE =  $2 \times 10^{-9}$  M; BAY K 8644 =  $10^{-7}$  M; TTX =  $10^{-6}$  M; Ryanodine =  $10^{-6}$  M. + = p < 0.05; a = p < 0.02; \* = p < 0.01; # = p < 0.005; \* = p < 0.001; ! = p < 0.0005



maximum rate of rise. Exposure to 5 mM cesium produced a greater increase in SCL and depolarized the maximum diastolic potential.

## 2. Norepinephrine and Bay K 8644

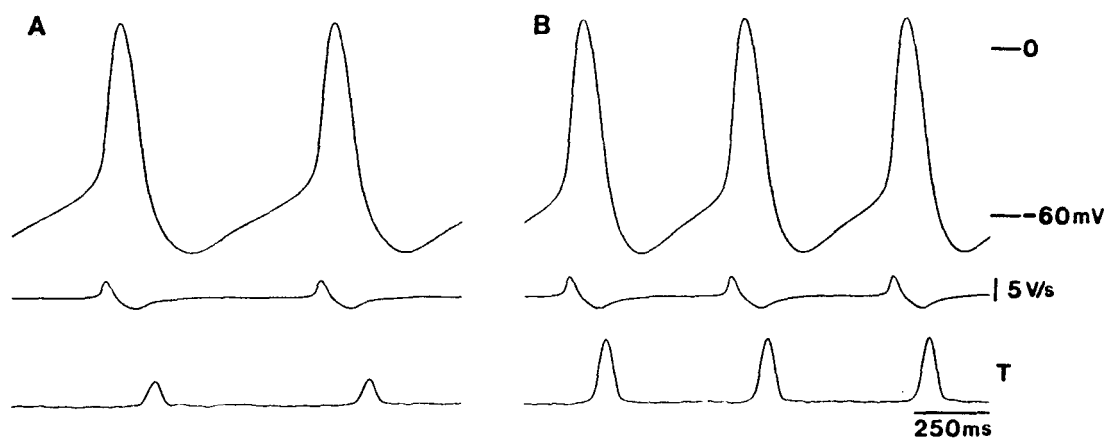
The role of the slow inward current was investigated by testing the effects of Bay K 8644 and norepinephrine (NE). As shown in Figure 15 and summarized in Table 4,  $10^{-7}$  M Bay K 8644 significantly decreased the SCL ( $-31.4 \pm 9.3\%$ ), increased overshoot potential and action potential amplitude, elicited a negative shift in maximum diastolic and takeoff potentials, increased maximum rate of rise, and increased tension threefold ( $n=2$ ). In addition, Bay K 8644 elicited a significantly greater increase in the slope of  $D_2$  ( $+57.5 \pm 12.3\%$ ) than in the slope of  $D_1$  ( $+14.9 \pm 3.5\%$ ) ( $p<0.01$ ).

Relatively low concentrations of NE ( $2 \times 10^{-9}$  M) had effects on pacemaker action potentials similar to those of Bay K 8644 (Table 4). In addition, NE elicited a significantly greater increase in the slope of  $D_2$  ( $+71.3 \pm 12.9\%$ ) than in the slope of  $D_1$  ( $+24.3 \pm 6.5\%$ ) ( $p<0.01$ ), resulting in a significant decrease in SCL ( $-32.0 \pm 3.2\%$ ). In five additional preparations,  $2 \times 10^{-9}$  M NE was administered in the presence of the  $\beta_1$ -adrenergic receptor blocking agent atenolol ( $10^{-6}$  M). Under these conditions, NE elicited only a small but significant decrease in SCL ( $-5.3 \pm 0.6\%$ ,  $p<0.005$ ) that was associated with a similar increase in  $D_1$  ( $+11.4 \pm 1.8\%$ ,  $p<0.05$ ) and  $D_2$  ( $+11.0 \pm 4.8\%$ , NS).

## 3. Verapamil and Tetrodotoxin

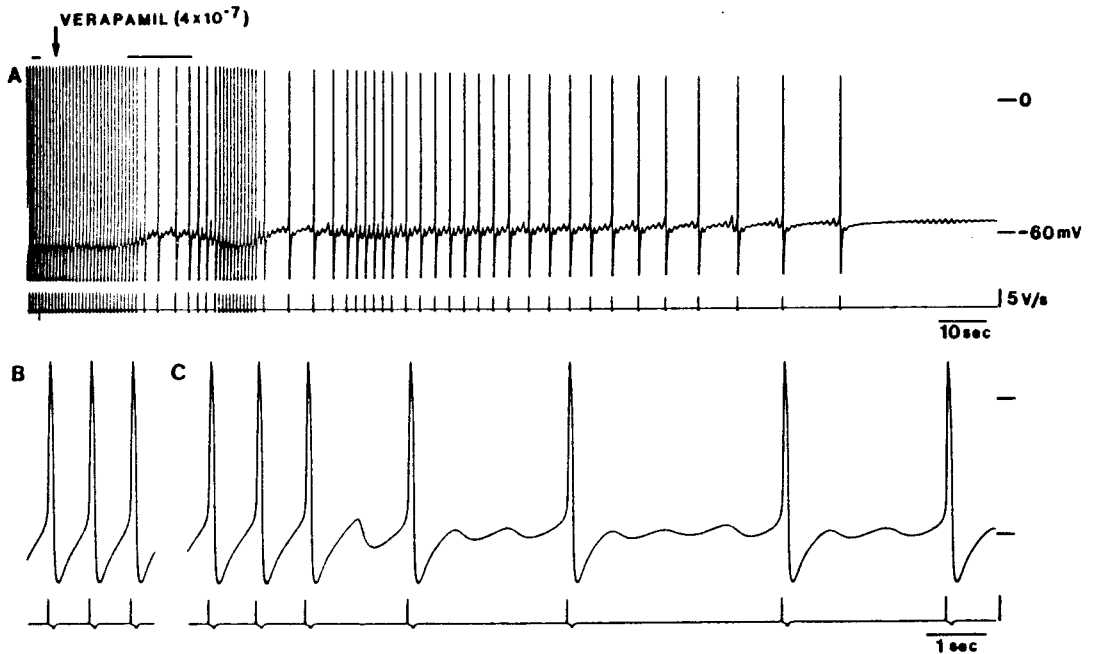
Figure 16 shows the effects of verapamil in pacemaker action potentials. At the left in panel A, the preparation was beating spontaneously under control conditions. Action potentials recorded at this time are shown more clearly in panel B. At the arrow in panel A, the preparation was exposed to  $4 \times 10^{-7}$  M verapamil. Initially, SCL gradually increased until the diastolic potential failed to reach threshold. Action

FIGURE 15  
EFFECT OF BAY K 8644 ON PACEMAKER ACTION POTENTIALS  
AND TENSION



Panel A = control; Panel B = effects of  $10^{-7}$  M BAY K 8644. The middle trace shows the first derivative of action potential voltage changes. All action potentials were recorded from the same cell. Bottom trace shows tension (T).

**FIGURE 16**  
**EFFECT OF VERAPAMIL ON PACEMAKER ACTION POTENTIALS**



Panel A = at the arrow, the preparation was exposed to  $4 \times 10^{-7}$  M verapamil. Panel B & C = selected portions of the signals shown in panel A (horizontal bars), shown at an expanded time scale. Note that the time scale in panel A is slower than in panels B & C. The bottom trace shows the first derivative of action potential voltage changes. All action potentials were recorded from the same cell.

potentials recorded at this time are shown in Panel C. Over the next several beats, the late diastolic slope was replaced with oscillatory potentials that initiated action potentials at irregular intervals. Note in panel C that although the diastolic potential was markedly affected, the action potential amplitude and rate of rise were essentially unchanged. With time (>30 seconds) there was a progressive decline in action potential amplitude and rate of rise and an increase in SCL. After approximately 2 minutes the diastolic oscillatory potentials failed to initiate activity and the preparation became quiescent. Similar results were found in a total of five experiments with verapamil and one experiment with nisoldipine ( $10^{-6}$  M), a more specific slow channel (L-type) antagonist. In six additional experiments, a decrease in extracellular calcium ( $[Ca]_o$ ) from control (1.8 mM) to 0.54 mM had effects similar to those of verapamil.

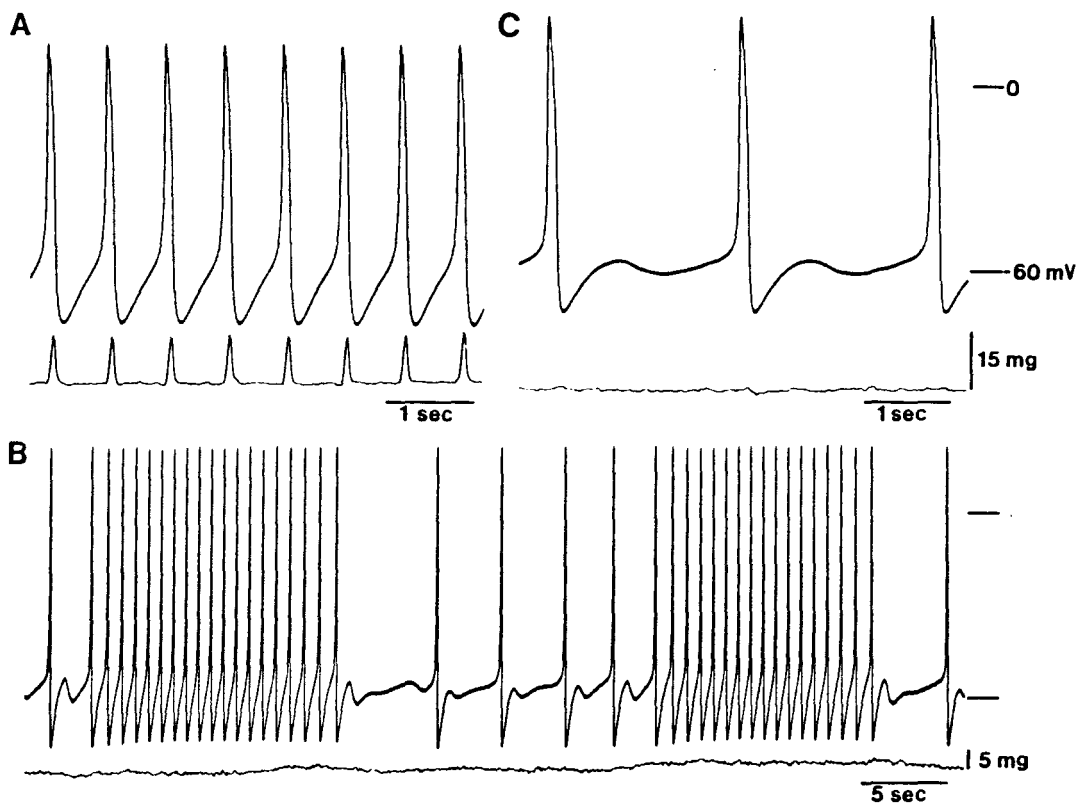
TTX ( $10^{-6}$  M) had no significant effect on maximum rate of rise of the upstroke. However, it elicited a small but significant decrease in overshoot potential and total amplitude (Table 4). Similar results were found in one additional experiment where the concentration was raised to  $10^{-5}$  M. In addition, TTX decreased the slope of  $D_1$  and  $D_2$ , shifted the takeoff potential more positive, and increased SCL ( $+23.9 \pm 9.2\%$ ), but only changes in  $D_2$  were statistically significant (Table 4).

#### 4. Ryanodine

The possibility that calcium entry may be influencing automaticity through a secondary release of intracellular calcium was assessed by exposure of spontaneous preparations to ryanodine. Figure 17A shows control action potentials and tension. Within the first 2 minutes of exposure to  $10^{-6}$  M ryanodine, the predominant effect was a gradual decrease in tension and a concomitant decrease in diastolic slope, leading to an increase in SCL. These changes continued until the diastolic membrane potential failed to reach threshold, resulting in a cyclic pattern of dysrhythmic activity

FIGURE 17

EFFECT OF RYANODINE ON SUBSIDIARY PACEMAKER ACTION POTENTIALS  
AND TENSION

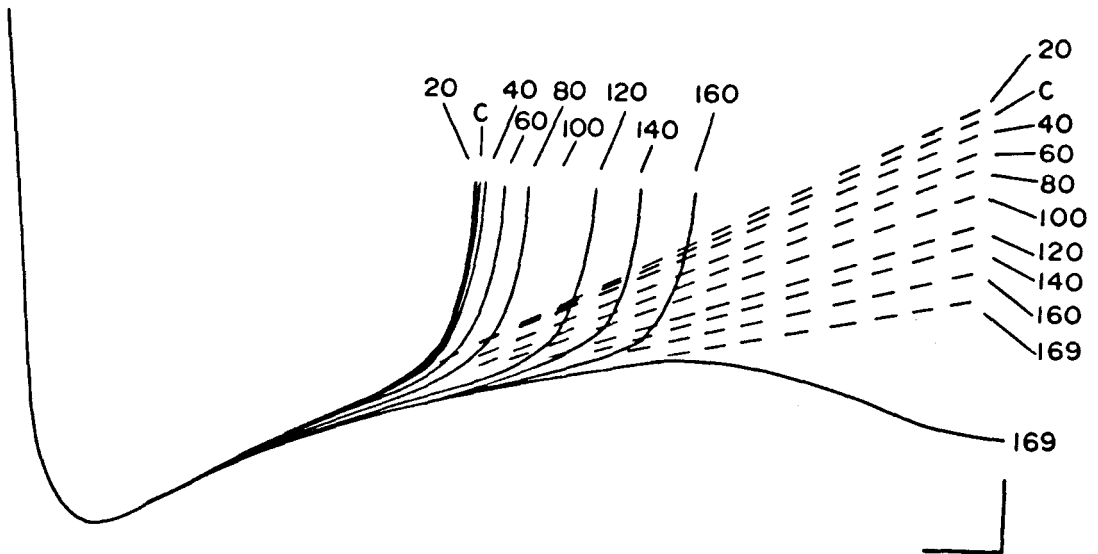


Panel A = control; panel B = early effects of  $10^{-6}$  M ryanodine after about 3 minutes of exposure; panel C = steady state effects of  $10^{-6}$  M ryanodine after about 15 minutes of exposure. Note that the time scale in panel B is 5 X slower than in panels A & C. All action potentials were recorded from the same cells. Bottom trace is tension.

panel B). Dysrhythmic activity lasted approximately 8-10 minutes before pacemaker rhythm stabilized at a prolonged cycle length. Panel C shows the steady state effects of ryanodine after about 15 minutes of exposure. It is apparent that ryanodine decreased the late diastolic slope ( $D_2$ ) and thereby prevented the diastolic potential from initially reaching threshold. As a result, the diastolic potential exhibited a late oscillation or delayed afterdepolarization and an increase in SCL. In the five preparations tested, ryanodine elicited a mean decrease in  $D_2$  slope of 32 mV/sec ( $-84.8 \pm 10.4\%$ ), which translates into a mean increase in SCL of 1,294 msec ( $+172 \pm 23\%$ ) (Table 4). Ryanodine abolished tension within 3-5 minutes ( $n=2$ ). Dysrhythmic activity elicited during early exposure to ryanodine occurred in four of five preparations tested. In addition, the steady state effects of ryanodine included a significant increase in overshoot potential, a marked increase in maximum rate of rise, and a positive shift in maximum diastolic potential. The takeoff potential, action potential duration, amplitude, and slope of  $D_1$  were not changed significantly. Since the effects of ryanodine were irreversible, recovery from the drug was not possible.

Figure 18 illustrates in more detail the specific effect of ryanodine on the slope of  $D_2$ . In this figure, every 20th action potential was traced and superimposed for the first 169 beats after exposure to ryanodine. Since there were no significant changes in maximum diastolic potential over this period (approximately 2 minutes), this portion of the action potential was superimposed. It is apparent that the predominant effect of ryanodine was a specific and progressive decrease in the slope of  $D_2$ , with little effect on the slope of  $D_1$ . At the 169th beat, the membrane potential failed to reach threshold. It should also be noted that ryanodine caused a brief initial shortening of the cycle length before lengthening occurred. This can be seen at the 20th (No. 20) action potential. In the five preparations tested, mean SCL significantly decreased by 27 msec within the first 60 seconds of ryanodine exposure (Table 4).

FIGURE 18  
 SUPERIMPOSED ACTION POTENTIALS DURING  
 RYANODINE ADMINISTRATION



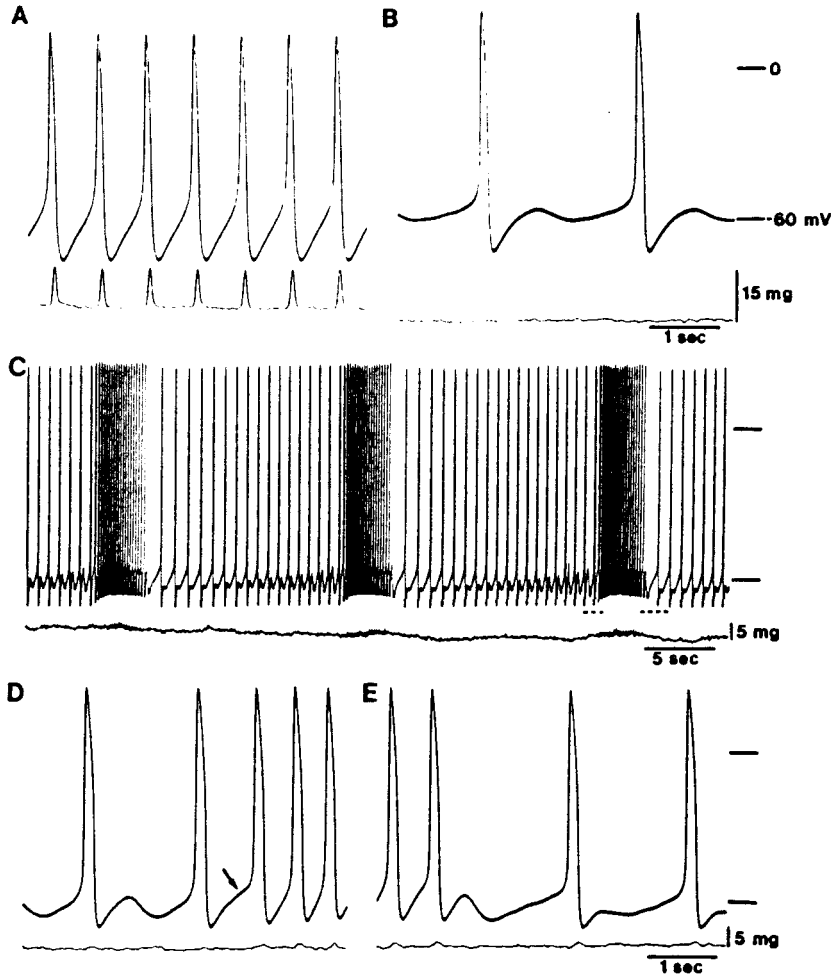
This illustration demonstrates the progressive effect of  $10^{-6}$  M ryanodine on the late phase of diastolic depolarization. Action potentials were superimposed using the maximum diastolic potential as reference point. C = control; numbers 20 through 169 indicate consecutive spontaneous beats. The dashed lines were drawn tangent with the late phase of diastolic depolarization for each beat to illustrate the changes in slope.

To assess the direct contribution of an increase in slow inward current on pacemaker automaticity, Bay K 8644 was administered after sarcoplasmic reticulum (SR) calcium release was blocked by ryanodine. Figure 19A shows control action potentials and tension. Panel B shows the steady state effects of ryanodine ( $10^{-6}$  M), that is, a decrease in  $D_2$ , an increase in SCL, and zero tension. Addition of Bay K 8644 ( $10^{-7}$  M) in the presence of ryanodine elicited a progressive increase in the amplitude of the early diastolic potential ( $D_1$ ), resulting in intermittent periods of regular pacemaker activity. Average SCL during these periods of regular activity ( $988 \pm 157$  msec) was significantly shorter than the SCL with ryanodine alone ( $2,038 \pm 172$  msec,  $p < 0.05$ ) and was not significantly different from the control SCL ( $821 \pm 61$  msec). This cyclic pattern of activity was similar to that seen during early exposure to ryanodine alone. In addition, tension returned to a small extent (approximately 2 mg), indicating an increase in intracellular calcium. This cyclic pattern of activity remained stable as long as Bay K 8644 was present. Panels D and E show an expanded view of the last period of regular activity shown in panel C (dashed lines). In Panel D, the onset of regular activity was initiated as the amplitude of the early diastolic potential increased, bringing the membrane potential to threshold (arrow). However, it is difficult to determine whether  $D_1$  was enhanced or  $D_2$  was restored. In panel E, as the maximum diastolic potential became more negative, the membrane potential failed initially to reach threshold, resulting in a delayed afterdepolarization superimposed on a slow diastolic depolarization and return to a prolonged SCL. Similar results were found in all four preparations tested with Bay K 8644 plus ryanodine. The effects of Bay K 8644 were reversible on washout of the drug (not shown).

To determine the contribution of the cesium-sensitive component after inhibition of the calcium mediated component, preparations were exposed to 1 mM cesium after at least 15 minutes of exposure to ryanodine ( $10^{-6}$  M). Figure 20A shows



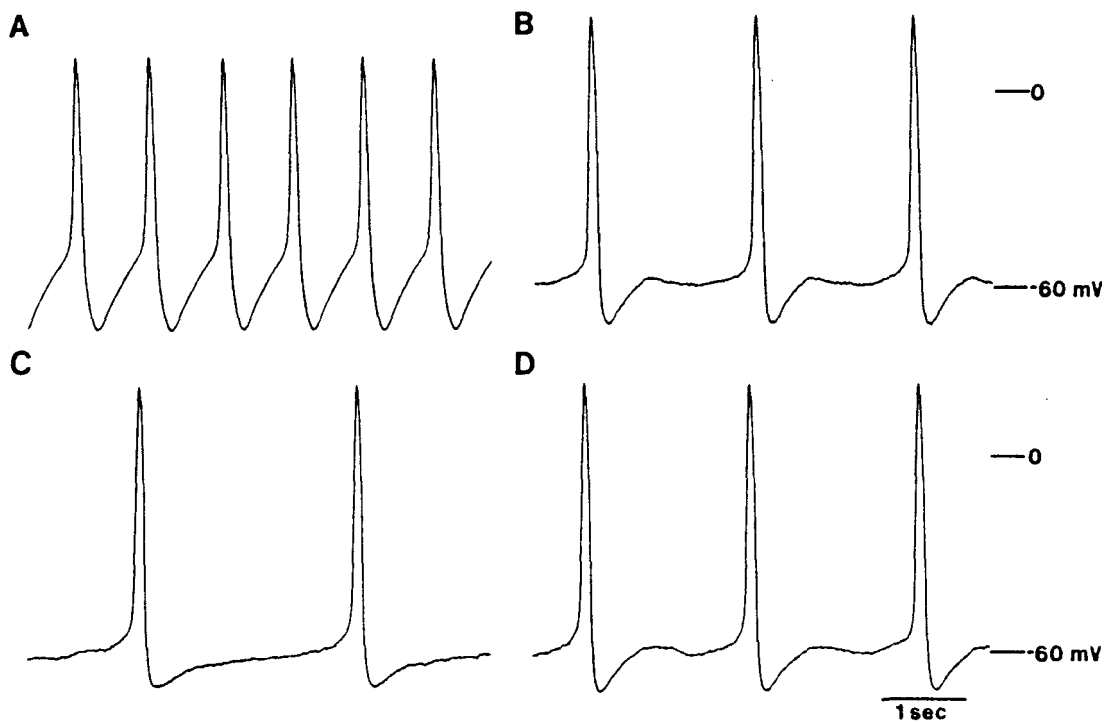
FIGURE 19  
EFFECT OF BAY K 8644 IN THE PRESENCE OF RYANODINE



The bottom trace in each panel is tension. Panel A = control; Panel B = steady state effect of  $10^{-6}$  M ryanodine alone; panel C = effect of  $10^{-7}$  M BAY K 8644 in the presence of ryanodine; panel D = expanded view of records in panel C (three dashed lines); panel E = expanded view of records in panel C (four dashed lines). Note that the time scale in panel C is 5 X slower than in panels A,B,D and E. All action potentials were recorded from the same cell.

FIGURE 20

## EFFECT OF CESIUM IN THE PRESENCE OF RYANODINE



Panel A = control; panel B = steady state effects of  $10^{-6}$  M ryanodine alone; panel C = effects of 1 mM cesium in the presence of  $10^{-6}$  M ryanodine; panel D = recovery after washout of cesium only. All action potentials were recorded from the same cell.

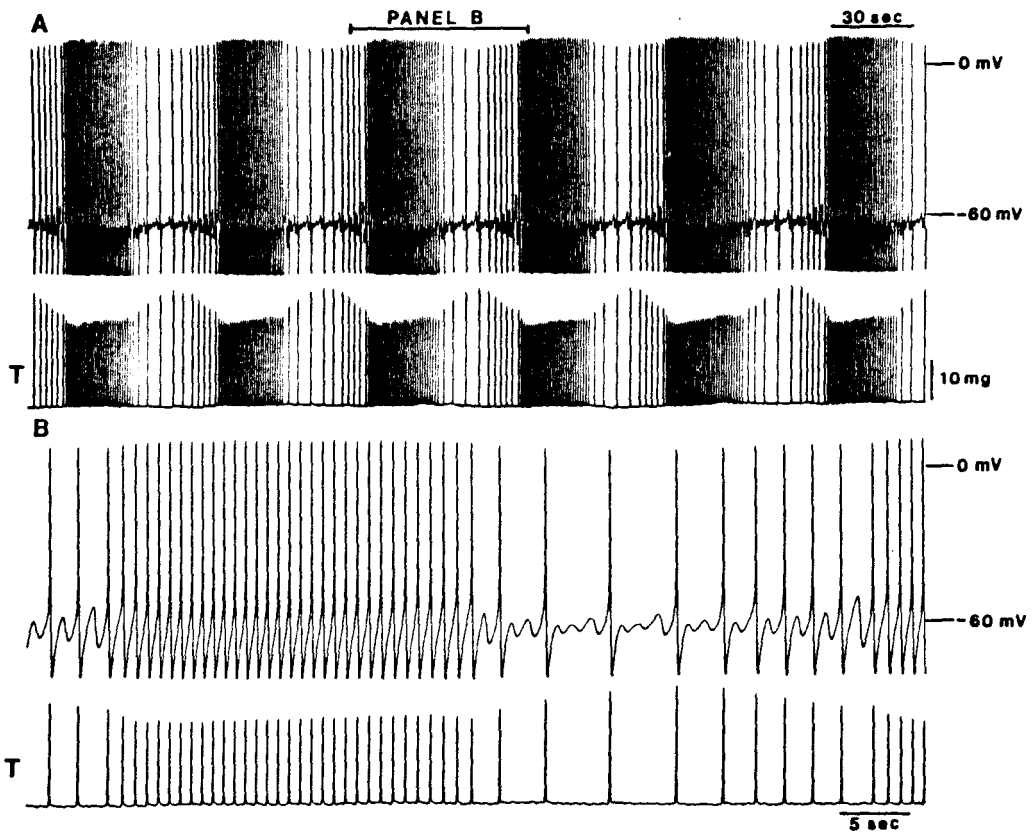
the control action potentials. Panel B shows the steady state effects of ryanodine, as previously described. In panel C, addition of 1 mM cesium decreased both the amplitude and slope of  $D_1$ , shifted the diastolic potential more negative, and further increased SCL. Panel D shows recovery after washout of cesium but still in the presence of ryanodine. In a total of six experiments, 1 mM cesium significantly increased mean SCL by  $462 \pm 98$  msec ( $+25.7 \pm 8\%$ ,  $p < 0.02$ ) and decreased the mean slope of  $D_1$  by  $15 \pm 3$  mV/sec ( $-39.3 \pm 8\%$ ,  $p < 0.005$ ). These changes were similar to those elicited by cesium under control conditions.

### C. CYCLIC BRADYDYSRHYTHMIAS GENERATED BY ATRIAL SUBSIDIARY PACEMAKERS

(J.Electrophys. 2:90-103,1988)

This work has shown that atrial muscle isolated from the ER region of cat right atrium normally generates stable subsidiary pacemaker activity (Fig 20A). In a few preparations, however, a consistent pattern of dysrhythmic activity developed spontaneously in preparations that previously exhibited rhythmic pacemaker activity. The records in Figure 21 show a typical example of this dysrhythmia. Panel A was recorded at a relatively slow chart speed in order to show the cyclic pattern and consistent nature of the activity. Panel B shows a portion of the records in panel A at an expanded time scale. Changes in SCL and maximum diastolic potential (MDP) during three periods of activity have been quantitated in the graph in Figure 22. As shown in Figure 21, periods of rhythmic pacemaker activity are cyclically interrupted by periods of irregular bradycardia. Periods of rhythmic pacemaker activity are characterized by gradual changes in cycle length: an initial decrease to about 800 msec followed by a gradual increase to about 1000 msec (Fig. 22). As cycle length progressively increased, the diastolic membrane potential eventually failed to reach

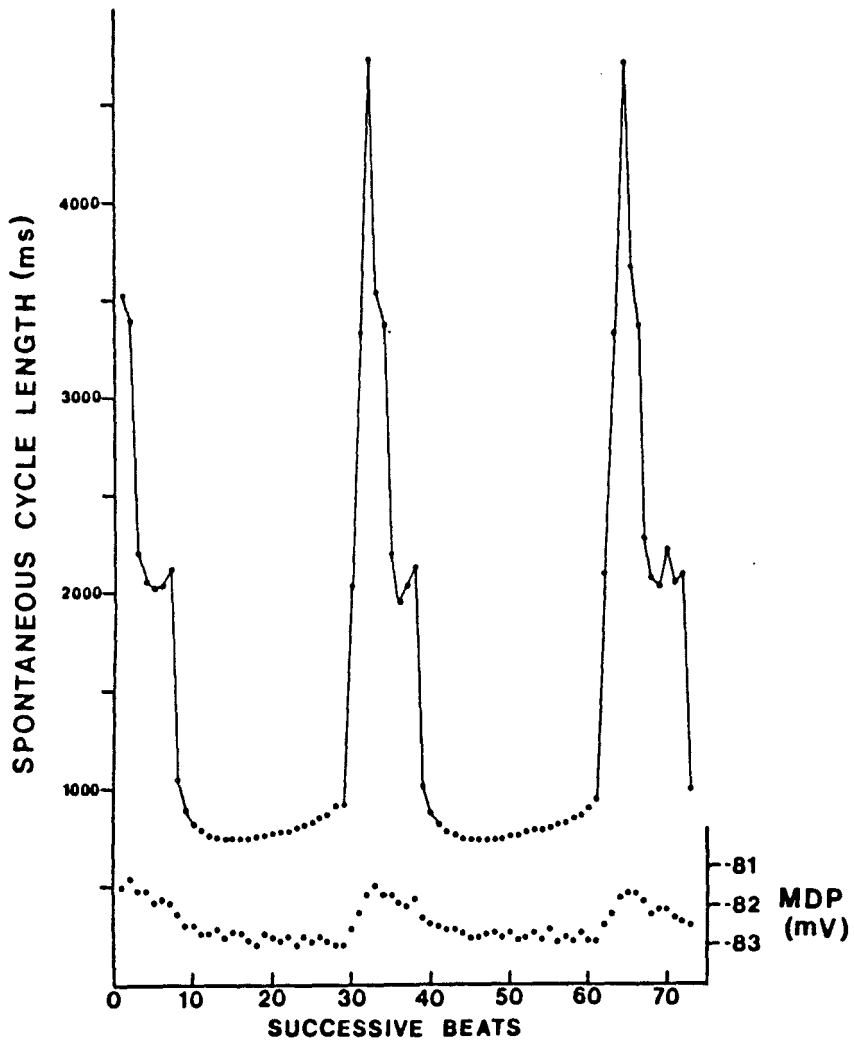
FIGURE 21  
 VOLTAGE AND TENSION RECORDS OF A TYPICAL  
 CYCLIC BRADYDYSRHYTHMIA



Action potentials and tension (T) recorded from a subsidiary atrial pacemaker exhibiting a typical cyclic bradydysrhythmia. The bar at the top of panel A, (labeled PANEL B), indicates the section of the recording that is illustrated in panel B, at an expanded time scale. Tyrode's solution contained 2.7 mM  $[Ca]_o$ , atenolol ( $10^{-6}$  M) plus atropine ( $10^{-7}$  M).

FIGURE 22

BEAT TO BEAT CHANGES IN SPONTANEOUS CYCLE LENGTH  
AND MAXIMUM DIASTOLIC POTENTIAL



Changes in spontaneous cycle length and maximum diastolic potential (MDP) for each successive beat during three cycles of a dysrhythmia. The lines connecting the spontaneous cycle length data points were included for clarity.

threshold (Fig. 21B), resulting in a single oscillation and an increase in SCL. Over the next three beats, SCL progressively increased as the earlier oscillations in diastolic potential failed to reach threshold. At this time, SCL reached a maximum of almost 5 sec (Fig. 22).

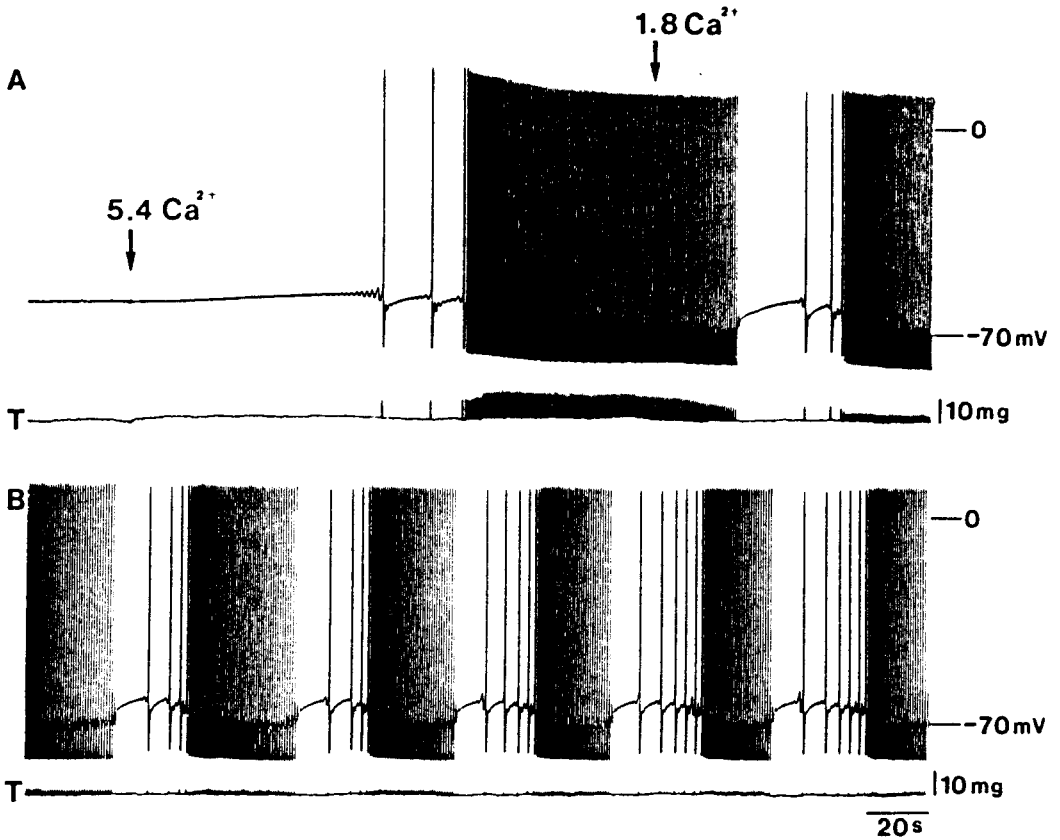
Cycle length then began to progressively decrease as the amplitude of the last diastolic oscillation in each interval increased and attained threshold. Eventually, only a single oscillation followed each action potential. This oscillation progressively increased in amplitude, producing irregular changes in SCL (Fig. 22). When the oscillation became large enough to reach threshold, another period of rhythmic pacemaker activity was initiated. It should be noted that, during the periods of bradycardia, the initial diastolic slope is unchanged and only the later phase of diastolic depolarization is decreased and exhibits oscillatory activity. The graph in Figure 22 shows that the MDP changed in phase with SCL. As SCL increased at the onset of a period of bradycardia, MDP became more positive and then, as SCL decreased, it became more negative. During periods of rhythmic pacemaker activity, the MDP hyperpolarized slightly. Action potential amplitude also exhibited frequency-dependent alterations. Amplitude reached its nadir at the longest cycle length and increased to a steady-state during periods of rhythmic activity. Frequency-dependent changes in tension are evident as well. Starting with a period of rhythmic activity, tension initially dipped and then exhibited a gradual positive staircase. As cycle length increased during the bradycardia, tension displayed a more marked positive staircase and then declined as cycle length shortened.

Cyclic bradydysrhythmias developed spontaneously in a total of 12 preparations which previously exhibited stable, rhythmic pacemaker activity. The dysrhythmia developed after variable periods of time in vitro, ranging from minutes to several hours, and invariably led to quiescence. One additional preparation exhibited the dysrhythmia

when first placed in the tissue bath. The spontaneous onset of the dysrhythmia was always associated with a gradual run-down in pacemaker activity, as characterized by an increase in spontaneous cycle length. However, it should be noted that increases in spontaneous cycle length were commonly observed in other experiments in which bradydysrhythmias did not appear. In seven preparations exhibiting the dysrhythmia, periods of rhythmic pacemaker activity averaged  $18.9 \pm 0.4$  sec and periods of bradycardia averaged  $18.8 \pm 1.4$  sec. Cyclic bradycardias lasted from only a few minutes up to 3 hours.

Bradydysrhythmias were also induced in four quiescent preparations by brief exposure to either relatively low concentrations of NE ( $2-4 \times 10^{-9}$  M;  $n=3$ ) or elevated  $[Ca]_o$  (2.7-5.4 mM;  $n=2$ ). Each of these preparations initially exhibited rhythmic spontaneous activity. Three of the four preparations exhibited periods of bradydysrhythmia before becoming quiescent. Figure 23 shows a typical response to high  $[Ca]_o$  of a quiescent preparation which had exhibited a bradydysrhythmia prior to quiescence. At the left in panel 23A, the resting membrane potential is recorded in Tyrode's solution containing 1.8 mM  $[Ca]_o$ ; At the arrow, raising  $[Ca]_o$  to 5.4 mM elicited a gradual depolarization of the resting membrane potential, the development of oscillatory prepotentials, and the initiation of sustained rhythmic activity. After approximately 2 minutes,  $[Ca]_o$  was returned to 1.8 mM. This resulted in a gradual decrease in tension, an increase in SCL, and after about 25 seconds, the development of a typical pattern of cyclic bradydysrhythmia. Brief exposure to NE had effects similar to those of elevated  $[Ca]_o$ . Although NE could induce bradydysrhythmias, its presence was not required to sustain them. Short exposures ( $\leq 2$  min) to NE could induce cyclic bradycardias which were sustained for up to 42 minutes. Moreover, in four experiments, cyclic bradycardias were unaffected by autonomic receptor blockade with atenolol ( $10^{-6}$  M) plus atropine ( $10^{-7}$  M).

FIGURE 23  
CYCLIC BRADYDYSRHYTHMIA INDUCED BY HIGH  $[Ca]_o$



Effect of high extracellular calcium concentration ( $[Ca]_o$ ) to induce the development of a cyclic bradydysrhythmia in a quiescent preparation. The preparation was exposed to  $5.4 \text{ mM } [Ca]_o$  for approximately 2 min. and then returned to control  $1.8 \text{ mM } [Ca]_o$ . The signals in panel A and B are continuous recordings and were taken from the same cell. Tyrode's solution contained atenolol ( $10^{-6} \text{ M}$ ) and atropine ( $10^{-7} \text{ M}$ ).

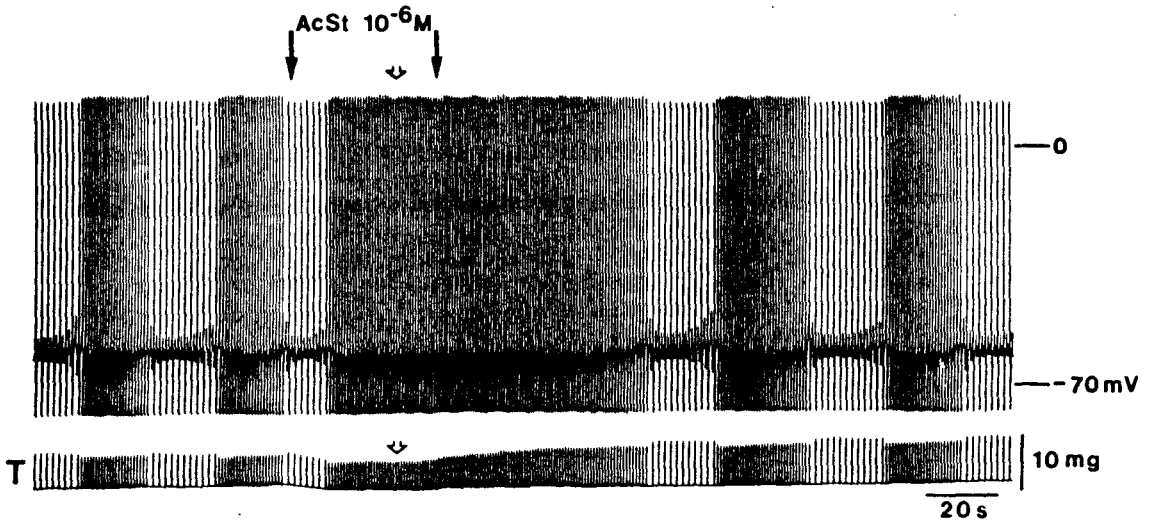


The frequency dependent changes in maximum diastolic potential suggested that activation of an electrogenic sodium pump current may be responsible for modulating the cyclic pattern of activity. To test this point, preparations exhibiting cyclic bradycardias were exposed to acetylstrophanthidin (AcSt) to inhibit sodium pump activity. As shown in Figure 24, before exposure to AcSt, periods of rhythmic pacemaker activity and bradycardia lasted approximately 19 and 18 sec, respectively. The preparation was exposed to  $10^{-6}$  M AcSt about 2 seconds after the onset of a period of bradycardia. Exposure to AcSt shortened the period of bradycardia, resulting in the initiation of rhythmic pacemaker activity 8 seconds earlier than under control conditions. It is also apparent that at 19 seconds (open arrow; upper trace), when the bradycardia would have reappeared before exposure to AcSt, pacemaker activity was now sustained. Also note, at this time, AcSt had no affect on tension (open arrow; lower trace). In fact, tension only began to increase above control values approximately 5 seconds after exposure to AcSt was discontinued (second solid arrow). Approximately 58 seconds after exposure to AcSt was discontinued, the bradycardia reappeared. Note that the bradycardia returned at a time when tension and presumably intracellular calcium were elevated. In three additional experiments (in which tension was not recorded), lower concentrations of AcSt ( $2-4 \times 10^{-7}$  M) had similar effects on pacemaker activity. In two of the three experiments, atenolol ( $10^{-6}$  M) and atropine ( $5 \times 10^{-7}$  M) were present. In one additional experiment where tension was measured, exposure to  $4 \times 10^{-7}$  M AcSt for approximately 3 minutes established sustained, rhythmic pacemaker activity and had no affect on tension.

The contribution of the electrogenic pump activity was tested further by electrically pacing dysrhythmic preparations to enhance pump activity. Preparations were electrically stimulated with a bipolar extracellular electrode using square wave pulses of 2-3 msec duration at 50% above threshold voltage. Pacing cycle length was set

FIGURE 24

## EFFECT OF ACETYLSTROPHANTHIDIN ON CYCLIC BRADYDYSRHYTHMIAS



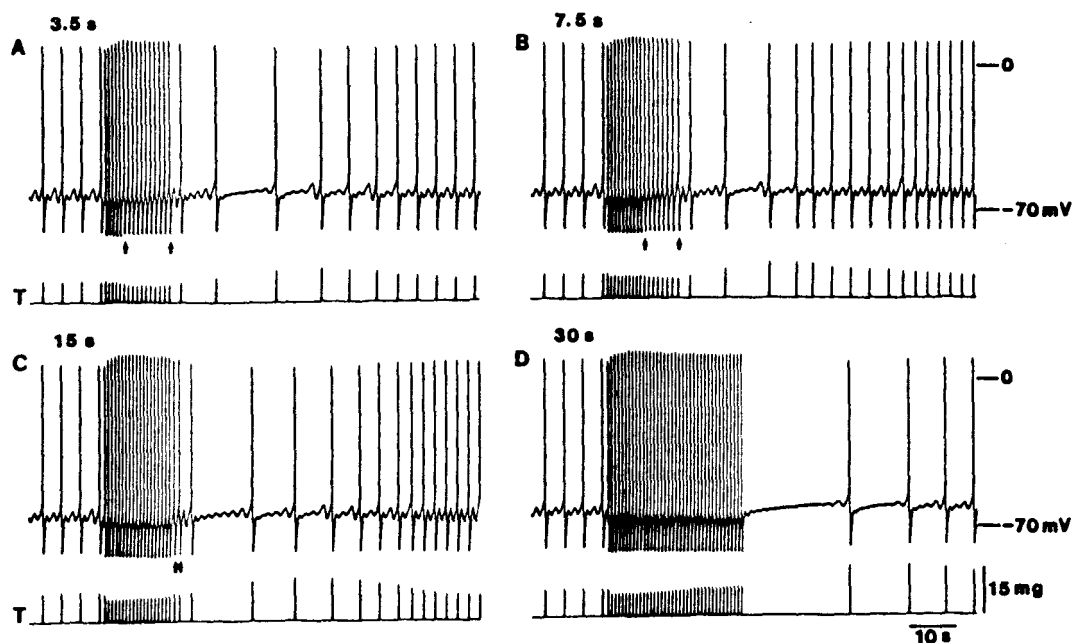
Effect of  $10^{-6}$  M acetylstrophanthidin (AcSt) on action potentials and tension (T) of a preparation exhibiting cyclic brady rhythms. AcSt was administered for 40 s (filled arrows). The upper open arrow indicates the time at which the brady rhythm would have re-appeared in the absence of AcSt. Note AcSt established rhythmic pacemaker activity at a time when tension was unchanged (lower open arrow).

at approximately the same cycle length that the preparation beat spontaneously during periods of rhythmic pacemaker activity. The pacing protocols were performed on preparations which initially exhibited cyclic dysrhythmias that stabilized into relatively rhythmic periods of bradycardia. Figure 25 shows the response to pacing at 800 msec for 3.5, 7.5, 15, and 30 seconds. The Tyrode's solution contained atenolol ( $10^{-6}$  M) and atropine ( $10^{-7}$  M) to prevent the effects of any endogenous neuromediators that may have been released by electrical stimulation (38). Shorter pacing periods resulted in the development of spontaneous action potentials immediately following the pacing period, which were inversely related in number to the pacing duration. Thus, pacing for 3.5, 7.5, and 15 seconds elicited 11, 8, and 2 spontaneous beats, respectively. At a longer pacing duration of 30 seconds, only suppression of pacemaker activity was elicited. Pacing for 60 seconds elicited a greater period of suppression (not shown). It should be noted that the banding created by the stimulus artifact (best illustrated in Fig. 25D) initially rises and then falls during the pacing period. This was due to the diastolic membrane potential becoming initially more positive and then more negative at the time of stimulation, resulting from an initial increase and then decrease, respectively, in the slope of diastolic depolarization. Qualitatively similar results were obtained in a total of three preparations tested.

The previous work has shown that intracellular calcium may mediate a component of subsidiary pacemaker automaticity. This suggested that the development of the dysrhythmia may be related to alterations in intracellular calcium and, thereby, automaticity. To test this hypothesis, dysrhythmic preparations were exposed to elevated  $[Ca]_o$  or NE to enhance intracellular calcium. Figure 26 shows action potentials and tension recorded from a preparation exhibiting cyclic bradycardias in 1.8 mM  $[Ca]_o$ . At the first arrow,  $[Ca]_o$  was increased from 1.8 to 5.4 mM. The tension recordings indicate that within 3-4 beats intracellular calcium was increased, and by the end of the

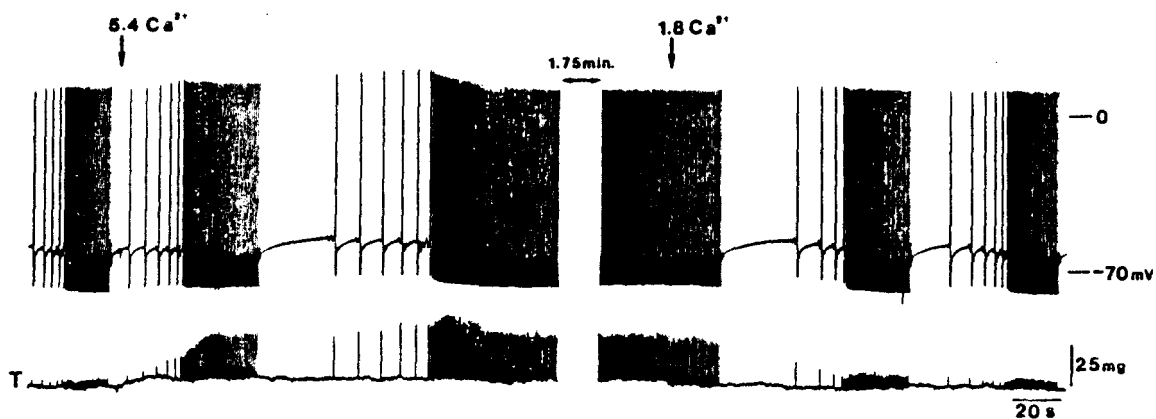
FIGURE 25

## EFFECT OF ELECTRICAL PACING OF DYSRHYTHMIC EUSTACHIAN RIDGE



Effect of electrical pacing on action potentials and tension (T) of a dysrhythmic preparation. The numbers at the top of panels A-D indicate the duration of pacing in seconds. The filled arrows in panel A-C indicate the first and last non-driven beats elicited immediately following each pacing period. Signals in each panel were recorded from the same cell.

FIGURE 26

EFFECT OF 5.4 mM  $[Ca]_o$  ON A DYSRHYTHMIC EUSTACHIAN RIDGE

Effect of 5.4 mM  $[Ca]_o$  on action potentials and tension (T) recorded from a dysrhythmic preparation. A 1.75 min. section of rhythmic pacemaker activity was deleted for clarity of presentation. Tyrode's solution contained atenolol ( $10^{-6}$  M) and atropine ( $10^{-7}$  M).

next period of rhythmic activity, tension was six times greater than control. This first period of rhythmic activity in 5.4 mM calcium was already longer in duration than control. In addition, the cycle length following this period was significantly longer and required more time to recover. Once pacemaker activity resumed, however, it remained stable as long as  $[Ca]_o$  was elevated. At the second arrow,  $[Ca]_o$  was returned to 1.8 mM and within about 25 seconds rhythmic pacemaker activity ended and the dysrhythmic pattern returned. Note that tension was still elevated when rhythmic activity ended and the bradycardia returned. Similar results were obtained in a total of five preparations where  $[Ca]_o$  was raised to 5.4 mM (n=3) or 2.7 mM (n=2).

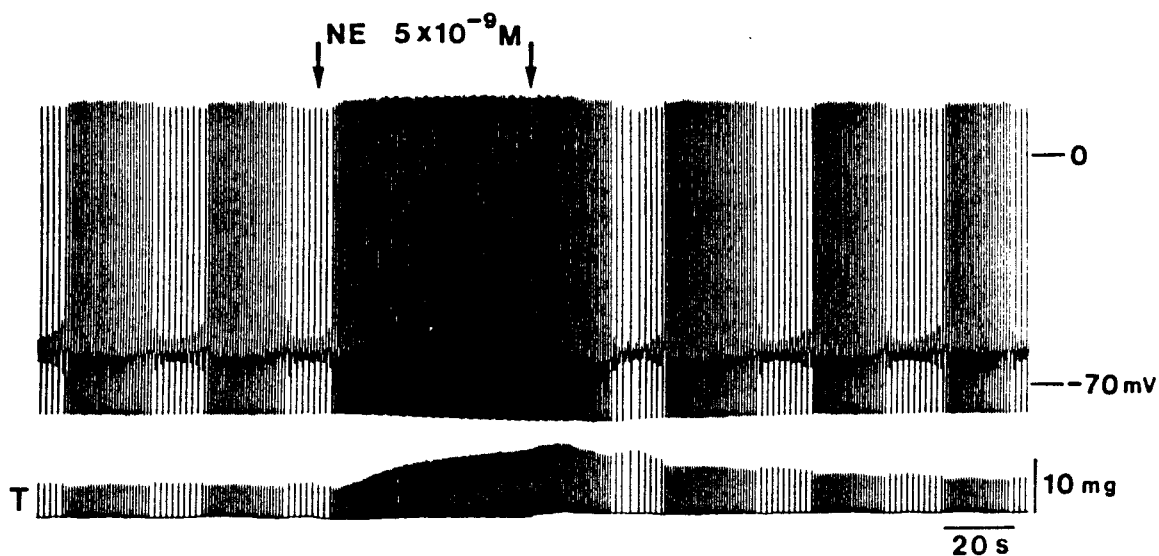
As shown in Figure 27, exposure of dysrhythmic preparations to  $5 \times 10^{-9}$  M NE also prevented development of bradycardias by establishing rhythmic pacemaker activity. Before exposure to NE, periods of rhythmic activity lasted about 23 seconds. NE was administered toward the end of a period of bradycardia for 60 seconds (arrows). It is apparent that NE established rhythmic activity and a progressive increase in tension. Approximately 23 seconds after NE was discontinued, the bradycardia returned even though tension was still elevated. Similar results were obtained in a total of five experiments with NE concentrations  $2-5 \times 10^{-9}$  M. Tension was measured in two of five experiments.

In two experiments, dysrhythmic preparations were briefly exposed (5 minutes) to verapamil ( $0.5$  to  $1.0 \times 10^{-7}$  M). Verapamil decreased periods of rhythmic pacemaker activity and prolonged periods of bradycardia (data not shown). Longer exposure resulted in bradycardias that led to quiescence.

In the previous study of normal subsidiary pacemaker function it was shown that ryanodine, a putative blocker of SR calcium release (339,497), specifically depressed the later phase ( $D_2$ ) of diastolic depolarization, significantly inhibiting automaticity. Figure 28 shows a typical experiment in which panel A shows control action potentials

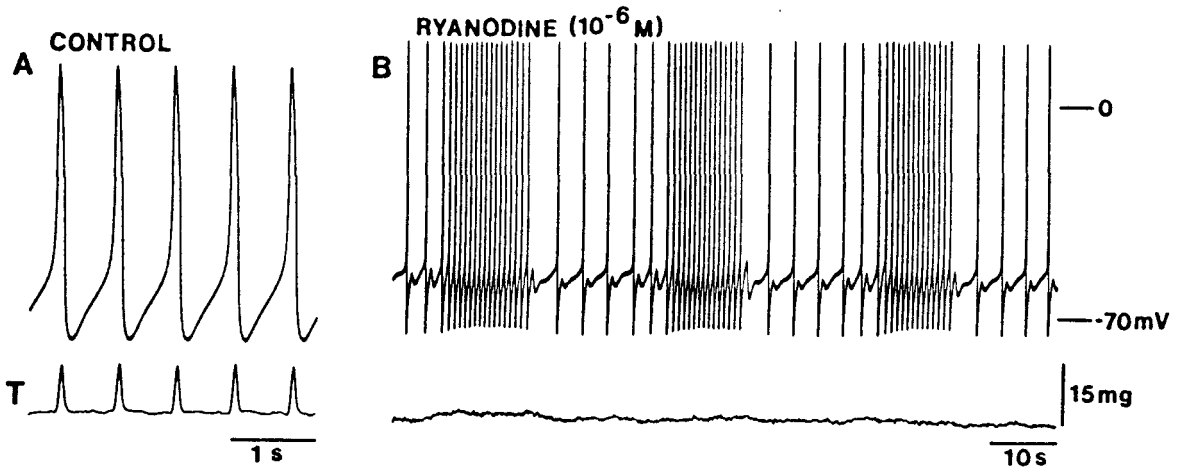
FIGURE 27

## EFFECT OF NOREPINEPHRINE ON CYCLIC BRADYDYSRHYTHMIAS



Effect of  $5 \times 10^{-9}$  M norepinephrine (NE) on action potentials and tension (T) recorded from a dysrhythmic preparation. NE was administered for approximately 60 s.

FIGURE 28  
RYANODINE INDUCED BRADYDYSRHYTHMIA



Effect of ryanodine on spontaneous action potentials and tension (T) recorded from a preparation exhibiting rhythmic pacemaker activity. Panel A shows control action potential configuration and tension (T). In panel B the preparation had been exposed to  $10^{-6}$  M ryanodine for approximately 3 min. Note that the time scale in Panel A is ten times greater than in panel B. Signals in panel A and B were recorded from the same cell.



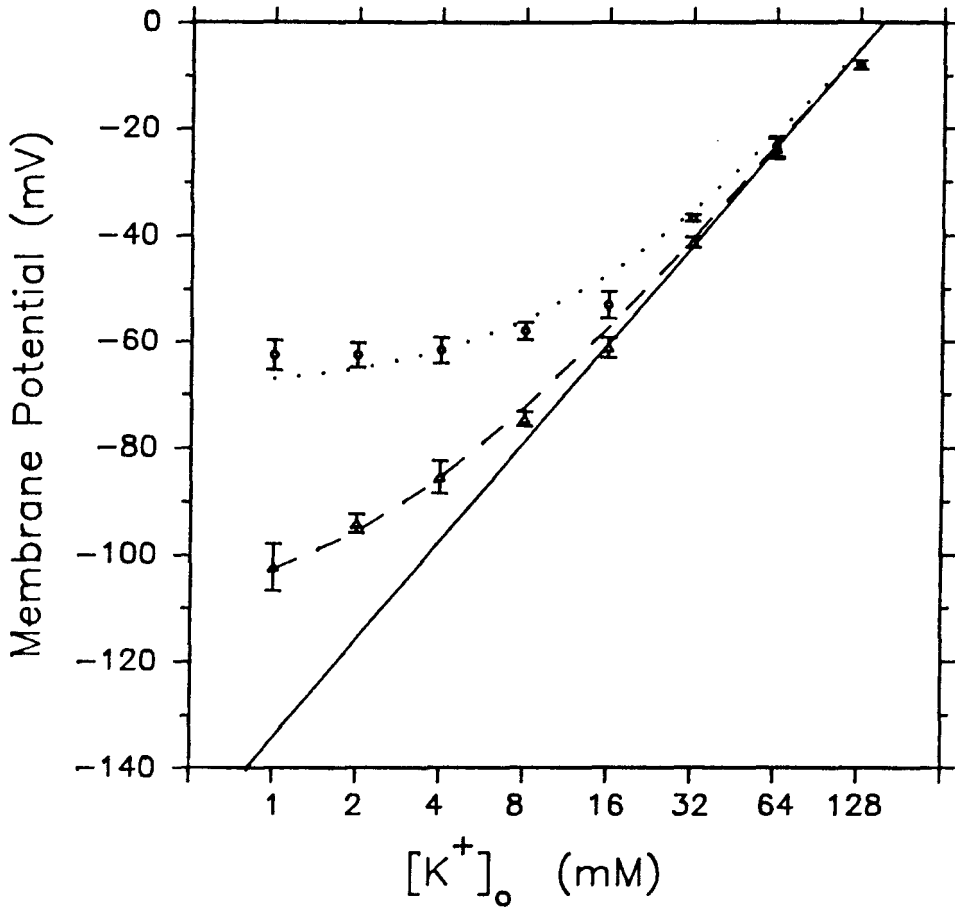
and tension recordings from a preparation exhibiting stable, rhythmic pacemaker activity. In panel B, the preparation had been exposed to  $10^{-6}$  M ryanodine for about 3 minutes. It is apparent that ryanodine elicited a pattern of cyclic bradycardia qualitatively similar to those preparations in which the dysrhythmia developed spontaneously or was induced. During the bradycardia, the later portion of diastolic depolarization is reduced, while the initial slope is unaffected. The oscillatory potentials during diastolic intervals are significantly attenuated compared to those in the dysrhythmias occurring spontaneously or were induced in quiescent preparations. Ryanodine also abolished tension. Dysrhythmias induced by ryanodine usually lasted 8-10 minutes. Over time, periods of bradycardia lengthened and periods of rhythmic pacemaker activity shortened until a rhythm with a prolonged cycle length ensued (not shown). Ryanodine induced cyclic bradycardias in four of five preparations tested.

#### D. SUBSIDIARY PACEMAKER RESISTANCE TO $[K]_o$

##### 1. $P_{Na}/P_K$ Ratio

It was shown that the MDP of spontaneously active Eustachian ridge preparations was not significantly different from SA node pacemakers. In addition, quiescent preparations in normal  $[K]_o$  exhibited resting membrane potentials (RMP) near -60 mV similar to SA node. This suggested that the passive membrane properties of the ER, specifically the  $P_{Na}/P_K$  ratio, might also be similar to that of nodal pacemaking fibers. In five ER preparations made quiescent by a background concentration of  $10^{-6}$  M verapamil, the RMP was recorded in 8 different extracellular potassium concentrations ( $[K]_o$ ; logarithmic changes), ranging from 1 mM to 128 mM. The sum  $[K]_o + [Na]_o$  was kept constant at 153 mM in the different solutions tested. The RMP stabilized within 3-4 minutes of the solution change. In Figure 29, the RMP is plotted against the  $\log [K]_o$  (open circles). In addition, if it is assumed that membrane of the ER cells is permeable

FIGURE 29

 $P_{Na}/P_K$  RATIO WITH AND WITHOUT ACETYLCHOLINE

Resting membrane potential was recorded at different  $[K^+]_o$  levels. Open circle or triangles (open circle: control; open triangle:  $10^{-4}$  M ACh) represent mean control values ( $N=5$ ) at all levels of  $[K^+]_o$  except  $[K^+]_o = 128$  mM ( $N=3$ ), and vertical bars indicate  $\pm$  S.E. Note the linear-log scale. Solid line is the calculated  $E_K$  at  $36^\circ$  C, and  $[K^+]_i = 155$  mM. Dotted line is calculated Goldman-Hodgkin-Katz equation with  $P_{Na}/P_K = 0.076$ , and dashed line has a  $P_{Na}/P_K = 0.015$ .

to only potassium ions then the equilibrium potential of potassium ( $E_K$ ) should accurately predict the RMP in the different potassium concentrations.  $E_K$  was calculated,

$$E_K = \frac{R T}{F} \ln \frac{[K]_o}{[K]_i} ,$$

and plotted for comparison (solid line).  $R$  is the gas constant,  $T$  is the absolute temperature, and  $F$  is the Faraday constant. The  $[K]_i$  is assumed to be 155 mM (53). Furthermore, it is assumed that the  $[K]_i$  remains relatively constant during these short changes in  $[K]_o$  (170). It is clear that at the lower levels of  $[K]_o$  that the equilibrium potential for potassium fails to accurately predict the measured values of RMP. This result suggests that the relatively low RMP may be secondary to either a low  $[K]_i$  or that the membrane is not exclusively permeable to potassium. The low RMP of cells in the canine coronary sinus, was predominantly due to a cellular permeability to sodium ions (53). Therefore, the Goldman (193), Hodgkin & Katz (225) equation was employed in a similar fashion:

$$V_m = \frac{R T}{F} \ln \frac{[K]_o + P_{Na}/P_K [Na]_o}{[K]_i + P_{Na}/P_K [Na]_i} ,$$

to determine if sodium permeability could also explain the relatively low RMP seen in this tissue. By setting the  $P_{Na}/P_K$  ratio to a value of 0.076, a line (dotted line) was generated that closely fit the data. Examination of the results of this line, shows that a large deviation from  $E_K$  results at the lower  $[K]_o$  levels. But when  $[K]_o$  is increased, the RMP more closely approximates  $E_K$ . Therefore, it is apparent that 155 mM is an accurate approximation of the  $[K]_i$ . Thus it is suggested that the relatively low RMP is due to a high  $P_{Na}/P_K$  ratio.

This conclusion can also be ascertained by a second method which experimentally decreases the  $P_{Na}/P_K$  ratio (53). A decrease in the  $P_{Na}/P_K$  ratio, by increasing the permeability to K ions should shift the RMP to more closely approximate  $E_K$ .

Stimulating muscarinic receptors are known to increase K permeability in atrial cells (84,180,235,329,521). Therefore, acetylcholine should decrease the  $P_{Na}/P_K$  ratio and hyperpolarize the membrane potential to values closer to  $E_K$ . The effect of  $[K]_o$  was repeated on the Eustachian ridge preparations. When the RMP had stabilized, the solution was switched to one containing  $10^{-4}$  M acetylcholine for short durations of 15-30 seconds. The resulting RMP was again plotted against  $\log [K]_o$  (open triangles, Figure 29), illustrating the shift toward  $E_K$ . The best fit curve (dashed line) according to the Goldman-Hodgkin-Katz equation had a  $P_{Na}/P_K$  ratio equal to 0.015 (five times less than above). Atropine, the muscarinic blocker, at concentrations of  $10^{-5}$  M blocked the effects produced by acetylcholine.

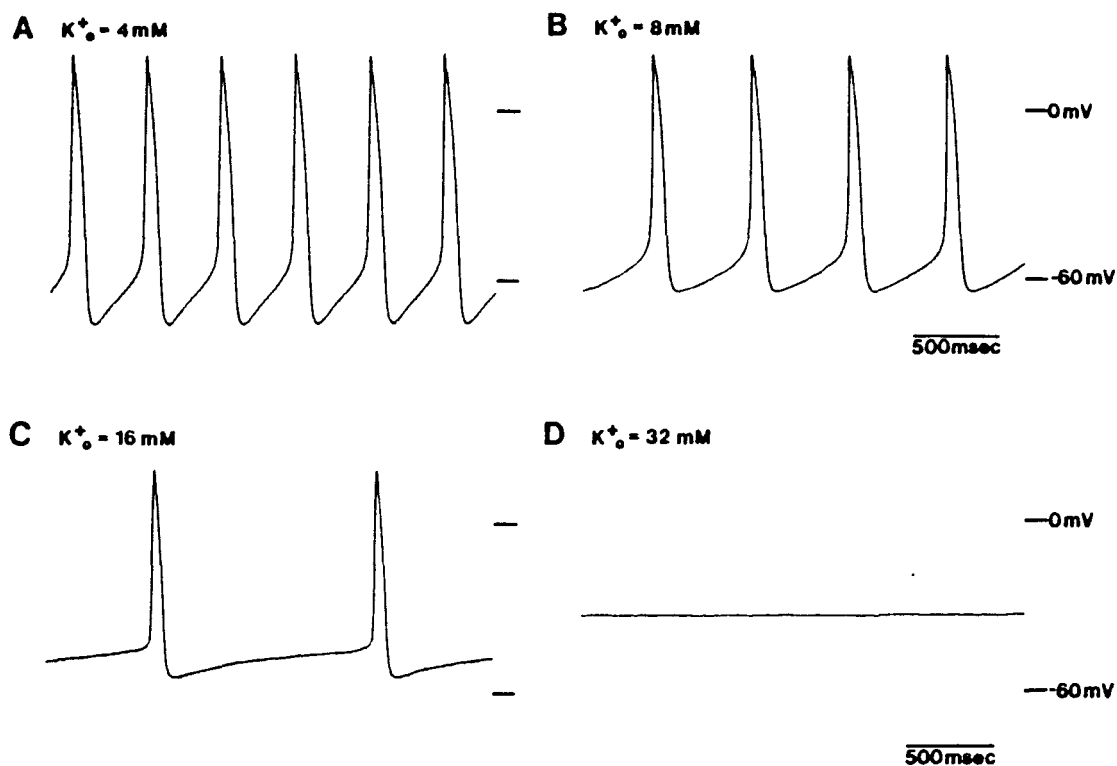
To directly assess sodium permeability, six preparations were studied in low sodium (50% of control). Exposing the tissues to low sodium for 30 seconds elicited a significant hyperpolarization of the RMP (control:  $-55.9 \pm 1.7$  mV vs. 50% Na:  $-61.0 \pm 2.2$  mV,  $p < .001$ ). During washout of the low sodium solutions it was noted that there were immediate depolarizations to levels above the control RMP.

## 2. Effect of $[K]_o$ on Spontaneous Activity

Many cardiac cells within the distribution of the SA ring bundle have been shown to be resistant to elevated  $[K]_o$  (53,110,228,335,336,549,550). The K resistance is associated with a high  $P_{Na}/P_K$  ratio, resulting from a low  $i_{K1}$  current density  $P_K$ , (183,386,450). This raises the question of whether the subsidiary pacemakers in the ER will exhibit K resistance.

Six spontaneously active ER tissues were each exposed to five different  $[K]_o$ , ranging from 1 mM to 16 mM. Action potentials were measured after equilibrating for 3-5 minutes. As shown in Figure 30, all preparations remained spontaneously active in

FIGURE 30

SUBSIDIARY PACEMAKER AUTOMATICITY IS RESISTANT TO HIGH  $[K]_o$ .

Atrial subsidiary pacemaker in the Eustachian ridge is resistant to elevated levels of  $[K]_o$ . Automatic activity persists in 16 mM  $[K]_o$ . At 32 mM  $[K]_o$ , activity is abolished and the RMP is approximately -34 mV.

16 mM  $[K]_o$ . At 8 mM  $[K]_o$ , SCL was significantly increased (Table 5, control:  $595 \pm 100$  ms vs. 8 mM:  $721 \pm 119$  ms;  $p < 0.01$ ), and the MDP was significantly decreased (control:  $-78 \pm 3.2$  mV vs. 8 mM:  $-68.9 \pm 3.0$  mV;  $p < 0.001$ ). In 16 mM  $[K]_o$ , the SCL, although more variable, increased further ( $8651 \pm 2367$  ms), and an additional significant depolarization of the MDP was seen ( $-54.1 \pm 2.1$  mV,  $p < 0.001$ ). Four of these preparations were also exposed to 32 mM  $[K]_o$ , all of these were rendered quiescent and had a mean RMP of  $-34.4$  mV.

## E. MECHANISMS OF INITIATION OF ATRIAL SUBSIDIARY

### PACEMAKER ACTIVITY

In several preparations (32%), the cat ER was found to be quiescent, but could initiate activity in the presence of relatively low concentrations of NE (1-10 nM). Initiation is a stimulation through ionic or pharmacologic manipulations of the preparation to generate automaticity without stimulated action potentials. A typical initiation sequence by NE is seen in Figure 31 (panel A). During the infusion of the NE containing solution, the RMP gradually depolarizes, forms oscillatory prepotentials, until reaching the threshold potential. Once threshold is reached, sustained rhythmic activity is maintained until washout of the NE. This study investigates the possible electrophysiologic mechanisms of initiation.

#### 1. Effect of Adrenergic Blockade

To determine the relative extent that the NE-induced responses were mediated via  $\alpha_1$  or  $\beta_1$  adrenergic receptors, preparations were pretreated with either  $10^{-6}$ M atenolol (selective beta-1 blocking agent) or  $10^{-6}$ M prazosin (selective alpha-1 blocking agent). Neither atenolol nor prazosin alone had any significant effect on the RMP. In all ten preparations tested, atenolol, but not prazosin, blocked initiation of activity by NE. In

TABLE 5

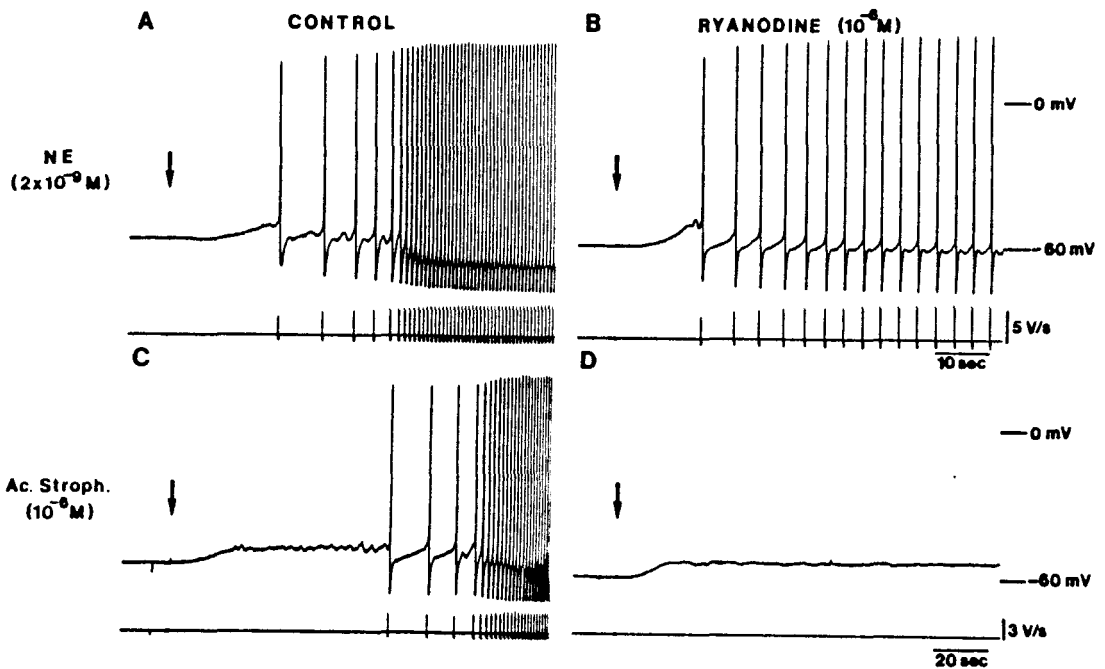
	SCL (ms)	MDP (mV)	OSP (mV)	AMP (mV)	TOP (mV)	APD (ms)	D1 (mV/s)	D2 (mV/s)	dv/dt (V/s)
CONTROL	595±100	-78.0±3.2	10.3±2.3	88.4±4.9	-60.6±1.5	98±7	60±4	47±7	9.6±1.5
1 mM [K] <sub>o</sub>	518±89	-81.3±4.5	6.6±2.2	87.9±6.2	-62.4±3.8	106±7	87±13	78±17	7.4±1.6
2 mM [K] <sub>o</sub>	602±91	-81.7±4.5 <sup>+</sup>	9.2±1.8 <sup>+</sup>	90.9±5.0 <sup>+</sup>	-62.1±1.9	103±7 <sup>+</sup>	74±7	62±9	8.4±1.2
8 mM [K] <sub>o</sub>	721±119	-68.9±3.0 <sup>*</sup>	11.0±1.4	80.8±3.5 <sup>*</sup>	-57.5±2.7	93±8	27±5 <sup>*</sup>	27±5 <sup>*</sup>	9.9±1.3
16 mM [K] <sub>o</sub>	3651±2367	-54.1±2.1 <sup>*</sup>	11.6±2.1	65.7±3.6 <sup>*</sup>	-46.4±2.3 <sup>*</sup>	81±6 <sup>*</sup>	18±4 <sup>*</sup>	10±4 <sup>*</sup>	6.9±0.9

Values represent mean ± standard error of the mean. SCL = spontaneous cycle length; MDP = maximum diastolic potential; OSP = overshoot potential; AMP = total amplitude; TOP = take-off potential; APD = action potential duration (60%); D1 = slope of early diastolic depolarization; D2 = slope of late diastolic depolarization.

<sup>+</sup> = p < 0.05; <sup>\*</sup> = p < 0.01; <sup>\*</sup> = p < 0.001

FIGURE 31

INITIATION OF ACTIVITY WITH NOREPINEPHRINE AND ACETYL-  
STROPHANTHIDIN: DIFFERENT EFFECTS OF RYANODINE



Panel A: Administration of  $2 \times 10^{-9}$  M NE to quiescent Eustachian ridge preparation (arrows in A and B), induced a depolarization of the RMP, causing small oscillatory prepotentials, until reaching threshold. Bottom trace shows first derivative of action potential voltage changes. Panel B: NE initiation in same preparation as in A, after equilibration in  $10^{-6}$  M ryanodine. Recordings in panels A and B are from the same preparation. Panel C: Administration of  $10^{-6}$  M AcSt initiates activity (arrows in C and D). Panel D: After equilibration in ryanodine, AcSt fails to initiate activity. Bottom traces are the first derivative of the action potential voltage changes. Recordings in panels C and D are from the same preparation.



3 additional experiments, 5-50 nM isoproterenol (a specific beta-1 receptor agonist) was also shown to initiate activity similar to NE. Furthermore, isoproterenol initiation was also blocked by  $10^{-6}$  M atenolol.

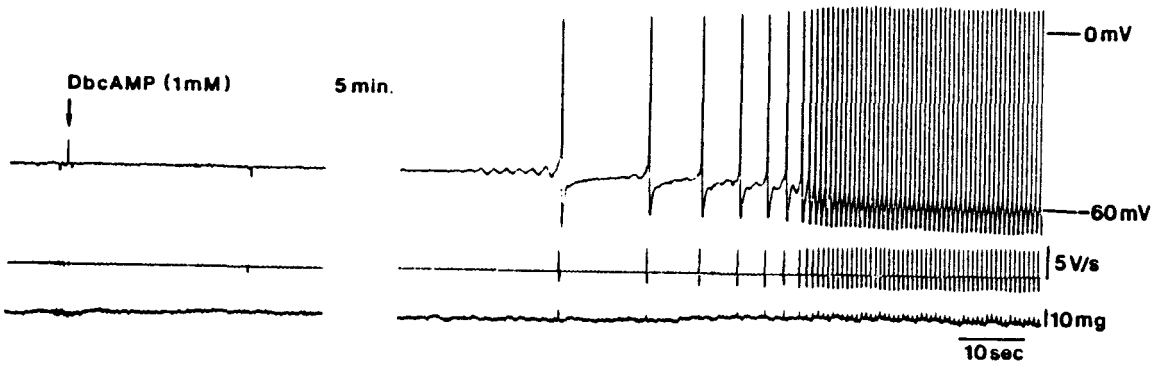
## 2. Effect of Dibutyryl Cyclic AMP (DBcAMP)

NE is known to affect myocardial tissues primarily through mechanisms involving activation of adenylate cyclase and increasing intracellular cAMP (211,373,399,530). To determine if NE initiation resulted from cAMP mediated events, dibutyryl cAMP was studied in five preparations at concentrations of either 0.5mM or 1 mM. Tissues were equilibrated in  $10^{-6}$  M atenolol and  $10^{-7}$  M atropine to block  $\beta_1$  and muscarinic receptors. Although the RMP remained fairly stable, after 5 minutes the oscillatory prepotentials eventually developed and grew in amplitude until threshold was reached (Figure 32). In all 5 preparations tested, DBcAMP caused initiation of subsidiary pacemaker activity. Cessation of activity occurred within 10 minutes following washout of DBcAMP.

## 3. Effect of Bay K 8644

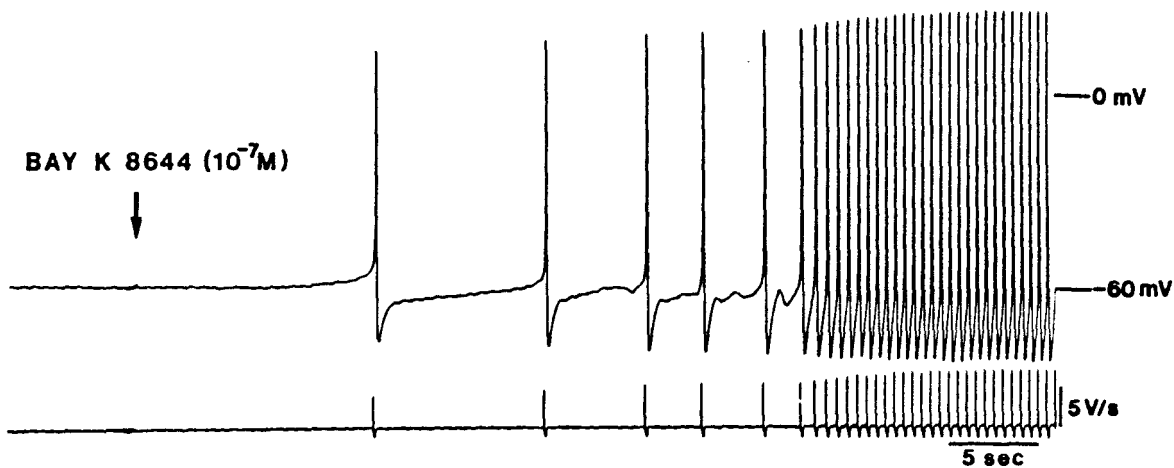
Enhancement of inward calcium currents by norepinephrine has been shown to be partially due to cAMP phosphorylation of L-type calcium channels (278,520,529). Bay K 8644 has been shown to activate the L-type calcium channels without cAMP phosphorylation (217,300,529). Six preparations were pretreated with  $10^{-6}$  M atenolol and  $10^{-7}$  M atropine, and then tested for the effects of  $10^{-7}$  M Bay K 8644. Bay K 8644 elicited a depolarization of the RMP, followed by oscillatory prepotentials, and pacemaker initiation (Figure 33). The activity continued until washout of Bay K 8644. In two preparations, the calcium channel blockers verapamil and nisoldipine, completely inhibited initiation by Bay K 8644.

FIGURE 32  
INITIATION OF ACTIVITY WITH DIBUTYRYL cAMP



The arrow indicates the time at which DbcAMP began being administered. After 5 minutes, oscillatory prepotentials developed and reached threshold to initiate activity. Middle trace is the differentiated voltage signals. Bottom trace is tension.

FIGURE 33  
INITIATION OF ACTIVITY WITH BAY K 8644



Arrow indicates exposure to Bay K 8644. RMP gradually depolarized and initiated activity.

#### 4. Effect of Cesium

To determine the possible role of the cesium-sensitive pacemaker current ( $i_f$ ) in the NE-induced responses, seven preparations were first equilibrated with 1 mM cesium before exposure to NE. Although cesium alone elicited a slight hyperpolarization of the RMP (control:  $-57.4 \pm 1.6$  mV vs Cs:  $-59.3 \pm 2.3$  mV;  $p > 0.05$ ), NE still elicited a depolarization of the RMP, oscillatory prepotentials, and pacemaker initiation similar to the effects of NE.

#### 4. Effect of Tetrodotoxin (TTX)

It is not known if NE initiation is related to enhancement of the fast sodium current ( $i_{Na}$ ). In three preparations, initial exposure to tetrodotoxin (TTX) produced a small, but insignificant, hyperpolarization of the RMP (control:  $-54.2 \pm 3.7$  mV vs. TTX:  $-56.4 \pm 2.9$  mV). Upon addition of NE, TTX did not affect any of the characteristics of NE initiation.

#### 5. Effect of Verapamil

To test the possibility that NE initiated activity by enhancing the slow inward current, seven preparations were tested in the presence of  $10^{-6}$  M verapamil. Verapamil blocked the NE-induced (4-10 nM) oscillatory prepotentials and initiation in all seven preparations tested. Although verapamil alone caused no significant change in the RMP (control:  $-59.7 \pm 2.2$  mV vs. verapamil:  $-60.7 \pm 1.7$  mV), NE still elicited a small depolarization of the RMP (verapamil:  $-60.7 \pm 1.7$  mV vs. verapamil + NE:  $-58.1 \pm 1.6$  mV,  $p < 0.001$ ). This depolarization was more than 4 mV short of reaching the threshold potential seen in the control initiation (Control NE TOP:  $-53.9 \pm 2.1$  mV vs. Verap + NE RMP:  $-58.1 \pm 1.6$  mV,  $p < 0.01$ ). Therefore, verapamil prevented initiation not only by blocking the action potential upstroke, but also by inhibiting the NE-induced

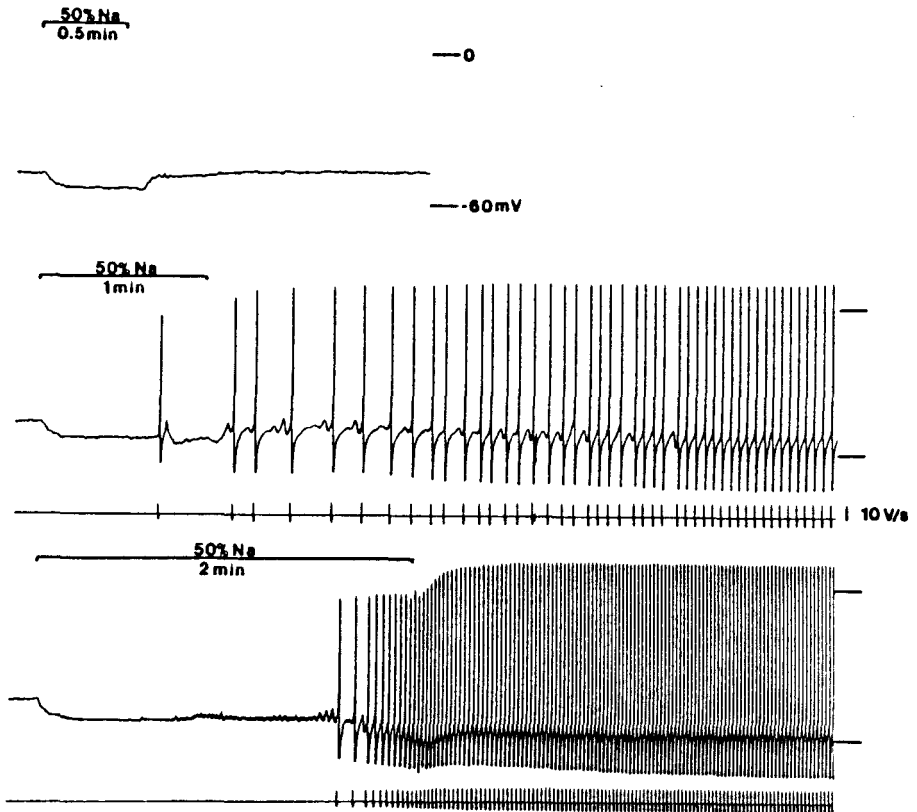
depolarization.

### 6. Effect of Low Sodium

The previous work has shown that calcium released from the SR may mediate a component of spontaneous activity. SR function can be enhanced by elevated levels of cAMP (46). Furthermore, the SR may generate oscillatory release of calcium in calcium overloaded states (153,281,301,346,398,531,573,574). Therefore, NE initiation of activity may be partially mediated by enhancement of an SR-mediated component by either or both of the above mechanisms. Thus it was questioned whether SR activation could initiate activity separate from activation of the L-type current.

Decreasing  $[Na]_o$  has been shown to increase  $[Ca]_i$  (571), probably through a Na/Ca exchange mechanism (140,292,325,370), resulting in voltage oscillations secondary to spontaneous oscillatory SR calcium release (153,531). To test if intracellular calcium overload can initiate subsidiary pacemaker activity, six preparations were exposed to low sodium (50% of control, sucrose replaced) for different durations of time (30, 60, and 120 seconds). All preparations were initially equilibrated in  $10^{-6}$  M atenolol and  $10^{-7}$  M atropine. Exposing the tissues to 50% sodium for 30 seconds elicited a significant hyperpolarization of the RMP (control:  $-55.9 \pm 1.7$  mV vs. 50%  $Na_{30}$ :  $-61.0 \pm 2.2$  mV,  $p < .001$ ). During washout of the low sodium solution there was an immediate depolarization, and the development of oscillatory potentials (Figure 34, panel A). In one of the six preparations, the depolarization reached threshold and initiated pacemaker activity. Exposure to 50% sodium for 60 seconds produced a similar hyperpolarization of the RMP (control:  $-55.5 \pm 1.4$  mV vs. 50%  $Na_{60}$ :  $-61.5 \pm 1.8$  mV,  $p < .001$ ). After returning to normal Tyrode's solution, three of six preparations depolarized to threshold and initiated pacemaker activity (Figure 34, panel B). Exposure to low  $[Na]_o$  for 120 seconds had similar effects on the RMP (control:  $-53.7 \pm$

FIGURE 34  
INITIATION OF ACTIVITY IN LOW SODIUM



Panel A: Brackets indicate a 30 sec exposure to low sodium solution (50%, replaced with 133 mM sucrose). Note that after the return to control solution, oscillatory potentials are seen. Panel B: The preparation was exposed to low sodium solution for 60 sec. One action potential is elicited at about 35 second into the exposure. After return to the control Tyrode's solution initiation of sustained activity is seen. Panel C: During the exposure to low sodium for 2 minutes, oscillatory prepotentials develop which result in a sustained rhythmic activity that persisted for several minutes after return to the control solution.

0.8 mV vs. 50%  $\text{Na}_{120}$ :  $-60.2 \pm 1.0$  mV,  $p < .001$ ). Pacemaker activity initiated in four of six preparations, two of which initiated activity before returning to 100% sodium (Figure 34, panel C).

### 7. Effect of Acetylstrophanthidin (AcSt)

Another method to create a calcium overloaded state, is through inhibition of the Na-K pump (121,531). Eleven quiescent preparations were first equilibrated in atenolol and atropine as above. The effect of administration of  $10^{-6}$  M AcSt was then studied. The RMP gradually depolarized, formed oscillatory prepotentials, and initiated activity in ten of the eleven preparations (Figure 31, panel C). Sustained rhythmic activity persisted until washout of the AcSt.

### 7. Effect of Ryanodine

The above experiments suggested that calcium overload without activation of calcium channels can initiate activity. Furthermore, initiation may be mediated by spontaneous oscillatory SR calcium release. To examine if initiation induced by NE was mediated by enhancement of an SR component, six preparations were studied in the presence of  $10^{-6}$  M ryanodine. All 6 tissues initiated activity in control stimulation by NE without ryanodine (Figure 31, panel A). Equilibration in ryanodine (20 minutes) was shown to have no significant effect on RMP (control:  $-59.5 \pm 2.3$  mV vs. ryanodine:  $-60.0 \pm 1.8$  mV). In the presence of ryanodine, norepinephrine again induced a depolarization of the RMP and initiated activity in all preparations (Figure 31, panel B). One notable characteristic difference, however, was that ryanodine caused a slower rate of the NE-induced automaticity. In fact, the SCL had almost doubled (Control NE:  $1327 \pm 459$  msec vs. RYAN + NE:  $2224 \pm 630$  msec;  $p < 0.05$ ).

Three of the six preparations, that initiated activity after exposure to  $10^{-7}$  M Bay

K 8644, were also reexamined after equilibration in  $10^{-6}$  M ryanodine. Again, ryanodine did not significantly change the RMP (control:  $-58.0 \pm 2.9$  mV vs. RYAN:  $-58.4 \pm 1.6$  mV). Reapplication of Bay K 8644 depolarized all three tissues and initiated pacemaker activity.

The effect of ryanodine was also studied in three of eleven preparations that initiated in the presence of AcSt. After equilibration in  $10^{-6}$  M ryanodine,  $10^{-6}$  M AcSt depolarized the RMP, but no oscillatory potentials developed. Initiation of activity by AcSt was blocked in all three preparations (Figure 31, panel D).



## CHAPTER V

### DISCUSSION

#### A. ELECTROPHYSIOLOGY AND ULTRASTRUCTURE OF EUSTACHIAN RIDGE FROM CAT RIGHT ATRIUM:

##### A COMPARISON WITH SA NODE

(J.Mol.Cell.Cardiol. 19:965-976, 1987)

##### 1. Electrophysiology

The present findings indicate that fibers within cat Eustachian ridge generate stable pacemaker activity and are functionally different or specialized compared to typical working atrial muscle. Similar results have been found for right atrial tissue isolated from the Eustachian ridge region of the dog (442). Pacemaker action potentials recorded from Eustachian ridge were similar to those recorded from SA node in that their maximum diastolic and take-off potentials were similar. However, as expected, subsidiary pacemaker spontaneous cycle length was significantly longer than that of SA node. Since the maximum diastolic and takeoff potentials were not significantly different, it seems likely that the longer cycle length of subsidiary pacemakers is due to their more gradual diastolic slope. Moreover, although both pacemaker action potentials take off from essentially the same membrane potential, the maximum rate of rise and overshoot of subsidiary pacemakers is significantly larger than in SA node. Even so, they were still only about 5 V/sec, suggesting activation of slow inward current during the upstroke. This is supported by the fact that subsidiary pacemaker action

potential upstroke and amplitude is suppressed by slow channel blockade and unaffected by tetrodotoxin.

Perhaps the simplest explanation for the electrophysiological differences between the two pacemakers is related to possible differences in ionic current mechanisms. However, since little is presently known about the ionic currents responsible for subsidiary atrial pacemaker activity, it would be premature to speculate on a specific hypothesis. An alternative or additional explanation may be related to the present morphological findings that the overall architecture of the two tissues differ. The present study, as well as others (262), shows that the cellular organization of the Eustachian ridge is more heterogeneous than that of SA node. Since pacemaker cells in both tissues are, presumably, electrotonically coupled to surrounding cells, differences in structural organization as well as passive membrane properties of individual units could strongly influence pacemaker characteristics. For example, subsidiary pacemaker cells in Eustachian ridge tissue may be more electrotonically influenced by adjacent non-automatic atrial muscle cells than are pacemaker cells in SA node. This could contribute to or be solely responsible for the relatively gradual diastolic slope and longer spontaneous cycle length of subsidiary pacemakers.

## 2. Morphology

All four Eustachian ridge and SA node preparations used for morphological study exhibited stable, spontaneous pacemaker activity. In order to compare the characteristics of pacemaker cells we restricted the morphological studies of each tissue to cross sections taken at the site of earliest pacemaker activation. P cells were invariably the predominant cell type found in each cross section and generally were located in clusters on the endocardial surface of the preparation. The idea that P cells are, in fact, responsible for generating pacemaker activity is strongly supported by the

work of Taylor et al., (505) in rabbit SA node. By using an intracellular marker they were able to directly correlate cells exhibiting primary pacemaker action potentials with cells exhibiting P cell ultrastructural characteristics. We felt that a similar approach of intracellular marking would be of limited value in this study since it is apparent, from this study as well as others (262), that Eustachian ridge tissue is not as homogenous as SA node. However, the present study does demonstrate that P cells were found consistently, in each preparation studied, at the endocardial site of earliest activation. It therefore seems reasonable to suppose that P cells are responsible for generating subsidiary pacemaker activity in Eustachian ridge, as they are in SA node.

Studies in rabbit atrioventricular valve tissues have also correlated pacemaker action potentials with the presence of P cells (31). On the other hand, although Bassett et al., (16) were able to record pacemaker action potentials from canine tricuspid valve tissue, ultrastructural studies did not reveal any P cells or other specialized morphological characteristics.

The presence of P cells in regions of the right atrium, outside of SA node, is not new (31,262,553). Sherf and James (262) have shown that in dog atrium, P cells are found in the Eustachian ridge and Bachmann's bundle. However, P cells were observed to be grouped in clusters only in Bachmann's bundle but not in Eustachian ridge. In contrast, the present findings show that P cells in cat Eustachian ridge were commonly found in clusters (Figure 9) surrounded by a single basal lamina. The discrepancy may be due to species differences. However, clustered pacemaker cell organization is typical of SA node P cells and may be important in synchronization of pacemaker activity.

The present morphological studies show that P cells in the Eustachian ridge are richly innervated with nerve fibers containing both clear and dense core vesicles. These would presumably correspond to cholinergic and adrenergic vesicles, respectively (353) that mediate the regulation of subsidiary pacemaker activity. Thus, application of

acetylcholine or norepinephrine decreases or increases subsidiary pacemaker automaticity, respectively (446). In vivo and in vitro studies of dog atrial subsidiary pacemakers showed a dependency on  $\beta$ -adrenergic stimulation for propagation of activity (269,422,442). Thus, sympathetic stimulation might allow better propagation and thereby prevent exit block as was seen in the dog (442).

The morphometric measurements show that P cells in the Eustachian ridge have ultrastructural characteristics that are not different from those found in SA node. However, only P cells in the Eustachian ridge exhibited paired subsarcolemmal cisternae directly apposed across adjacent cell borders. Paired cisternae were found within connected P cells or a connected P cell and transitional cell. Several considerations suggest that the apposition of cisternae was not a fortuitous association: 1) they were always observed at regions of cells connected by desmosomes, 2) cisternae were directly apposed and similar in length, and 3) similar structures were not found in SA node. One micrograph of the guinea pig AV node showed direct apposition of subsarcolemmal cisternae, although its presence was not mentioned in the paper (512). Since the present study is, as far as we know, the first ultrastructural study of P cells in cat Eustachian ridge, the presence of these structures may be species dependent.

The functional significance of paired subsarcolemmal cisternae is not clear. It is well known that calcium mediated calcium release from subsarcolemmal sites is essential to initiate cardiac contraction (153). However, based on myofibrillar content, it seems likely that contractile activity is of minor importance in these cells. Alternatively, calcium release from subsarcolemmal sites may influence cardiac electrical activity. Thus, calcium release from sarcoplasmic reticulum may mediate a transient inward current that is responsible for delayed afterdepolarizations and oscillatory membrane potentials (281). This calcium mediated inward current may also contribute to subsidiary pacemaker automaticity. Thus, ryanodine, a putative blocker

of calcium release from sarcoplasmic reticulum (497), specifically depresses the later portion of diastolic depolarization and significantly inhibits subsidiary pacemaker automaticity generated from the Eustachian ridge. It therefore seems possible that the specialized organization of apposed subsarcolemmal cisternae may, somehow, contribute importantly to subsidiary atrial pacemaker function.

Finally, the presence of P cells and pacemaker activity in Eustachian ridge tissue is not surprising. There is evidence that specialized zones of cells exist at junctions between the primordial chamber of the cardiac tube; between the sinus horn and atrium is the SA ring tissue (5). This region of tissue is visualized as extending from superior to inferior vena cava, along the length of the crista terminalis and extending into the posterior regions of the atrioventricular ring tissue. These cells ultimately form the developed sinoatrial node and the "posterior internodal pathway". In fact, based on morphological studies, a caudal extension of the SA node travels within and parallel with the crista terminalis, toward the posterior border of the coronary sinus ostium (515,517). Recent additional evidence for the existence of the SA ring tissue has been obtained through the use of monoclonal antibodies (197). Since the Eustachian ridge is within the distribution of the SA ring tissue it is not unexpected that it would contain cells with electrophysiological and ultrastructural pacemaker characteristics.

## B. MECHANISMS OF AUTOMATICITY IN SUBSIDIARY PACEMAKERS

### FROM CAT RIGHT ATRIUM

(Circ.Res. 64:648-657, 1989)

One of the main findings of this study is that calcium released from the sarcoplasmic reticulum may mediate a component of subsidiary pacemaker automaticity. This component contributes significantly during the last half of diastolic depolarization to bring the membrane potential to threshold. This interpretation is based primarily on

the fact that ryanodine abolished tension and elicited a relatively specific decrease in the late diastolic slope (D2), resulting in a significant inhibition of automaticity. Ryanodine has been shown to specifically interact with calcium release channels of the sarcoplasmic reticulum and thereby functionally eliminate SR calcium release (439). According to the work of Rousseau et al. (439), ryanodine causes a sudden increase in the open probability time of SR release channels, leading to a gradual depletion of SR calcium stores. This may account for the small, initial decrease, followed by the gradual increase in spontaneous cycle length, elicited by ryanodine in the present experiments. These findings may also be important in relation to the morphological studies on cat Eustachian ridge tissues. Those studies showed that the site of earliest pacemaker activation is correlated with presence of cells exhibiting P cell characteristics. Although these P cells are morphometrically identical to P cells found in SA node, Eustachian ridge P cells exhibit a unique apposition of prominent subsarcolemmal cisternae (junctional SR) not seen in SA node P cells. These subsarcolemmal cisternae not only have been determined to be the site from which calcium is released (271,514,571), but they also contain ryanodine receptors (79,239,307). Since P cells typically contain little myofibrillar material needed for contractile activity, it seems possible that the unique organization of cisternae found in Eustachian ridge P cells may, somehow, be related to the SR calcium mediated pacemaker component described here.

By inhibiting SR calcium release, ryanodine may also alter other intracellular calcium-dependent currents. Thus, ryanodine has been shown to reduce calcium-activated outward currents in Purkinje fibers (497) and to delay inactivation of slow inward current in ventricular myocytes (362). Either of these effects could account for the increases in action potential amplitude and rate of rise induced by ryanodine in the present study.

In voltage clamp studies of rabbit SA node, Brown et al., (69) have also presented evidence for a secondary component of slow inward current, possibly mediated by intracellular calcium release, that may bring the last third of the diastolic slope to threshold. In addition, Escande et al. (148) have shown that an SR calcium mediated component may participate in pacemaker activity recorded from abnormal, partially depolarized human atrial tissues. However, it is apparent from the present study, as well as those on SA node (69) that the participation of a calcium-mediated component in atrial pacemaker automaticity is not necessarily the result of abnormal function.

The calcium-mediated component proposed in the present experiments may be similar, if not identical, to the transient inward current associated with delayed afterdepolarizations (280,314). A study by Tseng and Wit (527) showed that transient inward currents are responsible for delayed afterdepolarizations recorded from atrial tissue isolated from the canine coronary sinus. In addition, Aronson et al., (8) reported that in coronary sinus, ryanodine suppresses delayed afterdepolarizations. If the transient inward current contributes a late component to the diastolic slope, then the time course of both events should be similar. In fact, the spontaneous pacemaker cycle lengths reported here, about 700 ms., are within the same order of magnitude as the time to peak of transient inward currents recorded in atrial muscle (527) as well as other preparations (582). In addition, interventions that raise or lower intracellular calcium cause a decrease or increase, respectively, in time to peak, and an increase or decrease, respectively, in amplitude of the transient inward current (527,582). As shown in the present study, interventions that are expected to raise (NE and BAY 8644) or lower (low  $[Ca]_o$  or slow channel block) intracellular calcium elicit decreases or increases, respectively, in spontaneous cycle length through changes in late diastolic slope.

Although transient inward currents and delayed afterdepolarization are usually recorded from tissues that are abnormally loaded with calcium (314,582), the pacemaker

tissues studied in the present experiments did not require interventions designed to load intracellular calcium. In fact, there is evidence that the transient inward current is normally present in atrial (8) as well as ventricular tissues (314,328), and is only enhanced by interventions that raise intracellular calcium. It therefore seems likely that calcium-mediated inward currents are normally present in cardiac tissues and may function in certain atrial cells as a major determinant of automaticity. In favor of this idea are the findings by Fabiato (152) that sarcoplasmic reticulum and calcium-induced release of SR calcium are more developed in atria than in ventricular tissue.

These experiments show that both NE and BAY K 8644 elicit a significantly greater increase in late (D2) than early (D1) diastolic slope. Since BAY K 8644 acts primarily through activation of the slow inward current channels (300,509), these findings suggest that a significant portion of the positive chronotropic effect of NE is mediated through an increase in slow inward current and subsequent SR calcium release. In addition, this effect of NE is mediated predominately through beta-1 adrenoceptors. This is consistent with the well known role of beta-1 receptors in mediating increases in slow inward current (528). Rozanski (440) has also reported that in rabbit tricuspid valve pacemakers the positive chronotropic response to isoproterenol (a selective beta receptor agonist) is associated with a significantly greater increase in the slope of D2 than D1.

Alternatively or in combination, the increase in diastolic slope observed in both NE and Bay K 8644 may be related to an increase in the  $i_f$  current. Adrenaline (63,64,67) and isoproterenol (126,201,384) are reported to increase  $i_f$  in the sinus node. In addition, both NE and Bay K 8644 significantly increased the MDP, which may have further activated  $i_f$  (63,78,122,123,125,126,129,348,385,591). Raising  $[Ca]_i$  may also increase  $i_f$  (201). Although Bay K 8644 can increase  $[Ca]_i$  (339), its effects on other currents that may contribute to automaticity, such as the cesium-sensitive  $i_f$  current are



unknown and therefore cannot be excluded.

Although TTX had little effect on action potential upstroke, it significantly increased SCL. This resulted from a positive shift in the takeoff potential and a decrease in the slope of diastolic depolarization. Perhaps the simplest explanation is that TTX acted by blocking fast sodium channels that carry inward current during diastole. However, Vassalle and Lee (551) have shown in Purkinje fibers that TTX directly reduces intracellular sodium activity and tension, suggesting a secondary decrease in intracellular calcium through sodium-calcium exchange. This suggests that the TTX-induced increase in SCL may also involve a secondary decrease in intracellular calcium.

Although these studies show that agents or interventions that alter slow inward current influence diastolic slope, they also show that these responses may be explained by secondary changes mediated by SR calcium release. It therefore is difficult to separate the direct from the indirect contribution of slow channel activation on automaticity. The finding that BAY K 8644 was able to elicit a partial positive chronotropic response in the presence of ryanodine may be interpreted as a direct contribution of slow inward current. On the other hand, the effects of BAY K 8644 may also be mediated indirectly through increases in free intracellular calcium independent of SR calcium release. Thus, BAY K 8644 elicited a measurable return of tension, in spite of the presence of ryanodine, indicating that intracellular calcium was increased (Figure 19C). This is consistent with the work of Marban and Wier (339) who showed in Purkinje fibers that BAY K 8644 in the presence of ryanodine increased the aequorin luminescence and contraction, although only to a small fraction of control. In fact, by opening SR calcium release channels (439), ryanodine may promote the accumulation of cytosolic calcium (30) by functionally eliminating the SR as a buffer of intracellular calcium. As a result, beat to beat increases in intracellular free calcium,

enhanced by BAY K 8644, may act directly on the sarcolemmal membrane to activate transient inward current and progressively enhance diastolic slope (Figure 19). In any case, without a functionally intact sarcoplasmic reticulum an increase in slow inward current elicits a limited and dysrhythmic positive chronotropic response. Although these experiments show that an increase in slow inward current may enhance pacemaker activity, it remains to be determined to what extent the slow inward current may contribute directly to automaticity under basal conditions.

The fact that pacemaker activity persists after exposure to ryanodine indicates that the calcium-mediated component is not the only mechanism operating. Indeed, the present experiments show that a cesium-sensitive component contributes significantly to diastolic depolarization. Cesium elicited a significant negative chronotropic effect under control conditions (Figure 14), and after exposure to ryanodine (Figure 20). This component would presumably correspond to the cesium-sensitive pacemaker current,  $i_f$ , found in SA node (63,126,129,348,385,591), Purkinje fibers (78,122,123,125,129), atrial muscle (83,138), as well as single right atrial myocytes isolated from cat heart (331). The fact that cesium inhibited D1 significantly more than D2 (see Table 4), suggests that the cesium-sensitive component contributes to a greater extent during early diastolic depolarization. This is consistent with the greater activation of  $i_f$  at more negative voltages (63,78,122,123,125,126,129,348,385,591). Rozanski (440) also found that in tricuspid valve pacemakers, 1 mM cesium specifically inhibited D1. However, spontaneous cycle length was not significantly increased in that tissue. Apparently, the contribution of the cesium-sensitive current to automaticity is variable among different types of atrial pacemakers. The present studies also indicate that although the cesium-sensitive component contributes significantly it is not essential to sustain automaticity. This conclusion is similar to that reported in studies of SA node (63,68,385), and other atrial pacemakers (440). Finally, even after inhibition of the cesium-sensitive current

plus inhibition of the calcium-mediated component by ryanodine, pacemaker activity persists. It appears that other mechanisms, such as slow inward current or a decreasing potassium current, may be operating to maintain automaticity.

### C. CYCLIC BRADYDYSRHYTHMIAS GENERATED BY ATRIAL

#### SUBSIDIARY PACEMAKERS

(J.Electrophys. 2:90-103, 1988)

The previous work has shown a unique apposition of the SR in the Eustachian ridge. Furthermore, SR calcium release mediates a significant contribution to the diastolic depolarization in the pacemaker activity of Eustachian ridge. Inhibition of this calcium-mediated component by ryanodine generated a cyclic bradycardia during the initial period of exposure to ryanodine. This dysrhythmia was almost identical to cyclic bradycardias generated under control conditions. The spontaneous appearance of this dysrhythmia suggests partial contribution from abnormal SR function.

This work reports a specific pattern of abnormal pacemaker rhythm generated by subsidiary atrial pacemakers maintained in vitro. The dysrhythmia usually developed spontaneously in otherwise normal preparations, and was characterized by cyclic periods of brady rhythm, frequency-dependent changes in maximum diastolic potential, action potential amplitude and tension, and diastolic oscillations in membrane potential. The cyclic nature of the activity suggested that a negative feedback system may be involved. This idea, coupled with the fact that changes in the maximum diastolic potential were in phase with changes in SCL suggested that stimulation of an electrogenic pump current may be operating to modulate pacemaker rhythms. It is well known that changes in pacemaker frequency can influence pump activity and that changes in pump activity can, in turn, influence pacemaker function

(94,174,445,545,579). In the present study, brief exposure to relatively low concentrations of AcSt prevented the development of brady rhythms by establishing stable, rhythmic pacemaker activity. Since the AcSt-induced changes in pacemaker rhythm were established in only a few seconds and its effects on electrical and mechanical activities did not correlate, it seems likely that AcSt acted through direct inhibition of sodium pump activity rather than through a secondary increase in intracellular calcium. Responses of dysrhythmic preparations to electrical pacing also supports the idea that electrogenic pump activity is a contributing factor. Although shorter pacing periods elicited spontaneous beats, the number of beats decreased as pacing duration increased. Moreover, longer durations of pacing (30 & 60 s), elicited complete pacemaker suppression. This progressive inhibition of pacemaker activity as pacing duration is increased is characteristic of overdrive suppression (545), resulting from stimulation of electrogenic sodium pump activity (94,174,445). It therefore seems likely that stimulation of a net outward electrogenic pump current during periods of rhythmic pacemaker activity may be responsible for the gradual increase in SCL, eventual failure of the diastolic potential to reach threshold and the onset of brady rhythms. As in any negative feedback loop, pump activity not only causes changes in SCL, it is also affected by them. As SCL initially increases during the brady rhythm, pump activity slows and net outward current decreases. This would account for the progressive depolarization of MDP during the first few beats of the brady rhythm. The progressive decrease in net outward current results in enhanced oscillatory potential amplitude and a progressive decrease in cycle length. As SCL decreases, pump activity is once again stimulated, resulting in a more negative MDP during the later portion of the brady period and into the next period of rhythmic pacemaker activity. The cycle repeats itself once again as another period of rhythmic pacemaker activity is initiated. This represents a negative feedback loop and appears to be the primary mechanism

responsible for the cyclic pattern of activity.

However, pacemaker activity does not normally overdrive suppress itself. Additional mechanisms must be involved to allow outward pump currents to modulate cycle length and thereby produce rhythm disorders. There are several lines of evidence indicating that this additional mechanism is related to a depression of automaticity caused by impaired intracellular calcium metabolism. Thus, interventions that augment calcium influx, such as exposure to high  $[Ca]_o$  or NE, prevent the development of brady rhythms by establishing stable, rhythmic pacemaker activity. In addition, short pacing periods, which increase intracellular calcium (306), enhance automaticity and elicit spontaneous action potentials immediately following the pacing period. On the other hand, verapamil inhibition of calcium influx through slow channels decreased periods of rhythmic pacemaker activity and prolonged periods of brady rhythm. Moreover, in preparations that became quiescent, interventions that raise intracellular calcium (NE or elevated  $[Ca]_o$ ) restored rhythmic pacemaker activity. However, once the calcium agonist was removed, pacemaker activity deteriorated into cyclic brady rhythms. Finally, ryanodine elicited dysrhythmias in normal preparations, that were similar to those that developed spontaneously or were induced in preparations that became quiescent. Taken together, these results suggest that the fundamental mechanism underlying development of the dysrhythmia is related to a depression of automaticity, due to impaired intracellular calcium metabolism. With automaticity depressed, even a small net outward current generated by stimulation of an electrogenic pump would have a relatively strong modulating influence on pacemaker activity. This would be especially true in pacemaker cells which are known to have a relatively high membrane resistance due to a low background potassium conductance (181). In fact, measurements in this preparation indicate a  $P_{Na}/P_K$  ratio of 0.076.

The fact that ryanodine could induce the development of cyclic brady rhythms

in normal preparations suggests that the depression of automaticity may be more specifically related to impaired calcium release from the sarcoplasmic reticulum. The ryanodine-induced dysrhythmias only appeared during early exposure (<10 min.) to the drug. It seems likely that this time-dependent effect may be related to ryanodine's mechanism of action. Thus, Rousseau et al (439) reports that ryanodine acts by reducing unit conductance and increasing open probability time of SR calcium release channels. The authors propose that by reducing the ability of the SR to handle calcium, ryanodine induces a time-dependent depletion of SR calcium. In heart cells, the calcium released into the cytosol would be extruded by the Na/Ca exchanger. In relation to the present work, the time-dependent depletion of SR calcium by ryanodine would result in a progressive inhibition of the calcium mediated component, resulting in a depression of automaticity. Similar considerations can be applied to preparations in which cyclic brady rhythms developed spontaneously. In these preparations a spontaneous run-down in intracellular calcium may lead to a decrease in SR calcium content and release, thereby depressing automaticity. The reason for this spontaneous run-down is not clear. In preparations that became quiescent, SR calcium may be depleted or too low to support pacemaker automaticity at all. Brief exposures to NE or high  $[Ca]_o$  could restore SR calcium enough to restore rhythmic pacemaker activity. However, once these calcium agonists are removed, SR calcium gradually runs down once again, allowing only a limited degree of automaticity and the development of the dysrhythmia. The similarities between the ryanodine-induced dysrhythmias and those that developed spontaneously or were induced in quiescent preparations, suggests that the fundamental mechanism underlying the onset of the dysrhythmia is impaired SR calcium release. Therefore it is proposed that the cyclic brady dysrhythmia results from an interaction between two phenomena: 1) a background depression of automaticity caused by impaired intracellular calcium metabolism, probably related to impaired SR calcium

release, and 2) frequency-dependent changes in electrogenic sodium pump current that act as a negative feedback mechanism to cyclically modulate pacemaker rhythm.

An alternative explanation for the depression of automaticity may be related to the effects of intracellular calcium on intercellular communication (116). A decrease in intracellular calcium, may reduce internal resistance. Better coupling between pacemaker and non-pacemaker fibers may depress automaticity and lead to dysrhythmias (264,539). Although this explanation cannot be ruled out, it is not consistent with the data. After exposure to AcSt (Figure 24), high  $[Ca]_o$  or NE, tension and presumably intracellular calcium were still elevated at a time when brady rhythms reappeared. In addition, changes in tension during dysrhythmias indicate that intracellular free calcium was highest during periods of brady rhythm, lowest at the onset of periods of rhythmic pacemaker activity and higher at the end of a period of rhythmic activity than at its onset (Figure 21). Whether these beat to beat changes in intracellular calcium can affect nexal resistance is not clear.

The fact that pacing dysrhythmic preparations elicited spontaneous beats immediately following short pacing periods, suggests that the first few action potentials during a period of rhythmic activity may be "triggering" subsequent beats in the period. The characteristics of this triggered activity, as well as rhythmic subsidiary pacemaker activity in general, are similar in some ways to triggered activity described in other atrial preparations (449,577-579). Both activities share a common mechanism i.e. an intracellular calcium mediated component. However, the primary distinctions between the two types of activities is that subsidiary pacemakers exhibit the property of automaticity. For example, as shown in the present study (figs. 25 & 26), suppression of subsidiary pacemaker activity does not result in arbitrarily long periods of quiescence; spontaneous oscillations in membrane potential lead to resumption of pacemaker activity. Since subsidiary pacemaker automaticity is based on an

intracellular calcium mediated component, it can be enhanced by interventions that raise intracellular calcium.

After discontinuing exposure to AcSt, high  $[Ca]_o$  or NE, the brady rhythm returned, even though tension, and presumably intracellular calcium, was still elevated (Figure 24,26,27). This apparent inconsistency may have several possible explanations. Fabiato (152) has shown that the absolute concentration of free calcium is not the only factor governing calcium-induced calcium release; the level of preload of SR calcium as well as the rate of change of free calcium are also important. Since automaticity of these pacemakers may be modulated by calcium-induced calcium release, these additional factors may also influence pacemaker rhythm responses. Another consideration stems from ultrastructural characteristics of this tissue. Cells correlated with pacemaker activity, i.e. P cells, have little myofibrillar material, and therefore probably contribute little to total tension development. This suggests that changes in tension may not accurately reflect changes in intracellular calcium within pacemaker cells, resulting in a dissociation between electrical and mechanical events. In addition, P cells in cat Eustachian ridge exhibit a unique structural organization of apposed subsarcolemmal cisternae, not described in ordinary atrial muscle, that may influence the way calcium is handled by subsidiary pacemaker cells. These structures may create a calcium pool that modulates electrical rather than contractile activity. Indeed, studies of cardiac tissue have provided evidence for different intracellular calcium pools that may serve different cellular functions (232,271,514,571).

These experiments demonstrate that right atrial subsidiary pacemakers can generate dysrhythmias characterized by periods of abnormally slow rhythm. The importance of these findings are apparent since bradycardia is a primary criterion used in the clinical diagnosis of atrial rhythm disorders such as sick sinus syndrome (160). Although electrocardiographic recordings of upright P waves are commonly used to



indicate that atrial rhythm disorders originate from within the sinus node, it has been shown that P wave polarity and morphology are poor indicators of the site of origin of atrial activation (558,559). In fact, upright P waves and P-R intervals within normal limits are recorded from dogs after surgical removal of the SA node, where right atrial subsidiary pacemakers control the heartbeat (420-422). It therefore seems possible that under pathological conditions, atrial pacemaker activation could shift from a failing sinus node to subsidiary pacemakers that are also suffering from depressed automaticity. Indeed, depressed automaticity of subsidiary atrial pacemakers has been proposed as a possible contributing factor in atrial dysrhythmias associated with sick sinus syndrome in man (435). In addition, with a background depression of subsidiary pacemaker automaticity, the influence of frequency-dependent electrogenic pump activity on pacemaker rhythm may be exaggerated. This is consistent with the fact that rapid atrial pacing in patients with sick sinus syndrome frequently results in prolonged periods of pacemaker suppression (338,435).

#### D. SUBSIDIARY PACEMAKER RESISTANCE TO $[K]_o$

The resting membrane potential of the Eustachian ridge is relatively low ( $-61.7 \pm 2.5$  mV, Figure 29) compared to typical atrial muscle cells. Furthermore, the RMP of cells within the Eustachian ridge exhibited a relative resistance to moderate increases in  $[K]_o$ . The relatively high  $P_{Na}/P_K$  ratio, determined to be 0.076, suggested the low RMP may be related to a decrease in potassium conductance. Low potassium conductance has also been observed in the cristae terminalis (182) and sinus node (386,475). Specifically, this has been attributed to a decreased  $i_{K1}$  (386,450). However, the resultant  $P_{Na}/P_K$  may also be associated with a higher sodium conductance. Support of this alternative was observed when low sodium exposure caused a significant 5 mV hyperpolarization. However, exposure to cesium elicited only a small hyperpolarization

of the RMP, suggesting that background sodium conductance is not carried by a cesium sensitive current as reported in embryonic cell aggregates (354). Boyden et al. (53) postulated that sodium influx may occur through pathways associated with transient inward current in cells within the coronary sinus. Although these mechanisms have been shown to be important in calcium overload conditions (96,279,280,282,527), it was not demonstrated whether they existed in control conditions to contribute to the RMP. Automaticity of the Eustachian ridge has a significant calcium mediated component during diastolic depolarization. The spontaneous activity observed in 104 out of 154 preparations, in a Tyrode's solution containing 1.8 mM  $\text{CaCl}_2$  and without norepinephrine, argues against a calcium overloaded condition. Therefore, in quiescent preparations in similar solutions, sodium entry via this pathway, either through a Na/Ca exchange, or a nonselective calcium mediated conductance cannot be excluded.

In either case, a decreased potassium or an increased sodium conductance, the  $P_{\text{Na}}/P_{\text{K}}$  ratio demonstrates that the RMP of cells within the Eustachian ridge are resistant to moderate elevations of  $[\text{K}]_o$ . This was further substantiated by the fact that these pacemakers sustained their automaticity in 16 mM  $[\text{K}]_o$ . Therefore, these results are in accordance with other tissues within the SA ring bundle also resistant to  $[\text{K}]_o$  (53,110,228,335,548,550).

#### E. MECHANISMS OF PACEMAKER INITIATION

This study has demonstrated two separate routes to initiation of pacemaker activity: ryanodine-sensitive and insensitive pathways. The ryanodine-sensitive pathway is invoked during conditions of elevated levels of  $[\text{Ca}]_i$  that presumably cause spontaneous oscillatory SR calcium release. Alternatively, the ryanodine-insensitive pathway requires the stimulation of voltage activated calcium channels. These two forms of initiation of activity through the development of oscillatory prepotentials is

distinct from triggered activity. Initiation through oscillations is generated from growing oscillations in membrane potential that reach threshold (543), whereas triggered activity is dependent upon a prior stimulated or propagated action potential (577). However the two forms of activity appear to have a common mechanism: a dependence on intracellular calcium. Therefore, the distinction between a ryanodine-sensitive oscillatory pathway and triggered activity may only be a matter of intracellular calcium concentrations (discussed below).

Cesium or TTX did not inhibit NE-induced initiation of activity. This fact strongly suggests that the mechanism of the initial depolarization was not related to an enhanced cesium-sensitive pacemaker current or the fast sodium current. Although NE increases  $i_f$  in the sinus node (63,64,67), the cesium-sensitive current does not appear important in the initiation of activity in Eustachian ridge.

The most likely mechanism responsible for NE-induced initiation is an enhancement of the slow inward current. The ability of atenolol, but not prazosin, to block the NE-induced effect suggested that initiation resulted from  $\beta_1$  receptor stimulation. Furthermore, isoproterenol (a specific  $\beta$  agonist) elicited responses similar to NE, which were also blocked by atenolol. The fact that DBcAMP mimics the effects of NE supports the idea that NE acts via stimulation of adenylate cyclase (211,373,399,530). Thus, phosphorylation of L-type calcium channels (278,520,529) may also be responsible for the NE-induced initiation seen in the Eustachian ridge.

Further support for a NE-induced increase in slow inward current comes from the finding that verapamil blocked NE-induced initiation, whereas BAY K 8644 mimicked it. Verapamil block of initiation can be interpreted simply as a blockade of the upstroke. Most notable however, was the fact that in the presence of verapamil, NE caused only a 2 mV depolarization. This depolarization was approximately one third of that required to reach the threshold potential under control conditions. In addition,

Bay K 8644, a specific calcium channel agonist that is not mediated via cAMP (217,300,529), also generated depolarization of the RMP until reaching the threshold potential. Therefore, it appears that the verapamil/Bay K 8644-sensitive calcium channels are important in the depolarization of the RMP prior to reaching threshold. The NE-induced depolarization of the RMP in the Eustachian ridge is in contrast to the effects of NE on coronary sinus (52). Boyden et al. (52) found that NE caused a significant hyperpolarization of the RMP, resulting from an increase in potassium permeability. If a similar mechanism exists in the Eustachian ridge, it is likely being masked by a stronger effect on calcium channels. The calcium channels which are affected presumably are L-type channels. Although T-type calcium channels have recently been shown to contribute to the later half of diastolic depolarization (202),  $\beta$ -adrenergic stimulation has affects only on L-type channels (19,202,374).

Alternatively, the conversion of a triggerable focus into an automatic focus, instead of enhancement of an automatic current such as  $i_L$ , might also have been responsible for the NE-induced initiation. It has been previously discussed that the activation of a triggered current would emerge only after an action potential, and thereby enhance diastolic depolarization. An example of a triggered current was the  $i_{Na/Ca}$  current. Elevated levels of  $[Ca]_i$  cause increases in the  $i_{ti}$  current (527,531). This current is generated by SR calcium release, and may be mediated by Na/Ca exchange (92,279,326). Moreover, it has been shown that SR calcium release during spontaneous activity in the ER contributes to the diastolic depolarization. If however, the ER tissue is quiescent and the SR spontaneously releases calcium, then oscillatory depolarizations of the RMP would be expected. Such spontaneous oscillations would suggest that the triggered current ( $i_{ti}$ ) was now active without a prior action potential and therefore would be a component of automatic activity. This suggests that the transition in the type of activity was likely mediated merely by elevation of  $[Ca]_i$ .

In a calcium overloaded condition, spontaneous oscillations of membrane potential and tension have been related to oscillatory SR calcium release (153,281,301,308,346,398,574). Thus, by increasing calcium influx, NE may be enhancing SR function to generate oscillatory release of calcium. In fact, Capagrossi et al., (81) have shown that synchronous SR release of calcium in single cells can depolarize the membrane potential past threshold and generate action potentials.

Two methods of loading intracellular calcium were used, low sodium or AcSt exposure. Both have been shown to develop oscillatory prepotentials and initiate activity in Purkinje fibers (98), and both techniques were shown to consistently develop oscillatory prepotentials and initiate activity in the Eustachian ridge. Thus it appears that SR release of calcium may provide an additional mechanism of initiation. Ryanodine would be expected to functionally eliminate an SR calcium release component (439,497). Repeating attempts to initiate activity through the two possibly different mechanisms, NE stimulation (cAMP mediated) and AcSt exposure (calcium overload mediated), resulted in two different results. Although ryanodine did not prevent NE-induced initiation, it abolished the ability of AcSt to initiate activity. Therefore, it appears that initiation of activity may indeed occur through at least two distinct pathways. This suggests that calcium overload initiates activity through a ryanodine-sensitive pathway, while NE initiates activity predominantly through a ryanodine-insensitive pathway. Thus, NE initiation is likely mediated by enhancement of the slow inward current. It is suggested that  $\beta_1$  receptor binding activates adenylate cyclase to increase intracellular cAMP, which can then phosphorylate and activate calcium channels. However, the fact that ryanodine significantly increased the cycle length of NE-induced activity, suggests that SR calcium release significantly contributed to the diastolic depolarization, similar to that seen in spontaneously active preparations.

The effect of ryanodine to inhibit AcSt initiation is consistent with the ability of ryanodine to reverse digitalis toxic dysrhythmias in the whole animal (206,277). Furthermore, ryanodine has recently been shown to inhibit ischemic and reperfusion dysrhythmias (507), which are also related to calcium overload (291,316). Lastly, ryanodine can inhibit triggered activity in calcium overloaded cells of the coronary sinus (8). Therefore a ryanodine-sensitive pathway exists in triggered activity as well as calcium overload-induced (AcSt) initiation of activity. Thus, SR calcium release, either activated by calcium overload or triggered by action potentials, can generate sustained rhythmic activity. The calcium-mediated automaticity (calcium overload resulting in spontaneous oscillatory SR calcium release) may be experimentally differentiated from triggered activity. Triggered and not automatic activity, has a bistability, and therefore can be experimentally annihilated by single pulse perturbations (190). It is speculated that fibers that generate triggered activity may be converted to the automatic calcium-mediated rhythm simply by a further increase in  $[Ca]_i$ . This mechanism may be related to the difficulty in distinguishing triggered and reentrant dysrhythmias (582) and therefore may identify a new mechanism of dysrhythmias.

## SUMMARY

Isolated preparations of the cat Eustachian ridge exhibit structural and functional similarities to that found in the sinus node. The morphological analysis revealed that the Eustachian ridge consisted of a variety of cells, with P cells being the most prominent at the site of earliest pacemaker activation. Furthermore, there were no significant differences from P cells within the SA node in cellular volume densities of cytoplasm, nucleus, mitochondria, or myofilaments. However, the Eustachian ridge exhibited a unique apposition of subsarcolemmal cisternae between cells not seen in the SA node.

The pacemaker activity recorded in the Eustachian ridge are slow response action potentials that can be inhibited by verapamil. The pacemaker action potentials exhibited two phases of diastolic depolarization, suggesting multiple mechanism of pacemaker activity. The earlier steeper slope ( $D_1$ ), was more inhibited by cesium than the later more gradual slope ( $D_2$ ), suggesting the involvement of the  $i_f$  pacemaker current. Ryanodine selectively inhibited the  $D_2$  portion, suggesting that SR calcium release mediates a significant component of late diastolic depolarization. In addition, the slow inward current may also directly contribute to the diastolic slope.

Although the Eustachian ridge typically exhibits rhythmic pacemaker activity, a small percentage of the preparations demonstrated cyclic bradycardias. The present findings suggest that the development of these dysrhythmias may be due to impaired  $[Ca]_i$  metabolism. This mechanism interacts with frequency dependent changes in electrogenic sodium pump activity which act as a negative feedback mechanism to cyclically modulate pacemaker rhythm.

Cells within the Eustachian ridge demonstrated characteristics which were typical of regions found within the SA ring bundle. Atrial subsidiary pacemakers within the Eustachian ridge exhibited a high  $P_{Na}/P_K$  ratio (0.076), and a relative resistance to moderate elevations of  $[K]_o$ . Pacemaker activity continued at 16 mM  $[K]_o$ .

Initiation of pacemaker activity can occur by either ryanodine-sensitive or insensitive pathways. Norepinephrine initiation is ryanodine-insensitive and may result from a  $\beta_1$  receptor stimulation of a cAMP mediated pathway to activate calcium channels. Calcium overload initiation of activity by acetylstrophanthidin toxicity was likely mediated by the spontaneous generation of oscillatory SR calcium release. This ryanodine-sensitive, calcium-mediated automaticity may identify another mechanism of dysrhythmias.

The calcium released from the sarcoplasmic reticulum in the cat Eustachian ridge likely contributes significantly to all forms of its pacemaker activity: rhythmic, dysrhythmic, and initiated.

The atrial subsidiary pacemakers are clinically important when the sinus node fails or is damaged. Further study into the specific currents will help establish the mechanisms of subsidiary pacemaker activity, and may better define the mechanisms of dysrhythmias. Continued emphasis should be communicated to cardiac surgeons on the location and functional importance of these pacemakers.



## BIBLIOGRAPHY

1. Agnarsson, U., T. Tajima and A.J. Pappano. Carbachol depolarizes and accelerates pacemaker activity in the sinoatrial node of chicks treated with pertussis toxin. J. Pharmacol. Exp. Ther. 247:150-155, 1988.
2. Akselrod, S., D. Gordon, F.A. Ubel, D.C. Shannon, A.C. Barger and R.J. Cohen. Power spectrum analysis of heart rate fluctuation: a quantitative probe of beat-to-beat cardiovascular control. Science 213:220-222, 1981.
3. Allen, D.G., D.A. Eisner and C.H. Orchard. Characterization of oscillations of intracellular calcium concentrations in ferret ventricular muscle. J. Physiol. 352:113-128, 1984.
4. Anderson, R.H., A.E. Becker, C. Brechenmacher, M.J. Davies and L. Rossi. The human atrioventricular junctional area - a morphologic study of the atrioventricular node and bundle. Eur. J. Cardiol. 3:11-25, 1975.
5. Anderson, R.H., A.E. Becker and A.C.G. Wenink. The development of the conducting tissues. In: Cardiac Arrhythmias in the Neonate, Infant and Child. eds. N.K. Roberts and H. Gelband. New York: Appleton-Century-Crofts, pp.1-28, 1977.
6. Anderson, R.H. and I.M. Taylor. Development of atrioventricular specialized tissue in human heart. Brit. Heart J. 34:1205-1214, 1972.
7. Arlock, P. and B.G. Katzung. Effects of sodium substitutes on transient inward current and tension in guinea-pig and ferret papillary muscle. J. Physiol. (Lond.) 360:105-120, 1985.
8. Aronson, R.S., P.F. Cranefield and A.L. Wit. The effects of caffeine and ryanodine on the electrical activity of the canine coronary sinus. J. Physiol. (Lond.) 368:593-610, 1985.
9. Arvanitaki, A. Proprieties Rhythmiques de la Matiere Vivante, Paris: Herman and Cie, 1938.
10. Aschoff, L. A discussion on some aspects of heart block. Brit. Med. J. 1103-1113, 1906.
11. Aschoff, L. Die Herzstoerungen in ihrer Beziehung zum spezifischen Muskelsystem des Herzens. Centralb. f. allg. Path. u. path. Anat. 21:433, 1910.
12. Ask, A., G. Stene-Larsen, K.B. Helle and F. Resch. Functional  $\beta_1$ - and  $\beta_2$ -adrenoceptors in the human myocardium. Acta Physiol. 123:81-88, 1985.

13. Ayettey, A.S. and V. Navaratnam. The T-tubule system in the specialized and general myocardium of the rat. J. Anat. **127**:125-140, 1978.
14. Baird, J.A. and J.S. Robb. Study, reconstruction, and gross dissection of the atrioventricular conducting system in the dog heart. Anat. Rec. **108**:747, 1950.
15. Barr, L., M.M. Dewey and W. Berger. Propagation of action potentials and the structure of the nexus in cardiac muscle. J. Gen. Physiol. **48**:797-823, 1965.
16. Bassett, A.L., J.J. Fenoglio, A.L. Wit, R.J. Myerburg and H. Gelband. Electrophysiologic and ultrastructural characteristics of the canine tricuspid valve. Am. J. Physiol. **230**:1366-1377, 1976.
17. Baumgarten, C.M. and H.A. Fozzard. The resting and pacemaker potentials. In: The Heart and Cardiovascular System. eds. H.A. Fozzard, E. Haber, R.B. Jennings, A.M. Katz and H.E. Morgan. New York: Raven Press, pp.601-626, 1986.
18. Baumgarten, C.M. and G. Isenberg. Depletion and accumulation of potassium in the extracellular clefts of cardiac Purkinje fibres during voltage-clamp hyperpolarization and depolarization. Pflug. Archiv. **368**:19-31, 1977.
19. Bean, B.P. Two Kinds of Calcium Channels in Canine Atrial Cells. J. Gen. Physiol. **86**:1-30, 1985.
20. Benfey, B.G. Cardiac  $\alpha$ -adrenoceptors. Can. J. Physiol. Pharmacol. **58**:1145-1147, 1980.
21. Bennett, H.S. Morphological aspects of extracellular polysaccharides. J. Histochem. Cytochem. **11**:14-23, 1963.
22. Bennett, P.B. and T.B. Begenisich. Catecholamines modulate the delayed rectifying potassium current (IK) in guinea pig ventricular myocytes. Pflug. Archiv. **410**:217-219, 1987.
23. Berger, R.D., J.P. Saul and R.J. Cohen. transfer function analysis of autonomic regulation. I. The canine atrial rate response. Am. J. Physiol. **256**:H142-H152, 1989.
24. Bergfeldt, L., O. Edhag and H. Vallin. Cardiac conduction disturbances, an underestimated manifestation in ankylosing spondylitis. A 25-year follow-up study of 68 patients. Acta Med. Scand. **212**:217-223, 1982.
25. Bergfeldt, L. and M. Rosenqvist. Atrial Arrhythmias - the dominating cardiac problem in three patients with HLA B27 associated rheumatic disorders. Acta Med. Scand. **224**:627-630, 1988.
26. Berridge, M.J. Inositol trphosphate and diacylglycerol as second messengers. Biochem. J. **220**:345-360, 1984.
27. Berridge, M.J. Inositol triphosphate and diacylglycerol: two interacting second messengers. Ann. Rev. Biochem. **56**:159-193, 1987.

28. Berridge, M.J. and P.E. Rapp. A comparative study of the function, mechanism and control of cellular oscillators. J. Exp. Biol. **81**:217-279, 1979.
29. Bers, D. Ryanodine and the calcium content of cardiac SR assessed by caffeine and rapid cooling contractures. Am. J. Physiol. **253**:C408-C415, 1987.
30. Bers, D.M. and K.T. Macleod. Cumulative depletions of extracellular calcium in rabbit ventricular muscle monitored with calcium-selective microelectrodes. Circ. Res. **58**:769-782, 1986.
31. Beskrovnova, N.N., V.V. Korolev, I.L. Kosharskaya and V.A. Makarychev. Morphofunctional characteristics of pacemaker formations in the atrioventricular valves of the heart. Bull. Exp. Biol. Med. **83**:600-604, 1977.
32. Bharati, S. and M. Lev. The conductin system in simple, regular (d-), complete transposition with ventricular septal defect. J. Thor. Cardiovas. Surg. **72**:194, 1976.
33. Bharati, S., M.E. Moltham, G. Veasy and M. Lev. Conduction system in two cases of sudden death two years after the Mustard procedure. J. Thor. Cardiovas. Surg. **77**:101, 1979.
34. Bilezikian, J.P., S.F. Steinberg, E.M. Horn, R.B. Robinson and M.R. Rosen. G protein-adrenergic interactions in the heart. Mol. Cell. Biochem. **82**:5-11, 1988.
35. Bilezikjian, L.M., E.G. Kranias, J.D. Potter and A. Schwartz. Studies on phosphorylation of canine cardiac sarcoplasmic reticulum by calmodulin-dependent protein kinase. Circ. Res. **49**:1356-1362, 1981.
36. Bink-Boelkens, M.T.E., H. Velvis, J.J. Homan van der Heide, A. Eygelaar and R.A. Hardjowijono. Dysrhythmias after atrial surgery in children. Am. Heart J. **106**:125-130, 1983.
37. Bleeker, W.K., A.J.C. Mackaay, M. Masson-Pevet, L.N. Bouman and A.E. Becker. Functional and morphological organization of the rabbit sinus node. Circ. Res. **46**:11-22, 1980.
38. Blinks, J.R. Field stimulation as a means of effecting the graded release of autonomic transmitters in isolated heart muscle. J. Pharmacol. Exp. Ther. **151**:221, 1966.
39. Blinks, J.R., C.B. Olson, B.R. Jewell and P. Braveny. Influence of caffeine and other methylxanthines on mechanical properties of isolated mammalian heart muscle. Evidence for a dual mechanism of action. Circ. Res. **30**:367-392, 1972.
40. Bode, D.C. and L.L. Brunton. Post-receptor modulation of the effects of cyclic AMP in isolated cardiac myocytes. Mol. Cell. Biochem. **82**:13-18, 1988.
41. Bohm, M., W. Schmitz, H. Scholz and A. Wilken. Pertussis toxin prevents adenosine receptor- and m-cholinergic-mediated sinus rate slowing and AV conduction block in the guinea-pig heart. Naunyn-Schmiedeberg's Arch. Pharmacol. **339**:152-158, 1989.

42. Boineau, J.P., R.B. Schuessler, D.B. Hackel, C.B. Miller and C.W. Brockus. Widespread distribution and rate differentiation of the atrial pacemaker complex. Am. J. Physiol. 239:H406-H415, 1980.
43. Boineau, J.P., R.B. Schuessler, C.R. Mooney, A.C. Wylds, C.B. Miller and R.D. Hudson. Multicentric origin of the atrial depolarization wave: the pacemaker complex. Circ. 58:1036-1048, 1978.
44. Boineau, J.P., R.B. Schuessler, W.R. Roeske, L.J. Autry, C.B. Miller and A.C. Wylds. The quantitative relation between sites of atrial impulse origin and cycle length. Am J Physiol. 245:H781-H789, 1983.
45. Bojsen-Moller, F. and J. Tranum-Jensen. Rabbit heart nodal tissue, sinuatrial ring bundle and atrioventricular connexions identified as a neuromuscular system. J. Anat. 112:367-382, 1972.
46. Boller, M. and L. Pott. B-adrenergic modulation of transient inward current in guinea-pig cardiac myocytes. Evidence for regulation of  $Ca^{2+}$  release from sarcoplasmic reticulum by a cyclic AMP dependent mechanism. Pflug. Archiv. 415:276-288, 1989.
47. Borman, M.C. and T.A. McMillan. Destruction of the sinoauricular node in dogs' hearts by radon. Am. Heart J. 3:208-218, 1927.
48. Borman, M.C. and W.J. Meek. Coronary sinus rhythm: rhythm subsequent to destruction by radon of the sino-auricular nodes in dogs. Arch Intern Med. 47:957, 1931.
49. Bossen, E.H., J.R. Sommer and R.G. Waugh. Comparative sterology of mouse atria. Tiss. Cell 13:71-77, 1981.
50. Bottiger, L.E. and O. Edhag. Heart block in ankylosing spondylitis and uropolyarthritis. Br. Heart J. 34:487-492, 1972.
51. Bouman, L.N., A.J.C. Mackaay, W.K. Bleeker and A.E. Becker. Pacemaker shifts in the sinus node: effects of vagal stimulation, temperature and reduction of extracellular calcium. In: The Sinus Node: Structure, Function, and Clinical Relevance. ed. F.I.M. Bonke. Boston: Martinus-Nijhoff, pp.245-257, 1978.
52. Boyden, P.A., P.F. Cranefield and D.C. Gadsby. Noradrenaline hyperpolarizes cells of the canine coronary sinus by increasing their permeability to potassium ions. J. Physiol. 339:185-206, 1983.
53. Boyden, P.A., P.F. Cranefield, D.C. Gadsby and A.L. Wit. The basis for the membrane potential of quiescent cells of the canine coronary sinus. J. Physiol. 339:161-183, 1983.
54. Bozler, E. The initiation of impulses in cardiac muscle. Am. J. Physiol. 138:273-282, 1943.
55. Brady, A.J. and J. Hecht. On the origin of the heart beat. Am. J. Med. 17:110, 1954.

56. Brandenburg, K. and P. Hoffman. Wo entstehen die normalen Bewegungsreize im Warmbluterherzen und welche Folgen für die Schlagfolge hat ihre reizlose Ausschaltung?. Med. Klin. 8:16, 1912.

57. Breckenridge, I.M., H. Celert and J. Stark. Mustard's operation for transposition of the great arteries. Lancet 1:1141, 1972.

58. Brewerton, D.A., D.H. Goddard and R.B. Moore. The myocardium in ankylosing spondylitis. A clinical, echocardiographic and histopathological study. Lancet 1:995-998, 1987.

59. Bristow, M.R. and R. Ginsberg.  $\beta_2$ -receptors present in myocardial cells in human ventricular myocardium. Am. J. Cardiol. 57:3F-6F, 1986.

60. Bristow, M.R., R. Ginsberg, V. Umans, M. Fowler, R. Rasmussen, P. Zera, R. Menlove, P. Shah and E.B. Stinson.  $\beta_1$ - and  $\beta_2$ -adrenergic-receptor subpopulation in nonfailing and failing human ventricular myocardium. Coupling of both receptor subtypes to muscle contraction and selective  $\beta_1$ -receptor down-regulation in heart failure. Circ. Res. 59:297-309, 1986.

61. Brodde, O.E., S. Motomura, M. Endoh and H.J. Schumann. Lack of correlation between the positive inotropic effect evoked by  $\alpha$ -adrenoreceptor stimulation and the levels of cyclic AMP and/or cyclic GMP in the isolated ventricle strip of the rabbit. J. Mol. Cell. Cardiol. 10:207-219, 1978.

62. Brooks, C.McC. and H.H. Lu. The Sinoatrial Pacemaker of the Heart, Springfield: Charles C. Thomas, pp. 1-179, 1972.

63. Brown, H. and D. DiFrancesco. Voltage-clamp investigations of membrane currents underlying pace-maker activity in rabbit sino-atrial node. J. Physiol. 308:331-351, 1980.

64. Brown, H., D. DiFrancesco and S. Noble. Cardiac pacemaker oscillation and its modulation by autonomic transmitters. J. Exp. Biol. 81:175-204, 1979.

65. Brown, H., K. Kimura and S. Noble. The relative contributions of various time-dependent membrane currents to pacemaker activity in the sino atrial node. In: Cardiac Rate and Rhythm: Physiological, Morphological and Developmental Aspects. eds.L.N. Bouman and H.J. Jongasma. Boston: Martinus-Nijhoff, pp.53-68, 1982.

66. Brown, H., D. Noble, S. Noble and A.I. Taupignon. Relationship between transient inward current and slow inward currents in the sino-atrial node of the rabbit. J. Physiol. 370:299-315, 1986.

67. Brown, H.F., D. DiFrancesco and S.J. Noble. How does adrenaline accelerate the heart. Nature (Lond.) 280:235-236, 1979.

68. Brown, H.F., J. Kimura, D. Noble, S.J. Noble and A. Taupignon. The ionic currents underlying pacemaker activity in rabbit sino-atrial node: experimental results and computer simulations. Proc. R. Soc. Lond. B222:329-347, 1984.

69. Brown, H.F., J. Kimura, D. Noble, S.J. Noble and A. Taupignon. The slow inward current,  $i_{si}$ , in the rabbit sino-atrial node investigated by voltage clamp and computer simulation. Proc. R. Soc. Lond. **B222**:305-328, 1984.

70. Brown, J.H. and S.L. Brown. Agonists differentiate muscarinic receptors that inhibit cyclic AMP formation from those that stimulate phosphoinositide metabolism. J. Biol. Chem. **259**:3777-3781, 1984.

71. Brown, J.H., I.L. Buxton and L.L. Brunton.  $\alpha$ 1-Adrenergic and muscarinic cholinergic stimulation of phosphoinositide hydrolysis in adult rat cardiomyocytes. Circ. Res. **57**:532-537, 1985.

72. Bruckner, R. and H. Scholz. Effects of alpha-adrenoceptor stimulation with phenylephrine in the presence of propranolol on force of contraction, slow inward current and cyclic AMP content in the bovine heart. Br. J. Pharmacol. **82**:223-232, 1984.

73. Brum, G., V. Flockerzi, F. Hofmann, W. Osterrieder and W. Trautwein. Injection of catalytic subunit of cAMP-dependent protein kinase into isolated cardiac myocytes. Pflugers Arch. **398**:147-154, 1983.

74. Brum, G., W. Osterrieder and W. Trautwein.  $\beta$ -adrenergic increase in the calcium conductance of cardiac myocytes studied with the patch clamp. Pflug. Archiv. **401**:111-118, 1984.

75. Burt, J.M. and D.C. Spray. Single-channel events and gating behavior of the cardiac gap junction channel. Proc. Natl. Acad. Sci. USA **85**:3431-3434, 1988.

76. Buxton, I.L. and L.L. Brunton. Action of the cardiac alpha1-adrenergic receptor: Activation of cyclic AMP degradation. J. Biol. Chem. **260**:6733-6737, 1985.

77. Cachelin, A.B., J.E. De Peyer, S. Kokubun and H. Reuter.  $Ca^{2+}$  channel modulation by 8-bromocyclic AMP in cultured heart cells. Nature **304**:462-464, 1983.

78. Callewaert, G., E. Carmeliet and J. Vereecke. Single cardiac Purkinje cells: general electrophysiology and voltage-clamp analysis of the pace-maker current. J. Physiol. **349**:643-661, 1984.

79. Campbell, K.P., C.M. Knudson, T. Imagawa, A.T. Leung, J.L. Sutko, S.D. Kahl, C.R. Raab and L. Madson. Identification and characterization of the high affinity ryanodine receptor of the junctional sarcoplasmic reticulum  $Ca^{2+}$  release channel. J. Biol. Chem. **262**:6460-6463, 1987.

80. Cannell, M.B. and W.J. Lederer. The arrhythmogenic current  $I_{Ca}$  in the absence of electrogenic sodium-calcium exchange in sheep cardiac Purkinje fibres. J. Physiol. (Lond.) **374**:201-219, 1986.

81. Capogrossi, M.C., S.R. Houser, A. Bahinski and E.G. Lakatta. Synchronous occurrence of spontaneous localized calcium release from the sarcoplasmic reticulum generates action potential in rat cardiac ventricular myocytes at normal resting membrane potential. Circ. Res. **61**:498-503, 1987.

82. Carmeliet, E. Chloride ions and the membrane potential of Purkinje fibres. J. Physiol. **156**:375-388, 1961.

83. Carmeliet, E. Existence of pacemaker current  $i_f$  in human atrial appendage fibres. J. Physiol. (Lond.) **357**:125P (abs), 1984.
84. Carmeliet, E. and K. Mubagwa. Changes by acetylcholine on membrane currents in rabbit cardiac Purkinje fibres. J. Physiol. **371**:201-217, 1986.
85. Carroll, J.D., W.H. Gasch and K.P.W.J. McAdam. Amyloid cardiomyopathy: characterization by a distinctive voltage/mass relation. Am. J. Cardiol. **49**:9, 1982.
86. Challice, C.E. Studies on the microstructure of the heart. I. The sinoatrial node and the sinoatrial ring bundle. J. Roy. Microsc. Soc. **85**:1-21, 1966.
87. Challice, C.E. and S. Viragh. The embryologic development of the mammalian heart. In: Ultrastructure of the Mammalian Heart, eds.C.E. Challice and S. Viragh. New York: Acad. Press, pp.91, 1973.
88. Chang, F., J. Gao, C. Tromba, I. Cohen and D. DiFrancesco. Acetylcholine reverses effects of  $\beta$ -agonists on pacemaker current in canine cardiac Purkinje fibers but has no direct action: A difference between primary and secondary pacemakers. Circ. Res. **66**:633-636, 1990.
89. Chapman, R.A. and C. Leoty. The time-dependent dose-dependent effects of caffeine on the contraction of the ferret heart. J. Physiol. **256**:287-314, 1976.
90. Chiba, S., K. Kubota and K. Hashimoto. Double peaked positive chronotropic response of the isolated blood-perfused SA node to caffeine. Tohoku J. Exp. Med. **107**:101-102, 1972.
91. Clarkson, P.M., B.G. Barratt-Boyes and J.M. Neutze. Late dysrhythmias and disturbances of conduction following Mustard operation for complete transposition of the great arteries. Circulation **53**:519-524, 1976.
92. Clusin, W.T., R. Fishmeister and R.L. DeHaan. Caffeine-induced current in embryonic heart cells: time course and voltage dependence. Am. J. Physiol. **245**:H528-H532, 1983.
93. Cohen, I., J. Daut and D. Noble. The effects of potassium and temperature on the pace-maker current,  $i_{K2}$ , in Purkinje fibres. J. Physiol. **260**:55-74, 1976.
94. Cohen, I., R. Falk and R. Kline. Membrane currents following activity in canine cardiac Purkinje fibers. Biophys J **33**:281-288, 1981.
95. Colborn, G.L. and E.Jr. Carsey. Electron microscopy of the sinoatrial node of the squirrel monkey *Saimiri sciureus*. J. Mol. Cell. Cardiol. **4**:525-536, 1972.
96. Colquhoun, D., E. Neher, H. Reuter and C.F. Stevens. Inward current channels activated by intracellular Ca in cultured cardiac cells. Nature **294**:752, 1981.
97. Coraboeuf, E. and G. Vassort. Effets de la tetrodotoxine, du tetraethylammonium et du manganes sur l'activite du myocarde de rat et de cobaye. C. R. Acad. Sci. **264**:1072-1075, 1967.

98. Cranefield, P.F. The Conduction of the Cardiac Impulse, Mount Kisco, New York: Futura Publishing Company, pp. 8, 1975.
99. Cranefield, P.F. Does spontaneous activity arise from phase 4 depolarization or from triggering?. In: The Sinus Node: Structure, Function and Clinical Relevance. ed. F.I.M. Bonke. Boston: Martinus-Nijhoff, pp.348-356, 1978.
100. Crevey, B.J., G.A. Langer and J.S. Frank. Role of calcium in maintenance of rabbit myocardial cell membrane structural and functional integrity. J. Mol. Cell. Cardiol. 10:1081-1100, 1978.
101. Dahl, G. and G. Isenberg. Decoupling of heart muscle cells: Correlation with increased cytoplasmic calcium activity and with changes of nexus ultrastructure. J. Membr. Biol. 53:63-75, 1980.
102. Dangman, K.H., K.P. Dresdner, Jr. and S. Zaim. Automatic and triggered impulse initiation in canine subepicardial ventricular muscle cells from border zones of 24-hour transmural infarcts. New mechanisms for malignant cardiac arrhythmias. Circ. 78:1020-1030, 1988.
103. Davies, A.B., M.R. Stephens and A.G. Davies. Carotid sinus hypersensitivity in patients presenting with syncope. Br. Heart J. 42:583, 1979.
104. Davis, J., M.M. Scheinman, M.A. Ruder, J.C. Griffin, J.M. Herre, W.E. Finkebeiner, M.C. Chin and M. Eldar. Ablation of cardiac tissue by an electrode catheter technique for treatment of ectopic supraventricular tachycardia in adults. Circulation 74:1044-1053, 1986.
105. Davis, L.D. Effects of autonomic neurohumors on transmembrane potentials of atrial plateau fibers. Am. J. Physiol. 229:1351-1364, 1975.
106. Davis, L.D., J.V. Temte, P.E. Helmer and Q.E. Murphy. Effects of cyclopropane and of hypoxia on transmembrane potentials of atrial, ventricular, and Purkinje fibers. Circ. Res. 18:692-704, 1966.
107. De Mello, W.C. Influence of the sodium pump on intercellular communication in heart fibers: Effect of intercellular injection of sodium ion on electrical coupling. J. Physiol. 263:171-197, 1976.
108. De Mello, W.C. Effect of 2-4-dinitrophenol on intracellular communication in mammalian cardiac fibers. Pflug. Archiv. 380:267-276, 1979.
109. De Mello, W.C. Intercellular communication in cardiac muscle. Circ. Res. 51:1-9, 1982.
110. De Mello, W.C. and B.F. Hoffman. Potassium ions and electrical activity of specialized cardiac fibers. Am. J. Physiol. 199:1125-1130, 1960.
111. Deanfield, J., J. Camm, F. Macartney, T. Cartwright, J. Douglas, J. Drew, M.R. De Leval and J. Stark. Arrhythmia and late mortality after Mustard and Senning operation for transposition of the great arteries. J. Thor. Cardiovas. Surg. 96:569-576, 1988.



112. DeHaan, R.L. In vitro models of entrainment of cardiac cells. In: Cardiac Rate and Rhythm. eds.L.N. Bouman and H.J. Jongasma. New York: Martinus-Nijhoff, pp.323-359, 1982.
113. DeHaan, R.L. and R.O. O'Rahilly. Embryology of the heart. In: The Heart. Ed. 4ed. J.W. Hurst. New York: McGraw-Hill, pp.6, 1978.
114. Deleze, J. and J.C. Herve. Effect of several uncouplers of cell-to-cell communication on gap junction morphology in mammalian heart. J. Membrane Biol. 74:203-215, 1983.
115. Deleze, J. and W.R. Leowenstein. Permeability of a cell junction during intracellular injection of divalent cations. J. Membr. Biol. 28:71-86, 1976.
116. DeMello, W.C. Ionic factors controlling cell communication in heart. In: Normal and Abnormal Conduction in the Heart. eds.A. Paes de Carvalho, B.F. Hoffman and M. Lieberman. Mt. Kisco, NY: Futura Publishing Co., pp.53, 1982.
117. Demoulin, J.C. and H.E. Kulbertus. Histopathological correlates of sinoatrial disease. Br. Heart J. 40:1384, 1978.
118. Desilets, M. and C.M. Baumgarten. Isoproterenol directly stimulates the Na-K pump in isolated cardiac myocytes. Am. J. Physiol. 251:H218-H225, 1986.
119. Dewey, M.M. and L. Barr. Intercellular connection between smooth muscle cells: The nexus. Science 137:670-672, 1962.
120. Dewey, M.M. and L. Barr. A study of the structure and distribution of the nexus. J. Cell Biol. 23:553-585, 1964.
121. Di Gennarro, M., P. Carbonin and M. Vassalle. On the mechanism by which caffeine abolishes the fast rhythms induced by cardotonic steroids. J. Mol. Cell. Cardiol. 16:851-862, 1984.
122. DiFrancesco, D. A study of the ionic nature of the pace-maker current in calf Purkinje fibres. J. Physiol. 314:377-393, 1981.
123. DiFrancesco, D. A new interpretation of the pace-maker current  $i_{K2}$  in Purkinje fibres. J. Physiol. 314:359-376, 1981.
124. DiFrancesco, D. The current  $i_{K2}$  in Purkinje fibres reinterpreted and identified with the current  $i_f$  in the sinus node. In: Cardiac Rate and Rhythm: Physiological, Morphological and Developmental Aspects. eds.L.N. Bouman and H.J. Jongasma. Boston: Martinus-Nijhoff, pp.69-91, 1982.
125. DiFrancesco, D. Block and activation of the pace-maker channel in calf purkinje fibers: effects of potassium, caesium and rubidium. J. Physiol. 329:485-507, 1982.
126. DiFrancesco, D., A. Ferroni, M. Massanti and C. Tromba. Properties of the hyperpolarizing-activated current ( $i_f$ ) in cells isolated from the rabbit sino-atrial node. J. Physiol. (Lond). 377:61-88, 1986.

127. DiFrancesco, D., A. Noma and W. Trautwein. Kinetics and magnitude of the time-dependent potassium current in the rabbit sino-atrial node. Pflug. Archiv. 381:271-279, 1979.
128. DiFrancesco, D., M. Ohba and C. Ojeda. Measurement and significance of the reversal potential for the pacemaker current ( $i_{K_2}$ ) in sheep Purkinje fibers. J. Physiol. 297:135-162, 1979.
129. DiFrancesco, D. and C. Ojeda. Properties of the current  $i_f$  in the sino-atrial node of the rabbit compared with those of the current  $i_{K_2}$  in Purkinje fibres. J. Physiol. (Lond.) 308:353-367, 1980.
130. DiFrancesco, D. and C. Tromba. Inhibition of the hyperpolarization-activated current ( $i_f$ ) induced by acetylcholine in rabbit sino-atrial node myocytes. J. Physiol. (Lond.) 405:477-491, 1988.
131. DiFrancesco, D. and C. Tromba. Muscarinic control of the hyperpolarization-activated current ( $i_f$ ) in rabbit sino-atrial node myocytes. J. Physiol. (Lond.) 405:493-510, 1988.
132. Draper, M.H. and S. Weidmann. Cardiac resting and action potentials recorded with an intracellular electrode. J. Physiol. (Lond.) 115:74-94, 1951.
133. Dreifuss, J.J. and L. Girardier. Etude de la propagation de l'excitation dans le ventricule de de rat au moyen de solutions hypertoniques. Pflugers Arch. Ges. Physiol. 292:13-33, 1966.
134. Dudel, J., K. Peper, R. Rudel and W. Trautwein. The effect of tetrodotoxin on the membrane current in cardiac muscle (Purkinje fibers). Pflugers Arch. Ges. Physiol. 295:213-226, 1967.
135. Dudel, J. and W. Trautwein. Der mechanismus der automatischen rhythmischen impulsbildung der herzmuskelfaser. Arch. f. d. ges. Physiol 267:553-565, 1958.
136. Dukes, I.D. and E.M. Vaughan Williams. Effects of selective  $\alpha_1$ -,  $\alpha_2$ -,  $B_1$ -,  $B_2$ -adrenceptor stimulation on potentials and contractions in the rabbit heart. J. Physiol. 355:523-546, 1984.
137. Duster, M.C., M.T.E. Bink-Boelkens, D. Wampler, P.C. Gillette, D.G. McNamara and D.A. Cooley. Long-term follow-up of dysrhythmias following the Mustard procedure. Am. Heart J. 109:1323-1326, 1985.
138. Earm, Y.E., Y. Shimoni and A.J. Spindler. A pace-maker-like current in the sheep atrium and its modulation by catecholamines. J. Physiol. (Lond.) 342:569-590, 1983.
139. Eisner, D.A. and W.J. Lederer. Inotropic and arrhythmogenic effects of potassium-depleted solutions on mammalian cardiac muscle. J. Physiol. 294:255-277, 1979.
140. Eisner, D.A. and W.J. Lederer. Na-Ca exchange: stoichiometry and electrogenicity. Am. J. Physiol. 248:C189-C202, 1985.

141. El-Said, G.M., P.C. Gillette, D.A. Cooley, C.E. Mullins and D.G. McNamara. Protection of the sinus node in Mustard's operation. Circulation 53:788-791, 1976.
142. El-Said, G.M., H.S. Rosenberg, C.E. Mullins, G.L. Hallman, D.A. Cooley and D.G. McNamara. Dysrhythmias after Mustard's operation for transposition of the great arteries. Am. J. Cardiol. 30:526-532, 1972.
143. Ellingsen, O., O.M. Sejersted, S. Leraand and A. Ilebekk. Catecholamine-induced myocardial potassium uptake by  $\beta_1$ -adrenoceptors and adenylate cyclase activation in the pig. Circ. Res. 60:540-550, 1987.
144. Endoh, M. and J.R. Blinks. Actions of sympathomimetic amines on the  $\text{Ca}^{2+}$  transients and contractions of rabbit myocardium: Reciprocal changes in myofibrillar responsiveness to  $\text{Ca}^{2+}$  mediated through  $\alpha$ - and  $\beta$ -adrenoceptors. Circ. Res. 62:247-265, 1988.
145. Endoh, M., M. Maruyama and T. Iijima. Attenuation of muscarinic cholinergic inhibition by islet-activating protein in the heart. Am. J. Physiol. 249:H309-H320, 1985.
146. Engelmann, T.W. Ueber den myogen ursprung der Herzthatigkeit und uber automatische Erregbarkeit als mormale Eigenschaft peripherischer nervenfasern. Pflugers Arch. Ges. Physiol. 65:535-576, 1879.
147. Erlanger, J. and J.R. Blackman. A study of relative rhythmicity and conductivity in various regions of the auricles of the mammalian heart. Am. J. Physiol. 19:125-174, 1907.
148. Escande, D., E. Coraboeuf and C. Planche. Abnormal pacemaking is modulated by sarcoplasmic reticulum in partially-depolarized myocardium from dilated right atria in humans. J. Mol. Cell. Cardiol. 19:231-241, 1987.
149. Euler, D.E., S.B. Jones, W.P. Gunnar, J.M. Loeb, D.K. Murdock and W.C. Randall. Cardiac arrhythmias in the conscious dog after excision of the sinoatrial node and crista terminalis. Circulation 59:468-475, 1979.
150. Eyster, J.A.E. and W.J. Meek. Experiments on the origin and conduction of the cardiac impulse. VI. Conduction of the excitation from the sino-auricular node to the right auricle and auriculoventricular node. Arch. Int. Med. 18:775-799, 1916.
151. Eyster, J.A.E. and W.J. Meek. Studies on the origin and conduction of the cardiac impulse. VIII. The permanent rhythm following destruction of the sino-auricular node. Am. J. Physiol. 61:117-129, 1922.
152. Fabiato, A. Calcium release in skinned cardiac cells: variation with species, tissues, and development. Federation Proc. 41:2238-2244, 1982.
153. Fabiato, A. and F. Fabiato. Contractions induced by a calcium-triggered release of calcium from the sarcoplasmic reticulum of single skinned cardiac cells. J Physiol (London) 249:469-495, 1975.
154. Fawcett, D.W. An Atlas of Fine Structure, The Cell, Philadelphia: W.B.Saunders Co., 1966.

155. Fawcett, D.W. and N.S. McNutt. The ultrastructure of the cat myocardium. J. Cell Biol. 42:1-45, 1969.
156. Feigl, E.O. Coronary physiology. Physiol. Rev. 63:1-205, 1983.
157. Feldt, R.H. Atrioventricular Canal Defects, Philadelphia: Saunder, pp. 1-12, 1976.
158. Fenoglio, J.J., T.D. Pham, A.L. Wit, A.L. Bassett and B.M. Wagner. Canine mitral complex: Ultrastructure and electromechanical properties. Circ. Res. 31:417-430, 1972.
159. Ferguson, D.G. and T.S. Leeson. Postnatal development of sarcolemmal invaginations in right atrial myocardium of the rat. Acta Anat. 117:289-302, 1983.
160. Ferrer, M.I. The sick sinus syndrome. Circ. 47:635-641, 1973.
161. Fischmeister, R. and H.C. Hartzell. Mechanism of action of acetylcholine on calcium current in single cells from frog ventricle. J. Physiol. 376:183-202, 1986.
162. Flavahan, N.A. and J.C. McGrath.  $\alpha$ 1-Adrenoceptors can mediate chronotropic responses in the rat heart. Br. J. Pharmacol. 73:586-588, 1981.
163. Flavahan, N.A. and J.C. McGrath.  $\alpha$ 1-Adrenoceptor activation can increase heart rate directly or decrease it indirectly through parasympathetic activation. Br. J. Pharmacol. 77:319-328, 1982.
164. Fleming, J.W. and A.M. Watanabe. Muscarinic cholinergic-receptor stimulation of specific GTP hydrolysis related to adenylate cyclase activity in canine cardiac sarcolemma. Circ. Res. 63:340-350, 1988.
165. Forbes, M.S. and N. Sperelakis. A labyrinthine structure formed from a transverse tubule of mouse ventricular myocardium. J. Cell Biol. 56:865-869, 1973.
166. Forbes, M.S. and N. Sperelakis. The presence of transverse tubules and axial tubules in the ventricular myocardium of embryonic and neonatal guinea-pigs. Cell Tissue Res. 166:83-90, 1976.
167. Forbes, M.S. and N. Sperelakis. The membrane systems and cytoskeletal elements of mammalian myocardial cells. In: Cell and Muscle Motility. eds. J.W. Shay and R.M. Dowben. New York: Plenum Press, pp.89-155, 1983.
168. Forbes, M.S. and N. Sperelakis. Ultrastructure of mammalian cardiac muscle. In: Physiology and Pathophysiology of the Heart. ed. N. Sperelakis. Boston: Martinus Nijhoff, pp.3-42, 1984.
169. Forssmann, W.G. and L. Girardier. A study of the T system in the rat heart. J. Cell Biol. 44:1-19, 1970.
170. Fozzard, H.A. and C.O. Lee. Influence of changes in extracellular potassium and chloride ions on membrane potential and intracellular potassium ion activity in rabbit ventricular muscle. J. Physiol. 256:663-689, 1976.

171. Frank, J.S., G.A. Langer, L.M. Nudd and K. Seraydarian. The myocardial cell surface, its histochemistry and effect of sialic acid and calcium removal on its structure and cellular ionic exchange. Circ. Res. 41:702-714, 1977.
172. Friesen, W.O. and G.D. Block. What is a biological oscillator?. Am. J. Physiol. 246:R847-R851, 1984.
173. Gadsby, D.C.  $\beta$ -adrenoreceptor agonists increase membrane  $K^+$  conductance in cardiac Purkinje fibres. Nature 306:691-693, 1983.
174. Gadsby, D.C. The Na/K pump of cardiac cells. Ann. Rev. Biophys. Bioeng. 13:373-398, 1984.
175. Gadsby, D.C. and P.F. Cranefield. Two levels of resting potential in cardiac Purkinje fibers. J. Gen. Physiol. 70:725-746, 1977.
176. Gadsby, D.C. and P.F. Cranefield. Effects of electrogenic sodium extrusion on the membrane potential of cardiac Purkinje fibers. In: Normal and Abnormal Conduction in the Heart. eds. A. Paes de Carvalho, B.F. Hoffman and M. Lieberman. Mt. Kisco, New York: Futura Publishing Co., pp.225, 1982.
177. Gadsby, D.C., R. Niedergerke and D.C. Ogden. The dual nature of membrane potential increase associated with activity of the sodium-potassium exchange pump in skeletal muscle fibers. Proc. R. Soc. Lond. Ser. B Biol. Sci. 198:463-472, 1977.
178. Geesbreght, J.M., W.C. Randall and G. Brynjolfson. Area localization of supraventricular pacemaker activity before and after SA node excision. Physiologist 13:202, 1970.
179. Gibson, R., D.J. Driscoll, P.C. Gillette, C.J. Hartley and M.L. Entman. The comparative electrophysiologic and hemodynamic effects of verapamil in puppies and adult dogs. Dev. Pharmacol. Ther. 2:104-116, 1981.
180. Giles, W. and S.J. Noble. Changes in membrane currents in bullfrog atrium produced by acetylcholine. J. Physiol. 261:103-123, 1976.
181. Giles, W., A. van Ginneken and E.F. Shibata. Ionic currents underlying cardiac pacemaker activity: a summary of voltage-clamp data from single cells. In: Cardiac Muscle: The Regulation of Excitation and Contraction. ed. R. Nathan. London, England: Academic Press, Inc., pp.1-27, 1986.
182. Giles, W.R. and E.F. Shibata. Voltage clamp of bull-frog cardiac pace-maker cells: a quantitative analysis of potassium currents. J. Physiol. (Lond.) 368:265-292, 1985.
183. Giles, W.R. and A.C.G. Van Ginneken. A transient outward current in isolated cells from the crista terminalis of rabbit heart. J. Physiol. (Lond.) 368:243-264, 1985.
184. Gillette, P.C. The mechanisms of supraventricular tachycardia in children. Circulation 54:133-139, 1976.

185. Gillette, P.C., G.M. El-Said, N. Sivarajan, C.E. Mullins, R.L. Williams and D.G. McNamara. Electrophysiological abnormalities after Mustard's operation for transposition of the great arteries. Br. Heart J. 36:186-191, 1974.
186. Gillette, P.C. and A.Jr. Garson. Electrophysiologic and pharmacologic characteristics of automatic ectopic atrial tachycardia. Circulation 56:571-575, 1977.
187. Gillette, P.C., J.D. Kugler, A.Jr. Garson, H.P. Gutgesell, D.F. Duff and D.G. McNamara. Mechanisms of cardiac arrhythmias after the mustard operation for transposition of the great arteries. Am. J. Cardiol. 45:1225-1230, 1980.
188. Gillette, P.C., D.G. Wampler, A.Jr. Garson, A. Zinner and D. Cooley. Treatment of atrial automatic tachycardia by ablation procedures. J. Am. Coll. Cardiol. 6:405-409, 1985.
189. Girardier, L., J.J. Dreifus and W.G. Forssmann. Micropinocytose de ferritine dans le cellules myocardiques de tortue et de rat. Acta Anat. 68:251, 1967.
190. Glass, L. and M.C. Mackey. From Clocks to Chaos: The Rhythms of Life, Princeton: Princeton University Press, pp. 3-248, 1988.
191. Glitsch, H.G. and L. Pott. Spontaneous tension oscillations in guinea-pig atrial trabeculae. Pflug. Archiv. 358:11-25, 1975.
192. Goldberg, J.M., J.M. Geesbreght, W.C. Randall and G. Brynjolfsson. Sympathetically induced pacemaker shifts following sinus node excision. Am. J. Physiol. 224:1468-1474, 1973.
193. Goldman, D.E. Potential, impedance, and rectification in membranes. J. Gen. Physiol. 27:37-60, 1943.
194. Goldreyer, B.N., J.J. Gallagher and A.N. Damato. The electrophysiologic demonstration of atrial ectopic tachycardia in man. Am. Heart J. 85:205, 1973.
195. Goodman, D., A.B.M. Van der Steen and R.T. Van Dam. Endocardial and epicardial activation pathways of the canine right atrium. Am. J. Physiol. 220:1-11, 1971.
196. Gorza, L., S. Schiaffino and M. Vitadello. Heart conduction system: A neural crest derivative?. Brain Res. 457:360-366, 1988.
197. Gorza, L. and M. Vitadello. Distribution of conducting system fibers in the developing and adult rabbit heart revealed by an antineurofilament antibody. Circ. Res. 65:360-369, 1989.
198. Greengard, P. Phosphorylated proteins as physiological effectors. Science 199:146-152, 1978.
199. Greenwood, R.D., A. Rosenthal, L.J. Sloss, M. LaCorte and A.S. Nadas. Sick sinus syndrome after surgery for congenital heart disease. Circulation 52:208-213, 1975.
200. Guckenheimer, J. Isochrons and phaseless sets. J. Math. Biol. 1:259-273, 1975.

201. Hagiwara, N. and H. Irisawa. Modulation by intracellular  $\text{Ca}^{++}$  of the hyperpolarization-activated inward current in rabbit single sino-atrial node cells. J. Physiol. 409:121-141, 1989.
202. Hagiwara, N., H. Irisawa and M. Kameyama. Contribution of two types of calcium currents to the pacemaker potentials of rabbit sino-atrial node cells. J. Physiol. 395:233-253, 1988.
203. Hagiwara, S., S. Miyazaki, W. Moody and J. Patlak. Blocking effects of barium and hydrogen ions on the potassium current during anomalous rectification in the starfish egg. J. Physiol. 279:167-185, 1978.
204. Hagiwara, S. and S. Nakajima. Tetrodotoxin and manganese ion: Effects on action potential of the frog heart. Science 149:1254-1255, 1965.
205. Hagiwara, S. and S. Nakajima. Differences in Na and Ca spikes as examined by application of tetrodotoxin, procaine, and manganese ions. J. Gen. Physiol. 49:793-806, 1966.
206. Hajdu, S. and E. Leonard. Action of ryanodine on mammalian cardiac muscle. Effects on contractility and reversal of digitalis-induced ventricular arrhythmias. Circ. Res. 9:1291-1298, 1961.
207. Hama, K. and T. Kanaseki. A comparative microanatomy of the ventricular myocardium. In: Electrophysiology and Ultrastructure of the Heart. eds. T. Sano, V. Mizuhira and K. Matsuda. Tokyo: Bunkodo, pp.27-40, 1967.
208. Hansford, R.G. and E.G. Lakatta. Ryanodine releases calcium from sarcoplasmic reticulum in calcium-tolerant rat cardiac myocytes. J. Physiol. 390:453-467, 1987.
209. Hardie, E.L., S.B. Jones, D.E. Euler, D.L. Fishman and W.C. Randall. Sinoatrial node artery distribution and its relation to hierarchy of cardiac automaticity. Am. J. Physiol. 241:H45-H53, 1981.
210. Harvey, W. Anatomical Studies on the Motion of the Heart and Blood, Springfield: Charles C. Thomas, pp. 42, 1970.
211. Hayes, J.S., L.L. Brunton and S.E. Mayer. Selective activation of particulate cAMP-dependent protein kinase by isoprenalol and prostaglandin E. J. Biol. Chem. 255:5113-5119, 1980.
212. Hays, M.D. and P.C. Gillette. Atrial automatic ectopic tachycardia successfully treated with encainide in a 4-week-old infant after Senning procedure. Am. Heart J. 117:489-492, 1989.
213. Hearse, D.J., S.M. Humphrey, W.G. Nayler, A. Slade and D. Border. Ultrastructure damage associated with reoxygenation of the anoxic myocardium. J. Mol. Cell. Cardiol. 7:315-324, 1975.
214. Hecht, H.H. Normal and abnormal transmembrane potentials of the spontaneously beating heart. NY Acad. Sci. 65:700, 1957.

215. Hescheler, J., M. Kameyama and W. Trautwein. On the mechanism of muscarinic inhibition of the cardiac Ca current. Pflug. Archiv. 407:182-189, 1986.
216. Hescheler, J., M. Kameyama, W. Trautwein, G. Mieskes and H.D. Soling. Regulation of cardiac calcium channel by protein phosphatases. Eur. J. Biochem. 165:261-266, 1987.
217. Hess, P., J.B. Lansman and R.W. Tsien. Different modes of Ca channel gating behavior favored by dihydropyridine Ca agonists and antagonists. Nature 311:538-544, 1984.
218. Hess, P. and W.G. Wier. Excitation-contraction coupling in cardiac Purkinje fibers. Effects of caffeine on the intracellular Ca<sup>2+</sup> transient, membrane currents, and contraction. J. Gen. Physiol. 83:417-433, 1984.
219. Hewett, K.W. and M.R. Rosen. Developmental changes in the rabbit sinus node action potential and its response to adrenergic agonists. J. Pharmacol. Exp. Ther. 235:308-312, 1985.
220. Hibbs, R.G. and V.J. Ferrans. An ultrastructural and histochemical study of rat atrium myocardium. Am. J. Anat. 124:251-270, 1969.
221. Hirano, Y., H.A. Fozzard and C.T. January. Characteristics of L- and T-type Ca<sup>++</sup> currents in canine cardiac Purkinje cells. Am. J. Physiol. 256:H1478-H1492, 1989.
222. Hiraoka, M. and T. Sano. Role of the sinoatrial ring bundle in internodal conduction. Am. J. Physiol. 231:319-325, 1976.
223. Hirobe, H. Studies on the spread of the right atrial activation by means of intracellular microelectrode. Jap. Circ. J. 25:583-593, 1961.
224. Hirota, A., K. Kamino and H. Komuro. Mapping of early development of electrical activity in the embryonic chick heart using multiple-site optical recording. J. Physiol. 383:711, 1987.
225. Hodgkin, A.L. and P. Horowicz. The effect of sodium ions on the electrical activity of the giant axon of the squid. J. Physiol. 108:37-77, 1949.
226. Hoffman, B.F. and P.F. Cranefield. The physiological basis of cardiac arrhythmias. Am. J. Med. 37:670-684, 1964.
227. Hoffman, B.F., M.R. Rosen and A.L. Wit. Electrophysiology and pharmacology of cardiac arrhythmias III. The cause and treatment of cardiac arrhythmias. Am. Heart J. 89:115, 1975.
228. Hogan, P.M. and L.D. Davis. Evidence for specialized fibers in the canine right atrium. Circ. Res. 23:387-396, 1968.
229. Hogan, P.M. and L.D. Davis. Electrophysiological characteristics of canine atrial plateau fibers. Circ. Res. 28:62-73, 1971.
230. Holsinger, J.W., A.G. Wallace and W.C. Sealy. The identification and surgical significance of the atrial internodal conduction tracts. Ann. Surg. 167:447-453, 1968.



231. Howse, H.P., V.J. Ferrans and R.G. Hibbs. A comparative histochemical and electronmicroscopic study of the surface coating of cardiac muscle cells. J. Mol. Cell. Cardiol. 1:157-168, 1970.
232. Hunter, D.R., R.A. Haworth and H.A. Berkoff. Modulation of cellular calcium stores in the perfused rat heart by isoproterenol and ryanodine. Circ. Res. 53:703-712, 1983.
233. Hurst, J.W. and R.B. Logue. The Heart, New York: McGraw Hill Book Company, pp. 294, 1966.
234. Hutter, O.F. and D. Noble. Anion conductance of cardiac muscle. J. Physiol. 157:335-350, 1961.
235. Hutter, O.F. and W. Trautwein. Effect of vagal stimulation on the sinus venosus of the frog's heart. Nature 176:512-513, 1955.
236. Iacono, G. and M. Vassalle. Acetylcholine increases intracellular sodium activity in sheep cardiac Purkinje fibers. Am. J. Physiol. 256:H1407-H1416, 1989.
237. Iijima, T., H. Irisawa and M. Kameyama. Membrane currents and their modification by acetylcholine in isolated single atrial cells of the guinea-pig. J. Physiol. 359:485-501, 1985.
238. Iijima, T. and N. Taira.  $\beta_2$ -adrenoceptor-mediated increase in the slow inward calcium current in atrial cells. Eur. J. Pharmacol. 163:357-360, 1989.
239. Inui, M., A. Saito and S. Fleischer. Isolation of the ryanodine receptor from cardiac sarcoplasmic reticulum and identity with feet structures. J. Biol. Chem. 262:15637-15642, 1987.
240. Irisawa, H. Electrical activity of rabbit sino-atrial node as studied by a double sucrose gap method. In: Proceedings of the Satellite Symposium of the XXVth International Congress of Physiological Sciences, ed. P. Rijlant. Bruxelles: Presses Academiques Europeanes, 1972.
241. Irisawa, H. Comparative physiology of the cardiac pacemaker mechanism. Physiol. Rev. 58:461-498, 1978.
242. Irisawa, H. and S. Kokubun. Modulation by intracellular ATP and cyclic AMP of the slow inward current in isolated single ventricular cells of the guinea-pig. J. Physiol. 338:321-327, 1983.
243. Irisawa, H. and A. Noma. Pacemaker mechanisms of rabbit sinoatrial node cells. In: Cardiac Rate and Rhythm: Physiological, Morphological and Developmental Aspects, eds. L.N. Bouman and H.J. Jongsma. Boston: Martinus-Nijhoff, pp.35-51, 1982.
244. Irisawa, H. and A. Noma. Pacemaker currents in mammalian nodal cells. J. Mol. Cell. Cardiol. 16:777-781, 1984.

245. Isaacson, R., J.L. Titus, J. Merideth, R.H. Feldt and D.C. McGoon. Apparent interruption of atrial conduction pathways after surgical repair of transposition of great arteries. Am. J. Cardiol. 30:533-535, 1972.
246. Isenberg, G. Cardiac purkinje fibers: Cesium as a tool to block inward rectifying potassium currents. Pflug. Archiv. 365:99-106, 1976.
247. Isenberg, G. and U. Klockner. Calcium currents of isolated bovine ventricular myocytes are fast and of large amplitude. Pflug. Archiv. 395:30-41, 1982.
248. Isenberg, G. and U. Klockner. Calcium tolerant ventricular myocytes prepared by preincubation in a "KB Medium". Pflugers Arch. 395:6-18, 1982.
249. Ishikawa, H. and E. Yamada. Differentiation of the sarcoplasmic reticulum and T-system in developing mouse cardiac muscle. In: Developmental and Physiological Correlates of Cardiac Muscle. eds.M. Lieberman and T. Sano. New York: Raven Press, pp.21-35, 1976.
250. Jaeger, . Archiv. f. klin. Med. 51:1, 1910.
251. Jalife, J. and C. Antzelevitch. Phase resetting and annihilation of pacemaker activity in cardiac tissue. Science 206:695-697, 1979.
252. James, T.N. The connecting pathways between the sinus node and AV node and between the right and left atrium in the human heart. Am. Heart J. 66:498-508, 1963.
253. James, T.N. Anatomy of the A-V node of the dog. Anat. Rec. 148:15-27, 1964.
254. James, T.N. The delivery and distribution of coronary collateral circulation. Chest 58:183-203, 1970.
255. James, T.N. The sinus node. Am. J. Cardiol. 40:965-986, 1977.
256. James, T.N. and R.E. Birk. Pathology of the cardiac conduction system in polyarteritis nodosa. Arch. Intern. Med. 117:561, 1966.
257. James, T.N., J.H. Isobe and J.H. Urthaler. Correlative electrophysiological and anatomical studies concerning the site of origin of escape rhythm during complete atrioventricular block in the dog. Circulation Research 45:108-119, 1979.
258. James, T.N. and R.A. Nadeau. Direct perfusion of the sinus node: An experimental model for pharmacologic and electrophysiologic studies of the heart. Henry Ford Hosp. Med. Bull. 10:21-25, 1962.
259. James, T.N. and R.A. Nadeau. Sinus bradycardia during injections directly into the sinus node artery. Am. J. Physiol. 204:9-15, 1963.
260. James, T.N. and L. Sherf. Ultrastructure of the human atrioventricular node. Circ. 37:1049-1070, 1968.
261. James, T.N. and L. Sherf. Specialized tissues and preferential conduction in the atrial of the heart. Am. J. Cardiol. 28:414-427, 1971.

262. James, T.N., L. Sherf, G. Fine and A.R. Morales. Comparative ultrastructure of the sinus node in man and dog. Circ. 34:139-163, 1966.
263. Janse, M.J. and R.H. Anderson. Specialized internodal atrial pathways - fact or fiction?. Eur. J. Cardiol. 2:117, 1974.
264. Janse, M.J. and F.J.L. van Capelle. Electrotonic interactions across an inexcitable region as a cause of ectopic activity in acute regional myocardial ischemia. Circ. Res. 50:527, 1982.
265. Jenden, D.J. and A.S. Fairhurst. The pharmacology of ryanodine. Pharm. Rev. 21:1-25, 1969.
266. Jennings, R.B., C.E. Ganote and K.A. Reimer. Ischemic tissue injury. Am. J. Path. 81:179-198, 1975.
267. Jones, S.B., D.E. Euler, E. Hardie, W.C. Randall and G. Brynjolfsson. Comparison of SA nodal and subsidiary atrial pacemaker function and location in the dog. Am. J. Physiol. 234:H471-H476, 1978.
268. Jones, S.B., D.E. Euler, W.C. Randall, G. Brynjolfsson and E.L. Hardie. Atrial ectopic foci in the canine heart: hierarchy of pacemaker automaticity. Am. J. Physiol. 238:H788-H793, 1980.
269. Jones, S.B., W.C. Randall, L.E. Rinkema, G.J. Rozanski and S.L. Lipsius. Autonomic control of right atrial pacemakers (Abstract). Federation Proc. 40:413, 1981.
270. Jordan, J.L., I. Yamaguchi and W.J. Mandel. Studies on the mechanism of sinus node dysfunction in the sick sinus syndrome. Circulation 57:217, 1978.
271. Jorgensen, A.O., R. Broderick, A.P. Somlyo and A.V. Somlyo. Two structurally distinct calcium storage sites in rat cardiac sarcoplasmic reticulum: An electron microprobe analysis study. Circ. Res. 63:1060-1069, 1988.
272. Jorgensen, A.O. and K.P. Campbell. Evidence for the presence of calsequestrin in two structurally different regions of the myocardial sarcoplasmic reticulum. J. Cell Biol. 98:1343-1352, 1984.
273. Jorgensen, A.O. and L.J. McGuffee. Immunoelectron microscopic localization of sarcoplasmic reticulum proteins crossfixed, freeze-dried, and low temperature-embedded tissue. J. Histochem. Cytochem. 35:723-732, 1987.
274. Jorgensen, A.O., A.C.-Y. Shen and K.P. Campbell. Ultrastructural localization of calsequestrin in adult rat atrial and ventricular muscle cells. J. Cell Biol. 101:257-268, 1985.
275. Jorgensen, A.O., A.C.-Y. Shen, P. Daly and D.H. MacLennan. Localization of  $Ca^{++}Mg^{++}ATPase$  of the sarcoplasmic reticulum in adult rat papillary muscle. J. Biol. Chem. 93:883-892, 1982.

276. Jundt, H., H. Porzig, H. Reuter and J.W. Stucki. The effects of substances releasing intracellular calcium ions on sodium-dependent calcium efflux from guinea-pig auricles. J. Physiol. 246:229-253, 1975.
277. Kahn, M., I. Shiffman, L.A. Kuhn and T.E. Jacobson. Effects of ryanodine in normal dogs and in those with digitalis-induced arrhythmias. Hemodynamic and electrocardiographic studies. Amer. J. Cardiol. 14:658-668, 1964.
278. Kameyama, M., F. Hofmann and W. Trautwein. On the mechanism of B-adrenergic regulation of the Ca channels in the guinea-pig heart. Pflug. Archiv. 405:285-293, 1985.
279. Karagueuzian, H. and B. Katzung. Voltage-clamp studies of transient inward current and mechanical oscillations induced by ouabain in ferret papillary muscle. J. Physiol. 327:255-271, 1982.
280. Kass, R.S., W.J. Lederer, R.W. Tsien and R. Weingart. Role of calcium ions in transient inward currents and aftercontractions induced by strophanthidin in cardiac Purkinje fibers. J. Physiol. (Lond.) 281:187-208, 1978.
281. Kass, R.S. and R.W. Tsien. Fluctuations in membrane current driven by intracellular calcium in cardiac Purkinje fibers. Biophys J 38:259-269, 1982.
282. Kass, R.S., R.W. Tsien and R. Weingart. Ionic basis of transient inward current induced by strophanthidin in cardiac Purkinje fibres. J. Physiol. 281:209-226, 1978.
283. Kaumann, A.J. and H. Lemoine. B<sub>2</sub>-adrenoceptor-mediated positive inotropic effect of adrenaline in human ventricular myocardium. Naunyn-Schmeideberg's Arch Pharmacol. 335:403, 1987.
284. Kawamura, K. and T. Konishi. Ultrastructure of the cell junction of heart muscle with special reference to its functional significance in excitation conduction and to the concept of "disease of the intercalated disc". Jap. Circ. J. 31:1533-1544, 1967.
285. Keely, S., T. Lincoln and J. Corbin. Interaction of acetylcholine and epinephrine on heart cyclic AMP-dependent protein kinase. Am. J. Physiol. 234:H432-H438, 1978.
286. Keith, A. and M. Flack. The form and nature of the muscular connections between the primary divisions of the vertebrate heart. J. Anat. Physiol. 41:172-189, 1906.
287. Keith, A. and I. Mackenzie. Recent researches on the anatomy of the heart. Lancet 1:101-103, 1910.
288. Keith, J.D., R.D. Rowe and P. Vlad. Heart Disease in Infancy and Childhood, Ed. 3 New York: The MacMillan Company, 1978.
289. Kentish, J.C., R.J. Barsotti, T.J. Lea, I.P. Mulligan, J. Patel and M. Ferenczi. Calcium release from cardiac sarcoplasmic reticulum induced by photorelease of calcium or Ins(1,4,5)P<sub>3</sub>. Am. J. Physiol. 258:H610-H615, 1990.
290. Kerr, C.R., A.O. Grant, T.L. Wenger and H.C. Strauss. Sinus node dysfunction. Cardiol. Clin. 1:187-207, 1983.

291. Kihara, Y., W. Grossman and J.P. Morgan. Direct measurement of changes in intracellular calcium transients during hypoxia, ischemia and reperfusion of the intact mammalian heart. Circ. Res. **65**:1029-1044, 1989.
292. Kimura, J., S. Miyamae and A. Noma. Identification of sodium-calcium exchange current in single ventricular cells of guinea-pig. J. Physiol. **384**:199-222, 1987.
293. Kimura, J., A. Noma and H. Irisawa. Na-Ca exchange current in mammalian heart cells. Nature **319**:596-597, 1986.
294. Kline, R. and M. Morad. Potassium efflux and accumulation in heart muscle. Evidence from  $K^+$  electrode experiments. Biophys. J. **16**:367-372, 1976.
295. Koch, W. Ueber die Bedeutung der Reizbildungsstellen (kardiomotorischen Zentren) des rechten Vorhofes beim Säugetierherzen. Arch. f. d. ges. Physiol **151**:275, 1913.
296. Kohl, C., W. Schmitz, H. Scholz and J. Scholz. Evidence for the existence of inositol tetrakisphosphate in mammalian heart: Effect of  $\alpha$ -adrenoceptor stimulation. Circ. Res. **66**:580-583, 1990.
297. Kohlhardt, M., B. Bauer, H. Krause and A. Fleckenstein. Differentiation of the transmembrane Na and Ca channels in mammalian cardiac fibers by the use of specific inhibitors. Pflug. Archiv. **335**:309, 1972.
298. Kohlhardt, M., H.R. Figulla and O. Tripathi. The slow membrane channel as the predominant mediator of the excitation process of the sinoatrial pacemaker cell. Basic Res. Cardiol. **71**:17, 1976.
299. Kohlhardt, M., H. Krause, M. Kubler and A. Herdey. Kinetics of inactivation and recovery of the slow inward current in the mammalian ventricular myocardium. Pflug. Archiv. **355**:1-17, 1975.
300. Kokubun, S. and H. Reuter. Dihydropyridine derivatives prolong the open state of Ca channels in cultured cardiac cells. Proc. Natl. Acad. Sci. **81**:4824-4827, 1984.
301. Kort, A.A. and E.G. Lakatta. Calcium-dependent mechanical oscillations occur spontaneously in unstimulated mammalian cardiac tissues. Circ. Res. **54**:396-404, 1984.
302. Korth, M. and V. Kuhlkamp. Muscarinic receptor-mediated increase of intracellular  $Na^+$  ion activity and force of contraction. Pflug. Archiv. **403**:266-272, 1985.
303. Korth, M., V.K. Sharma and S.S. Sheu. Stimulation of muscarinic receptors raises free intracellular  $Ca^{2+}$  concentration in rat ventricular myocytes. Circ. Res. **62**:1080-1087, 1988.
304. Kreitner, D. Evidence for the existence of a rapid sodium channel in the membrane of rabbit sinoatrial cells. J. Mol. Cell. Cardiol. **7**:655-662, 1975.
305. Kung, S.K. Herzblockstudien. Arch. f. exper. Path. u. Pharmakol. **155**:295, 1930.

306. Lado, M.G., S.S. Sheu and H.A. Fozzard. Changes in intracellular  $\text{Ca}^{2+}$  activity with stimulation in sheep cardiac Purkinje strands. Am. J. Physiol. **243**:H133, 1982.
307. Lai, F.A., H. Erickson, B.A. Block and G. Meissner. Evidence for a junctional feet-ryanodine receptor complex from sarcoplasmic reticulum. Biochem. Biophys. Res. Comm. **143**:704-709, 1987.
308. Lakatta, E.G. and D.L. Lappe. Diastolic scattered light fluctuation, resting force and twitch force in mammalian cardiac muscle. J. Physiol. **315**:369-394, 1981.
309. Langer, G.A., J.S. Frank and J.D. Philipson. Correlation of alterations in cation exchange and sarcolemmal ultrastructure produced by neuraminidase and phospholipases in cardiac cell tissue culture. Circ. Res. **49**:1289-1299, 1981.
310. Langer, G.A., J.S. Frank and K.D. Philipson. Ultrastructure and calcium exchange of the sarcolemma, sarcoplasmic reticulum and mitochondria of the myocardium. Pharmacol. Rev. **16**:331-376, 1982.
311. Langer, G.A. and L.M. Nudd. Addition and kinetic characterization of mitochondrial calcium in myocardial tissue culture. Am. J. Physiol. **239**:H769-H774, 1980.
312. Laskowski, M.B. and L.S. D'Agrosa. The ultrastructure of the sinu-atrial node of the bat. Acta Anat. **117**:85-102, 1983.
313. Le Peuch, C.J., J.C. Guilleux and J.G. Demaille. Phospholamban phosphorylation in the perfused rat heart is not solely dependent on  $\beta$ -adrenergic stimulation. FEBS Lett. **114**:165-168, 1980.
314. Lederer, W.J. and R.W. Tsien. Transient inward current underlying arrhythmogenic effects of cardiotonic steroids in Purkinje fibers. J. Physiol. (Lond.) **263**:73-100, 1976.
315. Lee, C.O. and M. Vassalle. Modulation of intracellular  $\text{Na}^+$  activity and cardiac force by norepinephrine and  $\text{Ca}^{2+}$ . Am. J. Physiol. **244**:C110-C114, 1983.
316. Lee, H.C., R. Mohabir, N. Smith, M.R. Franz and W.T. Clusin. Effects of ischemia on calcium-dependent fluorescence transients in rabbit hearts containing indol 1: Correlation with monophasic action potentials and contraction. Circulation **78**:1047-1059, 1988.
317. Levin, K.R. and E. Page. Quantitative studies in plasmalemmal folds and caveolae of rabbit ventricular myocardial cells. Circ. Res. **46**:244-255, 1980.
318. Lewis, A.B., G.G. Lindesmith, M. Takahashi, R.E. Stanton, B.L. Tucker, Q.R. Stiles and B. Meyer. Cardiac rhythm following the Mustard procedure for transposition of the great vessels. J. Thor. Cardiovas. Surg. **73**:919-926, 1977.
319. Lewis, T. Galvanometric curves yielded by cardiac beats generated in various areas of the auricular musculature. The pacemaker of the heart. Heart **2**:23-40, 1910.
320. Lewis, T., B.S. Oppenheimer and A. Oppenheimer. The site of origin of the mammalian heart-beat; the pacemaker in the dog. Heart **2**:147-169, 1910.

321. Lieberman, M. Physiologic development of impulse conduction in embryonic cardiac tissue. Am. J. Cardiol. 25:279-284, 1970.
322. Lindemann, J.P.  $\alpha$ -Adrenergic stimulation of sarcolemmal protein phosphorylation and slow responses in intact myocardium. J. Biol. Chem. 261:4860-4867, 1986.
323. Lindemann, J.P., L.R. Jones, D.R. Hathaway, B.G. Henry and A.M. Watanabe. B-adrenergic stimulation of phospholamban phosphorylation and  $\text{Ca}^{2+}$ -ATPase activity in guinea pig ventricles. J. Biol. Chem. 258:464-471, 1983.
324. Ling, G. and G.W. Gerard. The normal membrane potential of frog sartorius fibers. J. Cell. Comp. Physiol. 34:383-396, 1949.
325. Lipp, P. and L. Pott. Voltage dependence of sodium-calcium exchange current in guinea-pig atrial myocytes determined by means of an inhibitor. J. Physiol. 403:355-366, 1988.
326. Lipp, P. and L. Pott. Transient inward current in guinea-pig atrial myocytes reflects a change of sodium-calcium exchange current. J. Physiol. 397:601-630, 1988.
327. Lipsius, S. Triggered rhythms in atrial muscle. J. Electrocardiol. 20:33-37, 1987.
328. Lipsius, S.L. and W.R. Gibbons. Membrane currents, contractions, and aftercontractions in cardiac Purkinje fibers. Am. J. Physiol. 243:H77-H86, 1982.
329. Lipsius, S.L. and M. Vassalle. Effects of acetylcholine on potassium movements in the guinea-pig sinus node. J. Pharmacol. Exp. Ther. 201:669-677, 1977.
330. Lipsius, S.L. and M. Vassalle. Dual excitatory channels in the sinus node. J. Mol. Cell. Cardiol. 10:753-767, 1978.
331. Lipsius, S.L., J. Vereecke and E. Carmeliet. Pacemaker current ( $i_p$ ) and the inward rectifier ( $i_{K1}$ ) in single right atrial myocytes from cat heart. (abstract). Biophys. J. 49:351a, 1986.
332. Loeb, J.M., D.E. Euler, W.C. Randall, J.F. Moran and G. Brynjolfsson. Cardiac arrhythmias after chronic embolization of the sinus node artery: Alterations in parasympathetic pacemaker control. Circ. 61:192-198, 1980.
333. Lowenstein, W.R. Permeability of membrane junctions. Ann. NY Acad. Sci. 137:441-472, 1966.
334. Lowenstein, W.R. Junctional intercellular communication: The cell-to-cell membrane channel. Physiol. Rev. 61:829-913, 1981.
335. Lu, H.H. Shifts in pacemaker dominance within the sinoatrial region of cat and rabbit hearts resulting from increase of extracellular potassium. Circ Res 26:339-346, 1970.
336. Makarychev, V.A., I.L. Kosharskaya and L.S. Ul'yaninskii. Automatic activity of pacemaker cells of the atrioventricular valves of the rabbit heart. Bull. Exp. Biol. Med. 81:517-520, 1976.

337. Mandel, W., H. Hayakawa, R. Danzig and H.S. Marcus. Evaluation of sino-atrial node function in man by overdrive suppression. Circ. 44:59-66, 1971.
338. Mandel, W.J., H. Hayakawa, H.N. Allen, R. Danzig and A.I. Kermaier. Assessment of sinus node function in patients with the sick sinus syndrome. Circ. 46:761, 1972.
339. Marban, E. and W. Gil Wier. Ryanodine as a tool to determine the contributions of calcium entry and calcium release to the calcium transient and contraction of cardiac Purkinje fibers. Circulation Research 56:133-138, 1985.
340. Marquez-Montes, J., F. O'Connor, R. Burgos and J.L. Castillo-Olivares. Comparative electrophysiological evaluation of atrial activation and sinoatrial node function following Senning and Mustard procedures: An experimental study. Ann. Thorac. Surg. 36:692-699, 1983.
341. Martin, T.C., L. Smith, A. Hernandez and C.S. Weldon. Dysrhythmias following the Senning operation for dextro-transposition of the great arteries. J. Thor. Cardiovas. Surg. 85:928-932, 1983.
342. Masson-Pevet, M., W.K. Bleeker, A.J.C. Mackaay, L.N. Bouman and J.M. Houtkooper. Sinus node and atrium cells from the rabbit heart: A quantitative electron microscopic description after electrophysiological localization. J Mol Cell Cardiol 11:555-568, 1979.
343. Masson-Pevet, M., D. Gros and E. Besselsen. The caveolae in the rabbit sinus node and atrium. Cell Tissue Res. 208:183-196, 1980.
344. Masson-Pevet, M.A., W.K. Bleeker, E. Besselsen, B.W. Treysel and H.J. Jongsma. Pacemaker cell types in the rabbit sinus node: A correlative ultrastructural and electrophysiological study. J Mol Cell Cardiol 16:53-63, 1984.
345. Masters, S.B., M.W. Martin, T.K. Harden and J.H. Brown. Pertussis toxin does not inhibit muscarinic-receptor-mediated phosphoinositide hydrolysis or calcium mobilization. Biochem. J. 227:933-937, 1985.
346. Matsuda, H., A. Noma, Y. Kurachi and H. Irisawa. Transient depolarization and spontaneous voltage fluctuations in isolated single cells from guinea pig ventricles. Circ. Res. 51:142-151, 1982.
347. Maughan, D.N. Some effect of prolonged depolarization on membrane currents in bullfrog atrial muscle. J. Membr. Biol. 11:331-352, 1973.
348. Maylie, J. and M. Morad. Ionic currents responsible for the generation of pacemaker current in the rabbit sino-atrial node. J. Physiol. (Lond). 355:215-235, 1984.
349. Maylie, J., M. Morad and J. Weiss. A study of pace-maker potential in rabbit sino-atrial node: measurement of potassium activity under voltage clamp conditions. J. Physiol. 311:161-178, 1981.
350. McAllister, R.E. and D. Noble. The time and voltage dependence of the slow outward current in cardiac Purkinje fibres. J. Physiol. 186:632-662, 1966.



351. McNutt, N.S. Ultrastructure of intercellular junctions in adult and developing cardiac muscle. Am. J. Cardiol. 42:46-67, 1970.
352. McNutt, N.S. and D.W. Fawcett. The ultrastructure of the cat myocardium. II. Atrial muscle. J. Cell Biol. 42:46-67, 1969.
353. McNutt, N.S. and D.W. Fawcett. Myocardial ultrastructure. In: The Mammalian Myocardium. eds.G.A. Langer and A.J. Brady. New York: Wiley, pp.1-49, 1974.
354. Mead, R.H. and W.T. Clusin. Origin of the background sodium current and effects of sodium removal in cultured embryonic cardiac cells. Circ. Res. 55:67-77, 1984.
355. Mechmann, S. and L. Pott. Identification of Na-Ca exchange current in single cardiac myocytes. Nature 319:597-599, 1986.
356. Meek, W.J. and J.A.E. Eyster. Experiments on the origin and propagation of the impulse in the heart. III. The effect of vagal stimulation on the location of the pacemaker in auriculo-ventricular rhythm, and the effect of vagal stimulation on this rhythm. Heart 5:227-244, 1913.
357. Meek, W.J. and J.A.E. Eyster. Experiments on the origin and propagation of the impulse in the heart. IV. The effect of vagal stimulation and of cooling on the location of the pacemaker within the sino-auricular node. Am. J. Physiol. 34:368-383, 1914.
358. Meredith, J. and J.L. Titus. Anatomic atrial connections between sinus and A-V node. Circulation 37:566-579, 1968.
359. Mirowski, M., S.H. Lau, G.A. Bobb, C. Steiner and A.N. Damato. Studies on left atrial automaticity in dogs. Circ. Res. 26:317-325, 1970.
360. Mirowski, M., S.H. Lau, A.L. Wit, C. Steiner, G.A. Bobb, B. Tabatznik and A.N. Damato. Ectopic right atrial rhythms: Experimental and clinical data. Am. Heart J. 81:666-676, 1971.
361. Mitchell, M.R., T. Powell, D.A. Terrar and V.W. Twist. Characteristics of the second inward current in cells isolated from rat ventricular muscle. Proc. R. Soc. Lond. B219:447-469, 1983.
362. Mitchell, M.R., T. Powell, D.A. Terrar and V.W. Twist. Ryanodine prolongs Ca-currents while suppressing contraction in rat ventricular muscle cells. Br. J. Pharmac. (London) 81:13-15, 1984.
363. Miura, Y. and J. Inui. Multiple effects of  $\alpha$ -adrenoceptor stimulation on the action potential of the rabbit atrium. Naunyn-Schmiedeberg's Arch. Pharmacol. 325:47-53, 1984.
364. Moore, E.N., S.L. Jomain, J.H. Stuckey, J.W. Buchanan and B.F. Hoffman. Studies on ectopic atrial rhythms in dogs. Am. J. Cardiol. 19:676, 1967.
365. Moses, R.L. and W.C. Claycomb. Ultrastructure of cultured atrial cardiac muscle cells from adult rats. Am. J. Anat. 171:191-206, 1984.

366. Movsesian, M.A., M. Nishikawa and R.S. Adelstein. Phosphorylation of phospholamban by calcium-activated, phospholipid-dependent protein kinase. Stimulation of cardiac sarcoplasmic reticulum calcium uptake. J. Biol. Chem. **259**:8029-8032, 1984.
367. Movsesian, M.A., A.P. Thomas, M. Selak and J.R. Williamson. Inositol triphosphate does not release  $\text{Ca}^{2+}$  from permeabilized cardiac myocytes and sarcoplasmic reticulum. FEBS Lett. **185**:328-332, 1985.
368. Muir, A.R. Further observations on the cellular structure of cardiac muscle. J. Anat. **99**:27-46, 1965.
369. Muir, A.R. The effects of divalent cations on the ultrastructure of the perfused rat heart. J. Anat. **101**:239-261, 1967.
370. Mullins, L.J. The generation of electric currents in cardiac fibers by Na/Ca exchange. Am. J. Physiol. **236**:C103-c110, 1979.
371. MurPhree, S.S. and J.E. Saffitz. Delineation of the distribution of B-adrenergic receptor subtypes in canine myocardium. Circ. Res. **63**:117-125, 1988.
372. Mustard, W.T., J.D. Keith, G.A. Trusler, R. Fowler and L. Kidd. The surgical management of transposition of the great vessels. J. Thor. Cardiovas. Surg. **48**:953-958, 1964.
373. Nargeot, J., J.M. Nerbonne, J. Engels and H.A. Lester. Time course of the increase in myocardial slow inward current after a photochemically generated concentration jump of intracellular cyclic AMP. Proc. Natl. Acad. Sci. USA **80**:2395-2399, 1983.
374. Nilius, B., P. Hess, J.B. Lansman and R.W. Tsien. A novel type of cardiac calcium channel in ventricular cells. Nature **316**:443-446, 1985.
375. Nitter-hauge, S. and J.E. Otterstad. Characteristics of atrioventricular conduction disturbances in ankylosing spondylitis. Acta Med. Scand. **210**:197-200, 1981.
376. Noble, D. Potassium accumulation and depletion in frog atrial muscle. J. Physiol. **258**:579-613, 1976.
377. Noble, D. The surprising heart: A review of recent progress in cardiac electrophysiology. Journal of Physiology (London) **353**:1-50, 1984.
378. Noble, D. and T. Powell. The effects of series resistance on second inward current recorded under voltage clamp in ventricular muscle. J. Physiol. **345**:7P, 1983.
379. Noble, D. and R.W. Tsien. The kinetics and rectifier properties of the slow potassium current in cardiac Purkinje fibres. J. Physiol. **195**:185-214, 1968.
380. Noma, A. and H. Irisawa. Effects of  $\text{Na}^+$  and  $\text{K}^+$  on the resting membrane potential of the rabbit sinoatrial node cells. Jap. J. Physiol. **25**:287-302, 1975.
381. Noma, A. and H. Irisawa. A time- and voltage-dependent potassium current in the rabbit sinoatrial node cell. Pflug. Archiv. **366**:251-258, 1976.

382. Noma, A. and H. Irisawa. Membrane currents in the rabbit sinoatrial node as studied by the double microelectrode method. Pflugers Arch. 364:45-52, 1976.
383. Noma, A. and H. Irisawa. Ionic current in the isolated S-A and A-V node cells. Proc. Int. Union Physiol. Sci. 15:486-506, 1983.
384. Noma, A., H. Kotake and H. Irisawa. Slow inward current and its role mediating the chronotropic effect of epinephrine in the rabbit sinoatrial node. Pflug. Archiv. 388:1-9, 1980.
385. Noma, A., M. Morad and H. Irisawa. Does the "pacemaker current" generate the diastolic depolarization in the rabbit s.a. node cells?. Pflugers Arch. 397:190-194, 1983.
386. Noma, A., T. Nakayama, Y. Kurachi and H. Irisawa. Resting K conductance in pacemaker and non-pacemaker heart cells of the Rabbit. Japanese Journal of Physiol. 34:245-254, 1984.
387. Noma, A. and W. Trautwein. Relaxation of the ACh-induced potassium current in the rabbit sinoatrial node cell. Pflug. Archiv. 377:193-200, 1978.
388. Noma, A., K. Yanagihara and H. Irisawa. Inward current of the rabbit sinoatrial node. Pflug. Archiv. 372:43-51, 1977.
389. Nosek, T.M., M. Williams, S.T. Ziegler and R.E. Godt. Inositol triphosphate enhances calcium release in skinned cardiac and skeletal muscle. Am. J. Physiol. 250:C807-C811, 1986.
390. Oei, H.I., A.C.G. Van Ginneken, H.J. Jongasma and L.N. Bouman. Mechanisms of impulse generation in isolated cells from the rabbit sinoatrial node. J. Mol. Cell. Cardiol. 21:1137-1149, 1989.
391. Ohnishi, S., H. Kasanuki, K. Takamizawa, A. Takao and K. Hirose. Long-term management of bradyarrhythmias following open heart surgery: Surgical A-V block and sick sinus syndrome after surgery for secundum atrial septal defects treated with permanent cardiac pacing. Jap. Circ. J. 50:903-917, 1986.
392. Okada, T. Effect of verapamil on electrical activities of SA node, ventricular muscle and Purkinje fibers in isolated rabbit hearts. Jap. Circ. J. 40:329-341, 1976.
393. Olson, L.J., M.A. Gertz and W.D. Edwards. Senile cardiac amyloidosis with myocardial dysfunction: diagnosis by endomyocardial biopsy and immunohistochemistry. N. Engl. J. Med. 317:738, 1987.
394. Opthof, T., B. De Jonge and L.N. Bouman. Functional morphology of the mammalian sinoatrial node. Eur. Heart J. 8:1249-1259, 1987.
395. Opthof, T., B. De Jonge, H.J. Jongasma and L.N. Bouman. Functional morphology of the pig sinoatrial node. J. Mol. Cell. Cardiol. 19:1221-1236, 1987.

396. Opthof, T., B. De Jonge, J.C. Mackaay, W.K. Bleeker, M. Masson-Pevet, H.J. Jongsma and L.N. Bouman. Functional and morphological organization of the guinea-pig sinoatrial node compared with the rabbit sinoatrial node. J. Mol. Cell. Cardiol. **17**:549-565, 1985.
397. Opthof, T., B. DeJonge, M. Masson-Pevet, H.J. Jongsma and L.N. Bouman. Functional and morphological organization of the cat sinoatrial node. J Mol Cell Cardiol **18**:1015-1031, 1986.
398. Orchard, C.H., D.A. Eisner and D.G. Allen. Oscillations of intracellular Ca in mammalian cardiac muscle. Nature **304**:735-738, 1983.
399. Osterrieder, W., G. Brum, J. Hescheler, W. Trautwein, V. Flockerzi and F. Hofmann. Injection of subunits of cyclic AMP-dependent protein kinase into cardiac myocytes modulates Ca<sup>2+</sup> current. Nature **298**:576-578, 1982.
400. Osterrieder, W., A. Noma and W. Trautwein. On the kinetics of the potassium channel activated by acetylcholine in the S-A node of the rabbit heart. Pflug. Archiv. **386**:101-109, 1980.
401. Paes de Carvalho, A. Cellular electrophysiology of the atrial specialized tissues. In: The Specialized Tissues of the Heart. eds. A. Paes de Carvalho, W.C. De Mello and B.F. Hoffman. New York: Elsevier, pp.115-130, 1961.
402. Paes de Carvalho, A., W.C. DeMello and B. Hoffman. Electrophysiological evidence for specialized fiber types in rabbit atrium. Am. J. Physiol. **196**:483-488, 1959.
403. Pagani, M., F. Lombardi, S. Guzzetti, O. Rimoldi, R. Furlan, P. Pizzinelli, G. Sandrone, G. Malfatto, S. Dell'Orto, E. Piccaluga, M. Turiel, G. Baselli, S. Cerutti and A. Malliani. Power spectral analysis of heart rate and arterial pressure variabilities as a marker of sympatho-vagal interaction in man and conscious dog. Circ. Res. **59**:178-193, 1986.
404. Parratt, J.R. Effects of adrenergic activators and inhibitors on the coronary circulation. In: Handbook of Experimental Pharmacology: Adrenergic Activators and Inhibitors. ed. L. Szekers. Berlin: Springer-Verlag, pp.735-822, 1980.
405. Pastelin, G., R. Mendez and G.K. Moe. Participation of atrial specialized conduction pathways in atrial flutter. Circ. Res. **42**:386-393, 1978.
406. Patten, B.M. Initiation and early changes in the character of the heart beat in vertebrate embryos. Physiol. Rev. **29**:31-47, 1949.
407. Patten, B.M. Development of the sinoventricular conduction system. Univ. Mich. Med. Bull. **22**:1-21, 1956.
408. Pecker, M.S., W.-B. Im, J.K. Sonn and C.O. Lee. Effect of norepinephrine and cyclic AMP on intracellular sodium ion activity and contractile force in canine cardiac Purkinje fibers. Circ. Res. **59**:390-397, 1986.
409. Penefsky, Z.J. Studies on mechanism of inhibition of cardiac muscle contractile tension by ryanodine. Pflugers Arch. **347**:173-184, 1974.

410. Peper, K. and W. Trautwein. A note on the pace-maker current in Purkinje fibres. Pflug. Archiv. 309:356-361, 1969.
411. Peracchia, C. and L.L. Peracchia. Gap junction dynamics: Reversible effects of divalent cations. J. Cell Biol. 87:708-718, 1980.
412. Pfaffinger, P.J., J.M. Martin, D.D. Hunter, N.M. Nathanson and B. Hille. GTP-binding proteins couple cardiac muscarinic receptor to a K<sup>+</sup> channel. Nature 317:536-538, 1985.
413. Podolsky, R.J. and L.L. Constantin. Regulation by calcium of the contraction and relaxation of muscle fibers. Federation Proc. 23:933-999, 1964.
414. Pomeranz, B., R.J.B. Macaulay, M.A. Caudill, I. Kutz, D. Adam, D. Gordon, K.M. Kilborn, A.C. Barger, D.C. Shannon, R.J. Cohen and H. Benson. Assessment of autonomic function in humans by heart rate spectral analysis. Am. J. Physiol. 248:H151-H153, 1985.
415. Porter, K.R. and G.E. Palade. Studies on the endoplasmic reticulum. III. Its form and distribution in striated muscle cells. J. Biophys. Biochem. Cytol. 3:269-300, 1957.
416. Posner, P., E. Farrar and C. Lambert. Inhibitory effects of catecholamines in canine cardiac Purkinje fibers. Am. J. Physiol. 231:1415-1420, 1976.
417. Przybojewski, J.Z. Polyarteritis nodosa in the adult: Report of a case with repeated myocardial infarction and a review of cardiac involvement. S. Afr. Med. J. 60:512, 1981.
418. Racker, D.K. Atrioventricular node and input pathways: A correlated gross anatomical and histological study of the canine atrioventricular junctional region. Anat. Rec. 224:336-354, 1989.
419. Randall, W.C. Parasympathetic control of the heart. In: Neural Regulation of the Heart. ed. W.C. Randall. New York: Oxford, pp.97-129, 1977.
420. Randall, W.C., L.E. Rinkema, S.B. Jones, M.o.r.a.n. JF and G. Brynjolfsson. Overdrive suppression of atrial pacemaker tissues in the alert, awake dog before and chronically after excision of the sinoatrial node. Am. J. Cardiol. 49:1166-1175, 1982.
421. Randall, W.C., L.E. Rinkema, S.B. Jones, J.F. Moran and G. Brynjolfsson. Functional characterization of atrial pacemaker activity. Am. J. Physiol. 242:H98-H106, 1982.
422. Randall, W.C., J. Talano, M.P. Kaye, D.E. Euler, S.B. Jones and G. Brynjolfsson. Cardiac pacemakers in the absence of the SA node: responses to exercise and autonomic blockade. Am. J. Physiol. 234:H465-H470, 1978.
423. Randall, W.C., W.H. Wehrmacher and S.B. Jones. Hierarchy of supraventricular pacemakers. J Thorac Cardiovas Surg 82:797-800, 1981.
424. Rasmussen, K. Chronic sinoatrial heart block. Am. Heart J. 81:38-47, 1971.
425. Rasmussen, K. Chronic sinus node disease: natural course and indications for pacing. Eur. Heart J. 2:455-459, 1981.

426. Reeves, J.P. and C.C. Hale. The stoichiometry of the cardiac sodium-calcium exchange system. J. Biol. Chem. 259:7733-7739, 1984.
427. Reuter, H. The dependence of slow inward current in Purkinje fibres on the extracellular calcium concentration. J. Physiol. 192:479-492, 1967.
428. Reuter, H. Divalent cations as charge carriers in excitable membranes. Progr. Biophys. Mol. Biol. 26:3-43, 1973.
429. Reuter, H. Properties of two inward membrane currents in the heart. Ann. Rev. Physiol. 41:413-424, 1979.
430. Reuter, H. and H. Scholz. The regulation of the Ca conductance of cardiac muscle by adrenaline. J. Physiol. 264:49-62, 1977.
431. Reuter, H. and H. Scholz. A study on the ion selectivity and the kinetic properties of the calcium dependent slow inward current in mammalian cardiac muscle. J. Physiol. 264:17-47, 1977.
432. Reuter, H. and N. Seitz. The dependence of calcium efflux from cardiac muscle on temperature and external ion composition. J. Physiol. 195:451-470, 1968.
433. Revel, J.P. and M.F. Karnovsky. Hexagonal array of subunits in intercellular junctions of the mouse heart and liver. J. Cell Biol. 33:349-367, 1967.
434. Rokseth, R. and L. Hatle. Sinus arrest in acute myocardial infarction. Br. Heart J. 33:639, 1971.
435. Rosen, K.M., H.S. Loeb, M.Z. Sinno, S.H. Rahimtoola and R.M. Gunnar. Cardiac conduction in patients with symptomatic sinus node disease. Circ. 43:836, 1971.
436. Rosen, M.R., S.F. Steinberg, Y.K. Chow, J.P. Bilezikian and P. Danilo, Jr.. Role of a pertussis toxin-sensitive protein in the modulation of canine Purkinje fiber automaticity. Circ. Res. 62:315-323, 1988.
437. Ross, G. Adrenergic responses of the coronary vessels. Circ. Res. 39:461-465, 1976.
438. Rougier, O., G. Vassort, D. Garnier, Y.M. Gargouil and E. Coraboeuf. Existence and role of a slow inward current during the frog atrial action potential. Pflug. Archiv. 308:91-110, 1969.
439. Rousseau, E., J.S. Smith and G. Meissner. Ryanodine modifies conductance and gating behavior of single Ca<sup>2+</sup> release channel. Am. J. Physiol. 253:C364, 1987.
440. Rozanski, G.J. Electrophysiological properties of automatic fibers in rabbit atrioventricular valves. Am. J. Physiol. 253:H720-H727, 1987.
441. Rozanski, G.J. and J. Jalife. Automaticity in atrioventricular valve leaflets of rabbit heart. Am. J. Physiol. (Heart Circ.) 19:H397-H406, 1986.
442. Rozanski, G.J. and S.L. Lipsius. Electrophysiology of functional subsidiary pacemakers in canine right atrium. Am. J. Physiol. 249:H594-H603, 1985.

443. Rozanski, G.J., S.L. Lipsius and W.C. Randall. Functional characteristics of sinoatrial and subsidiary pacemaker activity in the canine right atrium. Circ. 67:1378-1387, 1983.
444. Rozanski, G.J., S.L. Lipsius, W.C. Randall and S.B. Jones. Alterations in subsidiary pacemaker function after prolonged subsidiary pacemaker dominance in the canine right atrium. J. Am. Coll. Cardiol. 4:535-542, 1984.
445. Rubenstein, D.S. and S.L. Lipsius. Mechanisms of bradycardia dysrhythmia. Circulation 70(II):223, 1984.(Abstract)
446. Rubenstein, D.S. and S.L. Lipsius. Electrophysiology of atrial pacemakers in the Eustachian ridge of the cat heart. Physiologist 27:215, 1984.(Abstract)
447. Rubenstein, J.J., C.L. Schulman, P.M. Yurchak and R.W. DeSanctis. Clinical spectrum of the sick sinus syndrome. Circulation 46:5-13, 1972.
448. Saalouke, M.G., J. Rios, L.W. Perry, S.R. Shapiro and L.P. Scott. Electrophysiologic studies after Mustard's operation for d-transposition of the great vessels. Am. J. Cardiol. 41:1104-1109, 1978.
449. Saito, T., M. Otoguro and T. Matsubara. Electrophysiological studies on the mechanism of electrically induced sustained rhythmic activity in the rabbit right atrium. Circ. Res. 42:199-206, 1978.
450. Sakmann, B., A. Noma and W. Trautwein. Acetylcholine activation of single muscarinic K channels in isolated pacemaker cells of the mammalian heart. Nature 303:250-253, 1983.
451. Sakmann, B. and G. Trube. Conductance properties of single inwardly rectifying potassium channels in ventricular cells from guinea-pig heart. J. Physiol. 347:641-657, 1984.
452. Sakmann, B. and G. Trube. Voltage-dependent inactivation of inward-rectifying single-channel current in the guinea-pig heart cell membrane. J. Physiol. 347:659-683, 1984.
453. Sano, T. and S. Yamagishi. Spread of excitation from the sinus node. Circ. Res. 16:423-430, 1965.
454. Sasaki, Y., M. Shimotori, K. Akahane, H. Yonekura, K. Hirano, R. Endoh, S. Koike, S. Kawa, S. Furata and T. Homma. Long-term follow-up of patients with sick sinus syndrome: A comparison among unpaced, ventricular inhibited paced, and physiologically paced groups. PACE 11:1575-1583, 1988.
455. Scheinman, M.M., D. Basu and M. Hollenberg. Electrophysiologic studies in patients with persistent atrial tachycardia. Circulation 50:266-273, 1974.
456. Scheinman, M.M., H.C. Strauss and C.T. Evans. Adverse effects of sympatholytic agents in patients with hypertension and sinus node dysfunction. Am. J. Med. 64:1013, 1978.

457. Scherf, D. Upper auriculo-ventricular rhythm (coronary sinus rhythm) experimentally produced. Proc. Soc. Exp. Biol. Med. 56:220-222, 1944.
458. Scherf, D., S. Blumenfeld and M. Yildiz. Experimental studies on A-V nodal rhythm following suppression of activity of the sinus node. Am. J. Cardiol. 10:234-238, 1962.
459. Scherf, D. and R. Harris. Coronary sinus rhythm. Am. Heart J. 32:443-456, 1946.
460. Scholz, H., R. Bruckner, A. Mugge and C. Reupcke. Myocardial alpha-adrenoceptors and positive inotropy. J. Mol. Cell. Cardiol. 18(Suppl 5):79-87, 1986.
461. Scholz, J., B. Schaefer, W. Schmitz, H. Scholz, m. Steinfath, M. Lohse, U. Schwabe and J. Puruunen. Alpha-1-adrenoceptor-mediated positive inotropic effect and inositol triphosphate increases in mammalian heart. J. Pharmacol. Exp. Ther. 245:327-335, 1988.
462. Schramm, M., G. Thomas, R. Towart and G. Franckowiak. Novel dihydropyridines with positive inotropic action through activation of Ca<sup>++</sup> channels. Nature 303:535-537, 1983.
463. Schramm, M., G. Thomas, R. Towart and G. Franckowiak. Activation of calcium channels by novel 1,4-dihydropyridines. A new mechanism for positive inotropics or smooth muscle stimulants. Arzneim-Forsch. Drug Res. 33:1268-1272, 1983.
464. Sealy, W.C., R.J. Bache, A.V. Seaber and S.K. Bhattacharga. The atrial pacemaking site after surgical exclusion of the sinoatrial node. J. Thorac. Cardiovasc. Surg. 65:841-850, 1973.
465. Sealy, W.C., J.C. Farmer, G. Young and I.W. Brown. Atrial dysrhythmia and atrial secundum defects. J. Thor. Cardiovasc. Surg. 57:245-250, 1969.
466. Sealy, W.C. and A.V. Seaber. Cardiac rhythm following exclusion of the sinoatrial node and most of the right atrium from the remainder of the heart. J. Thorac. Cardiovasc. Surg. 77:436-447, 1979.
467. Sealy, W.C. and A.V. Seaber. Surgical isolation of the atrial septum from the atria Identification of an atrial septal pacemaker. J. Thorac. Cardiovasc. Surg. 80:742-749, 1980.
468. Senning, A. Surgical correction of transposition of the great vessels. Surgery 45:966-980, 1959.
469. Seyama, I. Characteristics of the rectifying properties of the sino-atrial node cell of the rabbit. J. Physiol. 255:379-397, 1976.
470. Seyama, I. The effect of Na, K, and Cl ions on the resting membrane potential of sinoatrial node cell of the rabbit. Jap. J. Physiol. 27:577-588, 1977.
471. Seyama, I. Which ions are important for the maintenance of the resting membrane potential of the cells of the sinoatrial node of the rabbit?. In: The Sinus Node: Structure, Function and Clinical Relevance, ed. F.I.M. Bonke. Boston: Martinus-Nijhoff, pp.339-347, 1978.



472. Shah, A., I.S. Cohen and M.R. Rosen. Stimulation of cardiac alpha receptors increases Na/K pump current and decreases  $g_K$  via a pertussis toxin-sensitive pathway. Biophys. J. 54:219-225, 1988.
473. Sherf, L. and T.N. James. Fine structure of cells and their histologic organization within internodal pathways of the heart: Clinical and electrocardiographic implications. Am. J. Cardiol. 44:345-369, 1979.
474. Sheu, S.S. and M.P. Blaustein. Sodium/Calcium exchange and regulation of cell calcium and contractility in cardiac muscle, with a note about vascular smooth muscle. In: The Heart and Cardiovascular System. eds.H.A. Fozzard, R.B. Jennings, E. Haber, A.M. Katz and H.E. Morgan. New York: Raven Press, pp.509-536, 1986.
475. Shibata, E. and W. Giles. Cardiac pacemaker cells from the bullfrog sinus venosus lack an inwardly rectifying background K current. Biophys. J. 45:136a, 1984.
476. Shibata, E.F. and W.R. Giles. Ionic currents that generate the spontaneous diastolic depolarization in individual cardiac pacemaker cells. Proc. Natl. Acad. Sci. USA 82:7796-7800, 1985.
477. Siegelbaum, S.A. and R.W. Tsien. Calcium-activated transient outward current in calf cardiac Purkinje fibres. J. Physiol. 299:485-506, 1980.
478. Silka, M.J., P.C. Gillette, A.Jr. Garson and A. Zinner. Transvenous catheter ablation of a right atrial automatic ectopic tachycardia. J. Am. Coll. Cardiol. 5:999-1001, 1985.
479. Simonsen, E., B.L. Nielsen and J.S. Nielsen. Sinus node dysfunction in acute myocardial infarction. Acta Med. Scand. 208:463, 1980.
480. Sjostrand, F.S. and E. Andersson-Cedergren. Intercalated discs of heart muscle. In: The Structure and Function of Muscle. ed. G.E. Bourne. New York: Academic Press, pp.421-445, 1960.
481. Soejima, M. and A. Noma. Mode of regulation of the ACh-sensitive K channel by the muscarinic receptor in the rabbit atrial cells. Pflug. Archiv. 400:424-431, 1984.
482. Sommer, J.R. Purkinje fibers in the atrium. Federation Proc. 27:357, 1968.
483. Sommer, J.R. and E.A. Johnson. Ultrastructure of cardiac muscle. In: Handbook of Physiology: The Cardiovascular System. eds.R.M. Berne, N. Sperelakis and S.R. Geiger. Bethesda: American Physiological Society, pp.113-186, 1979.
484. Sommer, J.R. and R.A. Waugh. The ultrastructure of the mammalian cardiac muscle with special emphasis on the tubular membrane systems. Am. J. Path. 82:192-221, 1976.
485. Sorota, S., Y. Tsuji, T. Tajima and A.J. Pappano. Pertussis toxin treatment blocks hyperpolarization by muscarinic agonists in chick atrium. Circ. Res. 57:748-758, 1985.
486. Spach, M.S., M. Lieberman, J.C. Scott, R.C. Barr, E.A. Johnson and J.M. Kootsey. Excitation sequences of the atrial septum and AV node in isolated hearts of the dog and rabbit. Circ. Res. 29:156, 1971.

487. Spach, M.S., M. Lieberman, J.G. Scott, R.C. Barr, E.A. Johnson and J.M. Kootsey. Excitation sequences of the atrial septum and the AV node in isolated hearts of the dog and rabbit. Circ. Res. 29:156-172, 1971.
488. Sperelakis, N. Regulation of calcium slow channels of cardiac muscle by cyclic nucleotides and phosphorylation. J. Mol. Cell. Cardiol. 20(suppl II):75-105, 1988.
489. Sperelakis, N. and J. Schneider. A metabolic control mechanism for calcium ion influx that may protect the ventricular myocardial cell. Am. J. Cardiol. 37:1079-1085, 1976.
490. Sperelakis, N. and K. Shigenbou. Changes in membrane properties of chick embryonic hearts during development. J. Gen. Physiol. 60:430-453, 1972.
491. Spitzer, K.W. and J.L. Walker. Changes in liquid-junction potential following chloride replacement in cat papillary muscle. Pflug. Archiv. 382:281-284, 1979.
492. Stahlsberg, H. and R.L. DeHaan. The precardiac areas and formation of the tubular heart in the chick embryo. Dev. Biol. 19:128, 1969.
493. Steere, R.L. and J.R. Sommer. Stereo ultrastructure of nexus faces exposed by freeze-fracturing. J. Microscopic. 15:205-218, 1972.
494. Steinberg, S.F., L.M. Kaplan, T. Inouye, J.F. Zhang and R.B. Robinson. Alpha-1 adrenergic stimulation of 1,4,5-inositol triphosphate formation in ventricular myocytes. J. Pharmacol. Exp. Ther. 250:1141-1148, 1989.
495. Stiles, G.L. and R.J. Lefkowitz. Cardiac adrenergic receptors. Ann. Rev. Med. 35:149-164, 1984.
496. Strauss, H.C., M. Gilbert and R.H. Svenson. Electrophysiologic effects of propranolol on sinus node function in patients with sinus node dysfunction. Circulation 54:452, 1976.
497. Sutko, J.L. and J.L. Kenyon. Ryanodine modification of cardiac muscle responses to potassium-free solutions. J. Gen. Physiol. 82:385-404, 1983.
498. Sutko, J.L., J.T. Willerson, G.H. Templeton, L.R. Jones and H.R. Besch. Ryanodine: its alteration of cat papillary muscle contractile state and responsiveness to inotropic interventions and a suggested mechanism of action. J. Pharmacol. Exp. Ther. 209:37-47, 1979.
499. Tada, M. and A.M. Katz. Phosphorylation of the sarcoplasmic reticulum and sarcolemma. Ann. Rev. Physiol. 44:401-423, 1982.
500. Tada, M., M.A. Kirchberger, D.I. Repke and A.M. Katz. The stimulation of calcium transport in cardiac sarcoplasmic reticulum by adenosine 3',5'-monophosphate-dependent protein kinase. J. Biol. Chem. 249:6174-6180, 1974.
501. Tada, M., M. Yamada, M. Kadoma, M. Inui and F. Ohmori. Calcium transport by cardiac sarcoplasmic reticulum and phosphorylation of phospholamban. Mol. Cell. Biochem. 46:73-95, 1982.

502. Tajima, T., Y. Tsuji, J.H. Brown and A.J. Pappano. Pertussis toxin-insensitive phosphoinositide hydrolysis, membrane depolarization, and positive inotropic effect of carbachol in chick atria. Circ. Res. **61**:436-445, 1987.
503. Takaysu, M. Conduction of excitation from the sinus node to the atrioventricular node. Jap. Circ. J. **31**:373-380, 1967.
504. Tawara, S. Das Reizleitungssystem der Saugetierherzens. Jena 1906.
505. Taylor, J.J., L.S. D'Agrosa and E.M. Burns. The pacemaker cell of the sinoatrial node of the rabbit. Am J Physiol **235**:H407-H412, 1978.
506. Ten Eick, R., H. Nawrath, T.F. McDonald and W. Trautwein. On the mechanism of the negative inotropic effect of acetylcholine. Pflug. Archiv. **361**:207-213, 1976.
507. Thandroyen, F.T., J. McCarthy, K.P. Burton and L.H. Opie. Ryanodine and caffeine prevent ventricular arrhythmias during acute myocardial ischemia and reperfusion in rat heart. Circ. Res. **62**:306-314, 1988.
508. Thiene, G., M. Valente and L. Rossi. Involvement of the cardiac conducting system in panarteritis nodosa. Am. Heart J. **95**:716, 1978.
509. Thomas, G., M. Chung and C.J. Cohen. A dihydropyridine (BAY K 8644) that enhances calcium currents in guinea pig and calf myocardial cells. Circ. Res. **56**:87-96, 1985.
510. Thormann, J., F. Schwarz and R. Enlessen. Vagal tone, significance of electrophysiologic findings and clinical course in symptomatic sinus node dysfunction. Am. Heart J. **95**:725, 1978.
511. Tohse, N., M. Kameyama and H. Irisawa. Intracellular  $Ca^{2+}$  and protein kinase C modulate  $K^+$  current in guinea pig heart cells. Am. J. Physiol. **253**:H1321-H1324, 1987.
512. Tomita, Y. and V.J. Ferrans. Morphological study of sarcoplasmic reticulum in the atrioventricular node and bundle cells in the guinea pig hearts. Am. J. Anat. **180**:100-122, 1987.
513. Torii, H. Electron microscope observations of the S.A. and A.V. nodes and Purkinje fibers of the rabbit. Jap. Circ. J. **26**:39-65, 1962.
514. Tormey, J.McD. and E.S. Wheeler-Clark. Spatial resolution in electron probe analyses of sarcolemma and sarcoplasmic reticulum of cardiac muscle. Ann. NY Acad. Sci. **483**:260-269, 1986.
515. Trantum-Jensen, J. The fine structure of the atrial and atrio-ventricular (AV) junctional specialized tissues of the rabbit heart. In: The Conduction System of the Heart. eds.H.J.J. Wellens, K.I. Lie and M.J. Janse. Philadelphia: Lea & Febiger, pp.55-81, 1976.
516. Trantum-Jensen, J. The fine structure of the sinus node: A survey. In: The Sinus Node. ed. F.I.M. Bonke. Boston: Martinus-Nijhoff, pp.149-165p.1978.

517. Tranum-Jensen, J. and F. Bojsen-Moller. The ultrastructure of the sinuatrial ring bundle and of the caudal extension of the sinus node in the right atrium of the rabbit heart. Z. Zellforsch. 138:97-112, 1973.
518. Trautwein, W. Membrane currents in cardiac muscle fibers. Physiol. Rev. 53:793-835, 1973.
519. Trautwein, W. and A. Cavalie. Cardiac calcium channels and their control by neurotransmitters and drugs. J. Am. Coll. Cardiol. 6:1409-1416, 1985.
520. Trautwein, W., A. Cavalie, V. Flockerzi, F. Hofmann and D. Pelzer. Modulation of calcium channel function by phosphorylation in guinea pig ventricular cells and phospholipid bilayer membranes. Circ. Res. 61(Suppl I):I17-I23, 1987.
521. Trautwein, W. and J. Dudel. Zum mechanismus der membranwirkung des acetylcholin an der herzmuskelfaser. Pflug. Archiv. 266:324-334, 1958.
522. Trautwein, W. and D.G. Kassebaum. On the mechanism of spontaneous impulse generation in the pacemaker of the heart. J. Gen. Physiol. 45:317-330, 1961.
523. Trautwein, W. and K. Uchinozo. Electron microscopic and electrophysiologic study of the pacemaker in the sino-atrial node of the rabbit heart. Z. Zell 61:96-109, 1963.
524. Trautwein, W. and K. Zink. Uber membran-und aktion potentiale einzelner myokardfasern des kalt-und warmbluterherzens. Pflug. Archiv. 256:68-84, 1952.(Abstract)
525. Truex, R.C. and W.Q. Smythe. Reconstruction of the human atrioventricular node. Anat. Rec. 158:11-20, 1967.
526. Trusler, G.A., W.G. Williams, Y. Izukawa and P.M. Olley. Current results with the Mustard operation in isolated transposition of the great arteries. J. Thor. Cardiovas. Surg. 80:381-389, 1980.
527. Tseng, G.N. and A.L. Wit. Characteristics of a transient inward current that causes delayed afterdepolarizations in atrial cells of the canine coronary sinus. J. Mol. Cell. Cardiol. 19:1105-1119, 1987.
528. Tsien, R.W. Cyclic AMP and contractile activity in heart. In: Advances in Cyclic Nucleotide Research. eds.P. Greengard and G.A. Robison. NY: Raven Press, pp.363-420, 1977.
529. Tsien, R.W., B.P. Bean, P. Hess, J.B. Lansman, B. Nilius and M.C. Nowycky. Mechanisms of calcium channel modulation by B-adrenergic agents and dihydropyridine calcium agonists. J. Mol. Cell. Cardiol. 18:691-710, 1986.
530. Tsien, R.W., W. Giles and P. Greengard. Cyclic AMP mediates the action of adrenaline on the action potential plateau of cardiac Purkinje fibres. Nature New Biol. 240:181-183, 1972.
531. Tsien, R.W., R.S. Kass and R. Weingart. Cellular and subcellular mechanisms of cardiac pacemaker oscillations. J. Exp. Biol. 81:205-215, 1979.

532. Tsuchioka, Y., K. Matsumoto, H. Fujii, S. Masaoka, A. Yuasa, H. Tateishi, H. Matsuura, H. Sato and G. Kajiyama. Electrophysiological effects of propranolol in patients with sinus node dysfunction. Jap. Heart J. 29:319-324, 1988.
533. Tucek, S., V. Dolezal, J. Folbergrova, S. Hynie, F. Kolar and H. Ostadal. Pertussis toxin inhibits the negative inotropic and negative chronotropic muscarinic cholinergic effects on the heart. Pflug. Archiv. 408:167-172, 1987.
534. Turina, M., R. Siebenmann, P. Nussbaumer and A. Senning. Long-term outlook after atrial correction of great arteries. J. Thor. Cardiovas. Surg. 95:828-835, 1988.
535. Ullal, R.R., R.H. Anderson and C. Lincoln. Mustard's operation modified to avoid dysrhythmias and pulmonary and systemic venous obstruction. J. Thor. Cardiovas. Surg. 78:431-439, 1979.
536. Urthaler, F., C.R. Katholi, J.,J.r. Macy and T.N. James. Mathematical relationship between automaticity of the sinus node and the AV junction. Am. Heart J. 86:189-195, 1973.
537. Urthaler, F., C.R. Katholi, J.,J.r. Macy and T.N. James. Electrophysiological and mathematical characteristics of the escape rhythm during complete AV block. Cardiovasc. Res. 8:173-186, 1974.
538. Valdeolillos, M. and D.A. Eisner. The effects of ryanodine on calcium-overloaded sheep cardiac Purkinje fibers. Circ. Res. 56:452-456, 1985.
539. van Capelle, F.J.L. and D. Durrer. Computer simulation of arrhythmias in a network of coupled excitable elements. Circ. Res. 47:454, 1980.
540. Van Mierop, L.H.S. Location of pacemaker in chick embryo heart at the time of initiation of heartbeat. Am. J. Physiol. 212:407-415, 1967.
541. Van Mierop, L.H.S. The morphological development of the sinoatrial node in the mouse. Am. J. Cardiol. 25:204-212, 1970.
542. Van Mierop, L.H.S. Morphological development of the heart. In: Handbook of Physiology: The Cardiovascular System. eds.R.M. Berne, N. Sperelakis and S.R. Geiger. Bethesda, Maryland: American Physiological Society, pp.1-28, 1979.
543. Vassalle, M. Cardiac pacemaker potentials at different extra- and intracellular K concentrations. Am. J. Physiol. 208:770-775, 1965.
544. Vassalle, M. Analysis of cardiac pacemaker potential using a "voltage clamp" technique. Am. J. Physiol. 210:1335-1341, 1966.
545. Vassalle, M. Electrogenic suppression of automaticity in sheep and dog Purkinje fibers. Circ. Res. 27:361-377, 1970.
546. Vassalle, M. and O. Barnabei. Norepinephrine and potassium fluxes in cardiac Purkinje fibers. Pflug. Archiv. 322:287-303, 1971.

547. Vassalle, M. and M. Di Gennarro. Caffeine eliminates the oscillatory current in cardiac Purkinje fibers. Eur. J. Pharmacol. **94**:361-362, 1983.
548. Vassalle, M., K. Greenspan, S. Jomain and B.F. Hoffman. Effect of potassium on automaticity and conduction of canine hearts. Am. J. Physiol. **207**:334-340, 1964.
549. Vassalle, M., J.K. Greineder and J.H. Stuckey. Role of the sympathetic nervous system in the sinus node resistance to high potassium. Circ. Res. **32**:348-355, 1973.
550. Vassalle, M. and B.F. Hoffman. The spread of sinus activation during potassium administration. Circ Res **17**:285-295, 1965.
551. Vassalle, M. and C.O. Lee. The relationship among intracellular sodium activity, calcium, and strophanthidin inotropy in canine cardiac Purkinje fibers. J. Gen. Physiol. **83**:287-307, 1984.
552. Vassalle, M. and A. Mugelli. An oscillatory current in sheep cardiac Purkinje fibers. Circ. Res. **48**:618, 1981.
553. Viragh, S. and A. Porte. The fine structure of the conducting system of the monkey heart. I. The sino-atrial node and the internodal connections. Z. Zellforsch. **145**:191-211, 1973.
554. Viragh, S.Z. and C.E. Challice. The development of the conduction system in the mouse embryonic heart. I. The first embryonic A-V conduction pathway. Dev. Biol. **56**:382-396, 1977.
555. Vittone, L., C. Mundina, G. Chiappe de Cingolani and A. Mattiazzi. Correlation between myocardial relaxation and phospholamban phosphorylation. Acta Physiol. Pharmacol. **38**:213-227, 1988.
556. Vittone, L., C. Mundina, G. Chiappe de Cingolani and A. Mattiazzi. cAMP and calcium-dependent mechanisms of phospholamban phosphorylation in intact hearts. Am. J. Physiol. **258**:H318-H325, 1990.
557. Waddel, A.W. Adrenaline, noradrenaline and potassium fluxes in rabbit auricles. J. Physiol. **155**:209-220, 1961.
558. Waldo, A.L., W.A.H. MacLean, R.B. Karp, N.T. Kouchoukos and T.N. James. Sequence of retrograde atrial activation of the human heart: correlation with P wave polarity. Brit. Heart J. **39**:634, 1977.
559. Waldo, A.L., K.J. Vitikainen, G.A. Kaiser, J.R. Malm and B.F. Hoffman. The P wave and P-R interval: effects of the site of origin of atrial depolarization. Circ. **42**:653, 1970.
560. Wallenstein, S., C.L. Zucker and J.L. Fleiss. Some statistical methods useful in circulation research. Circ. Res. **47**:1-9, 1980.
561. Walsh, K.B. and R.S. Kass. Regulation of a heart potassium channel by protein kinase A and C. Science **242**:67-69, 1988.

562. Wang, D.Y., Q.Y. Gong and C.O. Lee. Effects of norepinephrine on intracellular sodium activity and membrane potential in beating and quiescent Purkinje fibers of sheep heart. Biophys. J. 53:166A, 1988.(Abstract)
563. Wasserstrom, J.A., D.J. Schwartz and H.A. Fozzard. Catecholamine effects on intracellular sodium activity and tension in dog heart. Am. J. Physiol. 243:H670-H675, 1982.
564. Watanabe, A.M., L.R. Jones, A.S. Manahan and H.C. Besch. Cardiac autonomic receptors: Recent concepts from radiolabelled ligand-binding studies. Circ. Res. 50:161-174, 1973.
565. Watanabe, A.M., J.P. Lindemann and J.W. Fleming. Mechanisms of muscarinic modulation of protein phosphorylation in intact ventricles. Fed. Proc. 43:2618-2623, 1984.
566. Weber, A. and R. Herz. The relationship between caffeine contracture of intact muscle and the effect of caffeine on reticulum. J. Gen. Physiol. 52:750-759, 1969.
567. Weibel, E.R., G.S. Kistler and W.F. Scherle. Practical stereological methods for morphometric cytology. J. Cell Biol. 30:23-38, 1966.
568. Weidmann, S. Effect of current flow on the membrane potential of cardiac muscle. J. Physiol. 115:227-236, 1951.
569. Weinberger, M.H., W. Aoi and D.P. Henry. Direct effect of beta-adrenergic stimulation on renin release by the rat kidney slice in vitro. Circ. Res. 37:318-324, 1975.
570. West, T.C. Ultramicroelectrode recording from the cardiac pacemaker. J Pharmacol Exp Ther 115:283-290, 1955.
571. Wheeler-Clark, E.S. and J.McD. Tormey. Electron probe X-ray microanalysis of sarcolemma and junctional sarcoplasmic reticulum in rabbit papillary muscles: Low sodium-induced calcium alterations. Circ. Res. 60:246-250, 1987.
572. White, C.W., M.L. Marcus and F.M. Abboud. Distribution of coronary artery flow to the canine right atrium and sinoatrial node. Circ. Res. 40:342-347, 1977.
573. Wier, W.G., M.B. Cannell, J.R. Berlin, E. Marban and W.J. Lederer. Cellular and subcellular heterogeneity of  $[Ca^{2+}]_i$  in single heart cells revealed by fura-2. Science 235:325-328, 1987.
574. Wier, W.G., A.A. Kort, M.D. Stern, E.G. Lakatta and E. Marban. Cellular calcium fluctuations in mammalian heart: Direct evidence from noise analysis of aequorin signals in Purkinje fibers. Proc. Natl. Acad. Sci. USA 80:7367-7371, 1983.
575. Winfree, A.T. Phase control of neural pacemakers. Science 197:761-763, 1977.
576. Winfree, A.T. When Time Breaks Down: The Three-Dimensional Dynamics of Electrochemical Waves and Cardiac Arrhythmias, Princeton: Princeton University Press, pp. 3-339, 1987.

577. Wit, A.L. and P.F. Cranefield. Triggered activity in cardiac muscle fibers of the simian mitral valve. Circ. Res. **38**:85-98, 1976.
578. Wit, A.L. and P.F. Cranefield. Triggered and automatic activity in the canine coronary sinus. Circ. Res. **41**:435-445, 1977.
579. Wit, A.L., P.F. Cranefield and D.C. Gadsby. Electrogenic sodium extrusion can stop triggered activity in the canine coronary sinus. Circ. Res. **49**:1029-1042, 1981.
580. Wit, A.L., J.J. Fenoglio, B.M. Wagner and A.L. Bassett. Electrophysiological properties of cardiac muscle in the anterior mitral valve leaflet and the adjacent atrium in the dog. Circ. Res. **32**:731-745, 1973.
581. Wit, A.L., J.L. Fenoglio, A.J. Hordorf and K. Reemtsma. Ultrastructure and transmembrane potentials of cardiac muscle in the human anterior mitral valve leaflet. Circ. **59**:1284-1292, 1979.
582. Wit, A.L. and M.R. Rosen. Afterdepolarizations and triggered activity. In: The Heart and Cardiovascular System. eds. H.A. Fozzard, R.B. Jennings, E. Haber and A.M. Katz. New York: Raven Press, pp.1449-1490, 1986.
583. Wittig, J.H., M.R. De Leval, J. Stark and A. Castenada. Intraoperative mapping of atrial activation before, during, and after the Mustard operation. J. Thor. Cardiovas. Surg. **73**:1-13, 1977.
584. Woods, W.T., R.E. Katholi, F. Urthaler and T.N. James. Electrophysiological effects of magnesium on cells in the canine sinus node and false tendon. Circ. Res. **44**:182-188, 1979.
585. Woods, W.T., F. Urthaler and T.N. James. Spontaneous action potentials of cells in the canine sinus node. Circ. Res. **39**:76-82, 1976.
586. Wybauw, R. Sur le point d'origine de la systole cardiaque dans l'oreillette droites. Arch. Internat. Physiol. **10**:78-89, 1910.
587. Yamada, K., M. Horiba, Y. Sakaida, M. Okajima, H. Horibe, H. Muraki, T. Kobayashi, A. Miyauchi and H. Oishi. Origination and transmission of impulse in the right auricle. Jap. Heart J. **6**:71-97, 1965.
588. Yamagishi, S. and T. Sano. Effect of tetrodotoxin on the pacemaker action potential of the sinus node. Proc. Jap. Acad. **42**:1194-1196, 1966.
589. Yamauchi, A. Electron microscopic observations on the development of SA and AV nodal tissues in the human embryonic heart. Z. Anat. Entw. Gesch. **124**:562-587, 1965.
590. Yanagihara, K. and H. Irisawa. Inward current activated during hyperpolarization in the rabbit sinoatrial node cell. Pflugers Arch. **385**:11-19, 1980.
591. Yanagihara, K., A. Noma and H. Irisawa. Reconstruction of sino-atrial node pace-maker potential based on the voltage clamp experiments. Jap. J. Physiol. **30**:841-857, 1980.



592. Yanigahara, K. and H. Irisawa. Potassium current during the pacemaker depolarization in rabbit sino-atrial node cell. Pflug. Archiv. 388:255-260, 1980.
593. Young, M.A. and S.F. Vatner. Regulation of large coronary arteries. Circ. Res. 59:579-596, 1986.
594. Young, M.L., D.L. Atkins, T.R. Lloyd and A.J. Wagman. Concealed atrial parasystole following the Senning operation. PACE 11:1504-1506, 1988.
595. Zahn, A. Experimentelle Untersuchungen ueber Reizbildung und Reizleitung im Atrioventrikulaknoten. Arch. f. d. ges. Physiol. 151:247, 1913.
596. Zaza, A., R.P. Kline and M.R. Rosen. Effects of  $\alpha$ -adrenergic stimulation on intracellular sodium activity and automaticity in canine cardiac Purkinje fibers. Circ. Res. 66:416-426, 1990.
597. Zuberbuhler, J.R. and S.R. Bauersfeld. Unusual arrhythmias after corrective surgery for transposition of the great vessels. Am. Heart J. 73:752-755, 1967.

APPROVAL SHEET

The thesis/dissertation submitted by Donald S. Rubenstein has been read and approved by the following committee:

Dr. Stephen L. Lipsius, Director  
Associate Professor, Physiology, Loyola University Chicago

Dr. Stephen B. Jones  
Associate Professor, Physiology, Loyola University Chicago

Dr. John F. Moran  
Professor, Medicine, Loyola University Chicago

Dr. Walter C. Randall  
Professor, Biology, Taylor University

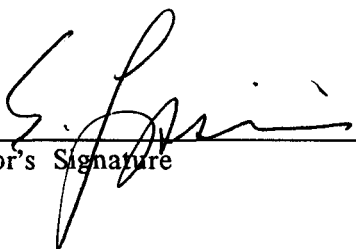
Dr. Andrew L. Wit  
Professor, Pharmacology, Columbia University

The final copies have been examined by the director of the thesis/dissertation and the signature which appears below verifies the fact that any necessary changes have been incorporated and that the thesis/dissertation is now given final approval by the Committee with reference to content and form.

The thesis/dissertation is therefore accepted in partial fulfillment of the requirements for the degree of Doctor of Philosophy.

Date

6/7/90

  
\_\_\_\_\_  
Director's Signature